

## CHAPTER 3: STRUCTURAL EVALUATION<sup>†</sup>

### 3.0 OVERVIEW

In this chapter, the structural components of the HI-STORM 100 System that are important to safety (ITS) are identified and described. The objective of the structural analyses is to ensure that the integrity of the HI-STORM 100 System is maintained under all credible loads for normal, off-normal, and design basis accident/natural phenomena. The chapter results support the conclusion that the confinement, criticality control, radiation shielding, and retrievability criteria set forth by 10CFR72.236(l), 10CFR72.124(a), 10CFR72.104, 10CFR72.106, and 10CFR72.122(l) are met. In particular, the design basis information contained in the previous two chapters and in this chapter provides sufficient data to permit structural evaluations to demonstrate compliance with the requirements of 10CFR72.24. To facilitate regulatory review, the assumptions and conservatism inherent in the analyses are identified along with a complete description of the analytical methods, models, and acceptance criteria. A summary of other material considerations, such as corrosion and material fracture toughness is also provided. Design calculations for the HI-TRAC transfer cask are included where appropriate to comply with the guidelines of NUREG-1536.

The organization of technical information in this chapter follows the format and content guidelines of USNRC Regulatory Guide 3.61 (February 1989). The FSAR ensures that the responses to the review requirements listed in NUREG-1536 (January 1997) are complete and comprehensive. The areas of NRC staff technical inquiries, with respect to structural evaluation in NUREG-1536, span a wide array of technical topics within and beyond the material in this chapter. To facilitate the staff's review to ascertain compliance with the stipulations of NUREG-1536, Table 3.0.1 "Matrix of NUREG-1536 Compliance - Structural Evaluation", is included in this chapter. A comprehensive cross-reference of the topical areas set forth in NUREG-1536, and the location of the required compliance information is contained in Table 3.0.1.

Section 3.7 describes in detail HI-STORM 100 System's compliance to NUREG-1536 Structural Evaluation Requirements.

The HI-STORM 100 System matrix of compliance table given in this section is developed with the supposition that the storage overpack is designated as a steel structure that falls within the purview of subsection 3.V.3 "Other Systems Components Important to Safety" (page 3-28 of NUREG-1536), and therefore, does not compel the use of reinforced concrete. (Please refer to Table 1.0.3 for an explicit statement of exception on this matter). The concrete mass installed in the HI-STORM 100 overpack is accordingly equipped with "plain concrete" for which the sole applicable industry code is ACI 318.1 (92). Plain concrete, in contrast to reinforced concrete, is the preferred shielding

---

<sup>†</sup> This chapter has been prepared in the format and section organization set forth in Regulatory Guide 3.61. However, the material content of this chapter also fulfills the requirements of NUREG-1536. Pagination and numbering of sections, figures, and tables are consistent with the convention set down in Chapter 1, Section 1.0, herein. Finally, all terms-of-art used in this chapter are consistent with the terminology of the glossary (Table 1.0.1) and component nomenclature of the Bill-of-Materials (Section 1.5).

material HI-STORM 100 because of three key considerations:

- (i) Plain concrete is more amenable to a void free pour than reinforced concrete in narrow annular spaces typical of ventilated vertical storage casks.
- (ii) The tensile strength bearing capacity of reinforced concrete is not required to buttress the steel weldment of the HI-STORM 100 overpack.
- (iii) The compression and bearing strength capacity of plain concrete is unaffected by the absence of rebars. A penalty factor, on the compression strength, pursuant to the provisions of ACI-318.1 is, nevertheless, applied to insure conservatism. However, while plain concrete is the chosen shielding embodiment for the HI-STORM 100 storage overpack, all necessary technical, procedural Q.C., and Q.A. provisions to insure nuclear grade quality will be implemented by utilizing the relevant sections from ACI-349 (85) as specified in Appendix 1.D.

In other words, guidelines of NUREG 1536 pertaining to reinforced concrete are considered to insure that the material specification, construction quality control and quality assurance of the shielding concrete comply with the provisions of ACI 349 (85). These specific compliance items are listed in the compliance matrix.

**TABLE 3.0.1**  
**MATRIX OF NUREG-1536 COMPLIANCE ITEMS – STRUCTURAL EVALUATION<sup>†</sup>**

PARAGRAPH IN NUREG-1536	NUREG-1536 COMPLIANCE ITEM	LOCATION IN FSAR CHAPTER 3	LOCATION OUTSIDE OF FSAR CHAPTER 3
IV.1.a	ASME B&PV Compliance		
	NB	3.1.1	Tables 2.2.6,2.2.7
	NG	3.1.1	Tables 2.2.6,2.2.7
IV.2	Concrete Material Specification		Appendix 1.D
IV.4	Lifting Devices	3.1; 3.4	
V.	Identification of SSC that are ITS		Table 2.2.6
“	Applicable Codes/Standards	3.6.1	Table 2.2.6
“	Loads		Table 2.2.13
“	Load Combinations	3.1.2.1.2; Tables 3.1.1- 3.1.5	Table 2.2.14
“	Summary of Safety Factors	3.4.3; 3.4.4.2; 3.4.4.3.1-3 3.4.6-3.4.9; Tables 3.4.3- 3.4.9	
“	Design/Analysis Procedures	Chapter 3	
“	Structural Acceptance Criteria		Tables 2.2.10-2.2.12

HOLTEC INTERNATIONAL COPYRIGHTED MATERIAL

**TABLE 3.0.1 (CONTINUED)**  
**MATRIX OF NUREG-1536 COMPLIANCE ITEMS – STRUCTURAL EVALUATION <sup>†</sup>**

PARAGRAPH IN NUREG-1536	NUREG-1536 COMPLIANCE ITEM	LOCATION IN FSAR CHAPTER 3	LOCATION OUTSIDE OF FSAR CHAPTER 3
“	Material/QC/Fabrication	Table 3.4.2	Chap. 9; Chap. 13
“	Testing/In-Service Surveillance		Chap. 9; Chap. 12
“	Conditions for Use		Table 1.2.6; Chaps. 8,9,12
V.1.a	Description of SSC	3.1.1	1.2
V.1.b.i.(2)	Identification of Codes & Standards		Tables 2.2.6, 2.2.7
V.1.b.ii	Drawings/Figures		1.5
“	Identification of Confinement Boundary		1.5; 2.3.2; 7.1; Table 7.1.1
“	Boundary Weld Specifications	3.3.1.4	1.5; Table 7.1.2
“	Boundary Bolt Torque	NA	
“	Weights and C.G. Location	Tables 3.2.1-3.2.4	
“	Chemical/Galvanic Reactions	3.4.1; Table 3.4.2	
V.1.c	Material Properties	3.3; Tables 3.3.1-3.3.5	1.A; 1.C; 1.D
“	Allowable Strengths	Tables 3.1.6-3.1.17	Tables 2.2.10-2.2.12; 1.D
“	Suitability of Materials	3.3; Table 3.4.2	1.A; 1.B; 1.D
“	Corrosion	3.3	
“	Material Examination before Fabrication		9.1.1

HOLTEC INTERNATIONAL COPYRIGHTED MATERIAL



**TABLE 3.0.1 (CONTINUED)**  
**MATRIX OF NUREG-1536 COMPLIANCE ITEMS – STRUCTURAL EVALUATION <sup>†</sup>**

PARAGRAPH IN NUREG-1536	NUREG-1536 COMPLIANCE ITEM	LOCATION IN FSAR CHAPTER 3	LOCATION OUTSIDE OF FSAR CHAPTER 3
“	Material Testing and Analysis		9.1; Table 9.1.1; 1.D
“	Material Traceability		9.1.1
“	Material Long Term Performance	3.3; 3.4.11; 3.4.12	9.2
“	Materials Appropriate to Load Conditions		Chap. 1
“	Restrictions on Use		Chap. 12
“	Temperature Limits	Table 3.1.17	Table 2.2.3
“	Creep/Slump	3.4.4.3.3.2	
“	Brittle Fracture Considerations	3.1.2.3; Table 3.1.18	
“	Low Temperature Handling		2.2.1.2
V.1.d.i.(1)	Normal Load Conditions		2.2.1; Tables 2.2.13,2.2.14
“	Fatigue	3.1.2.4	
“	Internal Pressures/Temperatures for Hot and Cold Conditions	3.4.4.1	2.2.2; Tables 2.2.1,2.2.3
“	Required Evaluations		
“	Weight+Pressure	3.4.4.3.1.2	
“	Weight/Pressure/Temp.	3.4.4.3.1.2	
“	Free Thermal Expansion	3.4.4.2	4.4.6; Table 4.4.10

HOLTEC INTERNATIONAL COPYRIGHTED MATERIAL

**TABLE 3.0.1 (CONTINUED)**  
**MATRIX OF NUREG-1536 COMPLIANCE ITEMS – STRUCTURAL EVALUATION <sup>†</sup>**

<b>PARAGRAPH IN NUREG-1536</b>	<b>NUREG-1536 COMPLIANCE ITEM</b>	<b>LOCATION IN FSAR CHAPTER 3</b>	<b>LOCATION OUTSIDE OF FSAR CHAPTER 3</b>
V.1.d.i.(2)	Off-Normal Conditions		2.2.2; Tables 2.2.13, 2.2.14; 11.1
V.1.d.i.(3)	Accident Level Events and Conditions	Tables 3.1.1, 3.1.2	2.2.3; Tables 2.2.13, 2.2.14; 11.2
V.1.d.i.(3).(a)	Storage Cask Vertical Drop	3.1.2.1.1.2; 3.4.10; 3.A	2.2.3.1
“	Storage Cask Tipover	3.1.2.1.1.1; 3.4.10; 3.A	2.2.3.2
“	Transfer Cask Horizontal Drop	3.4.9	2.2.3.1
V.1.d.i.(3).(b)	Explosive Overpressure	3.1.2.1.1.4	2.2.3.10
V.1.d.i.(3).(c)	Fire		
“	Structural Evaluations	3.4.4.2	2.2.3.3
“	Material Properties		11.2
“	Material Suitability	3.1.2.2; 3.3.1.1	Table 2.2.3; 11.2
V.1.d.i.(3).(d)	Flood		
“	Identification	3.1.2.1.1.3; 3.4.6	2.2.3.6
“	Cask Tipover	3.4.6	
“	Cask Sliding	3.4.6	
“	Hydrostatic Loading	3.1.2.1.1.3; 3.4.6	72-1008(3.H)
“	Consequences		11.2
V.1.d.i.(3).(e)	Tornado Winds		
“	Specification	3.1.2.1.1.5	2.2.3.5; Table 2.2.4
“	Drag Coefficients	3.4.8	
“	Load Combination	3.4.8	

HOLTEC INTERNATIONAL COPYRIGHTED MATERIAL

**TABLE 3.0.1 (CONTINUED)**  
**MATRIX OF NUREG-1536 COMPLIANCE ITEMS – STRUCTURAL EVALUATION<sup>†</sup>**

PARAGRAPH IN NUREG-1536	NUREG-1536 COMPLIANCE ITEM	LOCATION IN FSAR CHAPTER 3	LOCATION OUTSIDE OF FSAR CHAPTER 3
“	Overturning –Transfer	NA	
V.1.d.i.(3).(f)	Tornado Missiles		
“	Missile Parameters	3.1.2.1.1.5	Table 2.2.5
“	Tipover	3.4.8	
“	Damage	3.4.8.1; 3.4.8.2	
“	Consequences	3.4.8.1; 3.4.8.2	11.2
V.1.d.i.(3).(g)	Earthquakes		
“	Definition of DBE	3.1.2.1.1.6; 3.4.7	2.2.3.7; Table 2.2.8
“	Sliding	3.4.7	
“	Overturning	3.4.7	
“	Structural Evaluations	3.4.7	11.2
V.1.d.i.(4).(a)	Lifting Analyses		
“	Trunnions		
“	Requirements	3.1.2.1.2; 3.4.3.1; 3.4.3.2	72-1008(3.4.3); 2.2.1.2
“	Analyses	3.4.3.1; 3.4.3.2	72-1008(3.4.3)
“	Other Lift Analyses	3.4.3.7-3.4.3.9	
V.1.d.i.(4).(b)	Fuel Basket		
“	Requirements	3.1.2.1.2; Table 3.1.3	
“	Specific Analyses	3.4.4.2; 3.4.4.3; 3.6.3	72-1008(3.4.4.3.1.2; 3.4.4.3.1.6; 3.M; 3.H; 3.I)

HOLTEC INTERNATIONAL COPYRIGHTED MATERIAL

**TABLE 3.0.1 (CONTINUED)**  
**MATRIX OF NUREG-1536 COMPLIANCE ITEMS – STRUCTURAL EVALUATION <sup>†</sup>**

<b>PARAGRAPH IN NUREG-1536</b>	<b>NUREG-1536 COMPLIANCE ITEM</b>	<b>LOCATION IN FSAR CHAPTER 3</b>	<b>LOCATION OUTSIDE OF FSAR CHAPTER 3</b>
“	Dynamic Amplifiers	3.4.4.4.1	
“	Stability	3.4.4.3; 3.4.4.4	72-1008(Figures 3.4.27-32)
V.1.d.i.(4).(c)	Confinement Closure Lid Bolts		
“	Pre-Torque	NA	
“	Analyses	NA	
“	Engagement Length	NA	
“	Miscellaneous Bolting		
“	Pre-Torque	3.4.3.7; 3.4.3.8	
“	Analyses	3.4.4.3.2.2	
“	Engagement Length	3.4.3.5; 3.4.3.7; 3.4.3.8	
V.1.d.i.(4)	Confinement		
“	Requirements	3.1.2.1.2; Table 3.1.4	Chap. 7
“	Specific Analyses	3.6.3; Tables 3.4.3, 3.4.4	72-1008(3.E; 3.K; 3.I)
“	Dynamic Amplifiers	3.4.4.1	
“	Stability	3.4.4.3.1	72-1008(3.H)
“	Overpack		
“	Requirements	3.1.2.1.2; Tables 3.1.1, 3.1.5	
“	Specific Analyses	3.6.3; 3.4.4.3	

HOLTEC INTERNATIONAL COPYRIGHTED MATERIAL

**TABLE 3.0.1 (CONTINUED)**  
**MATRIX OF NUREG-1536 COMPLIANCE ITEMS – STRUCTURAL EVALUATION<sup>†</sup>**

PARAGRAPH IN NUREG-1536	NUREG-1536 COMPLIANCE ITEM	LOCATION IN FSAR CHAPTER 3	LOCATION OUTSIDE OF FSAR CHAPTER 3
“	Dynamic Amplifiers	3.4.4.3.2	
“	Stability	3.4.4.3; Table 3.1.1; 3.4.4.5	
“	Transfer Cask		
“	Requirements	3.1.2.1.2; Table 3.1.5	
“	Specific Analyses	3.4.4.3; 3.6.3	
“	Dynamic Amplifiers	3.4.4.4.1	
“	Stability	NA	2.2.3.1

<sup>†</sup> Legend for Table 3.0.1

Per the nomenclature defined in Chapter 1, the first digit refers to the chapter number, the second digit is the section number within the chapter; an alphabetic character in the second place means it is an appendix to the chapter.

72-1008                      HI-STAR 100 Docket Number where the referenced item is located  
NA                              Not Applicable for this item

### 3.1 STRUCTURAL DESIGN

#### 3.1.1 Discussion

The HI-STORM 100 System consists of three principal components: the Multi-Purpose Canister (MPC), the storage overpack, and the transfer cask. The MPC is a hermetically sealed, welded structure of cylindrical profile with flat ends and a honeycomb fuel basket. A complete description is provided in Subsection 1.2.1.1 wherein the anatomy of the MPC and its fabrication details are presented with the aid of figures. The MPCs utilized in the HI-STORM 100 System are identical to those for the HI-STAR 100 System submitted under Dockets 72-1008 and 71-9261. The evaluation of the MPCs presented herein draws upon the work described in those earlier submittals. In this section, the discussion is confined to characterizing and establishing the structural features of the MPC, the storage overpack, and the HI-TRAC transfer cask. Since a detailed discussion of the HI-STORM 100 Overpack and HI-TRAC transfer cask geometries is presented in Section 1.2, attention is focused here on structural capabilities and their inherent margins of safety for housing the MPC. Detailed design drawings for the HI-STORM 100 System are provided in Section 1.5.

The design of the MPC seeks to attain three objectives that are central to its functional adequacy, namely:

- **Ability to Dissipate Heat:** The thermal energy produced by the stored spent fuel must be transported to the outside surface of the MPC such that the prescribed temperature limits for the fuel cladding and for the fuel basket metal walls are not exceeded.
- **Ability to Withstand Large Impact Loads:** The MPC, with its payload of nuclear fuel, must be sufficiently robust to withstand large impact loads associated with the postulated handling accident events. Furthermore, the strength of the MPC must be sufficiently isotropic to meet structural requirements under a variety of handling and tip-over accidents.
- **Restraint of Free End Expansion:** The membrane and bending stresses produced by restraint of free-end expansion of the fuel basket are categorized as primary stresses. In view of the concentration of heat generation in the fuel basket, it is necessary to ensure that structural constraints to its external expansion do not exist.

Where the first two criteria call for extensive inter-cell connections, the last criterion requires the opposite. The design of the MPC seeks to realize all of the above three criteria in an optimal manner.

From the description presented in Chapter 1, the MPC enclosure vessel is the confinement vessel designed to meet ASME Code, Section III, Subsection NB stress limits. The enveloping canister shell, the baseplate, and the lid system form a complete confinement boundary for the stored fuel that is referred to as the "enclosure vessel". Within this cylindrical shell confinement vessel is an integrally welded assemblage of cells of square cross sectional openings for fuel storage, referred to herein as the fuel basket. The fuel basket is analyzed under the provisions of Subsection NG of Section III of the ASME Code. All multi-purpose canisters designed for deployment in the HI-

STORM 100 and HI-STAR 100 systems are exactly alike in their external dimensions. The essential difference between the MPCs lies in the fuel baskets. Each fuel storage MPC is designed to house fuel assemblies with different characteristics. Although all fuel baskets are configured to maximize structural ruggedness through extensive inter-cell connectivity, they are sufficiently dissimilar in structural details to warrant separate evaluations. Therefore, analyses for each of the MPC types were carried out to ensure structural compliance. Inasmuch as no new MPC designs are introduced in this application, and all MPC designs were previously reviewed by the USNRC under Docket 72-1008, the MPC analyses submitted under Docket Numbers 72-1008 and 71-9261 for the HI-STAR 100 System are not reproduced herein unless they need to be modified by HI-STORM 100 conditions or geometry differences. Analyses provided in the HI-STAR 100 System safety analysis reports that are applicable to the HI-STORM 100 System are referenced in this FSAR by docket number and subsection or appendix.

Components of the HI-STORM 100 System that are important to safety and their applicable design codes are defined in Chapter 2.

Some of the key structural functions of the MPC in the storage mode are:

1. To position the fuel in a subcritical configuration, and
2. To provide a confinement boundary.

Some of the key structural functions of the overpack in the storage mode are:

1. To serve as a missile barrier for the MPC,
2. To provide flow paths for natural convection,
3. To ensure stability of the HI-STORM 100 System, and
4. To maintain the position of the radiation shielding.
5. To allow movement of the overpack with a loaded MPC inside.

Some structural features of the MPCs that allow the system to perform these functions are summarized below:

- There are no gasketed ports or openings in the MPC. The MPC does not rely on any sealing arrangement except welding. The absence of any gasketed or flanged joints makes the MPC structure immune from joint leaks. The confinement boundary contains no valves or other pressure relief devices.

- The closure system for the MPCs consists of two components, namely, the MPC lid and the closure ring. The MPC lid can be either a single thick circular plate continuously welded to the MPC shell along its circumference or two dual lids welded around their common periphery. The MPC closure system is shown in the design drawings in Section 1.5. The MPC lid is equipped with vent and drain ports which are utilized for evacuating moisture and air from the MPC following fuel loading, and subsequent backfilling with an inert gas (helium) at a specified mass. The vent and drain ports are covered by a cover plate and welded before the closure ring is installed. The closure ring is a circular annular plate edge-welded to the MPC lid and shell. The two closure members are interconnected by welding around the inner diameter of the ring. Lift points for the MPC are provided in the MPC lid.
- The MPC fuel baskets consist of an array of interconnecting plates. The number of storage cells formed by this interconnection process varies depending on the type of fuel being stored. Basket designs containing cell configurations for PWR and BWR fuel have been designed and are explained in detail in Section 1.2. All baskets are designed to fit into the same MPC shell. Welding of the basket plates along their edges essentially renders the fuel basket into a multi-flange beam. Figure 3.1.1 provides an isometric illustration of a fuel basket for the MPC-68 design.
- The MPC basket is separated from its supports by a gap. The gap size decreases as a result of thermal expansion (depending on the magnitude of internal heat generation from the stored spent fuel). The provision of a small gap between the basket and the basket support structure is consistent with the natural thermal characteristics of the MPC. The planar temperature distribution across the basket, as shown in Section 4.4, approximates a shallow parabolic profile. This profile will create high thermal stresses unless structural constraints at the interface between the basket and the basket support structure are removed.
- The MPCs will be loaded with fuel with widely varying heat generation rates. The basket/basket support structure gap tends to be reduced for higher heat generation rates due to increased thermal expansion rates. Gaps between the fuel basket and the basket support structure are specified to be sufficiently large such that a gap exists around the periphery after any thermal expansion.
- In some early vintage MPCs, a small number of flexible thermal conduction elements (thin aluminum tubes) are interposed between the basket and the MPC shell. The elements are designed to be resilient. They do not provide structural support for the basket, and thus their resistance to thermal growth is negligible.



It is quite evident from the geometry of the MPC that a critical loading event pertains to the drop condition when the MPC is postulated to undergo a handling side drop (the longitudinal axis of the MPC is horizontal) or tip-over. Under the side drop or tip-over condition the flat panels of the fuel basket are subject to an equivalent pressure loading that simulates the deceleration-magnified inertia load from the stored fuel and the MPC's own metal mass.

The MPC fuel basket maintains the spent nuclear fuel in a subcritical arrangement. Its safe operation is assured by maintaining the physical configuration of the storage cell cavities intact in the aftermath of a drop event. This requirement is considered to be satisfied if the MPC fuel basket meets the stress intensity criteria set forth in the ASME Code, Section III, Subsection NG. Therefore, the demonstration that the fuel basket meets Subsection NG limits ensures that there is no impairment of ready retrievability (as required by NUREG-1536), and that there is no unacceptable effect on the subcritical arrangement.

The MPC confinement boundary contains no valves or other pressure relief devices. The MPC enclosure vessel is shown to meet the stress intensity criteria of the ASME Code, Section III, Subsection NB for all service conditions. Therefore, the demonstration that the enclosure vessel meets Subsection NB limits ensures that there is no unacceptable release of radioactive materials.

The HI-STORM 100 storage overpack is a steel cylindrical structure consisting of inner and outer low carbon steel shells, a lid, and a baseplate. Between the two shells is a thick cylinder of unreinforced (plain) concrete. Additional regions of fully confined (by enveloping steel structure) unreinforced concrete are attached to the lid and to the baseplate depending on the specific configuration (see applicable figures in previous chapters). The storage overpack serves as a missile and radiation barrier, provides flow paths for natural convection, provides kinematic stability to the system, and acts as a cushion for the MPC in the event of a tip-over accident. The storage overpack is not a pressure vessel since it contains cooling vents that do not allow for a differential pressure to develop across the overpack wall. The structural steel components of the HI-STORM 100 Overpack are designed to meet the stress limits of the ASME Code, Section III, Subsection NF, Class 3. Short versions of the HI-STORM 100 overpack, designated as the HI-STORM 100S, and the HI-STORM 100S Version B, are included in this revision. To accommodate nuclear plants with limited height access, the HI-STORM 100S has a re-configured lid and a lower overall height. There are minor weight redistributions but the overall bounding weight of the system is unchanged. The HI-STORM 100S Version B incorporates other improvements and modifications designed to improve fabricability and enhance some margins. Structural analyses are revisited if and only if the modified configuration cannot be demonstrated to be bounded by the original calculation. New or modified calculations focused on the HI-STORM 100S and the HI-STORM 100S Version B are clearly identified within the text of this chapter. Unless otherwise designated, general statements using the terminology "HI-STORM 100" also apply to the HI-STORM 100S and to the HI-STORM 100S Version B. The HI-STORM 100S overpacks can carry all MPCs and transfer casks that can be carried in the HI-STORM 100.

As discussed in Chapters 1 and 2, and Section 3.0, the principal shielding material utilized in the HI-STORM 100 Overpack is plain concrete. Plain concrete was selected for the HI-STORM 100 Overpack in lieu of reinforced concrete, because there is no structural imperative for incorporating tensile load bearing strength into the contained concrete. From a purely practical standpoint, the absence of rebars facilitate pouring and curing of concrete with minimal voids, which is an important consideration in light of its shielding function in the HI-STORM 100 Overpack. Plain concrete, however, acts essentially identical to reinforced concrete under compressive and bearing loads, even though ACI standards apply a penalty factor on the compressive and bearing strength of concrete in the absence of rebars (vide ACI 318.1).

Accordingly, the plain concrete in the HI-STORM 100 is considered as a structural material only to the extent that it may participate in supporting direct compressive loads. The allowable compression/bearing resistance is defined and quantified in the ACI 318.1-89(92) Building Code for Structural Plain Concrete.

In general, strength analysis of the HI-STORM 100 Overpack and its confined concrete is carried out only to demonstrate that the concrete is able to perform its radiation protection function and that retrievability of the MPC subsequent to any postulated accident condition of storage or handling is maintained.

A discrete ITS component in the HI-STORM 100 System is the HI-TRAC transfer cask. The HI-TRAC serves to provide a missile and radiation barrier during transport of the MPC from the fuel pool to the HI-STORM 100 Overpack. The HI-TRAC body is a double-walled steel cylinder that constitutes its structural system. Contained between the two steel shells is an intermediate lead cylinder. Attached to the exterior of the HI-TRAC body outer shell is a water jacket that acts as a radiation barrier. The HI-TRAC is not a pressure vessel since it contains a penetration in the HI-TRAC top lid that does not allow for a differential pressure to develop across the HI-TRAC wall. Nevertheless, in the interest of conservatism, structural steel components of the HI-TRAC are subject to the stress limits of the ASME Code, Section III, Subsection NF, Class 3.

Since both the HI-STORM 100 and HI-TRAC may serve as an MPC carrier, their lifting attachments are designed to meet the design safety factor requirements of NUREG-0612 [3.1.1] and ANSI N14.6-1993 [3.1.2] for single-failure-proof lifting equipment.

Table 2.2.6 provides a listing of the applicable design codes for all structures, systems, and components which are designated as ITS. Since no structural credit is required for the weld between the adjustable basket support pieces (i.e., shims and basket support flat plates), the adjustable basket supports are classified as NITS.

### 3.1.2 Design Criteria

Principal design criteria for normal, off-normal, and accident/environmental events are discussed in Section 2.2. In this section, the loads, load combinations, and allowable stresses used in the structural evaluation of the HI-STORM 100 System are presented in more detail.

Consistent with the provisions of NUREG-1536, the central objective of the structural analysis presented in this chapter is to ensure that the HI-STORM 100 System possesses sufficient structural capability to withstand normal and off-normal loads and the worst case loads under natural phenomenon or accident events. Withstanding such loadings enables the HI-STORM 100 System to successfully preclude the following negative consequences:

- unacceptable risk of criticality
- unacceptable release of radioactive materials
- unacceptable radiation levels
- impairment of ready retrievability of the SNF

The above design objectives for the HI-STORM 100 System can be particularized for individual components as follows:

- The objectives of the structural analysis of the MPC are to demonstrate that:
  1. Confinement of radioactive material is maintained under normal, off-normal, accident conditions, and natural phenomenon events.
  2. The MPC basket does not deform under credible loading conditions such that the subcriticality or retrievability of the SNF is jeopardized.
- The objectives of the structural analysis of the storage overpack are to demonstrate that:
  1. Tornado-generated missiles do not compromise the integrity of the MPC confinement boundary.
  2. The overpack can safely provide for on-site transfer of the loaded MPC and ensure adequate support to the HI-TRAC transfer cask during loading and unloading of the MPC.
  3. The radiation shielding remains properly positioned in the case of any normal, off-normal, or natural phenomenon or accident event.
  4. The flow path for the cooling airflow shall remain available under normal and off-normal conditions of storage and after a natural phenomenon or accident event.
  5. The loads arising from normal, off-normal, and accident level conditions exerted on the contained MPC do not exceed the structural design criteria of the MPC.

6. No geometry changes occur under any normal, off-normal, and accident level conditions of storage that may preclude ready retrievability of the contained MPC.
  7. A freestanding storage overpack can safely withstand a non-mechanistic tip-over event with a loaded MPC within the overpack. The HI-STORM 100A is specifically engineered to be permanently attached to the ISFSI pad. The ISFSI pad engineered for the anchored cask is designated as "Important to Safety". Therefore, the non-mechanistic tipover is not applicable to the HI-STORM 100A.
  8. The inter-cask transfer of a loaded MPC can be carried out without exceeding the structural capacity of the HI-STORM 100 Overpack, provided all required auxiliary equipment and components specific to an ISFSI site comply with their design criteria set forth in this FSAR and the handling operations are in full compliance with operational limits and controls prescribed in this FSAR.
- The objective of the structural analysis of the HI-TRAC transfer cask is to demonstrate that:
    1. Tornado generated missiles do not compromise the integrity of the MPC confinement boundary while the MPC is contained within HI-TRAC.
    2. No geometry changes occur under any postulated handling or storage conditions that may preclude ready retrievability of the contained MPC.
    3. The structural components perform their intended function during lifting and handling with the loaded MPC.
    4. The radiation shielding remains properly positioned under all applicable handling service conditions for HI-TRAC.
    5. The lead shielding, top lid, and transfer lid doors remain properly positioned during postulated handling accidents.

The aforementioned objectives are deemed to be satisfied for the MPC, the overpack, and the HI-TRAC, if stresses (or stress intensities, as applicable) calculated by the appropriate structural analyses are less than the allowables defined in Subsection 3.1.2.2, and if the diametral change in the storage overpack (or HI-TRAC), if any, after any event of structural consequence to the overpack (or transfer cask), does not preclude ready retrievability of the contained MPC.

Stresses arise in the components of the HI-STORM 100 System due to various loads that originate under normal, off-normal, or accident conditions. These individual loads are combined to form load

combinations. Stresses and stress intensities resulting from the load combinations are compared to their respective allowable stresses and stress intensities. The following subsections present loads, load combinations, and the allowable limits germane to them for use in the structural analyses of the MPC, the overpack, and the HI-TRAC transfer cask.

#### 3.1.2.1 Loads and Load Combinations

The individual loads applicable to the HI-STORM 100 System and the HI-TRAC cask are defined in Section 2.2 of this report (Table 2.2.13). Load combinations are developed by assembling the individual loads that may act concurrently, and possibly, synergistically (Table 2.2.14). In this subsection, the individual loads are further clarified as appropriate and the required load combinations are identified. Table 3.1.1 contains the load combinations for the storage overpack where kinematic stability is of primary importance. The load combinations where stress or load level is of primary importance are set forth in Table 3.1.3 for the MPC fuel basket, in Table 3.1.4 for the MPC confinement boundary, and in Table 3.1.5 for the storage overpack and the HI-TRAC transfer cask. Load combinations are applied to the mathematical models of the MPCs, the overpack, and the HI-TRAC. Results of the analyses carried out under bounding load combinations are compared with their respective allowable stresses (or stress intensities, as applicable). The analysis results from the bounding load combinations are also assessed, where warranted, to ensure satisfaction of the functional performance criteria discussed in the preceding subsection.

##### 3.1.2.1.1 Individual Load Cases

The individual loads that address each design criterion applicable to the structural design of the HI-STORM 100 System are catalogued in Table 2.2.13. Each load is given a symbol for subsequent use in the load combination listed in Table 2.2.14.

Accident condition and natural phenomena-induced events, collectively referred to as the "Level D" condition in Section III of the ASME Boiler & Pressure Vessel Codes, in general, do not have a universally prescribed limit. For example, the impact load from a tornado-borne missile, or the overturning load under flood or tsunami, cannot be prescribed as design basis values with absolute certainty that all ISFSI sites will be covered. Therefore, as applicable, allowable magnitudes of such loadings are postulated for the HI-STORM 100 System. The allowable values are drawn from regulatory and industry documents (such as for tornado missiles and wind) or from an intrinsic limitation in the system (such as the permissible "drop height" under a postulated handling accident). In the following, the essential characteristic of each "Level D" type loading is explained.

##### 3.1.2.1.1.1 Tip-Over

It is required to demonstrate that the free-standing HI-STORM 100 storage overpack, containing a loaded MPC, will not tip over as a result of a postulated natural phenomenon event, including tornado wind, a tornado-generated missile, a seismic or a hydrological event (flood). However, to demonstrate the defense-in-depth features of the design, a non-mechanistic tip-over scenario per NUREG-1536 is analyzed. Since the HI-STORM 100S and the HI-STORM 100S Version B have an

overall length that is less than the regular HI-STORM 100, the maximum impact velocity of the overpack will be reduced. Therefore, the results of the tipover analysis for the HI-STORM 100 (reported in Appendix 3.A) are bounding for the HI-STORM 100S and HI-STORM 100S Version B. The potential of the HI-STORM 100 Overpack tipping over during the lowering (or raising) of the loaded MPC into (or out of) it with the HI-TRAC cask mounted on it is ruled out because of the safeguards and devices mandated by this FSAR for such operations (Subsection 2.3.3.1 and Technical Specification 4.9). The physical and procedural barriers under the MPC handling operations have been set down in the FSAR to preclude overturning of the HI-STORM/HI-TRAC assemblage with an extremely high level of certainty. Much of the ancillary equipment needed for the MPC transfer operations must be custom engineered to best accord with the structural and architectural exigencies of the ISFSI site. Therefore, with the exception of the HI-TRAC cask, their design cannot be prescribed, a priori, in this FSAR. However, carefully drafted Design Criteria and conditions of use set forth in this FSAR eliminate the potential of weakening of the safety measures contemplated herein to preclude an overturning event during MPC transfer operations. Subsection 2.3.3.1 contains a comprehensive set of design criteria for the ancillary equipment and components required for MPC transfer operations to ensure that the design objective of precluding a kinematic instability event during MPC transfer operations is met. Further information on the steps taken to preclude system overturning during MPC transfer operations may be found in Chapter 8, Section 8.0.

In the HI-STORM 100A configuration, wherein the overpack is physically anchored to the ISFSI pad, the potential for a tip-over is a priori precluded. Therefore, the ISFSI pad need not be engineered to be sufficiently compliant to limit the peak MPC deceleration to Table 2.2.8 values. The stiffness of the pad, however, may be controlled by the ISFSI structural design and, therefore, may result in a reduced “carry height” from that specified for a freestanding cask. If a non-single failure proof lifting device is employed to carry the cask over the pad, determination of maximum carry height must be performed by the ISFSI owner once the ISFSI pad design is formalized.

#### 3.1.2.1.1.2 Handling Accident

A handling accident during transport of a loaded HI-STORM 100 storage overpack is assumed to result in a vertical drop. The HI-STORM 100 storage overpack will not be handled in a horizontal position while containing a loaded MPC. Therefore, a side drop is not considered a credible event.

HI-TRAC can be carried in a horizontal orientation while housing a loaded MPC. Therefore, a handling accident during transport of a loaded HI-TRAC in a horizontal orientation is considered to be a credible accident event.

As discussed in the foregoing, the vertical drop of the HI-TRAC and the tip-over of the assemblage of a loaded HI-TRAC on the top of the HI-STORM 100 storage overpack during MPC transfer operations do not need to be considered.

#### 3.1.2.1.1.3 Flood

The postulated flood event results into two discrete scenarios which must be considered; namely,

1. stability of the HI-STORM 100 System due to flood water velocity, and
2. structural effects of hydrostatic pressure and water velocity induced lateral pressure.

The maximum hydrostatic pressure on the cask in a flood where the water level is conservatively set at 125 feet is calculated as follows:

Using

$p$  = the maximum hydrostatic pressure on the system (psi),  
 $\gamma$  = weight density of water = 62.4 lb/ft<sup>3</sup>  
 $h$  = the height of the water level = 125 ft;

The maximum hydrostatic pressure is

$$p = \gamma h = (62.4 \text{ lb/ft}^3)(125 \text{ ft})(1 \text{ ft}^2/144 \text{ in}^2) = 54.2 \text{ psi}$$

The accident condition design external pressure for the MPC (Table 2.2.1) bounds the maximum hydrostatic pressure exerted by the flood.

#### 3.1.2.1.1.4 Explosion

The potential for explosive materials shall be evaluated based on site specific conditions as required in the HI-STORM 100 Technical Specification.

Pressure waves from an explosive blast in a property near the ISFSI site result in an impulsive aerodynamic loading on the stored HI-STORM 100 Overpacks. Depending on the rapidity of the pressure build-up, the inside and outside pressures on the HI-STORM METCON™ shell may not equalize, leading to a net lateral loading on the upright overpack as the pressure wave traverses the overpack. The magnitude of the dynamic pressure wave is conservatively set to a value below the magnitude of the pressure differential that would cause a tip-over of the cask if the pulse duration were set at one second. With the maximum design basis pressure pulse established (by setting the design basis pressure differential sufficiently low that cask tip-over is not credible due to the travelling pressure wave), the stress state under this condition requires analysis. The lateral pressure difference, applied over the overpack full height, causes axial and circumferential stresses and strains to develop. Level D stress limits must not be exceeded under this state of stress. It must also be demonstrated that no permanent ovalization of the cross section occurs that leads to loss of clearance to remove the MPC after the explosion.

Once the pressure wave traverses the cask body, then an elastic stability evaluation is warranted. An all-enveloping pressure from the explosion may threaten safety by buckling the overpack outer shell.

In contrast to the overpack, the MPC is a closed pressure vessel. Because of the enveloping overpack around it, the explosive pressure wave would manifest as an external pressure on the external surface of the MPC.

The maximum overpressure on the MPC resulting from an explosion is limited to the accident condition design external pressure specified in Table 2.2.1. The maximum external pressure differential on the overpack is limited to the accident condition design pressure differential specified in Table 2.2.1.

#### 3.1.2.1.1.5 Tornado

The three components of a tornado load are:

1. pressure changes,
2. wind loads, and
3. tornado-generated missiles.

Wind speeds and tornado-induced pressure drop are specified in Table 2.2.4. Tornado missiles are listed in Table 2.2.5. A central functional objective of a storage overpack is to maintain the integrity of the “confinement boundary”, namely, the multi-purpose canister stored inside it. This operational imperative requires that the mechanical loadings associated with a tornado at the ISFSI do not jeopardize the physical integrity of the loaded MPC. Potential consequences of a tornado on the cask system are:

- Instability (tip-over) due to tornado missile impact plus either steady wind or impulse from the pressure drop (only applicable for free-standing cask).
- Stress in the overpack induced by the lateral force caused by the steady wind or missile impact.
- Loadings applied on the MPC transmitted to the inside of the overpack through its openings or as a secondary effect of loading on the enveloping overpack structure.
- Excessive storage overpack permanent deformation that may prevent ready retrievability of the MPC.
- Excessive storage overpack permanent deformation that may significantly reduce the shielding effectiveness of the storage overpack.

Analyses must be performed to ensure that, due to the tornado-induced loadings:

- The loaded overpack does not become kinematically unstable (only applicable for free-standing cask).



- The overpack does not deform plastically such that the retrievability of the stored MPC is threatened.
- The MPC does not sustain an impact from an incident missile.
- The MPC is not subjected to inertia loads (acceleration or deceleration) in excess of its design basis limit set forth in Chapter 2 herein.
- The overpack does not deform sufficiently due to tornado-borne missiles such that the shielding effectiveness of the overpack is significantly affected.

The results obtained for the HI-STORM 100 bound the corresponding results for the HI-STORM 100S versions because of the reduced height. In the anchored configuration (HI-STORM 100A), the kinematic stability requirement stated above is replaced with the requirement that the stresses in the anchor studs do not exceed level D stress limits for ASME Section III, Class 3, Subsection NF components.

#### 3.1.2.1.1.6 Earthquake

Subsections 2.2.3.7 and 3.4.7 contain the detailed specification of the seismic inputs applied to the HI-STORM 100 System. The design basis earthquake is assumed to be at the top of the ISFSI pad. Potential consequences of a seismic event are sliding/overturning of a free-standing cask, overstress of the sector lugs and anchor studs for the anchored HI-STORM 100A, and lateral force on the overpack causing excessive stress and deformation of the storage overpack.

In the anchored configuration (HI-STORM 100A), a seismic event results in a fluctuation in the state of stress in the anchor bolts and a local bending action on the sector lugs.

Analyses must be performed to ensure that:

- The maximum axial stress in the anchor bolts remains below the Level D stress limits for Section III Class 3 Subsection NF components.
- The maximum primary membrane plus bending stress intensity in the sector lugs during the DBE event satisfies Level D stress limits of the ASME Code, Subsection NF.
- The anchor bolts will not sustain fatigue failure due to pulsation in their axial stress during the DBE event.
- The stress in the weld line joining the sector lugs to the HI-STORM 100 weldment is within Subsection NF limits for Level D condition.

#### 3.1.2.1.1.7 Lightning

The HI-STORM 100 Overpack contains over 25,000 lb of highly conductive carbon steel with over 700 square feet of external surface area. Such a large surface area and metal mass is adequate to dissipate any lightning that may strike the HI-STORM 100 System. There are no combustible materials on the HI-STORM 100 surface. Therefore, lightning will not impair the structural performance of components of the HI-STORM 100 System that are important to safety.

#### 3.1.2.1.1.8 Fire

The potential structural consequences of a fire are: the possibility of an interference developing between the storage overpack and the loaded MPC due to free thermal expansion; and, the degradation of material properties to the extent that their structural performance is affected during a subsequent recovery action. The fire condition is addressed to the extent necessary to demonstrate that these adverse structural consequences do not materialize.

#### 3.1.2.1.1.9 100% Fuel Rod Rupture

The effect on structural performance by 100% fuel rod rupture is felt as an increase in internal pressure. The accident internal pressure limit set in Chapter 2 bounds the pressure from 100% fuel rod rupture. Therefore, no new load condition has been identified.

#### 3.1.2.1.2 Load Combinations

Load combinations are created by summing the effects of several individual loads. The load combinations are selected for the normal, off-normal, and accident conditions. The loadings appropriate for HI-STORM 100 under the various conditions are presented in Table 2.2.14. These loadings are combined into meaningful combinations for the various HI-STORM 100 System components in Tables 3.1.1, and 3.1.3-3.1.5. Table 3.1.1 lists the load combinations that address overpack stability. Tables 3.1.3 through 3.1.5 list the applicable load combinations for the fuel basket, the enclosure vessel, and the overpack and HI-TRAC, respectively.

As discussed in Subsection 2.2.7, the number of discrete load combinations for each situational condition (i.e., normal, off-normal, etc.) is consolidated by defining bounding loads for certain groups of loadings. Thus, the accident condition pressure  $P_o^*$  bounds the surface loadings arising from accident and extreme natural phenomenon events, namely, tornado wind  $W'$ , flood  $F$ , and explosion  $E^*$ .

As noted previously, certain loads, namely earthquake  $E$ , flowing water under flood condition  $F$ , force from an explosion pressure pulse  $F^*$ , and tornado missile  $M$ , act to destabilize a cask. Additionally, these loads act on the overpack and produce essentially localized stresses at the HI-STORM 100 System to ISFSI interface. Table 3.1.1 provides the load combinations that are relevant to the stability analyses of freestanding casks. The site ISFSI DBE zero period acceleration (ZPA) must be bounded by the design basis seismic ZPA defined by the Load Combination C of Table 3.1.1 to demonstrate that the margin against tip-over during a seismic event is maintained.

The major constituents in the HI-STORM 100 System are: (i) the fuel basket, (ii) the enclosure vessel, (iii) the HI-STORM 100 (or HI-STORM 100S versions) Overpack, and (iv) the HI-TRAC transfer cask. The fuel basket and the enclosure vessel (EV) together constitute the multi-purpose canister. The multi-purpose canister (MPC) is common to HI-STORM 100 and HI-STAR 100, and as such, has been extensively analyzed in the storage FSAR and transport SAR (Dockets 72-1008 and 71-9261) for HI-STAR 100. Many of the loadings on the MPC (fuel basket and enclosure vessel) are equal to or bounded by loadings already considered in the HI-STAR 100 SAR documents. Where such analyses have been performed, their location in the HI-STAR 100 SAR documents is indicated in this HI-STORM 100 SAR for continuity in narration. A complete account of analyses and results for all load combinations for all four constituents parts is provided in Section 3.4 as required by Regulatory Guide 3.61.

In the following, the loadings listed as applicable for each situational condition in Table 2.2.14 are addressed in meaningful load combinations for the fuel basket, enclosure vessel, and the overpack. Each component is considered separately.

### Fuel Basket

Table 3.1.3 summarizes all loading cases (derived from Table 2.2.14) that are germane to demonstrating compliance of the fuel baskets to Subsection NG when these baskets are housed within HI-STORM 100 or HI-TRAC.

The fuel basket is not a pressure vessel; therefore, the pressure loadings are not meaningful loads for the basket. Further, the basket is structurally decoupled from the enclosure vessel. The gap between the basket and the enclosure vessel is sized to ensure that no constraint of free-end thermal expansion of the basket occurs. The demonstration of the adequacy of the basket-to -enclosure vessel (EV) gap to ensure absence of interference is a physical problem that must be analyzed.

The normal handling loads on the fuel basket in an MPC within the HI-STORM 100 System or the HI-TRAC transfer cask are identical to or bounded by the normal handling loads analyzed in the HI-STAR 100 FSAR Docket Number 72-1008.

Three accident condition scenarios must be considered: (i) drop with the storage overpack axis vertical; (ii) drop with the HI-TRAC axis horizontal; and (iii) storage overpack tipover. The vertical drop scenario is considered in the HI-STAR 100 FSAR.

The horizontal drop and tip-over must consider multiple orientation of the fuel basket, as the fuel basket is not radially symmetric. Therefore, two horizontal drop orientations are considered which are referred to as the 0 degree drop and 45 degree drop, respectively. In the 0 degree drop, the basket drops with its panels oriented parallel and normal to the vertical (see Figure 3.1.2). The 45-degree drop implies that the basket's honeycomb section is rotated meridionally by 45 degrees (Figure 3.1.3).

### Enclosure Vessel

Table 3.1.4 summarizes all load cases that are applicable to structural analysis of the enclosure vessel to ensure integrity of the confinement boundary.

The enclosure vessel is a pressure vessel consisting of a cylindrical shell, a thick circular baseplate at the bottom, and a thick circular lid at the top. This pressure vessel must be shown to meet the primary stress intensity limits for ASME Section III Class 1 at the design temperature and primary plus secondary stress intensity limits under the combined action of pressure plus thermal loads.

Normal handling of the enclosure vessel is considered in Docket 72-1008; the handling loads are independent of whether the enclosure vessel is within HI-STAR 100, HI-STORM 100, or HI-TRAC.

The off-normal condition handling loads are identical to the normal condition and, therefore, a separate analysis is not required.

Analyses presented in this chapter are intended to demonstrate that the maximum decelerations in drop and tip-over accident events are limited by the bounding values in Table 3.1.2. The vertical drop event is considered in the HI-STAR 100 FSAR Docket 72-1008.

The deceleration loadings developed in the enclosure vessel during a horizontal drop event are combined with those due to  $P_i$  (internal pressure) acting alone. The accident condition pressure is bounded by  $P_i^*$ . The design basis deceleration for the MPC in the HI-STAR 100 System is 60g's, whereas the design basis deceleration for the MPC in the HI-STORM 100 System is 45g's. The design pressures are identical. The fire event ( $T^*$  loading) is considered for ensuring absence of interference between the enclosure vessel and the fuel basket and between the enclosure vessel and the overpack.

It is noted that the MPC basket-enclosure vessel thermal expansion and stress analyses are reconsidered in this submittal to reflect the different MPC-to-overpack gaps that exist in the HI-STORM 100 Overpack versus the HI-STAR 100 overpack, coupled with the different design basis decelerations.

### Storage Overpack

Table 3.1.5 identifies the load cases to be considered for the overpack. These are in addition to the kinematic criteria listed in Table 3.1.1. Within these load cases and kinematic criteria, the following items must be addressed:

#### Normal Conditions

- The dead load of the HI-TRAC with the heaviest loaded MPC (dry) on top of the HI-STORM 100 Overpack must be shown to be able to be supported by the metal-concrete (METCON™) structure consisting of the two concentric steel shells and the radial ribs.

- The dead load of the HI-STORM 100 Overpack itself must be supportable by the steel structure with no credit for concrete strength other than self-support in compression.
- Normal handling loads must be accommodated without taking any strength credit from the contained concrete other than self-support in compression.

#### Accident Conditions

- Maximum flood water velocity for the overpack with an empty MPC must be specified to ensure that no sliding or tip-over occurs.
- Tornado missile plus wind on an overpack with an empty MPC must be specified to demonstrate that no cask tip-over occurs.
- Tornado missile penetration analysis must demonstrate that the postulated large and penetrant missiles cannot contact the MPC. The small missile must be shown not to penetrate the MPC pressure vessel boundary, since it can enter the overpack cavity through the vent ducts.
- Under seismic conditions, a fully loaded, free-standing HI-STORM 100 overpack must be demonstrated to not tip over under the maximum ZPA event. The maximum sliding of the overpack must demonstrate that casks will not impact each other.
- Under a non-mechanistic postulated tip-over of a fully loaded, freestanding HI-STORM 100 overpack, the overpack lid must not dislodge.
- Accident condition stress levels must not be exceeded in the steel and compressive stress levels in the concrete must remain within allowable limits.
- Accident condition induced gross general deformations of the storage overpack must be limited to values that do not preclude ready retrievability of the MPC.

As noted earlier, analyses performed using the HI-STORM 100 generally provide results that are identical to or bound results for the shorter HI-STORM 100S versions; therefore, analyses are not repeated specifically for the HI-STORM 100S unless the specific geometry changes significantly influence the safety factors.

#### HI-TRAC Transfer Cask

Table 3.1.5 identifies load cases applicable to the HI-TRAC transfer cask.

The HI-TRAC transfer cask must provide radiation protection, must act as a handling cask when carrying a loaded MPC, and in the event of a postulated accident must not suffer permanent

deformation to the extent that ready retrievability of the MPC is compromised. This submittal includes four types of transfer casks: a 125-ton HI-TRAC (referred to as the HI-TRAC 125), a modified version of the HI-TRAC 125 called the HI-TRAC 125D, a 100-ton HI-TRAC (referred to as the HI-TRAC 100), and a modified version of the HI-TRAC 100 called the HI-TRAC 100D. The details of these four transfer casks are provided in the design drawings in Section 1.5. The same steel structures (i.e., shell thicknesses, lid thicknesses, etc.) are maintained with the only major differences being in the amount of lead shielding, the water jacket configuration, the bottom flange, and the lower dead weight loading. Therefore, all structural analyses performed for the HI-TRAC 125 are repeated for the HI-TRAC 125D, the HI-TRAC 100, and the HI-TRAC 100D only if it cannot be clearly demonstrated that the HI-TRAC 125 calculation is bounding.

### 3.1.2.2 Allowables

The important to safety components of the HI-STORM 100 System are listed in Table 2.2.6. Allowable stresses, as appropriate, are tabulated for these components for all service conditions.

In Subsection 2.2.5, the applicable service level from the ASME Code for determination of allowables is listed. Table 2.2.14 provides a tabulation of normal, off-normal, and accident conditions and the service levels defined in the ASME Code, along with the applicable loadings for each service condition.

Allowable stresses and stress intensities are calculated using the data provided in the ASME Code and Tables 2.2.10 through 2.2.12. Tables 3.1.6 through 3.1.16 contain numerical values of the stresses/stress intensities for all MPC, overpack, and HI-TRAC load bearing materials as a function of temperature.

In all tables the terms  $S$ ,  $S_m$ ,  $S_y$ , and  $S_u$ , respectively, denote the design stress, design stress intensity, minimum yield strength, and the ultimate strength. Property values at intermediate temperatures that are not reported in the ASME Code are obtained by linear interpolation. Property values are not extrapolated beyond the limits of the Code in any structural calculation.

Additional terms relevant to the analyses are extracted from the ASME Code (Figure NB-3222-1, for example) as follows:

Symbol	Description	Notes
$P_m$	Average primary stress across a solid section	Excludes effects of discontinuities and concentrations. Produced by pressure and mechanical loads.
$P_L$	Average stress across any solid section	Considers effects of discontinuities but not concentrations. Produced by pressure and mechanical loads, including earthquake inertial effects.
$P_b$	Primary bending stress	Component of primary stress proportional to the distance from the centroid of a solid section. Excludes the effects of

Symbol	Description	Notes
		discontinuities and concentrations. Produced by pressure and mechanical loads, including earthquake inertial effects.
$P_e$	Secondary expansion stress	Stresses that result from the constraint of free-end displacement. Considers effects of discontinuities but not local stress concentration. (Not applicable to vessels.)
Q	Secondary membrane plus bending stress	Self-equilibrating stress necessary to satisfy continuity of structure. Occurs at structural discontinuities. Can be caused by pressure, mechanical loads, or differential thermal expansion.
F	Peak stress	Increment added to primary or secondary stress by a concentration (notch), or, certain thermal stresses that may cause fatigue but not distortion. This value is not used in the tables.

It is shown that there is no interference between component parts due to free thermal expansion. Therefore,  $P_e$  does not develop within any HI-STORM 100 component.

It is recognized that the planar temperature distribution in the fuel basket and the overpack under the maximum heat load condition is the highest at the cask center and drops monotonically, reaching its lowest value at the outside surface. Strictly speaking, the allowable stresses/stress intensities at any location in the basket, the enclosure vessel, or the overpack should be based on the coincident metal temperature under the specific operating condition. However, in the interest of conservatism, reference temperatures are established for each component, which are upper bounds on the metal temperature for each situational condition. Table 3.1.17 provides the reference temperatures for the fuel basket and the MPC canister utilizing Tables 3.1.6 through 3.1.16, and provides conservative numerical limits for the stresses and stress intensities for all loading cases. Reference temperatures for the MPC baseplate and the MPC lid are 400 degrees F and 550 degrees F, respectively, as specified in Table 2.2.3.

Finally, the lift devices in the HI-STORM 100 Overpack and HI-TRAC casks and the multi-purpose canisters, collectively referred to as "trunnions", are subject to specific limits set forth by NUREG-0612: the primary stresses in a trunnion must be less than the smaller of 1/10 of the material ultimate strength and 1/6 of the material yield strength under a normal handling condition (Load Case 01 in Table 3.1.5). The load combination D+H in Table 3.1.5 is equivalent to 1.15D. This is further explained in Subsection 3.4.3.

The region around the trunnions is part of the NF structure in HI-STORM 100 and HI-TRAC and NB pressure boundary in the MPC, and as such, must satisfy the applicable stress (or stress intensity) limits for the load combination. In addition to meeting the applicable Code limits, it is further required that the primary stress required to maintain equilibrium at the defined trunnion/mother structure interface must not exceed the material yield stress at three times the handling condition load

(1.15D). This criterion, mandated by Regulatory Guide 3.61, Section 3.4.3, insures that a large safety factor exists on non-local section yielding at the trunnion/mother structure interface that would lead to unacceptable section displacement and rotation.

### 3.1.2.3 Brittle Fracture

The MPC canister and basket are constructed from a series of stainless steels termed Alloy X. These stainless steel materials do not undergo a ductile-to-brittle transition in the minimum temperature range of the HI-STORM 100 System. Therefore, brittle fracture is not a concern for the MPC components. Such an assertion can not be made a priori for the HI-STORM storage overpack and HI-TRAC transfer cask that contain ferritic steel parts. In general, the impact testing requirements for the HI-STORM overpack and the HI-TRAC transfer cask are a function of two parameters: the Lowest Service Temperature (LST) and the normal stress level. The significance of these two parameters, as they relate to impact testing of the overpack and the transfer cask, is discussed below.

In normal storage mode, the LST of the HI-STORM storage overpack structural members may reach -40°F in the limiting condition wherein the spent nuclear fuel (SNF) in the contained MPCs emits no (or negligible) heat and the ambient temperature is at -40°F (design minimum per Chapter 2: Principal Design Criteria). During the HI-STORM handling operations, the applicable lowest service temperature is 0°F (which is the threshold ambient temperature below which lifting and handling of the HI-STORM 100 Overpack or the HI-TRAC cask is not permitted by the Technical Specification). Therefore, two distinct LSTs are applicable to load bearing metal parts within the HI-STORM 100 Overpack and the HI-TRAC cask; namely,

LST = 0°F for the HI-STORM overpack during handling operations and for the HI-TRAC transfer cask during all normal operating conditions.

LST = -40°F for the HI-STORM overpack during all non-handling operations (i.e., normal storage mode).

Parts used to lift the overpack or the transfer cask, which include the anchor block in the HI-STORM 100 overpack, and the pocket trunnions, the lifting trunnions and the lifting trunnion block in HI-TRAC, will henceforth be referred to as “significant-to-handling” (STH) parts. The applicable design code for these elements of the structure is ANSI N14.6. All other parts of the overpack and the transfer cask will be referred to as “NF” components. It is important to ensure that all materials designated as “NF” or “STH” parts possess sufficient fracture toughness to preclude brittle fracture. For the STH parts, the necessary level of protection against brittle fracture is deemed to exist if the NDT (nil ductility transition) temperature of the part is at least 40° below the LST. Therefore, the required NDT temperature for all STH parts is -40°F.

It is well known that the NDT temperature of steel is a strong function of its composition, manufacturing process (viz., fine grain vs. coarse grain practice), thickness, and heat treatment. For example, according to Burgreen [3.1.3], increasing the carbon content in carbon steels from 0.1% to 0.8% leads to the change in NDT from -50°F to approximately 120°F. Likewise, lowering of the



normalizing temperature in the ferritic steels from 1200°C to 900°C lowers the NDT from 10°C to -50°C [3.1.3]. It, therefore, follows that the fracture toughness of steels can be varied significantly within the confines of the ASME Code material specification set forth in Section II of the Code. For example, SA516 Gr. 70 (which is a principal NF material in the HI-STORM 100 Overpack) can have a maximum carbon content of up to 0.3% in plates up to four inches thick. Section II further permits normalizing or quenching followed by tempering to enhance fracture toughness. Manufacturing processes which have a profound effect on fracture toughness, but little effect on tensile or yield strength of the material, are also not specified with the degree of specificity in the ASME Code to guarantee a well defined fracture toughness. In fact, the Code relies on actual coupon testing of the part to ensure the desired level of protection against brittle fracture. For Section III, Subsection NF Class 3 parts, the desired level of protection is considered to exist if the lowest service temperature is equal to or greater than the NDT temperature (per NF 2311(b)(10)). Accordingly, the required NDT temperature for all load bearing metal parts in the HI-STORM 100 Overpack (NF and STH) is -40°F. Likewise, the NDT temperature for all NF parts in HI-TRAC (except for STH parts) is set equal to 0°F.

The STH components (HI-STORM bolt anchor block, HI-TRAC lifting trunnion, HI-TRAC lifting trunnion block, and HI-TRAC pocket trunnion) have thicknesses greater than 2". SA350-LF3 has been selected as the material for these items (except for the lifting trunnions) due to its capability to maintain acceptable fracture toughness at low temperatures (see Table 5 in SA350 of ASME Section IIA). Additionally, material for the HI-TRAC top flange, pool lid (100 ton) and pool lid outer ring (125 ton) has been defined as SA350-LF3, SA350-LF2, or SA203E (see Table A1.15 of ASME Section IIA) in order to achieve low temperature fracture toughness. The HI-TRAC lifting trunnion is fabricated from SB-637 Grade N07718, a high strength nickel alloy material. This material has a high resistance to fracture at low temperatures. All other steel structural materials in the HI-STORM 100 overpack and HI-TRAC cask are made of SA516 Gr. 70, SA515 Gr. 70, or SA36 (with some components having an option for SA203E or SA350-LF3 depending on material availability).

Either as-rolled or normalized SA516 Gr. 70 plate can be used to fabricate the overpack and the transfer cask. If the SA516 Gr. 70 plate is normalized, then it is exempt from impact testing per NF-2311(b). The specific reasons are:

1. The LST for handling operations is above the Minimum Design Temperature of SA516 Gr. 70 normalized plate (for thickness less than 2-1/2") per Figure NF-2311(b)-1, and;
2. During non-handling operations (i.e., normal storage mode), the maximum tensile stress in the HI-STORM overpack is less than the threshold limit of 6,000 psi specified in NF-2311(b)(7).

If the SA516 Gr. 70 plate is as-rolled (i.e., not normalized), then impact testing is required, except when the material is used for the following HI-STORM components: inner and outer shells, top plate, lid shear ring, lid shield ring, lid outer ring (for 100S Version B), and lid cover plate (for 100S Version B) and Base-Bottom Plate (for 100S Version B). The material for these components is

exempt from impact testing per NF-2311(b)(7) since the maximum stress under normal conditions, including handling operations, does not exceed 6,000 psi tension or is compressive.

Even though SA516 Gr. 70 normalized plate is exempt from impact testing per the above, certain components of the HI-STORM 100A overpack, namely the lug support ring, the gussets, and the baseplate, are impact tested, as a defense-in-depth measure, because they are potentially subject to high tensile stress levels (i.e., greater than 6,000 psi) during an earthquake.

Table 3.1.18 provides a summary of impact testing requirements to satisfy the requirements for prevention of brittle fracture.

#### 3.1.2.4 Fatigue

In storage, the HI-STORM 100 System is not subject to significant cyclic loads. Failure due to fatigue is not a concern for the HI-STORM 100 System.

In an anchored installation, however, the anchor studs sustain a pulsation in the axial load during the seismic event. The amplitude of axial stress variation under the DBE event is computed in this chapter and a significant margin of safety against fatigue failure during the DBE event is demonstrated.

The system is subject to cyclic temperature fluctuations. These fluctuations result in small changes of thermal expansions and pressures in the MPC. The loads resulting from these changes are small and do not significantly contribute to the "usage factor" of the cask.

Inspection of the HI-TRAC trunnions specified in Chapter 9 will preclude use of a trunnion that exhibits visual damage.

#### 3.1.2.5 Buckling

Certain load combinations subject structural sections with relatively large slenderness ratios (such as the enclosure vessel shell) to compressive stresses that may actuate buckling instability before the allowable stress is reached. Tables 3.1.4 and 3.1.5 list load combinations for the enclosure vessel and the HI-STORM 100/HI-TRAC structures; the cases which warrant stability (buckling) check are listed therein (note that a potential buckling load has already been identified as a consequence of a postulated explosion).

**TABLE 3.1.1****LOAD COMBINATIONS SIGNIFICANT TO HI-STORM 100 OVERPACK  
KINEMATIC STABILITY ANALYSIS**

<b>Loading Case</b>	<b>Combinations<sup>†</sup></b>	<b>Comment</b>	<b>Analysis of this Load Case Presented in:</b>
A	D + F	This case establishes flood water flow velocity with a minimum safety factor of 1.1 against overturning and sliding.	Subsection 3.4.6
B	D + M + W'	Demonstrate that the HI-STORM 100 Overpack with minimum SNF stored (minimum D) will not tip over.	Subsection 3.4.8
C	D + E	Establish the value of ZPA <sup>††</sup> that will not cause the overpack to tip over.	Subsection 3.4.7

---

<sup>†</sup> Loading symbols are defined in Table 2.2.13

<sup>††</sup> ZPA is zero period acceleration

---

HOLTEC INTERNATIONAL COPYRIGHTED MATERIAL

**TABLE 3.1.2**

**DESIGN BASIS DECELERATIONS FOR THE DROP EVENTS**

<b>Case</b>	<b>Value<sup>†</sup> (in multiples of acceleration due to gravity)</b>
Vertical axis drop (HI-STORM 100 Overpack only)	45
Horizontal axis (side) drop (HI-TRAC only)	45

---

<sup>†</sup> The design basis value is set from the requirements of the HI-STORM 100 System, as its components are operated as a storage system. The MPC is designed to higher loadings (60g's vertical and horizontal) when in a HI-STAR 100 overpack. Analysis of the MPC in a HI-STAR 100 overpack under a 60g loading is provided in HI-STAR 100 Docket Numbers 71-9261 and 72-1008.

**TABLE 3.1.3**

**LOADING CASES FOR THE FUEL BASKET**

Load Case I.D.	Loading <sup>†</sup>	Notes	Location Where this Case is Evaluated
F1	T, T'	Demonstrate that the most adverse of the temperature distributions in the basket will not cause fuel basket to expand and contact the enclosure vessel wall. Compute the secondary stress intensity and show that it is small.	Subsection 3.4.4.2
F2 (Note 1)	D + H	Conservatively add the stresses in the basket due to vertical and horizontal orientation handling to form a bounding stress intensity.	Table 3.4.9 of HI-STAR FSAR (Docket 72-1008)
F3 F3.a (Note 2)	D + H'	Vertical axis drop event	HI-STAR FSAR, Subsection 3.4.4.3.1.3
F3.b (Note 3)	D + H'	Side Drop, 0 degree orientation (Figure 3.1.2)	Table 3.4.6
F3.c (Note 3)	D + H'	Side Drop, 45 degree orientation (Figure 3.1.3)	Table 3.4.6

**Notes:**

1. Load Case F2 for the HI-STORM 100 System is identical to Load Case F2 for the HI-STAR 100 System in Docket Number 72-1008, Table 3.1.3.
2. Load Case F3.a is bounded by the 60g deceleration analysis performed for the HI-STAR 100 System in Docket Number 72-1008, Subsection 3.4.4.3.1.3. The HI-STORM 100 vertical deceleration loading is limited to 45g.
3. Load Cases F3.b and F3.c are analyzed here for a 45g deceleration, while the MPC is housed within a HI-STORM 100 Overpack or a HI-TRAC transfer cask. The initial clearance at the interface between the MPC shell and the HI-STORM 100 Overpack or HI-TRAC transfer cask is greater than or equal to the initial clearance between the MPC shell and the HI-STAR 100 overpack. This difference in clearance directly affects the stress field. The side drop analysis for the MPC in the HI-STAR 100 overpack under 60g's bounds the corresponding analysis of the MPC in HI-TRAC for 45 g's.

<sup>†</sup> The symbols used for the loadings are defined in Table 2.2.13.

**TABLE 3.1.4**

**LOADING CASES FOR THE ENCLOSURE VESSEL (CONFINEMENT BOUNDARY)**

Load Case I.D.	Load Combination <sup>†</sup>	Notes	Comments and Location Where this Case is Analyzed		
E1 (Note 1)					
E1.a	Design internal pressure, $P_i$	Primary stress intensity limits in the shell, baseplate, and closure ring	E1.a	Lid Baseplate Shell Supports	Docket 72-1008 3.E.8.1.1 Docket 72-1008 3.1.8.1 3.4.4.3.1.2 N/A
E1.b	Design external pressure, $P_o$	Primary stress intensity limits, buckling stability	E1.b	Lid Baseplate Shell  Supports	$P_i$ bounds $P_i$ bounds Docket 72-1008 Buckling methodology in 3.H N/A
E1.c	Design internal pressure, $P_i$ , Plus Temperature, T	Primary plus secondary stress intensity under Level A condition	E1.c	Lid, Baseplate, and Shell	Section 3.4.4.3.1.2
E2	$D + H + (P_i, P_o)^{\dagger\dagger}$	Vertical lift, internal operating pressure conservatively assumed to be equal to the normal design pressure. Principal area of concern is the lid assembly.	Lid Baseplate Shell  Supports	Docket 72-1008 3.E.8.1.2 3.4.3.6 Docket 72-1008 Table 3.4.9 (stress) Docket 72-1008 Buckling methodology in 3.H Docket 72-1008 Table 3.4.9	

<sup>†</sup> The symbols used for the loadings are defined in Table 2.2.13.

<sup>††</sup> The notation  $(P_i, P_o)$  means that both cases are checked with either  $P_o$  or  $P_i$  applied.

**TABLE 3.1.4 (CONTINUED)**

**LOADING CASES FOR THE ENCLOSURE VESSEL (CONFINEMENT BOUNDARY)**

<b>Load Case I.D.</b>	<b>Load Combination<sup>†</sup></b>	<b>Notes</b>	<b>Comments and Location Where this Case is Analyzed</b>	
E3				
E3.a (Note 2)	$D + H' + (P_o, P_i)$	Vertical axis drop event	E3.a	Lid Baseplate Shell Supports Docket 72-10083.E.8.2.1-2 Docket 72-10083.I.8.3 Docket 72-1008 Buckling methodology in 3.H N/A
E3.b (Note 3)	$D + H' + (P_i, P_o)$	Side drop, 0 degree orientation (Figure 3.1.2)	E3.b	Lid Baseplate Shell Supports End drop bounds End drop bounds Table 3.4.6 Table 3.4.6
E3.c (Note 3)	$D + H' + (P_i, P_o)$	Side drop, 45 degree orientation (Figure 3.1.3)	E3.c	Lid Baseplate Shell Supports End drop bounds End drop bounds Table 3.4.6 Table 3.4.6
E4	T	Demonstrate that interference with the overpack will not develop for T.	Section 3.4.4.2	

<sup>†</sup> The symbols used for the loadings are defined in Table 2.2.13.

**TABLE 3.1.4 (CONTINUED)**

**LOADING CASES FOR THE ENCLOSURE VESSEL (CONFINEMENT BOUNDARY)**

<b>Load Case I.D.</b>	<b>Load Combination<sup>†</sup></b>	<b>Notes</b>	<b>Comments and Location Where this Case is Analyzed</b>	
E5	$P_i^*$ or $P_o^* + D + T^*$	Demonstrate compliance with level D stress limits – buckling stability.	Lid	3.4.4.3.1.10
			Baseplate	3.4.4.3.1.10
			Shell	Docket 72-1008 Buckling methodology in 3.H
				3.4.4.3.1.2 (stress)
			Supports	N/A

Notes:

1. Load Cases E1.a, E1.b, and E2 are identical to the load cases presented in Docket Number 72-1008, Table 3.1.4. Design pressures and MPC weights are identical.
2. Load Case E3.a is bounded by the 60g deceleration analysis performed for the HI-STAR 100 System in Docket Number 72-1008. The HI-STORM 100 vertical deceleration loading is limited to 45g.
3. Load Cases E3.b and E3.c are analyzed in this HI-STORM 100 SAR for a 45g deceleration, while the MPC is housed within the HI-STORM 100 storage overpack. The interface between the MPC shell and storage overpack is not identical to the MPC shell and HI-STAR 100 overpack. The analysis for an MPC housed in HI-TRAC is not performed since results are bounded by those reported in the HI-STAR 100 TSAR for a 60g deceleration.

<sup>†</sup> The symbols used for the loadings are defined in Table 2.2.13.



**TABLE 3.1.5**

**LOAD CASES FOR THE HI-STORM 100 OVERPACK/HI-TRAC TRANSFER CASK**

Load Case I.D.	Loading <sup>†</sup>	Notes	Location in FSAR
01	D + H + T + (P <sub>o</sub> , P <sub>i</sub> )	Vertical load handling of HI-STORM 100 Overpack/HI-TRAC.	Overpack 3.4.3.5  HI-TRAC Shell 3.4.3.3, 3.4.3.4 Pool lid 3.4.3.8 Transfer lid 3.4.3.9
02			
02.a	D + H' + (P <sub>o</sub> , P <sub>i</sub> )	Storage Overpack: End drop; primary stress intensities must meet level D stress limits.	Overpack 3.4.4.3.2.3
02.b	D + H' + (P <sub>o</sub> , P <sub>i</sub> )	HI-TRAC: Horizontal (side) drop; meet level D stress limits for NF Class 3 components away from the impacted zone; show lids stay in-place. Show primary and secondary impact decelerations are within design basis. (This case is only applicable to HI-TRAC.)	HI-TRAC Shell 3.4.9.1 Transfer Lid 3.4.4.3.3.3 Slapdown 3.4.9.2
02.c	D + H'	Storage Overpack: Tip-over; any permanent deformations must not preclude ready retrieval of the MPC.	Overpack 3.4.10, 3.A

<sup>†</sup> The symbols used for the loadings are defined in Table 2.2.13

**TABLE 3.1.5 (CONTINUED)**

**LOAD CASES FOR THE HI-STORM 100 OVERPACK/HI-TRAC TRANSFER CASK**

<b>Load Case I.D.</b>	<b>Loading<sup>†</sup></b>	<b>Notes</b>	<b>Location in FSAR</b>
03	D (water jacket)	Satisfy primary membrane plus bending stress limits for water jacket (This case is only applicable to HI-TRAC).	3.4.4.3.3.4
04	M (penetrant missiles)	Demonstrate that no thru-wall breach of the HI-STORM overpack or HI-TRAC transfer cask occurs, and the primary stress levels are not exceeded. Small and intermediate missiles are examined for HI-STORM and HI-TRAC. Large missile penetration is also examined for HI-TRAC.	Overpack 3.4.8.1 HI-TRAC 3.4.8.2.1, 3.4.8.2.2
05	P <sub>o</sub>	Explosion: must not produce buckling or exceed primary stress levels in the overpack structure.	3.4.4.5.2, 3.4.7.2

**Notes:**

- Under each of these load cases, different regions of the structure are analyzed to demonstrate compliance.

---

<sup>†</sup> The symbols used for the loadings are defined in Table 2.2.13

**TABLE 3.1.6**

**DESIGN, LEVELS A AND B: STRESS INTENSITY**

**Code:** ASME NB  
**Material:** SA203-E  
**Service Conditions:** Design, Levels A and B  
**Item:** Stress Intensity

Temp. (Deg. F)	Classification and Value (ksi)					
	$S_m$	$P_m^{\dagger}$	$P_L^{\dagger}$	$P_L + P_b^{\dagger}$	$P_L + P_b + Q^{\dagger\dagger}$	$P_e^{\dagger\dagger}$
-20 to 100	23.3	23.3	35.0	35.0	69.9	69.9
200	23.3	23.3	35.0	35.0	69.9	69.9
300	23.3	23.3	35.0	35.0	69.9	69.9
400	22.9	22.9	34.4	34.4	68.7	68.7
500	21.6	21.6	32.4	32.4	64.8	64.8

**Definitions:**

$S_m$  = Stress intensity values per ASME Code  
 $P_m$  = Primary membrane stress intensity  
 $P_L$  = Local membrane stress intensity  
 $P_b$  = Primary bending stress intensity  
 $P_e$  = Expansion stress  
 $Q$  = Secondary stress  
 $P_L + P_b$  = Either primary or local membrane plus primary bending

Definitions for Table 3.1.6 apply to all following tables unless modified.

**Notes:**

1. Limits on values are presented in Table 2.2.10.

$\dagger$  Evaluation required for Design condition only.  
 $\dagger\dagger$  Evaluation required for Levels A and B only.  $P_e$  not applicable to vessels.

**TABLE 3.1.7****LEVEL D: STRESS INTENSITY**

**Code:** ASME NB  
**Material:** SA203-E  
**Service Condition:** Level D  
**Item:** Stress Intensity

Temp. (Deg. F)	Classification and Value (ksi)		
	$P_m$	$P_L$	$P_L + P_b$
-20 to 100	49.0	70.0	70.0
200	49.0	70.0	70.0
300	49.0	70.0	70.0
400	48.2	68.8	68.8
500	45.4	64.9	64.9

**Notes:**

1. Level D allowables per NB-3225 and Appendix F, Paragraph F-1331.
2. Average primary shear stress across a section loaded in pure shear may not exceed  $0.42 S_u$ .
3. Limits on values are presented in Table 2.2.10.
4.  $P_m$ ,  $P_L$ , and  $P_b$  are defined in Table 3.1.6.

**TABLE 3.1.8**

**DESIGN, LEVELS A AND B: STRESS INTENSITY**

**Code:** ASME NB  
**Material:** SA350-LF3  
**Service Conditions:** Design, Levels A and B  
**Item:** Stress Intensity

Temp. (Deg. F)	Classification and Value (ksi)					
	$S_m$	$P_m^\dagger$	$P_L^\dagger$	$P_L + P_b^\dagger$	$P_L + P_b + Q^{\dagger\dagger}$	$P_e^{\dagger\dagger}$
-20 to 100	23.3	23.3	35.0	35.0	69.9	69.9
200	22.8	22.8	34.2	34.2	68.4	68.4
300	22.2	22.2	33.3	33.3	66.6	66.6
400	21.5	21.5	32.3	32.3	64.5	64.5
500	20.2	20.2	30.3	30.3	60.6	60.6
600	18.5	18.5	27.75	27.75	55.5	55.5
700	16.8	16.8	25.2	25.2	50.4	50.4

Notes:

1. Source for  $S_m$  is ASME Code
2. Limits on values are presented in Table 2.2.10.
3.  $S_m$ ,  $P_m$ ,  $P_L$ ,  $P_b$ ,  $Q$ , and  $P_e$  are defined in Table 3.1.6.

$^\dagger$  Evaluation required for Design condition only.

$^{\dagger\dagger}$  Evaluation required for Levels A and B conditions only.  $P_e$  not applicable to vessels.

HOLTEC INTERNATIONAL COPYRIGHTED MATERIAL

**TABLE 3.1.9****LEVEL D, STRESS INTENSITY**

**Code:** ASME NB  
**Material:** SA350-LF3  
**Service Conditions:** Level D  
**Item:** Stress Intensity

Temp. (Deg. F)	Classification and Value (ksi)		
	P <sub>m</sub>	P <sub>L</sub>	P <sub>L</sub> + P <sub>b</sub>
-20 to 100	49.0	70.0	70.0
200	48.0	68.5	68.5
300	46.7	66.7	66.7
400	45.2	64.6	64.6
500	42.5	60.7	60.7
600	38.9	58.4	58.4
700	35.3	53.1	53.1

**Notes:**

1. Level D allowables per NB-3225 and Appendix F, Paragraph F-1331.
2. Average primary shear stress across a section loaded in pure shear may not exceed 0.42 S<sub>u</sub>.
3. Limits on values are presented in Table 2.2.10.
4. P<sub>m</sub>, P<sub>L</sub>, and P<sub>b</sub> are defined in Table 3.1.6.

**TABLE 3.1.10**

**DESIGN AND LEVEL A: STRESS**

**Code:** ASME NF  
**Material:** SA516, Grade 70, SA350-LF3, SA203-E  
**Service Conditions:** Design and Level A  
**Item:** Stress

Temp. (Deg. F)	Classification and Value (ksi)		
	S	Membrane Stress	Membrane plus Bending Stress
-20 to 650	17.5	17.5	26.3
700	16.6	16.6	24.9

**Notes:**

1. S = Maximum allowable stress values from Table 1A of ASME Code, Section II, Part D.
2. Stress classification per Paragraph NF-3260.
3. Limits on values are presented in Table 2.2.12.

**TABLE 3.1.11**

**LEVEL B: STRESS**

**Code:** ASME NF  
**Material:** SA516, Grade 70, SA350-LF3, and SA203-E  
**Service Conditions:** Level B  
**Item:** Stress

Temp. (Deg. F)	Classification and Value (ksi)	
	Membrane Stress	Membrane plus Bending Stress
-20 to 650	23.3	34.9
700	22.1	33.1

**Notes:**

1. Limits on values are presented in Table 2.2.12 with allowables from Table 3.1.10.



**TABLE 3.1.12****LEVEL D: STRESS INTENSITY**

**Code:** ASME NF  
**Material:** SA516, Grade 70  
**Service Conditions:** Level D  
**Item:** Stress Intensity

<b>Temp. (Deg. F)</b>	<b>Classification and Value (ksi)</b>		
	<b>S<sub>m</sub></b>	<b>P<sub>m</sub></b>	<b>P<sub>m</sub> + P<sub>b</sub></b>
-20 to 100	23.3	45.6	68.4
200	23.1	41.5	62.3
300	22.5	40.4	60.6
400	21.7	39.1	58.7
500	20.5	36.8	55.3
600	18.7	33.7	50.6
650	18.4	33.1	49.7
700	18.3	32.9	49.3

**Notes:**

1. Level D allowable stress intensities per Appendix F, Paragraph F-1332.
2. S<sub>m</sub> = Stress intensity values per Table 2A of ASME, Section II, Part D.
3. Limits on values are presented in Table 2.2.12.
4. P<sub>m</sub> and P<sub>b</sub> are defined in Table 3.1.6.

**TABLE 3.1.13**

**DESIGN, LEVELS A AND B: STRESS INTENSITY**

**Code:** ASME NB  
**Material:** Alloy X  
**Service Conditions:** Design, Levels A and B  
**Item:** Stress Intensity

Temp. (Deg. F)	Classification and Numerical Value					
	$S_m$	$P_m^\dagger$	$P_L^\dagger$	$P_L + P_b^\dagger$	$P_L + P_b + Q^{\dagger\dagger}$	$P_e^{\dagger\dagger}$
-20 to 100	20.0	20.0	30.0	30.0	60.0	60.0
200	20.0	20.0	30.0	30.0	60.0	60.0
300	20.0	20.0	30.0	30.0	60.0	60.0
400	18.7	18.7	28.1	28.1	56.1	56.1
500	17.5	17.5	26.3	26.3	52.5	52.5
600	16.4	16.4	24.6	24.6	49.2	49.2
650	16.0	16.0	24.0	24.0	48.0	48.0
700	15.6	15.6	23.4	23.4	46.8	46.8
750	15.2	15.2	22.8	22.8	45.6	45.6
800	14.9	14.9	22.4	22.4	44.7	44.7

**Notes:**

1.  $S_m$  = Stress intensity values per Table 2A of ASME II, Part D.
2. Alloy X  $S_m$  values are the lowest values for each of the candidate materials at temperature.
3. Stress classification per NB-3220.
4. Limits on values are presented in Table 2.2.10.
5.  $P_m$ ,  $P_L$ ,  $P_b$ ,  $Q$ , and  $P_e$  are defined in Table 3.1.6.

$^\dagger$  Evaluation required for Design condition only.

$^{\dagger\dagger}$  Evaluation required for Levels A, B conditions only.  $P_e$  not applicable to vessels.

HOLTEC INTERNATIONAL COPYRIGHTED MATERIAL

HI-STORM FSAR

HI-STORM 100 FSAR, NON-PROPRIETARY  
 REPORT PH-2002-444  
 REVISION 12  
 MARCH 12, 2014

3.1-37

Rev. 11

**TABLE 3.1.14****LEVEL D: STRESS INTENSITY**

**Code:** ASME NB  
**Material:** Alloy X  
**Service Conditions:** Level D  
**Item:** Stress Intensity

Temp. (Deg. F)	Classification and Value (ksi)		
	$P_m$	$P_L$	$P_L + P_b$
-20 to 100	48.0	72.0	72.0
200	48.0	72.0	72.0
300	46.2	69.3	69.3
400	44.9	67.4	67.4
500	42.0	63.0	63.0
600	39.4	59.1	59.1
650	38.4	57.6	57.6
700	37.4	56.1	56.1
750	36.5	54.8	54.8
800	35.8	53.7	53.7

**Notes:**

1. Level D stress intensities per ASME NB-3225 and Appendix F, Paragraph F-1331.
2. The average primary shear strength across a section loaded in pure shear may not exceed 0.42  $S_u$ .
3. Limits on values are presented in Table 2.2.10.
4.  $P_m$ ,  $P_L$ , and  $P_b$  are defined in Table 3.1.6.

**TABLE 3.1.15****DESIGN, LEVELS A AND B: STRESS INTENSITY**

**Code:** ASME NG  
**Material:** Alloy X  
**Service Conditions:** Design, Levels A and B  
**Item:** Stress Intensity

Temp. (Deg. F)	Classification and Value (ksi)				
	$S_m$	$P_m$	$P_m + P_b$	$P_m + P_b + Q$	$P_e$
-20 to 100	20.0	20.0	30.0	60.0	60.0
200	20.0	20.0	30.0	60.0	60.0
300	20.0	20.0	30.0	60.0	60.0
400	18.7	18.7	28.1	56.1	56.1
500	17.5	17.5	26.3	52.5	52.5
600	16.4	16.4	24.6	49.2	49.2
650	16.0	16.0	24.0	48.0	48.0
700	15.6	15.6	23.4	46.8	46.8
750	15.2	15.2	22.8	45.6	45.6
800	14.9	14.9	22.4	44.7	44.7

**Notes:**

1.  $S_m$  = Stress intensity values per Table 2A of ASME, Section II, Part D.
2. Alloy X  $S_m$  values are the lowest values for each of the candidate materials at temperature.
3. Classifications per NG-3220.
4. Limits on values are presented in Table 2.2.11.
5.  $P_m$ ,  $P_b$ ,  $Q$ , and  $P_e$  are defined in Table 3.1.6.

**TABLE 3.1.16****LEVEL D: STRESS INTENSITY**

**Code:** ASME NG  
**Material:** Alloy X  
**Service Conditions:** Level D  
**Item:** Stress Intensity

Temp. (Deg. F)	Classification and Value (ksi)		
	P <sub>m</sub>	P <sub>L</sub>	P <sub>L</sub> + P <sub>b</sub>
-20 to 100	48.0	72.0	72.0
200	48.0	72.0	72.0
300	46.2	69.3	69.3
400	44.9	67.4	67.4
500	42.0	63.0	63.0
600	39.4	59.1	59.1
650	38.4	57.6	57.6
700	37.4	56.1	56.1
750	36.5	54.8	54.8
800	35.8	53.7	53.7

**Notes:**

1. Level D stress intensities per ASME NG-3225 and Appendix F, Paragraph F-1331.
2. The average primary shear strength across a section loaded in pure shear may not exceed 0.42 S<sub>u</sub>.
3. Limits on values are presented in Table 2.2.11.
4. P<sub>m</sub>, P<sub>L</sub>, and P<sub>b</sub> are defined in Table 3.1.6.

**TABLE 3.1.17**

**REFERENCE TEMPERATURES AND STRESS LIMITS  
FOR THE VARIOUS LOAD CASES**

Load Case I.D.	Material	Reference Temperature <sup>†</sup> , ° F	Stress Intensity Allowables, ksi		
			P <sub>m</sub>	P <sub>L</sub> + P <sub>b</sub>	P <sub>L</sub> + P <sub>b</sub> + Q
F1	Alloy X	725	15.4	23.1	46.2
F2	Alloy X	725	15.4	23.1	46.2
F3	Alloy X	725	36.9	55.4	NL
E1	Alloy X	500	17.5	26.3	52.5
E2	Alloy X	500	17.5	26.3	52.5
E3	Alloy X	500	42.0	63.0	NL <sup>††</sup>
E4	Alloy X	500	17.5	26.3	52.5
E5	Alloy X	775	36.15	54.25	NL

**Notes:**

1. Q, P<sub>m</sub>, P<sub>L</sub>, and P<sub>b</sub> are defined in Table 3.1.6.
2. Reference temperatures for Load Cases E1-E4 are for MPC shell; for MPC lid and MPC baseplate, reference temperatures are 550 deg. F and 400 deg. F, respectively (per Table 2.2.3) and stress intensity allowables should be adjusted accordingly.

<sup>†</sup> Values for reference temperatures are chosen to bound the thermal results in Chapter 4. Lower temperature values may be used provided that they are at least equal to the calculated temperature for the specific component and location or otherwise justified.

<sup>††</sup> NL: No specified limit in the Code

HOLTEC INTERNATIONAL COPYRIGHTED MATERIAL

**TABLE 3.1.17 (CONTINUED)**

**REFERENCE TEMPERATURES AND STRESS LIMITS FOR THE VARIOUS LOAD CASES**

Load Case I.D.	Material	Reference Temperature, <sup>†,††</sup> ° F	Stress Intensity Allowables, ksi		
			P <sub>m</sub>	P <sub>L</sub> + P <sub>b</sub>	P <sub>L</sub> + P <sub>b</sub> + Q
O1	SA203-E	400	17.5	26.3	NL <sup>†††</sup>
	SA350-LF3	400	17.5	26.3	NL
	SA516 Gr. 70 SA515 Gr. 70	400	17.5	26.3	NL
O2	SA203-E	400	41.2	61.7	NL
	SA350-LF3	400	38.6	58.0	NL
	SA516 Gr. 70 SA515 Gr. 70	400	39.1	58.7	NL
O3	SA203-E	400	17.5	26.3	NL
	SA350-LF3	400	17.5	26.3	NL
	SA516 Gr. 70 SA515 Gr. 70	400	17.5	26.3	NL
O4	SA203-E	400	41.2	61.7	NL
	SA350-LF3	400	38.6	58.0	NL
	SA516 Gr. 70 SA515 Gr. 70	400	39.1	58.7	NL

Note:

1. P<sub>m</sub>, P<sub>L</sub>, P<sub>b</sub>, and Q are defined in Table 3.1.6.
2. Load Cases O1 and O3 are for Normal Conditions; therefore the values listed refer to allowable stress, not allowable stress intensity

<sup>†</sup> Values for reference temperatures are chosen to bound the thermal results in Chapter 4. Lower temperature values may be used provided that they are at least equal to the calculated temperature for the specific component and location or otherwise justified.

<sup>††</sup> For storage fire analysis, temperatures are defined by thermal solution

<sup>†††</sup> NL: No specified limit in the Code

HOLTEC INTERNATIONAL COPYRIGHTED MATERIAL

**TABLE 3.1.18  
FRACTURE TOUGHNESS TEST REQUIREMENTS**

<b>Material</b>	<b>Test Requirement</b>	<b>Test Temperature</b>	<b>Acceptance Criterion</b>
Bolting (SA193 B7)	Not required (per NF-2311(b)(13) and Note (e) to Figure NF-2311(b)-1)	-	-
Ferritic steel with nominal section thickness of 5/8" or less	Not required per NF-2311(b)(1)	-	-
SA36 (thickness greater than 5/8")	Not required per NF-2311(b)(7)	-	-
Normalized SA516 Gr. 70 (thickness greater than 5/8", but less than or equal to 2-1/2"), except when used for HI-STORM 100A baseplate, lug support ring, and gussets	Not required per NF-2311(b)(7), NF-2311(b)(13), and curve D in Figure NF-2311(b)-1	-	-
HI-STORM 100A baseplate, lug support ring, and gussets (See Note 2)	Per NF-2331	See Note 1. (Also must meet ASME Section IIA requirements)	Table NF-2331(a)-3 or Figure NF-2331(a)-2 (Also must meet ASME Section IIA requirements)
As-rolled SA516 Gr. 70, except when used for HI-STORM inner and outer shells, top plate, lid shear ring, lid shield ring, lid outer ring (for 100S Version B), and lid cover plate (for 100S Version B)	Per NF-2331	See Note 1. (Also must meet ASME Section IIA requirements)	Table NF-2331(a)-3 or Figure NF-2331(a)-2 (Also must meet ASME Section IIA requirements)
As-rolled SA516 Gr. 70 used for HI-STORM inner and outer shells, top plate, lid shear ring, lid shield ring, lid outer ring (for 100S Version B), and lid cover plate (for 100S Version B) and Base- Bottom Plate (for 100S Version B)	Not required per NF-2311(b)(7)	-	-
SA203, SA515 Gr. 70, SA350-LF2, SA350-LF3 (thickness greater than	Per NF-2331	See Note 1. (Also must meet ASME Section IIA requirements)	Table NF-2331(a)-3 or Figure NF-2331(a)-2

HOLTEC INTERNATIONAL COPYRIGHTED MATERIAL



5/8")			(Also must meet ASME Section IIA requirements)
Weld material	Test per NF-2430 if: 1) either of the base materials of the production weld requires impact testing, or; 2) either of the base materials is SA516 Gr. 70 with nominal section thickness greater than 5/8".	See Note 1	Per NF-2330

Notes:

1. Required NDT temperature = -40 deg. F for all materials in the HI-STORM 100 Overpack, -40 deg. F for HI-TRAC "STH" materials, and 0 deg. F for HI-TRAC "NF" materials.
2. In accordance with ASME Code Subsection NF, impact testing is not required for these components; specified testing is performed strictly for defense-in-depth.

**TABLE 3.1.19**

**DESIGN AND LEVEL A: STRESS**

**Code:** ASME NF  
**Material:** SA36  
**Service Conditions:** Design and Level A  
**Item:** Stress

<b>Temp. (Deg. F)</b>	<b>Classification and Value (ksi)</b>		
	<b>S</b>	<b>Membrane Stress</b>	<b>Membrane plus Bending Stress</b>
-20 to 650	14.5	14.5	21.8
700	13.9	13.9	20.9

**Notes:**

1. S = Maximum allowable stress values from Table 1A of ASME Code, Section II, Part D.
2. Stress classification per Paragraph NF-3260.
3. Limits on values are presented in Table 2.2.12.

**TABLE 3.1.20**

**LEVEL B: STRESS**

**Code:** ASME NF  
**Material:** SA36  
**Service Conditions:** Level B  
**Item:** Stress

<b>Temp. (Deg. F)</b>	<b>Classification and Value (ksi)</b>	
	<b>Membrane Stress</b>	<b>Membrane plus Bending Stress</b>
-20 to 650	19.3	28.9
700	18.5	27.7

**Notes:**

1. Limits on values are presented in Table 2.2.12 with allowables from Table 3.1.19.

**TABLE 3.1.21****LEVEL D: STRESS INTENSITY**

**Code:** ASME NF  
**Material:** SA36  
**Service Conditions:** Level D  
**Item:** Stress Intensity

Temp. (Deg. F)	Classification and Value (ksi)		
	$S_m$	$P_m$	$P_m + P_b$
-20 to 100	19.3	43.2	64.8
200	19.3	37.0	55.5
300	19.3	36.0	54.0
400	19.3	34.7	52.1
500	19.3	32.8	49.2
600	17.7	30.0	45.0
650	17.4	29.5	44.3
700	17.3	29.2	43.8

**Notes:**

1. Level D allowable stress intensities per Appendix F, Paragraph F-1332.
2.  $S_m$  = Stress intensity values per Table 2A of ASME, Section II, Part D.
3. Limits on values are presented in Table 2.2.12.
4.  $P_m$  and  $P_b$  are defined in Table 3.1.6.

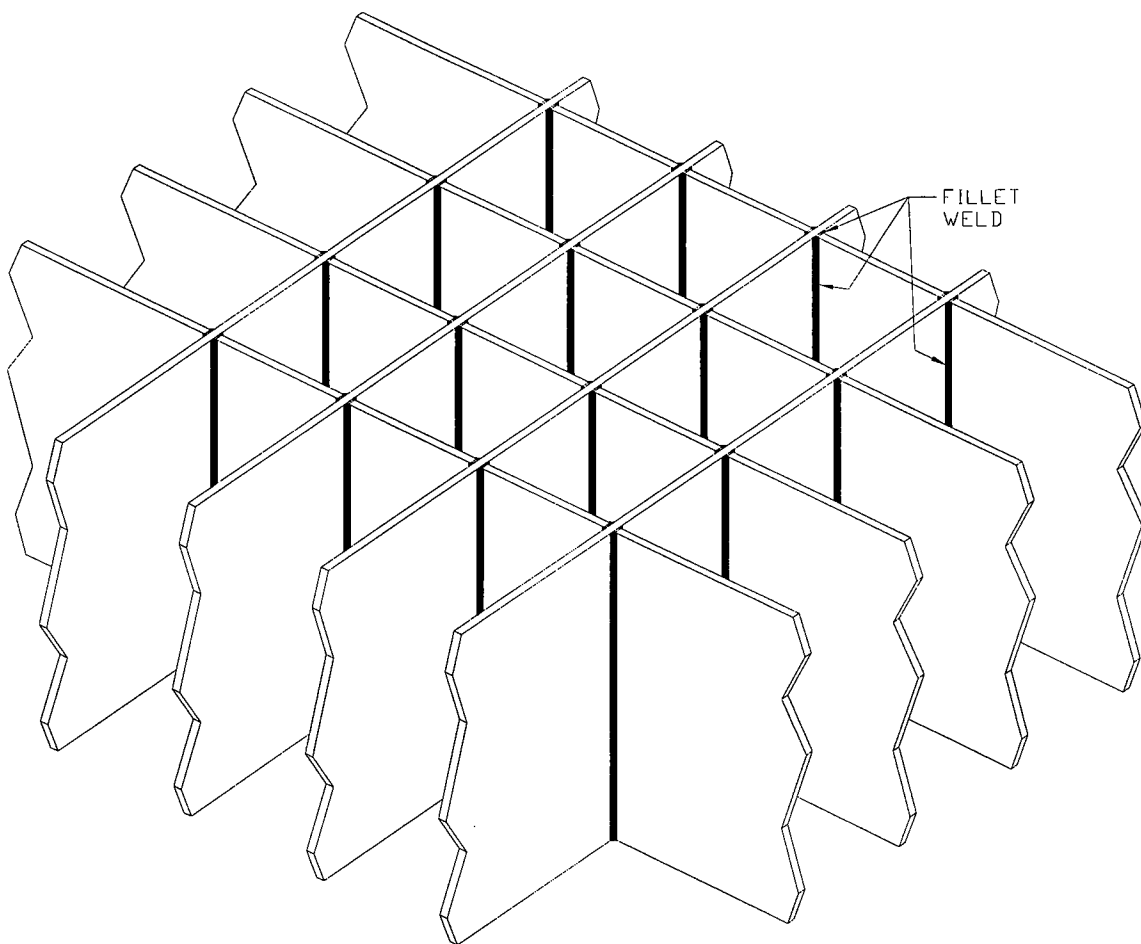
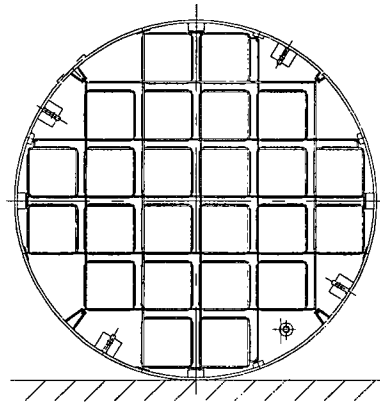
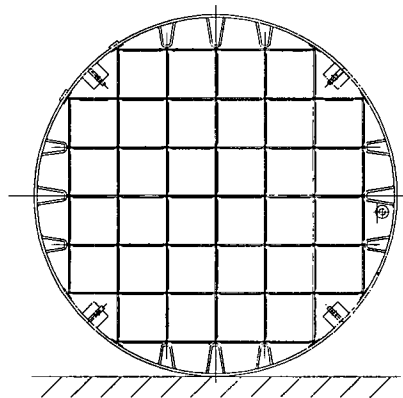


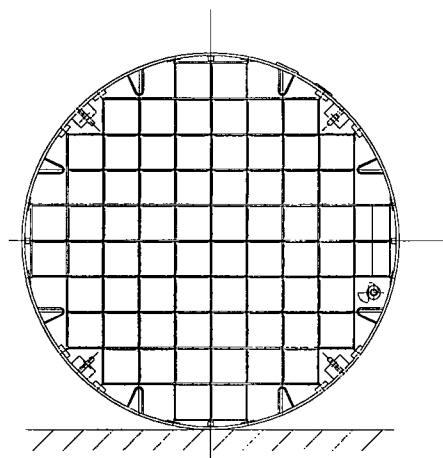
FIGURE 3.1.1; MPC-68 AND MPC-32 FUEL BASKET GEOMETRY



MPC-24



MPC-32



MPC-68

*FIGURE 3.1.2; 0° DROP ORIENTATIONS FOR THE MPCs*

REPORT HI-2002444

REV. 1

G:\SAR DOCUMENTS\HI-STORM FSAR\FIGURES\UFSAR-REV-1\CHP 3\3.1.2

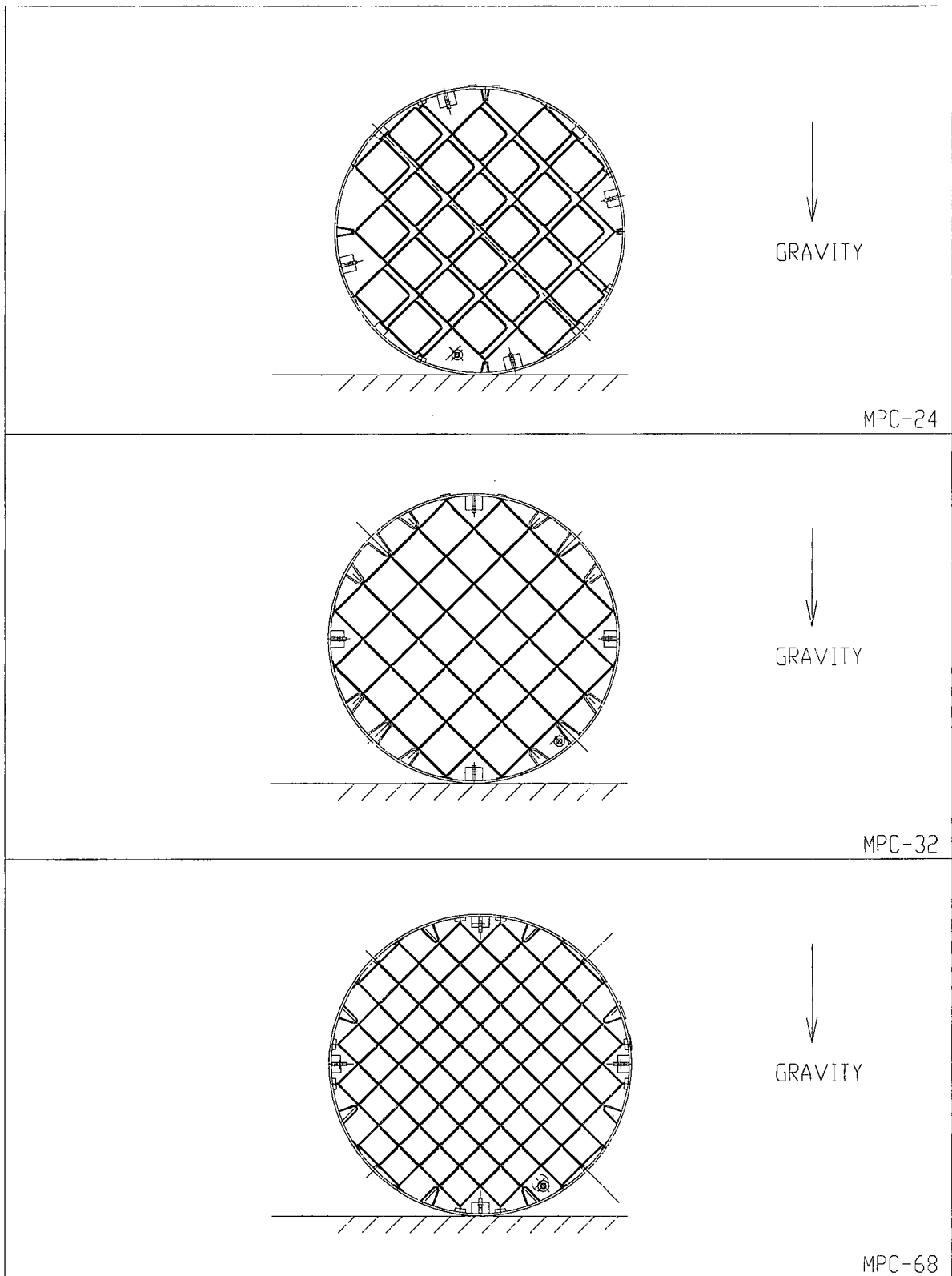


FIGURE 3.1.3; 45° DROP ORIENTATIONS FOR THE MPCs

REPORT HI-2002444

REV. 1

G:\SAR DOCUMENTS\HI-STORM FSAR\FIGURES\UFAR-REV-1\CHP 3\3.1.3

Tables 3.2.1 and 3.2.2 provide the calculated weights of the individual HI-STORM 100 components as well as the total system weights. The actual weights will vary within a narrow range of the calculated values due to the tolerances in metal manufacturing and fabrication permitted by the ASME Codes. Contained water mass during fuel loading is not included in this table.

The locations of the calculated centers of gravity (CGs) are presented in Table 3.2.3. All centers of gravity are located on the cask centerline since the non-axisymmetric effects of the cask system plus contents are negligible.

Table 3.2.4 provides the lift weight when the HI-TRAC transfer cask with the heaviest fully loaded MPC is being lifted from the fuel pool. The effect of buoyancy is neglected, and the weight of rigging is set at a conservative value.

In all weight tables, bounding values are also listed where necessary for use in structural calculations where their use will provide a conservative result.



**TABLE 3.2.1**  
**HI-STORM OVERPACK WEIGHT DATA**

<b>Item</b>	<b>Bounding Weight (lb)</b>
<b>MPC-24</b>	
• Without SNF	42,000
• Fully loaded with SNF and Fuel Spacers	90,000 <sup>†††</sup>
<b>MPC-32</b>	
• Without SNF	36,000
• Fully loaded with SNF and Fuel Spacers	90,000 <sup>†††</sup>
<b>MPC-68/68F/68FF</b>	
• Without SNF	39,000
• Fully loaded with SNF and Fuel Spacers	90,000 <sup>†††</sup>
<b>MPC-24E/EF</b>	
• Without SNF	45,000
• Fully loaded with SNF and Fuel Spacers	90,000 <sup>†††</sup>
<b>HI-STORM 100 Overpack<sup>†</sup></b>	
• Overpack top lid	23,000
• Overpack w/ lid (empty)	270,000
• Overpack w/ fully loaded MPC-24	360,000
• Overpack w/ fully loaded MPC-32	360,000
• Overpack w/ fully loaded MPC-68/68F/68FF	360,000
• Overpack w/ fully loaded MPC-24E/EF	360,000
<b>HI-STORM 100S(232) Overpack<sup>†</sup></b>	
• Overpack top lid	25,500 <sup>††</sup>
• Overpack w/ lid (empty)	270,000
• Overpack w/ fully loaded MPC-24	360,000
• Overpack w/ fully loaded MPC-32	360,000
• Overpack w/ fully loaded MPC-68/68F/68FF	360,000
• Overpack w/ fully loaded MPC-24E/EF	360,000

**TABLE 3.2.1 (CONTINUED)**  
**HI-STORM OVERPACK WEIGHT DATA**

<b>Item</b>	<b>Bounding Weight (lb)</b>
<b>HI-STORM 100S(243) Overpack<sup>†</sup></b>	
• Overpack top lid	25,500 <sup>††</sup>
• Overpack w/ lid (empty)	270,000
• Overpack w/ fully loaded MPC-24	360,000
• Overpack w/ fully loaded MPC-32	360,000
• Overpack w/ fully loaded MPC-68/68F/68FF	360,000
• Overpack w/ fully loaded MPC-24E/EF	360,000
<b>HI-STORM 100A Overpack<sup>†</sup></b>	Same as above
<b>HI-STORM 100S Version B(218) Overpack (values in parentheses use high density concrete in overpack body)</b>	
• Overpack top lid	29,000
• Overpack w/ lid (empty)	270,000 (305,000)
• Overpack w/ fully loaded MPC-24	360,000 (395,000)
• Overpack w/ fully loaded MPC-32	360,000 (395,000)
• Overpack w/ fully loaded MPC-68/68F/68FF	360,000 (395,000)
• Overpack w/ fully loaded MPC-24E/EF	360,000 (395,000)
<b>HI-STORM 100S Version B(229) Overpack (values in parentheses use high density concrete in overpack body)</b>	
• Overpack top lid	29,000
• Overpack w/ lid (empty)	270,000 (320,000)
• Overpack w/ fully loaded MPC-24	360,000 (410,000)
• Overpack w/ fully loaded MPC-32	360,000 (410,000)
• Overpack w/ fully loaded MPC-68/68F/68FF	360,000 (410,000)
• Overpack w/ fully loaded MPC-24E/EF	360,000 (410,000)

<sup>†</sup> The bounding weights for the HI-STORM 100S(232) and 100S(243) overpacks listed in the above table are based on a maximum concrete (dry) density of 160.8 pcf. For improved shielding effectiveness, higher density concrete (up to 200 pcf dry) can be poured in the radial cavity of each of the HI-STORM 100S overpacks. At 200 pcf, the bounding weights of an empty overpack and a fully loaded overpack increase to 320,000 lb and 410,000 lb, respectively. Higher density concrete cannot be used in the HI-STORM 100 or 100A overpacks.

<sup>††</sup> Based on a maximum concrete (dry) density of 155 pcf. For improved shielding effectiveness, higher density concrete (up to 200 pcf dry) can be poured in the HI-STORM 100S lids. At 200 pcf, the bounding weight of the lid increases to 28,000 lb.

<sup>†††</sup> Based on the following maximum fuel assembly weights (as applicable):  
1,680 lb per assembly (including non-fuel hardware) for PWR fuel that requires fuel spacers  
1,720 lb per assembly (including non-fuel hardware) for PWR fuel that does not require fuel spacers  
730 lb per assembly (including channels and DFCs) for BWR fuel

HOLTEC INTERNATIONAL COPYRIGHTED MATERIAL

HI-STORM FSAR

Report HI-2002444

HI-STORM 100 FSAR, NON-PROPRIETARY

REVISION 12

MARCH 12, 2014

3.2-3

Rev. 7

**TABLE 3.2.2**  
**HI-TRAC 125 TRANSFER CASK WEIGHT DATA**

<b>Item</b>	<b>Bounding Weight (lb)</b>
Top Lid	2,750
Pool Lid	12,500
Transfer Lid	24,500
HI-TRAC 125 w/ Top Lid and Pool Lid (water jacket filled)	143,500
HI-TRAC 125 w/ Top Lid and Transfer Lid (water jacket filled)	155,000
HI-TRAC 125 w/ Top Lid, Pool Lid, and fully loaded MPC-24 (water jacket filled)	226,000
HI-TRAC 125 w/ Top Lid, Pool Lid, and fully loaded MPC-32 (water jacket filled)	233,500
HI-TRAC 125 w/ Top Lid, Pool Lid, and fully loaded MPC-68/68F/68FF(water jacket filled)	231,000
HI-TRAC 125 w/ Top Lid, Pool Lid, and fully loaded MPC-24E/EF (water jacket filled)	229,000
HI-TRAC 125 w/ Top Lid, Transfer Lid, and fully loaded MPC-24 (water jacket filled)	237,500
HI-TRAC 125 w/ Top Lid, Transfer Lid, and fully loaded MPC-32 (water jacket filled)	245,000
HI-TRAC 125 w/ Top Lid, Transfer Lid, and fully loaded MPC-68/68F/68FF (water jacket filled)	242,500
HI-TRAC 125 w/ Top Lid, Transfer Lid, and fully loaded MPC-24E/EF (water jacket filled)	240,500

**TABLE 3.2.2 (CONTINUED)**  
**HI-TRAC 100 TRANSFER CASK WEIGHT DATA**

<b>Item</b>	<b>Bounding Weight (lb)</b>
Top Lid	1,500
Pool Lid	8,000
Transfer Lid	17,000
HI-TRAC 100 w/ Top Lid and Pool Lid (water jacket filled)	102,000
HI-TRAC 100 w/ Top Lid and Transfer Lid (water jacket filled)	111,000
HI-TRAC 100 w/ Top Lid, Pool Lid, and fully loaded MPC-24 (water jacket filled)	183,500
HI-TRAC 100 w/ Top Lid, Pool Lid, and fully loaded MPC-32 (water jacket filled)	191,000
HI-TRAC 100 w/ Top Lid, Pool Lid, and fully loaded MPC-68/68F/68FF (water jacket filled)	188,500
HI-TRAC 100 w/ Top Lid, Pool Lid, and fully loaded MPC-24E/EF (water jacket filled)	186,500
HI-TRAC 100 w/ Top Lid, Transfer Lid, and fully loaded MPC-24 (water jacket filled)	192,000
HI-TRAC 100 w/ Top Lid, Transfer Lid, and fully loaded MPC-32 (water jacket filled)	199,000
HI-TRAC 100 w/ Top Lid, Transfer Lid, and fully loaded MPC-68/68F/68FF (water jacket filled)	196,500
HI-TRAC 100 w/ Top Lid, Transfer Lid, and fully loaded MPC-24E/EF (water jacket filled)	194,500

**TABLE 3.2.2 (CONTINUED)**  
**HI-TRAC 125D TRANSFER CASK WEIGHT DATA**

<b>Item</b>	<b>Bounding Weight (lb)</b>
Top Lid	2,750
Pool Lid	12,500
HI-TRAC 125D w/ Top Lid and Pool Lid (water jacket filled)	146,000
HI-TRAC 125D w/ Top Lid, Pool Lid, and fully loaded MPC-24 (water jacket filled)	228,500
HI-TRAC 125D w/ Top Lid, Pool Lid, and fully loaded MPC-32 (water jacket filled)	236,000
HI-TRAC 125D w/ Top Lid, Pool Lid, and fully loaded MPC-68/68F/68FF (water jacket filled)	233,500
HI-TRAC 125D w/ Top Lid, Pool Lid, and fully loaded MPC-24E/EF (water jacket filled)	231,500

**TABLE 3.2.2 (CONTINUED)**  
**HI-TRAC 100D TRANSFER CASK WEIGHT DATA**

<b>Item</b>	<b>Bounding Weight (lb)</b>
Top Lid	1,500
Pool Lid	8,000
HI-TRAC 100D w/ Top Lid and Pool Lid (water jacket filled)	102,000
HI-TRAC 100D w/ Top Lid, Pool Lid, and fully loaded MPC-24 (water jacket filled)	183,500
HI-TRAC 100D w/ Top Lid, Pool Lid, and fully loaded MPC-32 (water jacket filled)	191,000
HI-TRAC 100D w/ Top Lid, Pool Lid, and fully loaded MPC-68/68F/68FF (water jacket filled)	188,500
HI-TRAC 100D w/ Top Lid, Pool Lid, and fully loaded MPC-24E/EF (water jacket filled)	186,500

**TABLE 3.2.3**  
**CENTERS OF GRAVITY OF HI-STORM SYSTEM CONFIGURATIONS**

<b>Component</b>	<b>Height of CG Above Datum<sup>†</sup> (in)</b>
MPC-24 (empty)	109.0
MPC-32 (empty)	113.2
MPC-68/68F/68FF (empty)	111.5
MPC-24E/EF (empty)	108.9
HI-STORM 100 Overpack (empty)	116.8
HI-STORM 100S(232) Overpack (empty)	111.7
HI-STORM 100S(243) Overpack (empty)	117.4
HI-STORM 100S Version B(218) Overpack (empty)(height using standard weight concrete bounds height calculated using high density concrete)	108.77(108.45)
HI-STORM 100S Version B(229) Overpack (empty)(height using standard weight concrete bounds height calculated using high density concrete)	114.27(113.94)
HI-STORM 100 Overpack w/ fully loaded MPC-24	118.8
HI-STORM 100 Overpack w/ fully loaded MPC-32	118.7
HI-STORM 100 Overpack w/ fully loaded MPC-68/68F/68FF	119.0
HI-STORM 100 Overpack w/ fully loaded MPC-24E/EF	119.2
HI-STORM 100S(232) Overpack w/ fully loaded MPC-24	113.8
HI-STORM 100S(232) Overpack w/ fully loaded MPC-32	113.7
HI-STORM 100S(232) Overpack w/ fully loaded MPC-68/68F/68FF	114.0
HI-STORM 100S(232) Overpack w/ fully loaded MPC-24E/EF	114.2
HI-STORM 100S(243) Overpack w/ fully loaded MPC-24	118.1
HI-STORM 100S(243) Overpack w/ fully loaded MPC-32	117.9
HI-STORM 100S(243) Overpack w/ fully loaded MPC-68/68F/68FF	118.2
HI-STORM 100S(243) Overpack w/ fully loaded MPC-24E/EF	118.4
HI-STORM 100S Version B(218) Overpack w/ fully loaded MPC-24	110.83
HI-STORM 100S Version B(218) Overpack w/ fully loaded MPC-32	111.88
HI-STORM 100S Version B(218) Overpack w/ fully loaded MPC-68/68F/68FF	111.45
HI-STORM 100S Version B(218) Overpack w/ fully loaded MPC-24E/EF	110.80

<sup>†</sup> See notes at end of table.

**TABLE 3.2.3 (CONTINUED)**  
**CENTERS OF GRAVITY OF HI-STORM SYSTEM CONFIGURATIONS**

<b>Component</b>	<b>Height of CG Above Datum<sup>†</sup> (in)</b>
HI-STORM 100S Version B(229) Overpack w/ fully loaded MPC-24	114.95
HI-STORM 100S Version B(229) Overpack w/ fully loaded MPC-32	116.00
HI-STORM 100S Version B(229) Overpack w/ fully loaded MPC-68/68F/68FF	115.58
HI-STORM 100S Version B(229) Overpack w/ fully loaded MPC-24E/EF	114.93
HI-TRAC 125 Transfer Cask w/ Top Lid, Transfer Lid, and fully loaded MPC-24 (water jacket filled)	99.5
HI-TRAC 125 Transfer Cask w/ Top Lid, Transfer Lid, and fully loaded MPC-32 (water jacket filled)	99.5
HI-TRAC 125 Transfer Cask w/ Top Lid, Transfer Lid, and fully loaded MPC-68/68F/68FF (water jacket filled)	99.8
HI-TRAC 125 Transfer Cask w/ Top Lid, Transfer Lid, and fully loaded MPC-24E/EF (water jacket filled)	100.1
HI-TRAC 100 Transfer Cask w/ Top Lid and Pool Lid (water jacket filled)	91.0
HI-TRAC 100 Transfer Cask w/ Top Lid and Transfer Lid (water jacket filled)	91.1
HI-TRAC 100 Transfer Cask w/ Top Lid, Pool Lid, and fully loaded MPC-24 (water jacket filled)	97.3
HI-TRAC 100 Transfer Cask w/ Top Lid, Pool Lid, and fully loaded MPC-32 (water jacket filled)	97.2
HI-TRAC 100 Transfer Cask w/ Top Lid, Pool Lid, and fully loaded MPC-68/68F/68FF (water jacket filled)	97.6
HI-TRAC 100 Transfer Cask w/ Top Lid, Pool Lid, and fully loaded MPC-24E/EF (water jacket filled)	98.0
HI-TRAC 100 Transfer Cask w/ Top Lid, Transfer Lid, and fully loaded MPC-24 (water jacket filled)	100.3
HI-TRAC 100 Transfer Cask w/ Top Lid, Transfer Lid, and fully loaded MPC-32 (water jacket filled)	100.3
HI-TRAC 100 Transfer Cask w/ Top Lid, Transfer Lid, and fully loaded MPC-68/68F/68FF (water jacket filled)	100.7
HI-TRAC 100 Transfer Cask w/ Top Lid, Transfer Lid, and fully loaded MPC-24E/EF (water jacket filled)	101.0

<sup>†</sup> See notes at end of table.



**TABLE 3.2.3 (CONTINUED)**  
**CENTERS OF GRAVITY OF HI-STORM SYSTEM CONFIGURATIONS**

<b>Component</b>	<b>Height of CG Above Datum (in)</b>
HI-TRAC 125D Transfer Cask w/ Top Lid and Pool Lid (water jacket filled)	92.4
HI-TRAC 125D Transfer Cask w/ Top Lid, Pool Lid, and fully loaded MPC-24 (water jacket filled)	97.6
HI-TRAC 125D Transfer Cask w/ Top Lid, Pool Lid, and fully loaded MPC-32 (water jacket filled)	97.5
HI-TRAC 125D Transfer Cask w/ Top Lid, Pool Lid, and fully loaded MPC-68/68F/68FF (water jacket filled)	97.8
HI-TRAC 125D Transfer Cask w/ Top Lid, Pool Lid, and fully loaded MPC-24E/EF (water jacket filled)	98.2
HI-TRAC 100D Transfer Cask w/ Top Lid and Pool Lid (water jacket filled)	87.0
HI-TRAC 100D Transfer Cask w/ Top Lid, Pool Lid, and fully loaded MPC-24 (water jacket filled)	99.2
HI-TRAC 100D Transfer Cask w/ Top Lid, Pool Lid, and fully loaded MPC-32 (water jacket filled)	101.2
HI-TRAC 100D Transfer Cask w/ Top Lid, Pool Lid, and fully loaded MPC-68/68F/68FF (water jacket filled)	100.4
HI-TRAC 100D Transfer Cask w/ Top Lid, Pool Lid, and fully loaded MPC-24E/EF (water jacket filled)	99.1

**Notes:**

1. The datum used for calculations involving the HI-STORM is the bottom of the overpack baseplate. The datum used for calculations involving the HI-TRAC is the bottom of the pool lid or transfer lid, as appropriate.
2. The datum used for calculations involving only the MPC is the bottom of the MPC baseplate.
3. The CG heights of the HI-STORM overpacks are calculated based on standard density concrete (i.e., 150 pcf dry). At higher densities, the CG heights are slightly lower, which makes the HI-STORM overpacks less prone to tipping.

**TABLE 3.2.4**  
**LIFT WEIGHT ABOVE POOL WITH HI-TRAC 125**

Item	Estimated Weight (lb)	Bounding Weight (lb)
HI-TRAC 125 w/ Top Lid and Pool Lid (water jacket filled)	142,976	
MPC-32 fully loaded with SNF and fuel spacers	89,765 <sup>†</sup>	
HI-TRAC 125 Top Lid	-2,730 <sup>††</sup>	
Water in MPC and HI-TRAC 125 Annulus	16,570	
Water in Water Jacket	-9,757 <sup>†††</sup>	
Lift yoke	4,200	
Inflatable annulus seal	50	
<b>TOTAL</b>	241,074	250,000

<sup>†</sup> Includes MPC closure ring.

<sup>††</sup> HI-TRAC top lid weight is included in transfer cask weight. However, the top lid is not installed during in-pool operations.

<sup>†††</sup> Total weight of HI-TRAC 125 includes water in water jacket. However, during removal from the fuel pool no water is in the water jacket since the water within the MPC cavity provides sufficient shielding.

HOLTEC INTERNATIONAL COPYRIGHTED MATERIAL

**TABLE 3.2.4 (CONTINUED)**  
**LIFT WEIGHT ABOVE POOL WITH HI-TRAC 100**

Item	Estimated Weight (lb)	Maximum Weight (lb)
HI-TRAC 100 w/ Top Lid and Pool Lid (water jacket filled)	100,194	
MPC-32 fully loaded with SNF and fuel spacers	89,765 <sup>†</sup>	
MPC closure ring	-140	
HI-TRAC 100 Top Lid	-1,203 <sup>††</sup>	
Water in MPC and HI-TRAC 100 Annulus	16,570	
Water in Water Jacket	-7,562 <sup>†††</sup>	
Lift yoke	3,200	
Inflatable annulus seal	50	
<b>TOTAL</b>	<b>200,874<sup>††††</sup></b>	<b>200,000</b>

Note: HI-TRAC transfer cask weight is without removable portion of pocket trunnion.

---

<sup>†</sup> Includes MPC closure ring.

<sup>††</sup> HI-TRAC top lid weight is included in transfer cask weight. However, the top lid is not installed during in-pool operations.

<sup>†††</sup> Total weight of HI-TRAC 100 includes water in water jacket. However, during removal from the fuel pool no water is in the water jacket since the water within the MPC cavity provides sufficient shielding.

<sup>††††</sup> Under worst case conditions, removal of a portion of water from the MPC may be required to reduce the in-pool lift weight.

---

HOLTEC INTERNATIONAL COPYRIGHTED MATERIAL

**TABLE 3.2.4 (CONTINUED)**  
**LIFT WEIGHT ABOVE POOL WITH HI-TRAC 125D**

Item	Estimated Weight (lb)	Bounding Weight (lb)
HI-TRAC 125D w/ Top Lid and Pool Lid (water jacket filled)	145,635	
MPC-32 fully loaded with SNF and fuel spacers	89,765 <sup>†</sup>	
HI-TRAC 125D Top Lid	-2,575 <sup>††</sup>	
Water in MPC and HI-TRAC 125D Annulus	16,570	
Water in Water Jacket	-8,955 <sup>†††</sup>	
Lift yoke	4,200	
Inflatable annulus seal	50	
<b>TOTAL</b>	<b>244,690</b>	<b>250,000</b>

---

<sup>†</sup> Includes MPC closure ring.

<sup>††</sup> HI-TRAC top lid weight is included in transfer cask weight. However, the top lid is not installed during in-pool operations.

<sup>†††</sup> Total weight of HI-TRAC 125D includes water in water jacket. However, during removal from the fuel pool no water is in the water jacket since the water within the MPC cavity provides sufficient shielding.

**TABLE 3.2.4 (CONTINUED)**  
**LIFT WEIGHT ABOVE POOL WITH HI-TRAC 100D**

<b>Item</b>	<b>Estimated Weight (lb)</b>	<b>Maximum Weight (lb)</b>
HI-TRAC 100D w/ Top Lid and Pool Lid (water jacket filled)	99,106	
MPC-32 fully loaded with SNF and fuel spacers	89,765 <sup>†</sup>	
MPC closure ring	-140	
HI-TRAC 100D Top Lid	-1,213 <sup>††</sup>	
Water in MPC and HI-TRAC 100D Annulus	16,570	
Water in Water Jacket	-7,665 <sup>†††</sup>	
Lift yoke	4,200	
Inflatable annulus seal	50	
<b>TOTAL</b>	<b>200,673<sup>††††</sup></b>	<b>200,000</b>

<sup>†</sup> Includes MPC closure ring.

<sup>††</sup> HI-TRAC top lid weight is included in transfer cask weight. However, the top lid is not installed during in-pool operations.

<sup>†††</sup> Total weight of HI-TRAC 100D includes water in water jacket. However, during removal from the fuel pool no water is in the water jacket since the water within the MPC cavity provides sufficient shielding.

<sup>††††</sup> Under worst case conditions, removal of a portion of water from the MPC may be required to reduce the in-pool lift weight.

HOLTEC INTERNATIONAL COPYRIGHTED MATERIAL

Table 2.2.6 provides a comprehensive listing of materials of construction, applicable code, and ITS designation for all functional parts in the HI-STORM 100 System. This section provides the mechanical properties used in the structural evaluation. The properties include yield stress, ultimate stress, modulus of elasticity, Poisson's ratio, weight density, and coefficient of thermal expansion. Values are presented for a range of temperatures which envelopes the maximum and minimum temperatures under all service conditions discussed in the preceding section where structural analysis is performed.

The materials selected for use in the MPC, HI-STORM 100 Overpack, and HI-TRAC transfer cask are presented in the Bills-of-Material in Section 1.5. In this chapter, the materials are divided into two categories, structural and nonstructural. Structural materials are materials that act as load bearing members and are, therefore, significant in the stress evaluations. Materials that do not support mechanical loads are considered nonstructural. For example, the HI-TRAC inner shell is a structural material, while the lead between the inner and outer shell is a nonstructural material. For nonstructural materials, the only property that is used in the structural analysis is weight density. In local deformation analysis, however, such as the study of penetration from a tornado-borne missile, the properties of lead in HI-TRAC and plain concrete in HI-STORM 100 are included.

### 3.3.1 Structural Materials

#### 3.3.1.1 Alloy X

A hypothetical material termed Alloy X is defined for all MPC structural components. The material properties of Alloy X are the least favorable values from the set of candidate alloys. The purpose of a least favorable material definition is to ensure that all structural analyses are conservative, regardless of the actual MPC material. For example, when evaluating the stresses in the MPC, it is conservative to work with the minimum values for yield strength and ultimate strength. This guarantees that the material used for fabrication of the MPC will be of equal or greater strength than the hypothetical material used in the analysis. In the structural evaluation, the only property for which it is not always conservative to use the set of minimum values is the coefficient of thermal expansion. Two sets of values for the coefficient of thermal expansion are specified, a minimum set and a maximum set. For each analysis, the set of coefficients, minimum or maximum that causes the more severe load on the cask system is used.

Table 3.3.1 lists the numerical values for the material properties of Alloy X versus temperature. These values, taken from the ASME Code, Section II, Part D [3.3.1], are used in all structural analyses. A minimum requirement on yield strength is set for MPC Lids in Table 3.3.1, to ensure that the lid internal threads have enough capacity under the lifted load as mandated by NUREG-0612. The maximum temperatures in some MPC components may exceed the allowable limits of temperature during short time duration loading operations, off-normal transfer operations, or storage accident events. However, no maximum temperature for Alloy X used at or within the confinement boundary exceeds 1000°F. As shown in ASME Code Case N-47-33 (Class 1 Components in

Elevated Temperature Service, 1995 Code Cases, Nuclear Components), the strength properties of austenitic stainless steels do not change due to exposure to 1000°F temperature for up to 10,000 hours. Therefore, there is no significant effect on mechanical properties of the confinement or basket material during the short time duration loading. A further description of Alloy X, including the materials from which it is derived, is provided in Appendix 1.A.

Two properties of Alloy X that are not included in Table 3.3.1 are weight density and Poisson's ratio. These properties are assumed constant for all structural analyses, regardless of temperature. The values used are shown in the table below.

PROPERTY	VALUE
Weight Density (lb/in <sup>3</sup> )	0.290
Poisson's Ratio	0.30

### 3.3.1.2 Carbon Steel, Low-Alloy and Nickel Alloy Steel

The carbon steels used in the structural qualification of the HI-STORM 100 System are SA516 Grade 70, SA515 Grade 70, and SA36. The nickel alloy and low alloy steels are SA203-E and SA350-LF3, respectively. These steels are not constituents of Alloy X. The material properties of SA516 Grade 70 and SA515 Grade 70 are shown in Tables 3.3.2. The material properties of SA203-E and SA350-LF3 are given in Table 3.3.3. The material properties of SA36 are shown in Table 3.3.6.

Two properties of these steels that are not included in Tables 3.3.2, 3.3.3 and 3.3.6 are weight density and Poisson's ratio. These properties are assumed constant for all structural analyses. The values used are shown in the table below.

PROPERTY	VALUE
Weight Density (lb/in <sup>3</sup> )	0.283
Poisson's Ratio	0.30

### 3.3.1.3 Bolting Materials

Material properties of the bolting materials used in the HI-STORM 100 System and HI-TRAC lifting trunnions are given in Table 3.3.4. The properties of representative anchor studs used to fasten HI-STORM 100A are listed in Table 1.2.7.

### 3.3.1.4 Weld Material

All weld materials utilized in the welding of the Code components comply with the provisions of the

appropriate ASME subsection (e.g., Subsection NB for the MPC enclosure vessel) and Section IX. All non-code welds will be made using weld procedures that meet Section IX of the ASME Code. The minimum tensile strength of the weld wire and filler material (where applicable) will be equal to or greater than the tensile strength of the base metal listed in the ASME Code.

### 3.3.2 Nonstructural Materials

#### 3.3.2.1 Solid Neutron Shield

The solid neutron shielding material in the HI-TRAC top lid and transfer lid doors is not considered as a structural member of the HI-STORM 100 System. Its load carrying capacity is neglected in all structural analyses except where such omission would be non-conservative. The only material property of the solid neutron shield that is important to the structural evaluation is weight density ( $1.63\text{g/cm}^3$ ).

#### 3.3.2.2 Solid Neutron Absorber

The fuel basket solid neutron absorber is not a structural member of the HI-STORM 100 System. Its load carrying capacity is neglected in all structural analyses. The only material property of the solid neutron absorber that is important to the structural evaluation is weight density. As the MPC fuel baskets can be constructed with neutron absorber panels of variable areal density, the weight that produces the most severe cask load is assumed in each analysis (density  $2.644\text{ g/cm}^3$ ).

#### 3.3.2.3 Concrete

The primary function of the plain concrete in the HI-STORM storage overpack is shielding. Concrete in the HI-STORM 100 Overpack is not considered as a structural member, except to withstand compressive, bearing, and penetrant loads. While concrete is not considered a structural member, its mechanical behavior must be quantified to determine the stresses in the structural members (steel shells surrounding it) under accident conditions. Table 3.3.5 provides the concrete mechanical properties. Allowable, bearing strength in concrete for normal loading conditions is calculated in accordance with ACI 318.1 -89 (92) [3.3.2]. The procedure specified in ASTM C-39 is utilized to verify that the assumed compressive strength will be realized in the actual in-situ pours. In addition, although the concrete is not reinforced (since the absence of reinforcement does not degrade the compressive strength), the requirements of ACI-349-85 [3.3.3] are imposed to insure the suitability of the concrete mix. Appendix 1.D provides additional information on the requirements on plain concrete for use in HI-STORM 100 storage overpack.

To enhance the shielding performance of the HI-STORM storage overpack, high density concrete can be used during fabrication. The permissible range of concrete densities is specified in Table 1.D.1. The structural calculations consider the most conservative density value (i.e., maximum or minimum weight), as appropriate.



#### 3.3.2.4 Lead

Lead is not considered as a structural member of the HI-STORM 100 System. Its load carrying capacity is neglected in all structural analysis, except in the analysis of a tornado missile strike where it acts as a missile barrier. Applicable mechanical properties of lead are provided in Table 3.3.5.

#### 3.3.2.5 Aluminum Heat Conduction Elements

In early vintage MPCs, aluminum heat conduction elements may be located between the fuel basket and MPC vessel. They are optional thin flexible elements whose sole function is to transmit heat as described in Chapter 4. They are not credited with any structural load capacity and are shaped to provide negligible resistance to basket thermal expansion. The total weight of the aluminum inserts is less than 1,000 lb. per MPC.

**TABLE 3.3.1**  
**ALLOY X MATERIAL PROPERTIES**

Temp. (Deg. F)	Alloy X				
	$S_y^{\ddagger}$	$S_u^{\dagger}$	$\alpha_{\min}$	$\alpha_{\max}$	E
-40	30.0 (33.0)	75.0 (70.0)	8.54	8.55	28.82
100	30.0 (33.0)	75.0 (70.0)	8.54	8.55	28.14
150	27.5 (30.25)	73.0 (68.1)	8.64	8.67	27.87
200	25.0 (27.5)	71.0 (66.2)	8.76	8.79	27.6
250	23.75 (26.12)	68.5 (63.85)	8.88	8.9	27.3
300	22.5 (24.75)	66.0 (61.5)	8.97	9.0	27.0
350	21.6 (23.76)	65.2 (60.75)	9.10	9.11	26.75
400	20.7 (22.77)	64.4 (60.0)	9.19	9.21	26.5
450	20.05 (22.06)	64.0 (59.65)	9.28	9.32	26.15
500	19.4 (21.34)	63.5 (59.3)	9.37	9.42	25.8
550	18.8 (20.68)	63.3 (59.1)	9.45	9.50	25.55
600	18.2 (20.02)	63.1 (58.9)	9.53	9.6	25.3
650	17.8 (19.58)	62.8 (58.6)	9.61	9.69	25.05
700	17.3 (19.03)	62.5 (58.4)	9.69	9.76	24.8
750	16.9 (18.59)	62.2 (58.1)	9.76	9.81	24.45
800	16.6 (18.26)	61.7 (57.6)	9.82	9.90	24.1

Definitions:

$S_y$  = Yield Stress (ksi)

$\alpha$  = Mean Coefficient of thermal expansion (in./in. per degree F x  $10^{-6}$ )

$S_u$  = Ultimate Stress (ksi)

E = Young's Modulus (psi x  $10^6$ )

Notes:

1. Source for  $S_y$  values is Table Y-1 of [3.3.1].
2. Source for  $S_u$  values is Table U of [3.3.1].
3. Source for  $\alpha_{\min}$  and  $\alpha_{\max}$  values is Table TE-1 of [3.3.1].
4. Source for E values is material group G in Table TM-1 of [3.3.1].

$\ddagger$  Values in the parentheses correspond to yield stress of MPC Lids which are 10% greater than the minimum yield stress values tabulated in Table 1.A.3. These higher values are only credited for the stress analysis of the MPC Lid lifting holes.

$\dagger$  The ultimate stress of Alloy X is dependent on the product form of the material (i.e., forging vs. plate). Values in parentheses are based on SA-336 forged materials (type F304, F304LN, F316, and F316LN), which are used solely for the one-piece construction MPC lids. All other values correspond to SA-240 plate material.

---

HOLTEC INTERNATIONAL COPYRIGHTED MATERIAL

HI-STORM FSAR  
REPORT HI-2002444

3.3-5

Rev. 11

**TABLE 3.3.2**  
**SA516 AND SA515, GRADE 70 MATERIAL PROPERTIES**

Temp. (Deg. F)	SA516 and SA515, Grade 70			
	S <sub>y</sub>	S <sub>u</sub>	α	E
-40	38.0	70.0	---	29.95
100	38.0	70.0	5.53 (5.73)	29.34
150	36.3	70.0	5.71 (5.91)	29.1
200	34.6	70.0	5.89 (6.09)	28.8
250	34.15	70.0	6.09 (6.27)	28.6
300	33.7	70.0	6.26 (6.43)	28.3
350	33.15	70.0	6.43 (6.59)	28.0
400	32.6	70.0	6.61 (6.74)	27.7
450	31.65	70.0	6.77 (6.89)	27.5
500	30.7	70.0	6.91 (7.06)	27.3
550	29.4	70.0	7.06 (7.18)	27.0
600	28.1	70.0	7.17 (7.28)	26.7
650	27.6	70.0	7.30 (7.40)	26.1
700	27.4	70.0	7.41 (7.51)	25.5
750	26.5	69.3	7.50 (7.61)	24.85

**Definitions:**

S<sub>y</sub> = Yield Stress (ksi)

α = Mean Coefficient of thermal expansion (in./in. per degree F x 10<sup>-6</sup>)

S<sub>u</sub> = Ultimate Stress (ksi)

E = Young's Modulus (psi x 10<sup>6</sup>)

**Notes:**

1. Source for S<sub>y</sub> values is Table Y-1 of [3.3.1].
2. Source for S<sub>u</sub> values is Table U of [3.3.1].
3. Source for α values is material group C in Table TE-1 of [3.3.1].
4. Source for E values is "Carbon steels with C less than or equal to 0.30%" in Table TM-1 of [3.3.1].
5. Values for SA515 are given in parentheses where different from SA516.

**TABLE 3.3.3**  
**SA350-LF3 AND SA203-E MATERIAL PROPERTIES**

Temp. (Deg. F)	SA350-LF3 and LF2			SA350-LF3/SA203-E		SA203-E		
	S <sub>m</sub>	S <sub>y</sub>	S <sub>u</sub>	E	α	S <sub>m</sub>	S <sub>y</sub>	S <sub>u</sub>
-20	23.3	37.5 (36.0)	70.0	28.2	---	23.3	40.0	70.0
100	23.3	37.5 (36.0)	70.0	27.6	6.27	23.3	40.0	70.0
200	22.8 (21.9)	34.2 (32.9)	68.5 (70.0)	27.1	6.54	23.3	36.5	70.0
300	22.2 (21.3)	33.2 (31.9)	66.7 (70.0)	26.7	6.78	23.3	35.4	70.0
400	21.5 (20.6)	32.2 (30.9)	64.6 (70.0)	26.1	6.98	22.9	34.3	68.8
500	20.2 (19.4)	30.3 (29.2)	60.7 (70.0)	25.7	7.16	21.6	32.4	64.9
600	18.5 (17.8)	- (26.6)	- (70.0)	-	-	-	-	-
700	16.8 (17.3)	- (26.0)	- (70.0)	-	-	-	-	-

**Definitions:**

- S<sub>m</sub> = Design Stress Intensity (ksi)
- S<sub>y</sub> = Yield Stress (ksi)
- S<sub>u</sub> = Ultimate Stress (ksi)
- α = Coefficient of Thermal Expansion (in./in. per degree F x 10<sup>-6</sup>)
- E = Young's Modulus (psi x 10<sup>6</sup>)

**Notes:**

1. Source for S<sub>m</sub> values is ASME Code.
2. Source for S<sub>y</sub> values is ASME Code.
3. Source for S<sub>u</sub> values is ratioing S<sub>m</sub> values.
4. Source for α values is material group E in Table TE-1 of [3.3.1].
5. Source for E values is material group B in Table TM-1 of [3.3.1].
6. Values for LF2 are given in parentheses where different from LF3.

**TABLE 3.3.4  
BOLTING MATERIAL PROPERTIES**

SB637-N07718					
Temp. (Deg. F)	S <sub>y</sub>	S <sub>u</sub>	E	α	S <sub>m</sub>
-100	150.0	185.0	29.9	---	50.0
-20	150.0	185.0	---	---	50.0
70	150.0	185.0	29.0	7.05	50.0
100	150.0	185.0	---	7.08	50.0
200	144.0	177.6	28.3	7.22	48.0
300	140.7	173.5	27.8	7.33	46.9
400	138.3	170.6	27.6	7.45	46.1
500	136.8	168.7	27.1	7.57	45.6
600	135.3	166.9	26.8	7.67	45.1
SA193 Grade B7 (2.5 to 4 inches diameter)					
Temp. (Deg. F)	S <sub>y</sub>	S <sub>u</sub>	E	α	-
100	95.0	115.00	-	5.73	-
200	88.5	107.13	-	6.09	-
300	85.1	103.02	-	6.43	-
400	82.3	99.63	-	5.9	-

**Definitions:**

S<sub>m</sub> = Design stress intensity (ksi)  
S<sub>y</sub> = Yield Stress (ksi)  
α = Mean Coefficient of thermal expansion (in./in. per degree F x 10<sup>-6</sup>)  
S<sub>u</sub> = Ultimate Stress (ksi)  
E = Young's Modulus (psi x 10<sup>6</sup>)

**Notes:**

1. Source for S<sub>m</sub> values is Table 4 of [3.3.1].
2. Source for S<sub>y</sub> values is ratioing design stress intensity values.
3. Source for S<sub>u</sub> values is ratioing design stress intensity values.
4. Source for α values is Tables TE-1 and TE-4 of [3.3.1], as applicable.
5. Source for E values is Table TM-1 of [3.3.1].
6. Source for S<sub>y</sub> values for SA193 bolts is Table Y-1 of [3.3.1]; source for S<sub>u</sub> is by ratioing S<sub>y</sub>.

HOLTEC INTERNATIONAL COPYRIGHTED MATERIAL

**TABLE 3.3.4 (CONTINUED)**  
**BOLTING MATERIAL PROPERTIES**

Temp. (Deg. F)	S <sub>y</sub>	S <sub>u</sub>	E	α	S <sub>m</sub>
SA193 Grade B7 (less than 2.5 inch diameter)					
100	105.0	125.00	-	5.73	-
200	98.0	116.67	-	6.09	-
300	94.1	112.02	-	6.43	-
400	91.5	108.93	-	6.74	-
SA705-630/SA564-630 (Age Hardened at 1075 degrees F)					
200	115.6	145.0	28.5	5.9	---
300	110.7	145.0	27.9	5.9	---
400	106.9	145.0	27.3	5.91	---
SA705-630/SA564-630 (Age Hardened at 1100 degrees F)					
200	106.3	140.0	28.5	5.9	---
300	101.9	140.0	27.9	5.9	---
400	98.3	136.3	27.3	5.91	---
SA705-630/SA564-630 (Age Hardened at 1150 degrees F)					
200	97.1	135.0	28.5	5.9	---
300	93.0	135.0	27.9	5.9	---

**Definitions:**

S<sub>m</sub> = Design stress intensity (ksi)  
S<sub>y</sub> = Yield Stress (ksi)  
α = Mean Coefficient of thermal expansion (in./in. per degree F x 10<sup>-6</sup>)  
S<sub>u</sub> = Ultimate Stress (ksi)  
E = Young's Modulus (psi x 10<sup>6</sup>)

**Notes:**

1. Source for S<sub>y</sub> values is Table Y-1 of [3.3.1].
2. Source for S<sub>u</sub> values is Table U of [3.3.1].
3. Source for α values is Tables TE-1 and TE-4 of [3.3.1], as applicable.
4. Source for E values is Table TM-1 of [3.3.1].

**TABLE 3.3.5**  
**CONCRETE AND LEAD MECHANICAL PROPERTIES**

PROPERTY	VALUE					
CONCRETE:						
Compressive Strength (psi)	See Table 1.D.1					
Nominal Density (lb/ft³)	See Table 1.D.1					
Allowable Bearing Stress (psi)	1,823 <sup>†</sup>					
Allowable Axial Compression (psi)	1,266 <sup>†</sup>					
Allowable Flexure, extreme fiber tension (psi)	187 <sup>†,††</sup>					
Allowable Flexure, extreme fiber compression (psi)	2,145 <sup>†</sup>					
Mean Coefficient of Thermal Expansion (in/in/deg. F)	5.5E-06					
Modulus of Elasticity (psi)	57,000 (compressive strength (psi)) <sup>1/2</sup>					
LEAD:	-40°F	-20°F	70°F	200°F	300°F	600°F
Yield Strength (psi)	700	680	640	490	380	20
Modulus of Elasticity (ksi)	2.4E+3	2.4E+3	2.3E+3	2.0E+3	1.9E+3	1.5E+3
Coefficient of Thermal Expansion (in/in/deg. F)	15.6E-6	15.7E-6	16.1E-6	16.6E-6	17.2E-6	20.2E-6
Poisson's Ratio	0.40					
Density (lb/cubic ft.)	708					

Notes:

- Concrete allowable stress values based on ACI 318.1-89 (92).
- Lead properties are from [3.3.5].

<sup>†</sup> Values listed correspond to concrete compressive stress = 3,300 psi

<sup>††</sup> No credit for tensile strength of concrete is taken in the calculations

HOLTEC INTERNATIONAL COPYRIGHTED MATERIAL

HI-STORM FSAR

REPORT HI-2002444

HI-STORM 100 FSAR, NON-PROPRIETARY

REVISION 12

MARCH 12, 2014

3.3-10

Rev. 11

**TABLE 3.3.6**  
**SA36 AND CARBON STEEL MATERIAL PROPERTIES**

Temp. (Deg. F)	SA36 AND CARBON STEEL			
	S <sub>y</sub>	S <sub>u</sub>	α	E
-40	36.0	58.0	---	29.95
100	36.0	58.0	5.53	29.34
150	34.4	55.4	5.71	29.1
200	32.8	52.8	5.89	28.8
250	32.35	52.1	6.09	28.6
300	31.9	51.4	6.26	28.3
350	31.35	50.5	6.43	28.0
400	30.8	49.6	6.61	27.7
450	29.95	48.3	6.77	27.5
500	29.1	46.9	6.91	27.3
550	27.85	44.9	7.06	27.0
600	26.6	42.9	7.17	26.7
650	26.1	42.1	7.30	26.1
700	25.9	41.7	7.41	25.5

**Definitions:**

S<sub>y</sub> = Yield Stress (ksi)

α = Mean Coefficient of thermal expansion (in./in. per degree F x 10<sup>-6</sup>)

S<sub>u</sub> = Ultimate Stress (ksi)

E = Young's Modulus (psi x 10<sup>6</sup>)

**Notes:**

1. Source for S<sub>y</sub> values is Table Y-1 of [3.3.1].
2. Source for S<sub>u</sub> values is ratioing S<sub>y</sub> values.
3. Source for α values is material group C in Table TE-1 of [3.3.1].
4. Source for E values is "Carbon steels with C less than or equal to 0.30%" in Table TM-1 of [3.3.1].



### 3.4 GENERAL STANDARDS FOR CASKS

#### 3.4.1 Chemical and Galvanic Reactions

In this section, it is shown that there is no credible mechanism for significant chemical or galvanic reactions in the HI-STORM 100 System during long-term storage operations (including HI-STORM 100S and HI-STORM 100A).

The MPC, which is filled with helium, provides a nonaqueous and inert environment. Insofar as corrosion is a long-term time-dependent phenomenon, the inert gas environment in the MPC precludes the incidence of corrosion during storage on the ISFSI. Furthermore, the only dissimilar material groups in the MPC are: (1) the neutron absorber material and stainless steel and (2) aluminum (found in some early vintage MPCs) and stainless steel. Neutron absorber materials and stainless steel have been used in close proximity in wet storage for over 30 years. Many spent fuel pools at nuclear plants contain fuel racks, which are fabricated from neutron absorber materials and stainless steel materials, with geometries similar to the MPC. Not one case of chemical or galvanic degradation has been found in fuel racks built by Holtec. This experience provides a sound basis to conclude that corrosion will not occur in these materials. Additionally, the aluminum conduction inserts and stainless steel basket are very close on the galvanic series chart. Aluminum, like other metals of its genre (e.g., titanium and magnesium) rapidly passivates in an aqueous environment, leading to a thin ceramic ( $\text{Al}_2\text{O}_3$ ) barrier, which renders the material essentially inert and corrosion-free over long periods of application. The physical properties of the material, e.g., thermal expansion coefficient, diffusivity, and thermal conductivity, are essentially unaltered by the exposure of the aluminum metal stock to an aqueous environment.

The aluminum in the optional heat conduction elements (found in some early vintage MPCs) will quickly passivate in air and in water to form a protective oxide layer that prevents any significant hydrogen production during MPC cask loading and unloading operations. The aluminum in the neutron absorber material may also react with the water to generate hydrogen gas. The exact rate of generation and total amount of hydrogen generated is a function of a number of variables (see Section 1.2.1.3.1) and cannot be predicted with any certainty. Therefore, to preclude the potential for hydrogen ignition during lid welding or cutting, the operating procedures in Chapter 8 require monitoring for combustible gas and purging the space beneath the MPC lid with an inert gas during these activities. Once the MPC cavity is drained, dried, and backfilled with helium, the source of the hydrogen gas (the aluminum-water reaction) is eliminated.

The HI-STORM 100 storage overpack and the HI-TRAC transfer cask each combine low alloy and nickel alloy steels, carbon steels, neutron and gamma shielding materials, and bolting materials. All of these materials have a long history of non-galvanic behavior within close proximity of each other. The internal and external steel surfaces of each of the storage overpacks are sandblasted and coated to preclude surface oxidation. The HI-TRAC coating does not chemically react with borated water. Therefore, chemical or galvanic reactions involving the storage overpack materials are highly unlikely and are not expected.

In accordance with NRC Bulletin 96-04 [3.4.7], a review of the potential for chemical, galvanic, or other reactions among the materials of the HI-STORM 100 System, its contents and the operating environments, which may produce adverse reactions, has been performed. Table 3.4.2 provides a listing of the materials of fabrication for the HI-STORM 100 System and evaluates the performance of the material in the expected operating environments during short-term loading/unloading operations and long-term storage operations. As a result of this review, no operations were identified which could produce adverse reactions beyond those conditions already analyzed in this FSAR.

#### 3.4.2 Positive Closure

There are no quick-connect/disconnect ports in the confinement boundary of the HI-STORM 100 System. The only access to the MPC is through the storage overpack lid, which weighs over 23,000 pounds (see Table 3.2.1). The lid is fastened to the storage overpack with large bolts. Inadvertent opening of the storage overpack is not feasible; opening a storage overpack requires mobilization of special tools and heavy-load lifting equipment.

#### 3.4.3 Lifting Devices

As required by Reg. Guide 3.61, in this subsection, analyses for all lifting operations applicable to the deployment of a member of the HI-STORM 100 family are presented to demonstrate compliance with applicable codes and standards.

The HI-STORM 100 System has the following components and devices participating in lifting operations: lifting trunnions located at the top of the HI-TRAC transfer cask, lid lifting connections for the HI-STORM 100 lid and for other lids in the HI-TRAC transfer cask, connections for lifting and carrying a loaded HI-STORM 100 vertically, and lifting connections for the loaded MPC.

Analyses of HI-STORM 100 storage overpack and HI-TRAC transfer cask lifting devices are reported in this submittal. Analyses of MPC lifting operations are presented in the HI-STAR 100 FSAR (Docket Number 72-1008, Subsection 3.4.3) and are also applicable here.

The evaluation of the adequacy of the lifting devices entails careful consideration of the applied loading and associated stress limits. The load combination  $D+H$ , where  $H$  is the "handling load", is the generic case for all lifting adequacy assessments. The term  $D$  denotes the dead load. Quite obviously,  $D$  must be taken as the bounding value of the dead load of the component being lifted. In all lifting analyses considered in this document, the handling load  $H$  is assumed to be  $0.15D$ . In other words, the inertia amplifier during the lifting operation is assumed to be equal to  $0.15g$ . This value is consistent with the guidelines of the Crane Manufacturer's Association of America (CMAA), Specification No. 70, 1988, Section 3.3, which stipulates a dynamic factor equal to  $0.15$  for slowly executed lifts. Thus, the "apparent dead load" of the component for stress analysis purposes is  $D^* = 1.15D$ . Unless otherwise stated, all lifting analyses in this report use the "apparent dead load",  $D^*$ , as the lifted load.

Analysis methodology to evaluate the adequacy of the lifting device may be analytical or numerical. For the analysis of the trunnion, an accepted conservative technique for computing the bending stress is to assume that the lifting force is applied at the tip of the trunnion "cantilever" and that the stress state is fully developed at the base of the cantilever. This conservative technique, recommended in NUREG-1536, is applied to all trunnion analyses presented in this SAR and has also been applied to the trunnions analyzed in the HI-STAR 100 FSAR.

In general, the stress analysis to establish safety pursuant to NUREG-0612, Regulatory Guide 3.61, and the ASME Code, requires evaluation of three discrete zones which may be referred to as (i) the trunnion, (ii) the trunnion/component interface, hereinafter referred to as Region A, and (iii) the rest of the component, specifically the stressed metal zone adjacent to Region A, herein referred to as Region B. During this discussion, the term "trunnion" applies to any device used for lifting (i.e., trunnions, lift bolts, etc.)

Stress limits germane to each of the above three areas are discussed below:

- i. Trunnion: NUREG-0612 requires that under the "apparent dead load",  $D^*$ , the maximum primary stress in the trunnion be less than 10% of the trunnion material ultimate strength and less than 1/6th of the trunnion material yield strength. Because of the materials of construction selected for trunnions in all HI-STORM 100 System components, the ultimate strength-based limit is more restrictive in every case. Therefore, all trunnion safety factors reported in this document pertain to the ultimate strength-based limit.
- ii. Region A: Trunnion/Component Interface: Stresses in Region A must meet ASME Code Level A limits under applied load  $D^*$ . Additionally, Regulatory Guide 3.61 requires that the primary stress under  $3D^*$ , associated with the cross-section, be less than the yield strength of the applicable material. In cases involving section bending, the developed section moment may be compared against the plastic moment at yield. The circumferential extent of the characteristic cross-section at the trunnion/component interface is calculated based on definitions from ASME Section III, Subsection NB and is defined in terms of the shell thickness and radius of curvature at the connection to the trunnion block. By virtue of the construction geometry, only the mean shell stress is categorized as "primary" for this evaluation.
- iii. Region B: Typically, the stresses in the component in the vicinity of the trunnion/component interface are higher than elsewhere. However, exceptional situations exist. For example, when lifting a loaded MPC, the MPC baseplate, which supports the entire weight of the fuel and the fuel basket, is a candidate location for high stress even though it is far removed from the lifting location (which is located in the top lid).

Even though the baseplate in the MPC would normally belong to the Region B category, for conservatism it was considered as Region A in the HI-STAR 100 SAR.

The pool lid and the transfer lid of the HI-TRAC transfer cask also fall into this dual category. In general, however, all locations of high stress in the component under D\* must also be checked for compliance with ASME Code Level A stress limits.

Unless explicitly stated otherwise, all analyses of lifting operations presented in this report follow the load definition and allowable stress provisions of the foregoing. Consistent with the practice adopted throughout this chapter, results are presented in dimensionless form, as safety factors, defined as

$$\text{Safety Factor, } \beta = \frac{\text{Allowable Stress in the Region Considered}}{\text{Computed Maximum Stress in the Region}}$$

The safety factor, defined in the manner of the above, is the added margin over what is mandated by the applicable code (NUREG-0612 or Regulatory Guide 3.61).

In the following subsections, we briefly describe each of the lifting analyses performed to demonstrate compliance with regulations. Summary results are presented for each of the analyses.

It is recognized that stresses in Region A are subject to two distinct criteria, namely Level A stress limits under D\* and yield strength at 3D\*. We will identify the applicable criteria in the summary tables, under the column heading "Item", using the "3D\*" identifier.

All of the lifting analyses reported on in this Subsection are designated as Load Case 01 in Table 3.1.5.

#### 3.4.3.1 125 Ton HI-TRAC Lifting Analysis - Trunnions

The lifting device in the HI-TRAC 125 cask is presented in Holtec Drawing 1880 (Section 1.5 herein). The two lifting trunnions for HI-TRAC are spaced at 180 degrees. The trunnions are designed for a two-point lift in accordance with the aforementioned NUREG-0612 criteria. Figure 3.4.21 shows the overall lifting configuration. The lifting analysis demonstrates that the stresses in the trunnions, computed using the conservative methodology described previously, comply with NUREG-0612 provisions.

Specifically, the following results are obtained:

<b>HI-TRAC 125 Lifting Trunnions<sup>†</sup></b>		
	<b>Value (ksi)</b>	<b>Safety Factor</b>
Bending stress	16.09	1.13
Shear stress	7.26	1.50
<sup>†</sup> The lifted load is 245,800 lb.(a value that bounds the actual lifted weight from the pool after the lift yoke weight is eliminated per Table 3.2.4).		

Note that the safety factor presented in the previous table represents the additional margin beyond the mandated limit of 6 on yield strength and 10 on tensile strength.

Similar calculations have been performed for the HI-TRAC 125D cask, which differs from the HI-TRAC 125 with respect to the material options for the lifting trunnions. The lifting trunnions for the HI-TRAC 125 are fabricated from SB637-N07718; the lifting trunnions for the HI-TRAC 125D can be fabricated from either SB637-N07718 or SA564-630. The bounding results for the HI-TRAC 125D are:

<b>HI-TRAC 125D Lifting Trunnions<sup>†</sup></b>		
	<b>Value (ksi)</b>	<b>Safety Factor</b>
Bending stress	13.57	1.03
Shear stress	7.26	1.16
<sup>†</sup> The lifted load is 245,800 lb.(a value that bounds the actual lifted weight from the pool after the lift yoke weight is eliminated per Table 3.2.4).		

#### 3.4.3.2 125 Ton HI-TRAC Lifting - Trunnion Lifting Block Welds, Bearing, and Thread Shear Stress (Region A)

As part of the Region A evaluation, the weld group connecting the lifting trunnion block to the inner and outer shells, and to the HI-TRAC top flange, is analyzed. Conservative analyses are also performed to determine safety factors for bearing stress and for thread shear stress at the interface between the trunnion and the trunnion block. The following results are obtained for the HI-TRAC 125 and 125D transfer casks:

<b>125 Ton HI-TRAC Lifting Trunnion Block (Region A Evaluation)</b>			
<b>Item</b>	<b>Value (ksi)</b>	<b>Allowable (ksi)</b>	<b>Safety Factor</b>
Trunnion Block Bearing Stress	5.95	11.4	1.91
Trunnion Block Thread Shear Stress	5.05	6.84	1.35
Weld Shear Stress (3D*)	4.35 <sup>†</sup>	11.4	2.62

<sup>†</sup> No quality factor has been applied to the weld group. (Subsection NF or NUREG-0612 do not apply penalty factors to the structural welds).

#### 3.4.3.3 125 Ton HI-TRAC Lifting - Structure near Trunnion (Region B/Region A)

A three-dimensional elastic model of the HI-TRAC 125 metal components is analyzed using the ANSYS finite element code. The structural model includes, in addition to the trunnion and the trunnion block, a portion of the inner and outer HI-TRAC shells and the HI-TRAC top flange. Stress results over the characteristic interface section are summarized and compared with allowable strength limits per ASME Section III, Subsection NF, and per Regulatory Guide 3.61. The results show that the primary stresses in the HI-TRAC 125 structure comply with the level A stress limits for Subsection NF structures.

The results from the analysis are summarized below:

<b>HI-TRAC 125 Trunnion Region (Regions A and B)</b>			
<b>Item</b>	<b>Value (ksi)</b>	<b>Allowable (ksi)</b>	<b>Safety Factor</b>
Membrane Stress	6.50	17.5	2.69
Membrane plus Bending Stress	8.71	26.25	3.01
Membrane Stress (3D*)	19.5	34.6	1.77

The results above are also valid for the HI-TRAC 125D since the dimensions and the configuration of the inner shell, outer shell, top flange, and the trunnion block are the same in both the HI-TRAC 125 and 125D transfer casks, and the dimension used in the finite element model for the trunnion length conservatively bounds both transfer casks.

#### 3.4.3.4 100 Ton HI-TRAC Lifting Analysis

The lifting trunnions and the trunnion blocks for the 100 Ton HI-TRAC are identical to the trunnions analyzed for the 125 Ton HI-TRAC. However, the outer shell geometry (outer diameter) is different. A calculation performed in the spirit of strength-of-materials provides justification that, despite the difference in local structure at the attachment points, the stresses in the body of the HI-TRAC 100 Ton unit meet the allowables set forth in Subsection 3.1.2.2.

Figure 3.4.10 illustrates the differences in geometry, loads, and trunnion moment arms between the body of the 125-Ton HI-TRAC and the body of the 100-Ton HI-TRAC. It is reasonable to assume that the level of stress in the 100 Ton HI-TRAC body, in the immediate vicinity of the interface (Section X-X in Figure 3.4.10), is proportional to the applied force and the bending moment applied. In the figure, the subscripts 1 and 0 refer to 100 Ton and 125 Ton casks, respectively. Figure 3.4.10 shows the location of the area centroid (with respect to the outer surface) and the loads and moment arms associated with each construction. Conservatively, neglecting all other interfaces between the top of the trunnion block and the top flange and between the sides of the trunnion block and the shells, equilibrium is maintained by developing a force and a moment in the section comprised of the two shell segments interfacing with the base of the trunnion block.

The most limiting stress state is in the outer shell at the trunnion block base interface. The stress level in the outer shell at Section X-X is proportional to  $P/A + Mc/I$ . Evaluating the stress for a unit width of section permits an estimate of the stress state in the HI-TRAC 100 outer shell if the corresponding stress state in the HI-TRAC 125 is known (the only changes are the applied load, the moment arm and the geometry). Using the geometry shown in Figure 3.4.10 gives the result as:

$$\text{Stress (HI-TRAC 100 outer shell)} = 1.242 \times \text{Stress (HI-TRAC 125 outer shell)}$$

The tabular results in the previous subsection can be adjusted accordingly and are reported below:

<b>100 Ton HI-TRAC Near Trunnion (Region A and Region B)</b>	
<b>Item</b>	<b>Safety Factor</b>
Membrane Stress	2.17
Membrane plus Bending Stress	2.42
Membrane Stress (3D*)	1.43

#### 3.4.3.5 HI-STORM 100 Lifting Analyses

There are two vertical lifting scenarios for the HI-STORM 100 storage overpack carrying a fully loaded MPC. Figure 3.4.17 shows a schematic of these lifting scenarios. Both lifting scenarios are examined using finite element models that focus on the local regions near the lift points. The analysis is based on the geometry of the HI-STORM 100; the alterations to the lid and to the length of the overpack barrel to configure the HI-STORM 100S have no effect on the conclusions reached in the area of the baseplate. Therefore, there is no separate analysis for the baseplate, inboard of the inner shell, for the HI-STORM 100S as the results are identical to or bounded by the results presented here. Since the upper portion of the HI-STORM 100S, the HI-STORM 100S lid, and the radial ribs and anchor block have a different configuration than the HI-STORM 100, separate calculations have been performed for these areas of the HI-STORM 100S. Similarly, where differences in construction between the HI-STORM 100 and the HI-STORM 100S Version B exist, separate calculations have been performed and the results summarized here.

Scenario #1 considers a "bottom lift" where the fully loaded HI-STORM 100 storage overpack is lifted vertically by four synchronized hydraulic jacks each positioned at one of the four inlet air vents. This lift allows for installation and removal of "air pads" which may be used for horizontal positioning of HI-STORM 100 at the ISFSI pad.

Scenario #2, labeled the "top lift scenario" considers the lifting of a fully loaded HI-STORM 100 vertically through the four lifting lugs located at the top end.

No structural credit is assumed for the HI-STORM concrete in either of the two lifting scenarios except as a vehicle to transfer compressive loads.

For the bottom lift, a three-dimensional one-quarter symmetry finite element model of the bottom region of the HI-STORM 100 storage overpack is constructed. The model includes the inner shell, the outer shell, the baseplate, the inlet vent side and top plates, and the radial plates connecting the inner and outer shells.

In the finite element analysis, the concrete is modeled as an equivalent pressure load applied over the baseplate as well as the four horizontal inlet vent plates. In reality, the concrete is supported only at the four inlet vents, directly above the hydraulic jacks. In other words, the concrete has sufficient strength to carry its own weight between these four support locations. The average shear stress in the concrete on a vertical cross section at the edge of an inlet vent is calculated as:

$$\tau_{concrete} = \frac{\rho V}{2A}$$

where:

$\rho$  equals the weight density of concrete;

$V$  equals the volume of unsupported concrete between two adjacent inlet vents;

---

HOLTEC INTERNATIONAL COPYRIGHTED MATERIAL



A cross-sectional area of concrete at location of maximum shear stress;

For  $\rho = 160.8 \text{ lb/ft}^3$ ,  $V = 231 \text{ ft}^3$ , and  $A = 5,665 \text{ in}^2 (= 27.5 \text{ in} \times 206 \text{ in})$ , the average shear stress is only 3.28 psi, which is negligible compared to the allowable shear stress of 126.5 psi for 4,000 psi compressive strength concrete. If the density of concrete is increased to  $200 \text{ lb/ft}^3$ , the shear stress increases by roughly 0.8 psi. Clearly, the concrete can support this load. Moreover, the positive effect that the concrete strength has on the results outweighs any adverse impact due to high density concrete. Therefore, the safety factors reported in this subsection (where the concrete is treated like water) for the bottom lift remain conservative for concrete densities up to  $200 \text{ lb/ft}^3$ .

For the analysis of the "top lift" scenario, a three-dimensional 1/8-symmetry finite element model of the top segment of HI-STORM 100 storage overpack is constructed. The metal HI-STORM 100 material is modeled (shells, radial plates, lifting block, ribs, vent plates, etc.) using shell or solid elements. Lumped weights are used to ensure that portions of the structure not modeled are, in fact, properly represented as part of a lifted load. The model is supported vertically at the lifting lug. The results are reported in tabular form at the end of this subsection.

The finite element results for the HI-STORM 100, as well as the results of similar analyses for the HI-STORM 100S, are based on inner and outer shell thicknesses of 1-1/4" and 3/4", respectively. Per Bill of Material 1575 and Drawing 3669, the thickness of both shells may be changed to 1" as an option for the HI-STORM 100 and 100S overpacks. With respect to the lifting analyses, the 1" thick inner and outer shells would have a negligible effect on the maximum calculated stress in the inlet vent horizontal plate, the HI-STORM baseplate, and the radial ribs. Therefore, the safety factors reported below for the HI-STORM 100 and 100S are valid for either thickness option.

To provide an alternate calculation to demonstrate that the bolt anchor blocks are adequate, we compute the average normal stress in the net metal area of the block under three times the lifted load. Further conservatism is introduced by including an additional 15% for dynamic amplification, i.e., the total load is equal to  $3D^*$ .

The average normal load in one bolt anchor block is

$$\text{Load} = 3 \times 1.15 \times 360,000 \text{ lb.}/4 = 310,500 \text{ lb.} \quad (\text{Weight comes from Table 3.2.1})$$

The net area of the bolt anchor block is

$$\text{Area} = (3.14159)/4 \times (5'' \times 5'' - 3.25'' \times 3.25'') = 11.34 \text{ sq. inch} \quad (\text{Dimensions from BM-1575})$$

Therefore, the safety factor (yield strength at 350 degrees F/calculated stress from Table 3.3.3) is

$$\text{SF} = 31,400 \text{ psi} / (\text{Load}/\text{Area}) = 1.14$$

The shear stress in the threads of the lifting block is also examined. This analysis considers a

cylindrical area of material under an axial load resisting the load by shearing action. The diameter of the area is the basic pitch diameter of the threads, and the length of the cylinder is the thread engagement length.

The analysis also examines the capacity of major welds in the load path and the compression capacity of the pedestal shield and pedestal shield shell.

The table below summarizes key results obtained from the analyses described above for the HI-STORM 100.

<b>HI-STORM 100 Top and Bottom Lifting Analyses<sup>†‡</sup></b>			
<b>Item</b>	<b>Value (ksi)</b>	<b>Allowable (ksi)</b>	<b>Safety Factor</b>
Primary Membrane plus Bending - Bottom Lift - Inlet Vent Plates - Region B	8.0	26.3	3.28
Primary Membrane - Top Lift - Radial Rib Under Lifting Block - Region B	6.67	17.5	2.63
Primary Membrane plus Bending – Top Lift - Baseplate – Region B	7.0	26.3	3.75
Primary Membrane Region A (3D*)	19.97	33.15	1.66
Primary Membrane plus Bending Region A (3D*)	24.02	33.15	1.38
Lifting Block Threads - Top Lift – Region A (3D*)	10.67	18.84	1.76
Lifting Stud - Top Lift –Region A (3D*)	43.733	108.8	2.49
Welds – Anchor Block-to-Radial Rib Region B	5.74	19.695	3.43
Welds – Anchor Block-to-Radial Rib Region A (3D*)	17.21	19.62	1.14
Welds – Radial Rib-to-Inner and Outer Shells Region B	5.83	21.00	3.60
Welds – Radial Rib-to-Inner and Outer Shells Region A (3D*)	17.49	19.89	1.13
Weld – Baseplate-to Inner Shell Region A (3D*)	1.59	19.89	12.48
Weld – Baseplate-to-Inlet Vent Region A (3D*)	14.89	19.89	1.33
Pedestal Shield Concrete (3D*)	0.096	1.266	13.19
Pedestal Shell (3D*)	3.269	33.15	10.14

<sup>†</sup> Regions A and B are defined at beginning of Subsection 3.4.3

<sup>‡</sup> The lifted load is 360000 lb. and an inertia amplification of 15% is included.

It is concluded that all structural integrity requirements are met during a lift of the HI-STORM 100 storage overpack under either the top lift or the bottom lift scenario. All factors of safety are greater than 1.0 using criteria from the ASME Code Section III, Subsection NF for Class 3 plate and shell supports and from USNRC Regulatory Guide 3.61.

Similar calculations have been performed for the HI-STORM 100S where differences in configuration warrant. The results are summarized in the table below:

<b>HI-STORM 100S Top and Bottom Lifting Analyses<sup>†‡</sup></b>			
<b>Item</b>	<b>Value (ksi)</b>	<b>Allowable (ksi)</b>	<b>Safety Factor</b>
Primary Membrane plus Bending - Bottom Lift - Inlet Vent Plates - Region A (3D*)	9.824	33.15	3.374
Lifting Block Threads - Top Lift - Region A (3D*)	7.950	18.840	2.37
Lifting Stud - Top Lift - Region A (3D*)	49.806	83.7	1.68
Welds - Anchor Block-to-Radial Rib Region B	5.556	21.0	3.78
Welds - Anchor Block-to-Radial Rib Region A (3D*)	16.670	18.84	1.13
Welds - Radial Rib-to-Inner and Outer Shells Region B	5.631 <sup>*</sup>	21.00	3.73 <sup>*</sup>
Welds - Radial Rib-to-Inner and Outer Shells Region A (3D*)	16.895 <sup>*</sup>	19.89	1.18 <sup>*</sup>
Weld - Baseplate-to Inner Shell Region A (3D*)	1,592	19.89	12.49
Weld - Baseplate-to-Inlet Vent Region A (3D*)	8.982	19.89	2.214
Radial Rib Membrane Stress - Bottom Lift Region A (3D*)	10.58	33.15	3.132
Pedestal Shield Concrete (3D*)	0.095	1.535	16.17
Pedestal Shell (3D*)	3.235	33.15	10.24

<sup>†</sup> Regions A and B are defined at beginning of Subsection 3.4.3

<sup>‡</sup> The lifted load is 410,000 lb and an inertia amplification of 15% is included. The increased weight (over the longer HI-STORM 100) comes from conservatively assuming an increase in concrete weight density in the HI-STORM 100S overpack and lid to provide additional safety margin.

\* Result is specific to HI-STORM 100S overpacks fabricated with full height radial plates. For HI-STORM 100S overpacks fabricated with shorter top and bottom radial plates (i.e., two-piece configuration), the results tabulated below for the HI-STORM 100S Version B overpack, for the radial rib to inner and outer shell welds, are bounding.

HOLTEC INTERNATIONAL COPYRIGHTED MATERIAL

HI-STORM FSAR

REPORT HI-2002444

HI-STORM 100 FSAR, NON-PROPRIETARY

REVISION 12

MARCH 12, 2014

3.4-12

Rev. 10

Similar calculations have been performed for the HI-STORM 100S, Version B where differences in configuration warrant. The results are summarized in the table below for the heaviest HI-STORM 100S Version B (using high density concrete and with SA 564-630 stud material):

HI-STORM 100S Version B Top and Bottom Lifting Analyses			
Item	Value (ksi)	Allowable (ksi)	Safety Factor
Primary Membrane - Bottom Lift - Inlet Vent Plates - Region A (3D*)	27.06	33.15	1.22
Primary Membrane + Bending - Bottom Lift - Inlet Vent Plates - Region A (3D*)	20.455	33.15	1.62
Lifting Block Threads - Top Lift -Region A (3D*)	9.315	19.620	2.11
Lifting Stud - Top Lift -Region A (3D*)	49.369	108.8	2.20
Welds - Anchor Block-to-Radial Rib Region B	5.507	19.695	3.58
Welds - Anchor Block-to-Radial Rib Region A (3D*)	16.523	19.620	1.19
Welds - Radial Rib-to-Inner and Outer Shells Region B	6.120	21.00	3.43
Welds - Radial Rib-to-Inner and Outer Shells Region A (3D*)	18.36	19.89	1.08
Weld - Baseplate-to Inner Shell Region A (3D*)	2.724	19.89	7.302
Radial Rib to Inner and Outer Shell - Bottom Lift Region A (3D*)	18.360	19.89	1.08

For the longest HI-STORM 100S, Version B, with high-density concrete, the lifted load is 406,400 lb.

It is concluded that all structural integrity requirements are met during a lift of the HI-STORM 100, HI-STORM 100S, and HI-STORM 100S, Version B storage overpacks under either the top lift or the bottom lift scenario. All factors of safety are greater than 1.0 using criteria from the ASME Code Section III, Subsection NF for Class 3 plate and shell supports and from USNRC Regulatory Guide 3.61.

#### 3.4.3.6 MPC Lifting Analysis

The MPC can be inserted or removed from an overpack by lifting cleats that are designed for installation into threaded holes in the top lid. The strength requirements of the attachment bolts and base metal are examined based on the requirements of NUREG 0612. Sufficiency of thread engagement length and bolt pre-load are also considered. The MPC top closure is examined considering the top lid as "Region B", where satisfaction of ASME Code Level A requirements is demonstrated. The analysis also considers highly stressed regions of the top closure as "region A" where applied load is 3D\*. The MPC baseplate is analyzed under normal handling and subject to the allowable strengths appropriate to a component considered in "Region B". Finally, the baseplate region is further analyzed where loading is "3D\*" consistent with the MPC baseplate being considered as "Region A". The definitions of "Region A", "Region B", and "3D\*" as they apply to lifting analyses have been introduced at the beginning of this subsection.

The following table summarizes the minimum safety factors from these analyses. As stated earlier, safety factors tabulated below represent margins that are over and beyond those implied by the loading magnification mandated in NUREG 0612 or Regulatory Guide 3.61, as appropriate.

Summary of MPC Lifting Analyses			
Item	Thread Engagement Safety Factor (NUREG-0612)	Region A Safety Factor (Note 1)	Region B Safety Factor (Note 1)
MPC	1.013 (Note 2)	1.54	1.08

Notes:

1. Safety factor is for MPC baseplate.
2. The Safety Factor is calculated at 475°F based on a minimum yield strength of 33 ksi at room temperature for MPC Lids.

When dual lids are used on the MPC, the outer lid transfers the entire lifted load to the peripheral weld. The maximum bending stress in the outer lid from the lifted load can be conservatively computed by strength of materials theory using the solution for a simply supported circular plate under a central concentrated load equal to 115% of the bounding MPC load. The calculation and result are presented below using tabular results from Timoshenko, Strength of Materials, Vol. II, 3<sup>rd</sup> Edition.

$$P = 90,000 \text{ lb.} \times 1.15$$

$$\text{Outer Diameter } a = 67.375''$$

$$\text{Effective Central Diameter where load is applied } b = 13.675'' \text{ (conservative assumption)}$$

$$a/b = 5$$

$$\text{Lid thickness } = 4.75'' \text{ (Dual lids)}$$

From the reference,  $k=1.745$  and the maximum bending stress under the amplified lifted load is

$$\sigma = kP/h^2 = 8005 \text{ psi}$$

Table 3.4.7 provides results for the stress in the lid under normal condition internal pressure. For the case with dual lids, the stress must be doubled. From the table, the pressure stress is

$$S = 2 \times 1,633 \text{ psi}$$

Therefore, the combined bending stress at the center of the dual lid is 11,271. Using the allowable strength from Table 3.4.7, the safety factor is

$$SF = 25,450 \text{ psi} / 11,271 \text{ psi} = 2.258$$

### 3.4.3.7 Miscellaneous Lid Lifting Analyses

The HI-STORM 100 lid lifting analysis is performed to ensure that the threaded connections provided in the lid are adequately sized. The lifting analysis of the top lid is based on a vertical orientation of loading from an attached lifting device. The top lid of the HI-STORM 100 storage overpack is lifted using four lugs that are threaded into holes in the top plate of the lid (Holtec Drawing 1495, Section 1.5). It is noted that failure of the lid attachment would not result in any event of safety consequence because a free-falling HI-STORM 100 lid cannot strike a stored MPC (due to its size and orientation). Operational limits on the carry height of the HI-STORM 100 lid above the top of the storage overpack containing a loaded MPC preclude any significant lid rotation out of the horizontal plane in the event of a handling accident. Therefore, contact between the top of the MPC and the edge of a dropped lid due to uncontrolled lowering of the lid during the lid placement operation is judged to be a non-credible scenario. Except for location of the lift points, the lifting device for the HI-STORM 100S and for the HI-STORM 100S, Version B lid is the same as for the regular HI-STORM 100 lid. Since the lid weight for the HI-STORM 100S, Version B bounds the HI-STORM 100 and the HI-STORM 100S, the calculated safety factors for the lifting of the HI-STORM 100S lid are reduced and are also reported in the summary table below.

In addition to the HI-STORM 100 top lid lifting analysis, the strength qualification of the lid lifting holes, and associated lid lifting devices, for the HI-TRAC pool lid and top lid has been performed. The qualification is based on the Regulatory Guide 3.61 requirement that a load factor of 3 results in stresses less than the yield stress. The results for the HI-TRAC 125 bound the results for the HI-TRAC 125D, the HI-TRAC 100, and the HI-TRAC 100D, since the lid weights used in the calculation are greater than or equal to all other HI-TRAC lid weights. Example commercially available lifting structures are considered and it is shown that thread engagement lengths are acceptable. Loads to lifting devices are permitted to be at a maximum angle of 45 degrees from vertical. A summary of results, pertaining to the various lid lifting operations, is given in the table below:

<b>Summary of HI-STORM 100 Lid Lifting Analyses</b>		
<b>Item</b>	<b>Dead Load (lb)</b>	<b>Minimum Safety Factor</b>
HI-STORM 100 (100S) Top Lid Lifting	23,000 (29,000 <sup>†</sup> )	4.925 (3.906)
HI-TRAC Pool Lid Lifting	12,500	3.594 (Note 1)
HI-TRAC Top Lid Lifting	2,750	11.3
<sup>†</sup> Bounding weight of HI-STORM 100S, Version B top lid with 200 pcf concrete.		

Note 1: Safety Factor is calculated based on a conservative thread engagement of 1".

The analysis demonstrates that thread engagement is sufficient for the threaded holes used solely for lid lifting and that commercially available lifting devices engaging the threaded holes, are available.

We note that all reported safety factors are based on an allowable strength equal to 33.3% of the yield strength of the lid material when evaluating shear capacity of the internal threads and based on the working loads of the commercially available lifting devices associated with the respective threaded holes.

3.4.3.8 HI-TRAC Pool Lid Analysis - Lifting MPC From the Spent Fuel Pool (Load Case 01 in Table 3.1.5)

During lifting of the MPC from the spent fuel pool, the HI-TRAC pool lid supports the weight of a loaded MPC plus water (see Figure 3.4.21). Calculations are performed to show structural integrity under this condition for both the HI-TRAC 100 and the HI-TRAC 125 transfer casks. In accordance with the general guidelines set down at the beginning of Subsection 3.4.3, the pool lid is considered as both Region A and Region B for evaluating safety factors. The analysis shows that the stress in the pool lid top plate is less than the Level A allowable stress under pressure equivalent to the heaviest MPC, contained water, and lid self weight (Region B evaluation). Stresses in the lids and bolts are also shown to be below yield under three times the applied lifted load (Region A evaluation using Regulatory Guide 3.61 criteria). The threaded holes in the HI-TRAC pool lid are also examined for acceptable engagement length under the condition of lifting the MPC from the pool. It is demonstrated that the pool lid peripheral bolts have adequate engagement length into the pool lid to permit the transfer of the required load. The safety factor is defined based on the strength limits imposed by Regulatory Guide 3.61.

The following table summarizes the results of the analyses for the HI-TRAC pool lid for each of the four transfer cask types. Results given in the following table compare calculated stress (or load) and allowable stress (or load). In all cases, the safety factor is defined as the allowable value divided by the calculated value.



HI-TRAC Pool Lid Lifting a Loaded MPC Evaluation <sup>†</sup>			
Item	Value (ksi)	Allowable (ksi)	Safety Factor
Lid Bending Stress - HI-TRAC 125/125D - Region B Analysis - Pool Lid Top Plate	10.1	26.3	2.604
Lid Bending Stress - HI-TRAC 125/125D - Region B Analysis - Pool Lid Bottom Plate	5.05	26.3	5.208
Lid Bending Stress - HI-TRAC 100/100D - Region B Analysis - Pool Lid Top Plate	10.06	26.3	2.614
Lid Bending Stress - HI-TRAC 100/100D - Region B Analysis - Pool Lid Bottom Plate	6.425	26.3	4.093
Lid Bolt Stress - HI-TRAC 125 – (3D*)	18.92	95.0	5.02
Lid Bolt Stress - HI-TRAC 100 – (3D*)	18.21	95.0	5.216
Lid Bolt Force - HI-TRAC 125D – (3D*)	25.77 <sup>‡</sup>	84.05 <sup>‡</sup>	3.262
Lid Bolt Force - HI-TRAC 100D – (3D*)	24.80 <sup>‡</sup>	84.05 <sup>‡</sup>	3.389
Lid Bending Stress - HI-TRAC 125/125D - Region A Analysis - Pool Lid Top Plate (3D*)	30.3	33.15	1.094
Lid Bending Stress - HI-TRAC 125/125D - Region A Analysis - Pool Lid Bottom Plate (3D*)	15.15	33.15	2.188
Lid Bending Stress - HI-TRAC 100/100D – Region A Analysis - Pool Lid Top Plate (3D*)	30.19	33.15	1.098
Lid Bending Stress - HI-TRAC 100/100D – Region A Analysis - Pool Lid Bottom Plate (3D*)	19.28	33.15	1.72
Lid Thread Engagement Length (HI-TRAC 125)	137.4 <sup>‡</sup>	267.9 <sup>‡</sup>	1.949

<sup>†</sup> Region A and B defined at beginning of Subsection 3.4.3.

<sup>‡</sup> Calculated and allowable value for this item in (kips).

### 3.4.3.9 HI-TRAC Transfer Lid Analysis - Lifting MPC Away from Spent Fuel Pool (Load Case 01 in Table 3.1.5)

During transfer to or from a storage overpack using a HI-TRAC 125 or a HI-TRAC 100, the HI-TRAC transfer lid supports the weight of a loaded MPC. Figure 3.4.21 illustrates the lift operation. In accordance with the general lifting analysis guidelines, the transfer lid should be considered as both a Region A (Regulatory Guide 3.61 criteria) and a Region B location (ASME Section III, Subsection NF for Class 3 plate and shell structures) for evaluation of safety factors. The HI-TRAC 125 transfer lid and the HI-TRAC 100 transfer lid are analyzed separately because of differences in geometry. The HI-TRAC 125D and HI-TRAC 100D employ specially designed mating devices in combination with the pool lid to transfer a loaded MPC to or from a storage overpack. Thus, a transfer lid analysis is not performed for the HI-TRAC 125D or the HI-TRAC 100D. Results for the HI-TRAC 125D and HI-TRAC 100D pool lids are presented in the previous subsection.

It is shown that the transfer lid doors can support a loaded MPC together with the door weight without exceeding ASME NF stress limits and the more conservative limits of Regulatory Guide 3.61. It is also shown that the connecting structure transfers the load to the cask body without overstress. The following tables summarize the results for both HI-TRAC casks:

HI-TRAC 125 Transfer Lid – Lifting Evaluation <sup>†</sup>			
Item	Value (ksi)	Allowable (ksi)	Safety Factor
HI-TRAC 125 - Door Plate – (3D*)	9.381	32.7	3.486
HI-TRAC 125 - Door Plate – Region B	3.127	26.25	8.394
HI-TRAC 125 – Wheel Track (3D*)	26.91	36.0	1.338
HI-TRAC 125 - Door Housing Bottom Plate-Region B	7.701	26.25	3.409
HI-TRAC 125 - Door Housing Bottom Plate-(3D*)	23.103	32.7	1.415
HI-TRAC 125 - Door Housing Stiffeners- (3D*)	4.131	32.7	7.913
HI-TRAC 125 - Housing Bolts-Region B	29.96	57.5	1.919
HI-TRAC 125 – Housing Bolts (3D*)	89.88	95.0	1.057
HI-TRAC 125 – Lid Top Plate (3D*)	30.907	32.7	1.058

<sup>†</sup> Region A and B defined at beginning of Subsection 3.4.3

HI-TRAC 100 Transfer Lid – Lifting Evaluation <sup>†</sup>			
Item	Value (ksi)	Allowable (ksi)	Safety Factor
HI-TRAC 100 - Door Plate – (3D*)	22.188	32.7	1.474
HI-TRAC 100 - Door Plate – Region B	7.396	26.25	3.549
HI-TRAC 100 – Wheel Track (3D*)	13.011	36.0	2.767
HI-TRAC 100 – Door Housing Bottom Plate- Region B	7.447	26.25	3.525
HI-TRAC 100 – Door Housing Bottom Plate- (3D*)	22.336	32.7	1.464
HI-TRAC 100 – Door Housing Stiffeners- (3D*)	4.917	32.7	6.65
HI-TRAC 100 – Welds Connecting Door Housing Stiffeners (3D*)	11.802	32.7	2.771
HI-TRAC 100 - Housing Bolts-Region B	22.478	57.5	2.558
HI-TRAC 100 – Housing Bolts (3D*)	67.423	95.0	1.409
HI-TRAC 100 – Lid Top Plate (3D*)	19.395	32.7	1.686

<sup>†</sup> Region A and B defined at beginning of Subsection 3.4.3

HOLTEC INTERNATIONAL COPYRIGHTED MATERIAL

HI-STORM FSAR

REPORT HI-2002444

3.4-18

Rev. 10

HI-STORM 100 FSAR, NON-PROPRIETARY  
REVISION 12  
MARCH 12, 2014

### 3.4.3.10 HI-TRAC Bottom Flange Evaluation during Lift (Load Case 01 in Table 3.1.5)

During a lifting operation, the HI-TRAC transfer cask body supports the load of a loaded MPC, and the transfer lid (away from the spent fuel pool) or the pool lid plus contained water (lifting from the spent fuel pool). In either case, the load is transferred to the bottom flange of HI-TRAC through the bolts and a state of stress in the flange and the supporting inner and outer shells is developed. Figure 3.4.21 illustrates the lifting operation. This area of the HI-TRAC 125 is analyzed to demonstrate that the required limits on stress are maintained for both ASME and Regulatory Guide 3.61. The bottom flange is considered as an annular plate subject to a total bolt load acting at the bolt circle and supported by reaction loads developed in the inner and outer shells of HI-TRAC. The solution for maximum flange bending stress is found in the classical literature and stresses and corresponding safety factors developed for the bottom flange and for the outer and inner shell weld shear stress. Since the welds are partial penetration, weld stress evaluation bounds an evaluation of direct stress. The table below summarizes the results of the evaluation.

<b>Safety Factors in HI-TRAC Bottom Flange During a Lift Operation</b>			
<b>Item</b>	<b>Value(ksi)</b>	<b>Allowable(ksi)</b>	<b>Safety Factor</b>
Bottom Flange – Region B	7.798	26.25	3.37
Bottom Flange (3D*)	23.39	33.15	1.42
Outer Shell (3D*)	4.773	33.15	6.94

The bottom flanges of the HI-TRAC 125D and HI-TRAC 100D are different from the HI-TRAC 125 in several respects. Namely, the thickness of the bottom flange is less, and the groove weld connecting the bottom flange to the inner shell is smaller. In addition, the bottom flange of the HI-TRAC 125D and HI-TRAC 100D is reinforced by eight gusset plates, whereas the HI-TRAC 125 bottom flange is not reinforced. Therefore, to account for these differences, the evaluation described above has been repeated for the HI-TRAC 125D and the HI-TRAC 100D. The results are summarized in the tables below. Note that the following results are conservative since the HI-TRAC 125D and HI-TRAC 100D bottom flange evaluations neglect the reinforcing strength of the gusset plates.

<b>Safety Factors in HI-TRAC 125D Bottom Flange During a Lift Operation</b>			
<b>Item</b>	<b>Value(ksi)</b>	<b>Allowable(ksi)</b>	<b>Safety Factor</b>
Bottom Flange – Region B	9.594	26.25	2.74
Bottom Flange (3D*)	28.78	33.15	1.15
Outer Shell (3D*)	4.710	33.15	7.04

Safety Factors in HI-TRAC 100D Bottom Flange During a Lift Operation			
Item	Value(ksi)	Allowable(ksi)	Safety Factor
Bottom Flange – Region B	8.646	26.25	3.04
Bottom Flange (3D*)	25.94	33.15	1.28
Outer Shell (3D*)	5.499	33.15	6.03

#### 3.4.3.11 Conclusion

Synopses of lifting device, device/component interface, and component stresses, under all contemplated lifting operations for the HI-STORM 100 System have been presented in the foregoing. The HI-STORM storage overpack and the HI-TRAC transfer cask have been evaluated for limiting stress states. The results show that all factors of safety are greater than 1.

#### 3.4.4 Heat

The thermal evaluation of the HI-STORM 100 System is reported in Chapter 4.

##### 3.4.4.1 Summary of Pressures and Temperatures

Design pressures and design temperatures for all conditions of storage are listed in Tables 2.2.1 and 2.2.3, respectively.

##### 3.4.4.2 Differential Thermal Expansion

Consistent with the requirements of Reg. Guide 3.61, Load Cases F1 (Table 3.1.3) and E4 (Table 3.1.4) are defined to study the effect of differential thermal expansion among the constituent components in the HI-STORM 100 System. The temperatures necessary to perform the differential thermal expansion analyses for the MPC in the HI-STORM 100 and HI-TRAC casks are provided in Chapter 4. The material presented in Subsection 4.4.5 demonstrates that a physical interference between discrete components of the HI-STORM 100 System (e.g. storage overpack and enclosure vessel) will not develop due to differential thermal expansion during any operating condition.

##### 3.4.4.2.1 Normal Hot Environment

Closed form calculations are performed in Subsection 4.4.6 to demonstrate that initial gaps between the HI-STORM 100 storage overpack or the HI-TRAC transfer cask and the MPC canister, and between the MPC canister and the fuel basket, will not close due to thermal expansion of the system components under loading conditions, defined as F1 and E4 in Tables 3.1.3 and 3.1.4, respectively. To assess this in the most conservative manner, the thermal solutions computed in Chapter 4, including the thermosiphon effect, are surveyed for the following information.

- The radial temperature distribution in each of the fuel baskets at the location of peak center metal temperature.
- The highest and lowest mean temperatures of the canister shell for the hot environment condition.

Using the above temperature information, simplified thermoelastic solutions of equivalent axisymmetric problems are used to obtain conservative estimates of gap closures. The following procedure, which conservatively neglects axial variations in temperature distribution, is utilized.

1. Use the surface temperature information for the fuel basket to define a parabolic distribution in the fuel basket that bounds (from above) the actual temperature distribution. Using this result, generate a conservatively high estimate of the radial and axial growth of the different fuel baskets using classical closed form solutions for thermoelastic deformation in cylindrical bodies.
2. Use the temperatures obtained for the canister to predict an estimate of the radial and axial growth of the canister to check the canister-to-basket gaps.
3. Use the temperatures obtained for the canister to predict an estimate of the radial and axial growth of the canister to check the canister-to-storage overpack and canister-to-HI-TRAC gaps.
4. For given initial clearances, compute the operating clearances.

The results are summarized in Table 4.4.10 for normal storage conditions. The clearances between the MPC basket and canister structure, as well as between the MPC shell and storage overpack or HI-TRAC inside surface, are sufficient to preclude a temperature induced interference from differential thermal expansions under normal operating conditions.

#### 3.4.4.2.2 Fire Accident

It is shown in Chapter 4 that the fire accident has a small effect on the MPC temperatures because of the short duration of the fire accidents and the large thermal inertia of the storage overpack. Therefore, a structural evaluation of the MPC under the postulated fire event is not required. The conclusions reached in Subsection 3.4.4.2.1 are also appropriate for the fire accident with the MPC housed in the storage overpack. Analysis of fire accident temperatures of the MPC housed within the HI-TRAC for thermal expansion is unnecessary, as the HI-TRAC, directly exposed to the fire, expands to increase the gap between the HI-TRAC and MPC.

As expected, the external surfaces of the HI-STORM 100 storage overpack that are directly exposed to the fire event experience maximum rise in temperature. The outer shell and top plate in the top lid are the external surfaces that are in direct contact with heated air from fire. The table below, extracted from data provided in Chapter 4, provides the maximum temperatures attained at the key locations in HI-STORM 100 storage overpack under the postulated fire event.

<b>Component</b>	<b>Maximum Fire Condition Temperature (Deg. F)</b>
Storage Overpack Inner Shell	300
Storage Overpack Radial Concrete Mid-Depth	184
Storage Overpack Outer Shell	570
Storage Overpack Lid	<570

The following conclusions are readily reached from the above table.

- The maximum metal temperature of the carbon steel shell most directly exposed to the combustion air is well below 600°F (Table 2.2.3 applicable short-term temperature limit). 600°F is well below the permissible temperature limit in the ASME Code for the outer shell material.
- The bulk temperature of concrete is well below the normal condition temperature limit of 300°F specified in Table 2.2.3 and Appendix 1.D. ACI-349-85 permits 350°F as the short-term temperature limit; the shielding concrete in the HI-STORM 100 Overpack, as noted in Appendix 1.D, will comply with the specified compositional and manufacturing provisions of ACI-349-85. As the detailed information in Section 4.6 shows, the radial extent in the concrete where the local temperature exceeds 350°F begins at the outer shell/concrete interface and ends in less than one-inch. Therefore, the potential loss in the shielding material's effectiveness is less than 4% of the concrete shielding mass in the overpack annulus.
- The metal temperature of the inner shell does not exceed 300°F at any location, which is below the accident condition temperature limit of 400°F specified in Table 2.2.3 for the inner shell.
- The presence of a stitch weld between the overpack inner shell and the overpack top plate ensures that there will be no pressure buildup in the concrete annulus due to the concrete losing water that then turns to steam.

The above summary confirms that the postulated fire event will not jeopardize the structural integrity of the HI-STORM 100 Overpack or significantly diminish its shielding effectiveness.

The above conclusions, as relevant, also apply to the HI-TRAC fire considered in Chapter 4. Water jacket over-pressurization is precluded by the safety valve set point. The non-structural effects of loss of water have been evaluated in Chapter 5 and shown to meet regulatory limits. Therefore, it is concluded that the postulated fire event will not cause significant loss in storage overpack or HI-

TRAC shielding function.

#### 3.4.4.3 Stress Calculations

This subsection presents calculations of the stresses in the different components of the HI-STORM 100 System from the effects of mechanical load case assembled in Section 3.1. Loading cases for the MPC fuel basket, the MPC enclosure vessel, the HI-STORM 100 storage overpack and the HI-TRAC transfer cask are listed in Tables 3.1.3 through 3.1.5, respectively. The load case identifiers defined in Tables 3.1.3 through 3.1.5 denote the cases considered.

The purpose of the analyses is to provide the necessary assurance that there will be no unacceptable risk of criticality, unacceptable release of radioactive material, unacceptable radiation levels, or impairment of ready retrievability of fuel from the MPC and the MPC from the HI-STORM 100 storage overpack or from the HI-TRAC transfer cask.

For all stress evaluations, the allowable stresses and stress intensities for the various HI-STORM 100 System components are based on bounding high metal temperatures to provide additional conservatism (Table 3.1.17 for the MPC basket, for example).

In addition to the loading cases germane to stress evaluations mentioned above, three cases pertaining to the stability of HI-STORM 100 are also considered (Table 3.1.1).

The results of various stress calculations on components are reported. The calculations are either performed directly as part of the text, or carried out in a separate calculation report that provides details of strength of materials evaluations or finite element numerical analysis. The specific calculations reported in this subsection are:

1. MPC stress calculations
2. HI-STORM 100 storage overpack stress calculations
3. HI-TRAC stress calculations

The MPC calculations reported in this document are complemented by analyses in the HI-STAR 100 Dockets. As noted earlier in this chapter, calculations for MPC components that are reported in HI-STAR 100 FSAR and SAR (Docket Numbers 72-1008 or 71-9261) are not repeated here unless geometry or load changes warrant reanalysis. For example, analysis of the MPC lid under normal conditions is not included in this submittal since neither the MPC lid loading nor geometry is affected by the MPC being placed in HI-TRAC or HI-STORM 100. MPC stress analyses reported herein focus on the basket and canister stress distributions due to the design basis (45g) lateral deceleration imposed by a non-mechanistic tip-over of the HI-STORM 100 storage overpack or a horizontal drop of HI-TRAC. In the submittals for the HI-STAR 100 FSAR and SAR (Docket Numbers 72-1008 and 71-9261, for storage and transport, respectively), the design basis deceleration was 60g. In this submittal the design basis deceleration is 45g. However, since the geometry of the MPC external boundary condition, viz. canister-to-storage overpack gap, has changed, a reanalysis of the MPC stresses under the lateral deceleration loads is required. This analysis is performed and the

results are summarized in this subsection.

The HI-STORM 100 storage overpack and the HI-TRAC transfer cask have been evaluated for certain limiting load conditions that are germane to the storage and operational modes specified for the system in Tables 3.1.1 and 3.1.5. The determination of component safety factors at the locations considered in the HI-STORM 100 storage overpack and in the HI-TRAC transfer cask is based on the allowable stresses permitted by the ASME Code Section III, Subsection NF for Class 3 plate and shell support structures.

#### 3.4.4.3.1 MPC Stress Calculations

The structural function of the MPC in the storage mode is stated in Section 3.1. The calculations presented here demonstrate the ability of the MPC to perform its structural function. The purpose of the analyses is to provide the necessary assurance that there will be no unacceptable risk of criticality, unacceptable release of radioactive material, or impairment of ready retrievability.

##### 3.4.4.3.1.1 Analysis of Load Cases E.3.b, E.3.c (Table 3.1.4) and F.3.b, F.3.c (Table 3.1.3)

Analyses are performed for each of the MPC designs. The following subsections describe the model, individual loads, load combinations, and analysis procedures applicable to the MPC. Unfortunately, unlike vertical loading cases, where the analyses performed in the HI-STAR 100 dockets remain fully applicable for application in HI-STORM 100, the response of the MPC to a horizontal loading event is storage overpack-geometry dependent. Under a horizontal drop event, for example, the MPC and the fuel basket structure will tend to flatten. The restraint to this flattening offered by the storage overpack will clearly depend on the difference in the diameters of the storage overpack internal cavity and that of the outer surface of the MPC. In the HI-STORM 100 storage overpack, the diameter difference is larger than that in HI-STAR 100; therefore, the external restraint to MPC ovalization under a horizontal drop event is less effective. For this reason, the MPC stress analysis for lateral loading scenarios must be performed anew for the HI-STORM 100 storage overpack; the results from the HI-STAR 100 analyses will not be conservative. The HI-TRAC transfer casks and HI-STAR 100 overpack inner diameters are identical. Therefore, the analysis of the MPC in the HI-STAR 100 overpack under 60g's for the side impact (Docket 72-1008) bounds the analysis of the MPC in the HI-TRAC under 45g's.

#### Description of Finite Element Models of the MPCs Under Lateral Loading

A finite element model of each MPC is used to assess the effects of the accident loads. The models are constructed using ANSYS [3.4.1], and they are identical to the models used in Holtec's HI-STAR 100 submittals in Docket Numbers 72-1008 and 71-9261. The following model description is common to all MPCs.

The MPC structural model is two-dimensional. It represents a one-inch long cross section of the MPC fuel basket and MPC canister.



The MPC model includes the fuel basket, the basket support structures, and the MPC shell. A basket support is defined as any structural member that is welded to the inside surface of the MPC shell. A portion of the storage overpack inner surface is modeled to provide the correct restraint conditions for the MPC. Figures 3.4.1 through 3.4.9 show typical MPC models. The fuel basket support structure shown in the figures is a multi-plate structure consisting of solid shims or support members having two separate compressive load supporting members. For conservatism in the finite element model some dual path compression members (i.e., "V" angles) are simulated as single columns. Therefore, the calculated stress intensities in the fuel basket angle supports from the finite element solution are conservatively overestimated in some locations.

The ANSYS model is not intended to resolve the detailed stress distributions in weld areas. Individual welds are not included in the finite element model. A separate analysis for basket welds and for the basket support "V" angles is performed outside of ANSYS.

No credit is taken for any load support offered by the neutron absorber panels, sheathing, and the aluminum heat conduction elements. Therefore, these so-called non-structural members are not represented in the model. The bounding MPC weight used, however, does include the mass contributions of these non-structural components.

The model is built using five ANSYS element types: BEAM3, PLANE82, CONTAC12, CONTAC26, and COMBIN14. The fuel basket and MPC shell are modeled entirely with two-dimensional beam elements (BEAM3). Plate-type basket supports are also modeled with BEAM3 elements. Eight-node plane elements (PLANE82) are used for the solid-type basket supports. The gaps between the fuel basket and the basket supports are represented by two-dimensional point-to-point contact elements (CONTAC12). Contact between the MPC shell and the storage overpack is modeled using two-dimensional point-to-ground contact elements (CONTAC26) with an appropriate clearance gap.

Two orientations of the deceleration vector are considered. The 0-degree drop model includes the storage overpack-MPC interface in the basket orientation illustrated in Figure 3.1.2. The 45-degree drop model represents the storage overpack-MPC interface with the basket oriented in the manner of Figure 3.1.3. The 0-degree and the 45-degree drop models are shown in Figures 3.4.1 through 3.4.6. Table 3.4.1 lists the element types and number of elements for current MPCs.

A contact surface is provided in the model used for drop analyses to represent the interface between the storage overpack channels and the MPC. As the MPC makes contact with the storage overpack, the MPC shell deforms to mate with the channels that are welded at equal intervals around the storage overpack inner surface. The nodes that define the elements representing the fuel basket and the MPC shell are located along the centerline of the plate material. As a result, the line of nodes that forms the perimeter of the MPC shell is inset from the real boundary by a distance that is equal to half of the shell thickness. In order to maintain the specified MPC shell/storage overpack gap dimension, the radius of the storage overpack channels is decreased by an equal amount in the model.

The three discrete components of the HI-STORM 100 System, namely the fuel basket, the MPC shell, and the storage overpack or HI-TRAC transfer cask, are engineered with small diametral clearances which are large enough to permit unconstrained thermal expansion of the three components under the rated (maximum) heat duty condition. A small diametral gap under ambient conditions is also necessary to assemble the system without physical interference between the contiguous surfaces of the three components. The required gap to ensure unrestricted thermal expansion between the basket and the MPC shell is small and will further decrease under maximum heat load conditions, but will introduce a physical nonlinearity in the structural events involving lateral loading (such as side drop of the system) under ambient conditions. It is evident from the system design drawings that the fuel basket that is non-radially symmetric is in proximate contact with the MPC shell at a discrete number of locations along the circumferences. At these locations, the MPC shell, backed by the channels attached to the storage overpack, provides a support line to the fuel basket during lateral drop events. Because the fuel basket, the MPC shell, and the storage overpack or HI-TRAC are all three-dimensional structural weldments, their inter-body clearances may be somewhat uneven at different azimuthal locations. As the lateral loading is increased, clearances close at the support locations, resulting in the activation of the support from the storage overpack or HI-TRAC.

The bending stresses in the basket and the MPC shell at low lateral loading levels which are too small to close the support location clearances are secondary stresses since further increase in the loading will activate the storage overpack's or HI-TRAC's transfer cask support action, mitigating further increase in the stress. Therefore, to compute primary stresses in the basket and the MPC shell under lateral drop events, the gaps should be assumed to be closed. However, in the analyses, we have conservatively assumed that an initial gap of 0.1875" exists, in the direction of the applied deceleration, at all support locations between the fuel basket and the MPC shell and that the clearance gap between the shell and the storage overpack at the support locations is 3/16". In the evaluation of safety factors for the MPC-24, MPC-32, and MPC-68, the total stress state produced by the applied loading on these configurations is conservatively compared with primary stress levels, even though the self-limiting stresses should be considered secondary in the strict definition of the Code. To illustrate the conservatism, we have eliminated the secondary stress (that develops to close the clearances) in the comparison with primary stress allowable values and report safety factors for the MPC-24E that are based only on primary stresses necessary to maintain equilibrium with the inertia forces.

ANSYS requires that for a static solution all bodies be constrained to prevent rigid body motion. Therefore, in the 0 degree and 45 degree drop models, two-dimensional linear spring elements (COMBIN14) join the various model components, i.e., fuel basket and enclosure vessel, at the point of initial contact. This provides the necessary constraints for the model components in the direction of the impact. By locating the springs at the points of initial contact, where the gaps remain closed, the behavior of the springs is identical to the behavior of a contact element. Linear springs and contact elements that connect the same two components have equal stiffness values.

#### Description of Individual Loads and Boundary Conditions Applied to the MPCs

---

HOLTEC INTERNATIONAL COPYRIGHTED MATERIAL

The method of applying each individual load to the MPC model is described in this subsection. The individual loads are listed in Table 2.2.14. A free-body diagram of the MPC corresponding to each individual load is given in Figures 3.4.7-3.4.9. In the following discussion, reference to vertical and horizontal orientations is made. Vertical refers to the direction along the cask axis, and horizontal refers to a radial direction.

Quasi-static structural analysis methods are used. The effects of any dynamic load factors (DLFs) are included in the final evaluation of safety factors. All analyses are carried out using the design basis decelerations in Table 3.1.2.

The MPC models used for side drop evaluations are shown in Figures 3.4.1 through 3.4.6. In each model, the fuel basket and the enclosure vessel are constrained to move only in the direction that is parallel to the acceleration vector. The storage overpack inner shell, which is defined by three nodes needed to represent the contact surface, is fixed in all degrees of freedom. The fuel basket, enclosure vessel, and storage overpack inner shell are all connected at one location by linear springs, as described in Subsection 3.4.4.3.1.1 (see Figure 3.4.1, for example). Detailed side drop evaluations here focus on an MPC within a HI-STORM 100 storage overpack. Since the analyses performed in Docket Number 72-1008 for the side drop condition in the HI-STAR 100 storage overpack demonstrates a safe condition under a 60g deceleration, no new analysis is required for the MPC and contained fuel basket and fuel during a side drop in the HI-TRAC, which is limited to a 45g deceleration (HI-TRAC and HI-STAR 100 overpacks have the same inside dimensions).

### Accelerations

During a side impact event, the stored fuel is directly supported by the cell walls in the fuel basket. Depending on the orientation of the drop, 0 or 45 degrees (see Figures 3.4.8 and 3.4.9), the fuel is supported by either one or two walls. In the finite element model this load is effected by applying a uniformly distributed pressure over the full span of the supporting walls. The magnitude of the pressure is determined by the weight of the fuel assembly, the axial length of the fuel basket support structure, the width of the cell wall, and the impact acceleration. It is assumed that the load is evenly distributed along an axial length of basket equal to the fuel basket support structure. For example, the pressure applied to an impacted cell wall during a 0-degree side drop event is calculated as follows:

$$p = \frac{a_n W}{L c}$$

where:

p = pressure

a<sub>n</sub> = ratio of the impact acceleration to the gravitational acceleration

W = weight of a stored fuel assembly

$L$  = axial length of the fuel basket support structure

$c$  = width of a cell wall

For the case of a 45-degree side drop the pressure on any cell wall equals  $p$  (defined above) divided by the square root of 2.

It is evident from the above that the effect of deceleration on the fuel basket and canister metal structure is accounted for by amplifying the gravity field in the appropriate direction.

#### Internal Pressure

Design internal pressure is applied to the MPC model. The inside surface of the enclosure vessel shell is loaded with pressure. The magnitude of the internal pressure applied to the model is taken from Table 2.2.1.

For this load condition, the center node of the fuel basket is fixed in all degrees of freedom to numerically satisfy equilibrium.

#### Temperature

Temperature distributions are developed in Chapter 4 and applied as nodal temperatures to the finite element model of the MPC enclosure vessel (confinement boundary). Maximum design heat load has been used to develop the temperature distribution used to demonstrate compliance with ASME Code stress intensity levels.

#### Analysis Procedure

The analysis procedure for this set of load cases is as follows:

1. The stress intensity and deformation field due to the combined loads is determined by the finite element solution. Results are postprocessed and tabulated in the calculation package associated with this FSAR.
2. The results for each load combination are compared to allowables. The comparison with allowable values is made in Subsection 3.4.4.4.

##### 3.4.4.3.1.2 Analysis of Load Cases E1.a and E1.c (Table 3.1.4)

Since the MPC shell is a pressure vessel, the classical Lamé's calculations should be performed to demonstrate the shell's performance as a pressure vessel. We note that dead load has an insignificant effect on this stress state. We first perform calculations for the shell under internal pressure. Subsequently, we examine the entire confinement boundary as a pressure vessel subject to both

internal pressure and temperature gradients. Finally, we perform confirmatory hand calculations to gain confidence in the finite element predictions.

The stress from internal pressure is found for normal and accident pressures conditions using classical formulas:

Define the following quantities:

$P$  = pressure,  $r$  = MPC radius, and  $t$  = shell thickness.

Using classical thin shell theory, the circumferential stress,  $\sigma_1 = Pr/t$ , the axial stress  $\sigma_2 = Pr/2t$ , and the radial stress  $\sigma_3 = -P$  are computed for both normal and accident internal pressures. The results are given in the following table (conservatively using the outer radius for  $r$ ):

<b>Classical Shell Theory Results for Normal and Accident Internal Pressures</b>				
<b>Item</b>	<b><math>\sigma_1</math> (psi)</b>	<b><math>\sigma_2</math> (psi)</b>	<b><math>\sigma_3</math> (psi)</b>	<b><math>\sigma_1 - \sigma_3</math> (psi)</b>
P= 100 psi	6838	3419	-100	6938
P= 200 psi	13675	6838	-200	13875

- Finite Element Analysis (Load Case E1.a and E1.c of Table 3.1.4)

The MPC shell, the top lid, and the baseplate together form the confinement boundary (enclosure vessel) for storage of spent nuclear fuel. In this section, we evaluate the operating condition consisting of dead weight, internal pressure, and thermal effects for the hot condition of storage. The top and bottom plates of the MPC enclosure vessel (EV) are modeled using plane axisymmetric elements, while the shell is modeled using the axisymmetric thin shell element. The thickness of the top lid varies in the different MPC types and can be either a single thick lid, or two dual lids welded around their common periphery; the minimum thickness top lid is modeled in the finite element analysis. As applicable, the results for the MPC top lid are modified to account for the fact that in the dual lid configuration, the two lids act independently under mechanical loading. The temperature distributions for all MPC constructions are nearly identical in magnitude and gradient and reflect the thermosiphon effect inside the MPC. Temperature differences across the thickness of both the baseplate and the top lid exist during HI-STORM 100's operations. There is also a thermal gradient from the center of the top lid and baseplate out to the shell wall. The metal temperature profile is essentially parabolic from the centerline of the MPC out to the MPC shell. There is also a parabolic temperature profile along the length of the MPC canister. Figure 3.4.11 shows a sketch of the confinement boundary structure with identifiers A-I locating points where temperature input data is used to represent a continuous temperature distribution for analysis purposes. The overall dimensions of the confinement boundary are also shown in the figure.

The temperatures for confinement thermal stress analysis are determined from the thermal numerical analyses supporting the results in Chapter 4. The MPC-68 is identified to have the maximum through thickness thermal gradients. For conservatism, a bounding temperature profile is defined for all MPC types and used as input for thermal stress analysis. The particular thermal inputs used are for an MPC inside of a HI-STORM 100 or 100S; the corresponding inputs for an MPC inside of a HI-STORM 100S Version B are not bounding. Because of the intimate contact between the two lid plates when the MPC lid is a two-piece unit, there is no significant thermal discontinuity through the thickness; thermal stresses arising in the MPC top lid will be bounding when there is only a single lid. Therefore, for thermal stresses, results from the analysis that considers the lid as a one-piece unit are used and are amplified to reflect the increase in stress in the dual lid configuration.

Figure 3.4.12 shows details of the finite element model of the top lid (considered as a single piece), canister shell, and baseplate. The top lid is modeled with 40 axisymmetric quadrilateral elements; the weld connecting the lid to the shell is modeled by a single element solely to capture the effect of the top lid attachment to the canister offset from the middle surface of the top lid. The MPC canister is modeled by 50 axisymmetric shell elements, with 20 elements concentrated in a short length of shell appropriate to capture the so-called "bending boundary layer" at both the top and bottom ends of the canister. The remaining 10 shell elements model the MPC canister structure away from the shell ends in the region where stress gradients are expected to be of less importance. The baseplate is modeled by 20 axisymmetric quadrilateral elements. Deformation compatibility at the connections is enforced at the top by the single weld element, and deformation and rotation compatibility at the bottom by additional shell elements between nodes 106-107 and 107-108.

The geometry of the model is listed below (terms are defined in Figure 3.4.12):

$$\begin{aligned}
 H_t &= 9.5" \text{ (the minimum total thickness lid is assumed)} \\
 R_L &= 0.5 \times 67.25" \text{ (Bill of Materials for Top Lid)} \\
 L_{MPC} &= 190.5" \text{ (Design Drawings in Section 1.5)} \\
 t_s &= 0.5" \\
 t_{BP} &= 0.5 \times 68.375" \\
 \beta &= 2\sqrt{R_s t_s} \approx 12" \text{ (the "bending boundary layer")}
 \end{aligned}$$

Stress analysis results are obtained for two cases as follows:

- a. internal pressure = 100 psi
- b. internal pressure = 100 psi plus applied temperatures

For this configuration, dead weight of the top lid acts to reduce the stresses due to pressure. For

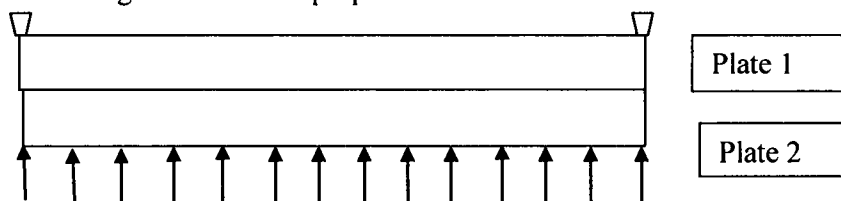
example, the equivalent pressure simulating the effect of the weight of the top lid is an external pressure of 3 psi, which reduces the pressure difference across the top lid to 97 psi. The dead weight of the top lid is neglected to provide additional conservatism in the results. The dead weight of the baseplate, however, adds approximately 0.73 psi to the effective internal pressure acting on the base. The effect of dead weight is still insignificant compared to the 100 psi design pressure, and is therefore neglected. The thermal loading in the confinement vessel is obtained by developing a parabolic temperature profile to the entire length of the MPC canister and to the top lid and baseplate. The temperature data provided at locations A-I in Figure 3.4.11 and 3.4.12 are sufficient to establish the profiles. Through-thickness temperatures are assumed linearly interpolated between top and bottom surfaces of the top lid and baseplate. Finally, in the analysis, all material properties and expansion coefficients are considered to be temperature-dependent in the model.

Results for stress intensity are reported for the case of internal pressure alone and for the combined loading of pressure plus temperature (Load Case E1.c in Table 3.1.4). Tables 3.4.7 and 3.4.8 report results at the inside and outside surfaces of the top lid and baseplate at the centerline and at the extreme radius. Canister results are reported in the "bending boundary layer" and at a location near mid-length of the MPC canister. In the tables, the calculated value is the value from the finite element analysis, the categories are  $P_m$  = primary membrane;  $P_L + P_b$  = local membrane plus primary bending; and  $P_L + P_b + Q$  = primary plus secondary stress intensity. The allowable strength value is obtained from the appropriate table in Section 3.1 for Level A conditions, and the safety factor SF is defined as the allowable strength divided by the calculated value. Allowable strengths for Alloy X are taken at 550 degrees F, 400 degrees F, and 500 degrees F, respectively, for the MPC lid, baseplate, and canister shell. The results given in Tables 3.4.7 and 3.4.8 demonstrate the ruggedness of the MPC as a confinement boundary. Since mechanically induced stresses in the top lid are increased when a dual lid configuration is considered, the stress results obtained from an analysis of a single top lid must be corrected to reflect the maximum stress state when a dual lid configuration is considered. The modifications required are based on the following logic:

Consider the case of a simply supported circular plate of thickness  $h$  under uniform lateral pressure " $q$ ". Classical strength of materials provides the solution for the maximum stress, which occurs at the center of the plate, in the form:

$$\sigma_s = 1.225q(a/h)^2 \quad \text{where } a \text{ is the radius of the plate and } h \text{ is the plate thickness.}$$

Now consider the MPC simply supported top lid as fabricated from two plates "1" and "2", of thickness  $h_1$  and  $h_2$ , respectively, where the lower surface of plate 2 is subjected to the internal pressure " $q$ ", the upper surface of plate 1 is the outer surface of the helium retention boundary, and the lower surface of plate 1 and the upper surface of plate 2 are in contact. The following sketch shows the dual lid configuration for the purposes of this discussion:



HOLTEC INTERNATIONAL COPYRIGHTED MATERIAL

From classical plate theory, if it is assumed that the interface pressure between the two plates is uniform and that both plates deform to the same central deflection, then if

$$h_1 + h_2 = h, \text{ and if } h_2/h_1 = r$$

the following relations exist between the maximum stress in the two individual plates,  $\sigma_1$ ,  $\sigma_2$  and the maximum stress  $\sigma_s$  in the single plate of thickness “h” (assuming that all three plates are the same material):

$$\frac{\sigma_1}{\sigma_s} = \frac{(1+r)^2}{(1+r^3)} \qquad \frac{\sigma_2}{\sigma_s} = \frac{(1+r)^2}{(1+r^3)} r$$

Since the two lid thicknesses are the same in the dual lid configuration,  $r = 1.0$  so that the stresses in plates 1 and 2 are both two times larger than the maximum stress computed for the single plate lid having the same total thickness. In Tables 3.4.7 and 3.4.8, bounding results for the single lid configuration are reported; a doubling of the calculated stress values (and a halving of the top lid safety factors) results when the dual lid configuration is considered.

Per the design drawings in Section 1.5, the top plate in the dual lid configuration is stainless steel (Alloy X), and the bottom plate is fabricated from stainless steel or carbon steel with a stainless steel covering. Although the top and bottom plates may be different materials, the stress amplification factor of 2, which is used to convert the results from the one-piece MPC lid to the dual lid configuration as explained above, is conservative since carbon steel has a higher Young’s modulus than stainless steel. Therefore, the carbon steel bottom plate would be stiffer, and the stress in the top plate would be less versus the dual lid configuration with stainless steel top and bottom plates.



## Evaluation of MPC Baseplate Alternate Support Configuration

The stress state in the MPC baseplate and adjacent canister is evaluated to assess the effect of the discrete support of the MPC under the action of vertical loading plus pressure and temperature. The alternate MPC supports consist of bearing pads (shims) at six locations around the periphery plus a central support to transfer vertical loads to the HI-STORM. The baseplate of the MPC has been previously analyzed under loading from the fuel basket and the fuel assemblies assuming the baseplate plate continuously supported around the periphery by the MPC canister shell (e.g., this condition arises during lifting and lowering of the MPC into the storage overpack). To evaluate the effect of a discrete support configuration, a finite element model of  $\frac{1}{2}$  of the baseplate is constructed using shell elements and includes a sufficient portion of the MPC canister to simulate the canister-to-baseplate joint and the bending boundary layer in the canister shell. Vertical loads from fuel assemblies and fuel basket are applied to the baseplate as a uniform pressure and a ring loading, respectively (these loads have been applied in the same manner in the evaluation of the baseplate under the MPC lowering condition for HI-STORM 100 system). The total vertical load is resisted at the peripheral and central discrete support locations. Under normal conditions of storage, the baseplate/canister is subject to normal service pressure and temperature plus the one-g dead weight loading. The state of stress in the MPC under design pressure and normal operating temperature has been previously considered using an axi-symmetric finite element model, and the results are discussed above (see "Finite Element Analysis") and summarized in Tables 3.4.7 and 3.4.8 (Level A condition). In Table 3.4.8, although the actual metal temperatures were used to develop the solution for the thermal stresses, the allowable stresses were conservatively chosen at the design temperature rather than at the actual operating temperature as befits a Level A analysis.

The stress intensities arising in the MPC baseplate and in the lower portion of the canister from the added vertical load are added to the previously determined stress intensities arising from internal pressure and temperature (reported in Table 3.4.8 and adjusted downward for actual service pressure) to obtain the total stress intensity for the Level A normal operating condition. The computed stress intensities are then amplified to simulate the vertical seismic event and again summed with the results from Table 3.4.8 to obtain the total stress intensity for the Level D condition.

The primary and secondary stress intensities in the MPC baseplate and canister shell are computed for the Level A normal operating condition. The maximum primary stress intensity in the MPC baseplate is also determined for the Level D vertical seismic event. All computed safety factors are above 1.0.

#### 3.4.4.3.1.3 Elastic Stability and Yielding of the MPC Basket under Compression Loads (Load Case F3 in Table 3.1.3)

This load case corresponds to the scenario wherein the loaded MPC is postulated to drop causing a compression state in the fuel basket panels.

##### a. Elastic Stability

Following the provisions of Appendix F of the ASME Code [3.4.3] for stability analysis of Subsection NG structures, (F-1331.5(a)(1)), a comprehensive buckling analysis is performed using ANSYS. For this analysis, ANSYS's large deformation capabilities are used. This feature allows ANSYS to account for large nodal rotations in the fuel basket, which are characteristic of column buckling. The interaction between compressive and lateral loading, caused by the deformation, is exactly included. Subsequent to the large deformation analysis, the basket panel that is most susceptible to buckling failure is identified by a review of the results. The lateral displacement of a node located at the mid-span of the panel is measured for the range of impact decelerations. The buckling or collapse load is defined as the impact deceleration for which a slight increase in its magnitude results in a disproportionate increase in the lateral displacement.

The stability requirement for the MPC fuel basket under lateral loading is satisfied if two-thirds of the collapse deceleration load is greater than the design basis horizontal acceleration (Table 3.1.2). This analysis was performed for the HI-STAR 100 submittal (Docket Number 72-1008) under a 60g deceleration loading. Within the HI-STAR 100 FSAR (Docket Number 72-1008), Figures 3.4.27 through 3.4.32 are plots of lateral displacement versus impact deceleration for the MPC-24, MPC-32, and MPC-68. It should be noted that the displacements (in the HI-STAR 100 FSAR) in Figures 3.4.27 through 3.4.31 are expressed in  $1 \times 10^{-1}$  inch and Figure 3.4.32 is expressed in  $1 \times 10^{-2}$  inch. The plots in the HI-STAR 100 FSAR clearly show that the large deflection collapse load of the MPC fuel basket is greater than 1.5 times the design basis deceleration for all baskets in all orientations. The results for the MPC-24E are similar. Thus, the requirements of Appendix F are met for lateral deceleration loading under Subsection NG stress limits for faulted conditions.

An alternative solution for the stability of the fuel basket panel is obtained using the methodology espoused in NUREG/CR-6322 [3.4.13]. In particular, we consider the fuel basket panels as wide plates in accordance with Section 5 of NUREG/CR-6322. We use eq.(19) in that section with the "K" factor set to the value appropriate to a clamped panel. Material properties are selected corresponding to a metal temperature of 600 degrees F which bounds computed metal temperatures at the periphery of the basket. In general, the basket periphery sees the largest loading in an impact scenario. The critical buckling stress is:

$$\sigma_{cr} = \left( \frac{\pi}{K} \right)^2 \frac{E}{12(1-\nu^2)} \left( \frac{h}{a} \right)^2$$

where  $h$  is the panel thickness,  $a$  is the unsupported panel length,  $E$  is the Young's Modulus of Alloy X at 600 degrees F,  $\nu$  is Poisson's Ratio, and  $K=0.65$  (per Figure 6 of NUREG/CR-6322).

The MPC-24 has a small  $h/a$  ratio; the results of the finite element stress analyses under design basis deceleration load show that this basket is subject to the highest compressive load in the panel. Therefore, the critical buckling load is computed using the geometry of the MPC-24. The following table shows the results from the finite element stress analysis and from the stability calculation.

Panel Buckling Results From NUREG/CR-6322			
Item	Finite Element Stress (ksi)	Critical Buckling Stress (ksi)	Factor of Safety
Stress	12.585	44.44	3.531

For a stainless steel member under an accident condition load, the recommended safety factor is 2.12. We see that the calculated safety factor exceeds this value; therefore, we have independently confirmed the stability predictions of the large deflection analysis based on classical plate stability analysis by employing a simplified method.

Stability of the basket panels, under longitudinal deceleration loading, is demonstrated in the following manner. Under 60g deceleration in Docket Number 71-9261, the axial compressive stress was computed for all fuel basket types, and the bounding result was determined as:

4,074 psi (for MPC 24E)

For the 45g design basis decelerations for HI-STORM 100, the basket axial stresses are reduced by 25%.

The above values represent the amplified weight, including the nonstructural sheathing and the neutron absorber material, divided by the bearing area resisting axial movement of the basket. To demonstrate that elastic instability is not a concern, the buckling stress for an MPC-24 flat panel is computed.

For elastic stability, Reference [3.4.8] provides the formula for critical axial stress as

$$\sigma_{cr} = \frac{4 \pi^2 E}{12 (1 - \nu^2)} \left( \frac{T}{W} \right)^2$$

where T is the panel thickness and W is the width of the panel, E is the Young's Modulus at the metal temperature and  $\nu$  is the metal Poisson's Ratio. The following table summarizes the calculation for the critical buckling stress using the formula given above:

Elastic Stability Result for a Flat Panel	
Reference Temperature	725 degrees F
T (MPC-24)	5/16 inch
W	10.777 inch
E	24,600,000 psi
Critical Axial Stress	74,781 psi

It is noted the critical axial stress is an order of magnitude greater than the computed basket axial stress reported in the foregoing and demonstrates that elastic stability under longitudinal deceleration load is not a concern for any of the fuel basket configurations.

#### b. Yielding

The safety factor against yielding of the basket under longitudinal compressive stress from a design basis inertial loading is given, using the bounding result for the MPC-24E, by

$$SF = 17,100/4,074 = 4.197$$

Therefore, plastic deformation of the fuel basket under design basis deceleration is not credible.

#### 3.4.4.3.1.4 MPC Baseplate Analysis (Load Case E2)

Minimum safety factors have been reported for Load Case E2 in Subsection 3.4.3.6 where an evaluation has been performed for stresses under three times the apparent load D\*. A bounding analysis is performed in the HI-STAR 100 FSAR (Docket Number 72-1008, Appendix 3.I) to

evaluate the stresses in the MPC baseplate during a vertical end drop (Load Case E3.a). During a fire (Load Case E5), the MPC baseplate is subjected to the accident internal pressure, dead load, and the fire temperature (which serves only to lower the allowable strengths). The results for Load Cases E3.a and E5 are summarized below:

MPC Baseplate Minimum Safety Factors – Load Cases E3.a and E5			
Item	Value (ksi)	Allowable (ksi)	Safety Factor
Center of Baseplate – Primary Bending (Load Case E3.a) (Note 1)	35.93	67.32	1.87
Center of Baseplate – Primary Bending (Load Case E5)	46.38	54.23	1.17

Notes:

1. Detailed analysis presented in Appendix 3.I of HI-STAR 100 FSAR (Docket 72-1008).

#### 3.4.4.3.1.5 Analysis of the MPC Top Closure (Load Case E2)

The FSAR for the HI-STAR 100 System (Docket Number 72-1008, Appendix 3.E) contains stress analysis of the MPC top closure during lifting. Loadings in that analysis are also valid for the HI-STORM 100 System. From Table 2.2.1, the off-normal design internal pressure is 110 psi, or ten percent greater than the normal design pressure. Whereas Level A service limits are used to establish allowables for the normal design pressure, Level B service limits are used for off-normal loads. Since Subsection NB of the ASME Code permits an identical 10% increase in allowable stress intensity values for primary stress intensities generated by Level B Service Loadings, it stands to reason that the safety factors reported for normal pressure are also valid for the case of off-normal design internal pressure.

#### 3.4.4.3.1.6 Structural Analysis of the Fuel Support Spacers (Load Case E3.a)

Upper and lower fuel support spacers are utilized to position the active fuel region of the spent nuclear fuel within the poisoned region of the fuel basket. It is necessary to ensure that the spacers will continue to maintain their structural integrity after an accident event. Ensuring structural integrity implies that the spacer will not buckle under the maximum compressive load, and that the maximum compressive stress will not exceed the compressive strength of the spacer material (Alloy X). Detailed calculations in Docket Number 72-1008, Appendix 3.J, demonstrate that large structural margins in the fuel spacers are available for the entire range of spacer lengths which may be used in HI-STORM 100 applications (for the various acceptable fuel types). The calculations for the HI-STORM 100 45g load are bounded by those for the HI-STAR 100 60g load.

#### 3.4.4.3.1.7 External Pressure (Load Case E1.b, Table 3.1.4)

The design external pressure for the MPC is zero psig. The outer surface of the MPC shell is conservatively subject to a net external pressure of 2 psig. The methodology for analysis of the MPC under this external pressure is provided in the HI-STAR 100 FSAR Docket Number 72-1008. Using the identical methodology with input loads and decelerations appropriate to the HI-STORM, safety factors > 1.0 are obtained for all relevant load cases.

#### 3.4.4.3.1.8 Miscellaneous MPC Structural Evaluations

Calculations are performed to determine the minimum fuel basket weld size, the capacity of the sheathing welds, the stresses in the MPC cover plates, and the stresses in the fuel basket supports. The following paragraphs briefly describe each of these evaluations.

The fillet welds in the fuel basket honeycomb are made by an autogenous operation that has been shown to produce highly consistent and porosity free weld lines. However, Subsection NG of the ASME Code permits only 40% quality credit on double fillet welds which can be only visually examined (Table NG-3352-1). Subsection NG, however, fails to provide a specific stress limit on such fillet welds. In the absence of a Code mandated limit, Holtec International's standard design procedure requires that the weld section possess as much load resistance capability as the parent metal section. Since the loading on the honeycomb panels is essentially that of section bending, it is possible to develop a closed form expression for the required weld throat thickness "t" corresponding to panel thickness "h".

The sheathing is welded to the fuel basket cell walls to protect and position the neutron absorber material. Force equilibrium relationships are used to demonstrate that the sheathing weld is adequate to support a 45g deceleration load applied vertically and horizontally to the sheathing and the confined neutron absorber material. The analysis assumes that the weld is continuous and then modifies the results to reflect the amplification due to intermittent welding.

The MPC cover plates are welded to the MPC lid during loading operations. The cover plates are part of the confinement boundary for the MPC. No credit is taken for the pressure retaining abilities of the quick disconnect couplings for the MPC vent and drain. Therefore, the MPC cover plates must meet ASME Code, Section III, Subsection NB limits for normal, off-normal, and accident conditions. Conservatively, the accident condition pressure loading is applied, and it is demonstrated that the Level A limits for Subsection NB are met where possible.

The fuel basket internal to the MPC canister is supported by a combination of angle fuel basket supports and flat plate or solid bar fuel basket supports. These fuel basket supports are subject to significant load only when a lateral acceleration is applied to the fuel basket and the contained fuel. The quasi-static finite element analyses of the MPC's, under lateral inertia loading, focused on the structural details of the fuel basket and the MPC shell. Basket supports were modeled in less detail, which served only to properly model the load transfer path between fuel basket and canister. Safety

factors reported for the fuel basket supports from the finite element analyses, are overly conservative, and do not reflect available capacity of the fuel basket angle support. A strength of materials analysis of the fuel basket angle supports is performed to complement the finite element results. Weld stresses in the load path are computed, direct stress in the support members is evaluated, and stability of the support legs is examined for all fuel basket support configurations.

The results of these evaluations are summarized in the tables below.

Minimum Weld Sizes for Fuel Baskets			
Basket Type	Panel Thickness (h), in	t/h Ratio	Minimum Weld Size (t), in
MPC-24	5/16	0.566	0.177
MPC-68	1/4	0.522	0.130
MPC-32	9/32	0.578	0.163
MPC-24E	5/16	0.516	0.161

Miscellaneous Stress Results for MPC			
Item	Stress (ksi)	Allowable Stress (ksi)	Safety Factor
Shear Stress in Sheathing Weld	7.724	27.93	3.62
Bending Stress in MPC Cover Plate (Level A)	14.08	25.425	1.81
Bending Stress in MPC Cover Plate (Level D)	28.16	61.02	2.17
Shear Stress in MPC Cover Plate Weld	7.55	18.99	2.52
Shear Stress in Fuel Basket Support Weld	19.78	26.67	1.35
Combined Stress in Fuel Basket Support Plates	32.393	59.1	1.82
Load in Basket Support Legs (Stability)	2.185 kips/in	8.886 kips/in	4.07

#### 3.4.4.3.1.9 Structural Integrity of Damaged Fuel Containers

The damaged fuel containers or canisters (DFCs) to be deployed in the HI-STAR 100 System transport package have been evaluated to demonstrate that the containers are structurally adequate to support the mechanical loads postulated during normal operations, while in long-term storage, and during a hypothetical end drop. The evaluations address the following damaged/failed fuel containers for transportation in the HI-STAR 100 System:

---

HOLTEC INTERNATIONAL COPYRIGHTED MATERIAL

- Holtec-designed MPC-24E (PWR) DFC
- Holtec-designed MPC-68 (BWR) DFC
- Transnuclear-designed DFC for Dresden Unit 1 fuel
- Transnuclear-designed Thoria Rod Canister for Dresden Unit 1

The structural load path in each of the analyzed containers is evaluated using basic strength of materials formulations. The various structural components are modeled as axial or bending members and their stresses are computed. Depending on the particular DFC, the load path includes components such as the container sleeve and collar, various weld configurations, load tabs, closure components and lifting bolts. Axial plus bending stresses are computed, together with applicable bearing stresses and weld stresses. Comparisons are then made with the appropriate allowable strengths at temperature. Input data for all DFCs comes from the applicable drawings. The design temperature for lifting evaluations is set at 150°F (since the DFC is in the spent fuel pool). The design temperature for accident conditions is set at 725°F.

*For those DFCs designed to be handled when loaded, the DFC lift point(s) must be designed in accordance with Item 3 in Section 5.1.6 of NUREG-0612 [3.1.1]. The remaining components of the damaged fuel container are governed by the stress limits of the ASME Code Section III, Subsection NG [3.4.10] and Section III, Appendix F [3.4.3], as applicable.*

The following table presents the minimum safety factors, from all of the stress computations, for each of the above listed DFCs.

DFC Type	Loading Condition – DFC Component	Calculated Stress (ksi)	Allowable Stress (ksi)	Safety Factor = (Allowable Stress) / (Calculated Stress)	Remarks
Holtec-designed MPC-24E (PWR) DFC					
	60g End Drop – Baseplate-to-Container Sleeve Welds	3.95	26.59	6.73	ASME Level D stress limit
Holtec-designed MPC-68 (BWR) DFC					
	60g End Drop – Baseplate-to-Container Sleeve Welds	1.59	26.59	16.7	ASME Level D stress limit
Transnuclear-designed DFC for Dresden Unit 1	Normal Lift – Lid Frame Assembly	0.527	4.583	8.70	Bearing stress
	60g End Drop – Bottom Assembly	12.32	37.92	3.08	ASME Level D stress limit
Transnuclear-designed Thoria Rod Canister for Dresden Unit 1	Normal Lift – Lid Frame Assembly	0.373	4.583	12.3	Bearing stress
	60g End Drop – Bottom Assembly	8.73	37.92	4.34	ASME Level D stress limit

HOLTEC INTERNATIONAL COPYRIGHTED MATERIAL

HI-STORM FSAR

REPORT HI-2002444

HI-STORM 100 FSAR, NON-PROPRIETARY

REVISION 12

MARCH 12, 2014

3.4-40

Rev. 10



The table above demonstrates that the DFCs are structurally adequate to support the mechanical loads postulated during normal operations and during a hypothetical end drop. Moreover, since the HI-STAR design basis handling accident bounds the corresponding load for HI-STORM (60g vs. 45g), the DFCs can be carried safely in both the HI-STAR and HI-STORM Systems.

#### 3.4.4.3.1.10 Analysis of MPC Baseplate and Closure Lid (Load Case E5)

During a fire (Load Case E5), the MPC baseplate is subjected to the accident pressure plus dead load, and the fire temperature (which serves only to lower the allowable strengths). The results of this analysis are summarized below:

MPC Baseplate Minimum Safety Factors – Load Cases E5			
Item	Value (ksi)	Allowable (ksi)	Safety Factor
Center of Baseplate – Primary Bending (Load Case E5)	46.32	54.23	1.17

The closure lid and the closure lid peripheral weld are also examined for maximum stresses developed during the storage fire. The closure lid is modeled as a single simply supported plate and is subject to dead load plus accident internal pressure. Results are presented for both the single and dual lid configuration (in parentheses). The results for minimum safety factor are reported in the table below:

MPC Top Closure Lid – Minimum Safety Factors – Load Case E5			
Item	Stress (ksi) or Load (lb.)	Allowable Stress (ksi) or Load Capacity (lb.)	Safety Factor
Lid Bending Stress – Load Case E5	3.158/(6.316)	54.225	17.17/(8.58)
Lid-to-Shell Peripheral Weld Load – Load Case E5	713,047	1,477,000 <sup>†</sup>	2.07

<sup>†</sup> Based on 0.625" single groove weld and conservatively includes a quality factor of 0.45.

We note from the above that all safety factors are greater than 1.0.

#### 3.4.4.3.2 HI-STORM 100 Storage Overpack Stress Calculations

The structural functions of the storage overpack are stated in Section 3.1. The analyses presented here demonstrate the ability of components of the HI-STORM 100 storage overpack to perform their structural functions in the storage mode. Load Cases considered are given in Table 3.1.5. The nomenclature used to identify the load cases (Load Case Identifier) considered is also given in Table 3.1.5.

The purpose of the analyses is to provide the necessary assurance that there will be no unacceptable release of radioactive material, unacceptable radiation levels, or impairment of ready retrievability of the MPC from the storage overpack. Results obtained using the HI-STORM 100 configuration are identical to or bound results for the HI-STORM 100S configuration.

3.4.4.3.2.1 HI-STORM 100 Compression Under the Static Load of a Fully Loaded HI-TRAC Positioned on the Top of HI-STORM 100 (Load Case 01 in Table 3.1.5)

During the loading of HI-STORM 100, a HI-TRAC transfer cask with a fully loaded MPC may be placed on the top of a HI-STORM 100 storage overpack. During this operation, the HI-TRAC may be held by a single-failure-proof lifting device so a handling accident is not credible. The HI-STORM 100 storage overpack must, however, possess the compression capacity to support the additional dead load. The following analysis provides the necessary structural integrity demonstration; safety factors are large and results for the HI-STORM 100 overpack are representative of the margins for the 100S and 100S Version B overpacks.

Define the following quantities for analysis purposes:

$W_{HT}$  = Bounding weight of HI-TRAC 125D (loaded w/ MPC-32) = 236,000 lb (Table 3.2.2)

$W_{MD}$  = Weight of mating device = 15,000 lb

$W_{TOTAL} = W_{HT} + W_{MD} = 251,000$  lb

The total weight of the HI-TRAC 125D plus the mating device is greater than the weight of a loaded HI-TRAC 125 with the transfer lid. Therefore, the following calculations use the weight for the HI-TRAC 125D as input.

The dimensions of the compression components of HI-STORM 100 are as follows:

outer diameter of outer shell =	$D_o = 132.5"$
thickness of outer shell =	$t_o = 0.75"$ (1" for HI-STORM 100S Version B)
outer diameter of inner shell =	$D_i = 76"$
thickness of inner shell =	$t_i = 1.25"$ (1" for HI-STORM 100S Version B)
thickness of radial ribs =	$t_r = 0.75"$ (ribs are not full-length for HI-STORM 100S Version B; HI-STORM 100S can be fabricated with full or partial length ribs)

In what follows, detailed results are provided using the classic HI-STORM 100 dimensions. While Bill of Material 1575 provides the option to fabricate the inner and outer shells from 1" thick material, the above dimensions (i.e.,  $t_o$  and  $t_i$ ) are used because they minimize the total cross sectional metal area.

The metal area of the outer shell is

$$A_o = \frac{\pi}{4} (D_o^2 - (D_o - 2t_o)^2) = \frac{\pi}{4} (132.5^2 - 131^2) \\ = 310.43 \text{ in}^2$$

The metal area of the radial ribs is

$$A_r = 4 t_r (D_o - 2 t_o - D_i) / 2 = \frac{3}{2} (131 - 76) = 82.5 \text{ in}^2$$

The metal area of the inner shell is

$$A_i = \frac{\pi}{4} (76^2 - 73.5^2) = 293.54 \text{ in}^2$$

In the HI-STORM 100, there are four radial ribs that extend full length and can carry load. For the HI-STORM 100S and the HI-STORM 100S Version B, the radial ribs are not counted as part of the compression load carrying area since they are not required to be full-length. The concrete radial shield can also support compression load. The area of concrete available to support compressive loading is

$$A_{\text{concrete}} = \frac{\pi}{4} ((D_o - 2t_o)^2 - (D_i)^2) - A_r \\ = \frac{\pi}{4} (131^2 - 76^2) - 82.5 \text{ in}^2 \\ = (8,994 - 82.5) \text{ in}^2 = 8,859.5 \text{ in}^2$$

The areas computed above are calculated at a section below the air outlet vents. To correct the above areas for the presence of the air outlet vents (HI-STORM 100 only since HI-STORM 100S and HI-STORM 100S, Version B have the air outlet vents located in the lid), we note that Bill-of-Materials 1575 in Chapter 1 gives the size of the horizontal plate of the air outlet vents as:

Peripheral width =  $w = 16.5''$

Radial depth =  $d = 27.5''$  (over concrete in radial shield)

Using these values, the following final areas are obtained:

$$A_o = A_o(\text{no vent}) - 4t_o w = 260.93 \text{ sq. inch}$$

$$A_i = A_i(\text{no vent}) - 4t_i w = 211.04 \text{ sq. inch}$$

$$A_{\text{concrete}} = A_{\text{concrete}}(\text{no vent}) - 4dw = 7044.2 \text{ sq. inch}$$

The loading case is a Level A load condition. The load is apportioned to the steel and to the concrete in accordance with the values of EA for the two materials ( $E(\text{steel}) = 28,000,000 \text{ psi}$  and  $E(\text{concrete}) = 3,605,000 \text{ psi}$ ).

$$\begin{aligned} EA(\text{steel}) &= 28 \times 10^6 \text{ psi} \times (260.93 + 211.04 + 82.5) \text{ in}^2 \\ &= 15,525.2 \text{ lb} \times 10^6 \text{ lbs.} \end{aligned}$$

$$\begin{aligned} EA(\text{concrete}) &= 3.605 \times 10^6 \times (7044.2) \text{ in}^2 \\ &= 25,394.3 \times 10^6 \text{ lb.} \end{aligned}$$

Therefore, the total HI-TRAC load will be apportioned as follows:

$$F_{\text{STEEL}} = (15,525.2 / 40,919.5) \times 251,000 = 95,231.5 \text{ lb.}$$

$$F_{\text{CONCRETE}} = (25,394.3 / 40,919.5) \times 251,000 = 155,768.5 \text{ lb.}$$

Therefore, if the load is apportioned as above, with all load-carrying components in the path acting, the compressive stress in the steel is

If we conservatively neglect the compression load bearing capacity of concrete, then

$$\sigma_{\text{STEEL}} = \frac{251,000}{554.5} = 452.7 \text{ psi}$$

If we include the concrete, then the maximum compressive stress in the concrete is:

$$\sigma_{\text{CONCRETE}} = \frac{F_{\text{CONCRETE}}}{A_{\text{CONCRETE}}} = 22.1 \text{ psi}$$

It is clear that HI-STORM 100 storage overpack can support the dead load of a fully loaded HI-TRAC 125D and the mating device placed on top for MPC transfer into or out of the HI-STORM 100 storage overpack cavity. The calculated stresses at a cross-section through the air outlet ducts are small and give rise to large factors of safety. The metal cross-section at the base of the HI-STORM storage overpack will have a slightly larger metal area (because the width of the air-inlet ducts is smaller) but will be subject to additional dead load from the weight of the supported metal components of the HI-STORM storage overpack plus the loaded HI-TRAC weight. At the base of the storage overpack, the additional stress in the outer shell and the radial plates is due solely to the

weight of the component. Based on the maximum concrete density, the additional stress in these components is computed as:

$$\Delta\sigma = (200\text{lb./cu.ft.}) \times 18.71 \text{ ft./144 sq.in./sq.ft.} = 26.0 \text{ psi}$$

This stress will be further increased by a small amount because of the material cut away by the air-inlet ducts; however, the additional stress still remains small. The inner shell, however, is subject to additional loading from the top lid of the storage overpack and from the radial shield. From the Structural Calculation Package (HI-981928)(see Subsection 3.6.4 for the reference), and from Table 3.2.1, the following weights are obtained (for conservatism, use the 100S, Version B lid weight with 200 pcf concrete even though the shell geometry is for the classic HI-STORM 100):

HI-STORM 100S, Version B Top Lid weight < 29,000 lb.

HI-STORM 100 Inner Shell weight < 19,000 lb.

HI-STORM 100 Shield Shell weight < 11,000 lb.

Note that the shield shell was removed from the HI-STORM 100 design as of June 2001. However, it is conservative to include the shield shell weight in the following calculations.

Using the calculated inner shell area at the top of the storage overpack for conservatism, gives the metal area of the inner shell as:

$$A_i = A_i(\text{no vent}) - 4t_i w = 211.04 \text{ sq. inch}$$

Therefore, the additional stress from the HI-STORM 100S, Version B storage overpack components, at the base of the overpack, is:

$$\Delta\sigma = 280 \text{ psi}$$

and a maximum compressive stress in the inner shell predicted as:

$$\text{Maximum stress} = 453 \text{ psi} + 280 \text{ psi} = 733 \text{ psi}$$

The safety factor at the base of the storage overpack inner shell (minimum section) is

$$SF = 17,500\text{psi}/733 \text{ psi} = 23.9$$

The preceding analysis is bounding for the 100 Ton HI-TRAC transfer cask because of the lower HI-TRAC weight.

The preceding analysis is representative of all overpacks since the bounding lid weight from the Version B has been used. Based on the computed safety factor, it is concluded that all versions of the HI-STORM 100 and HI-STORM 100S can safely support the heaviest HI-TRAC while performing a vertical fuel transfer operation.

#### 3.4.4.3.2.2 HI-STORM 100 Lid Integrity Evaluation (Load Case 02.c, Table 3.1.5)

A non-mechanistic tip over of the HI-STORM 100 results in high decelerations at the top of the storage overpack. The storage overpack lid diameter is less than the storage overpack outer diameter. This ensures that the storage overpack lid does not directly strike the ground but requires analysis to demonstrate that the lid remains intact and does not separate from the body of the storage overpack. Figure 3.4.19 shows the scenario.

The HI-STORM 100 overpack has two lid designs, which rely on different mechanisms to resist separation from the overpack body. The original design relies solely on the lid studs to resist the shear and axial loads on the lid. In the new design, the bolt holes are enlarged and a shear ring is welded to the underside of the lid top plate. These changes insure that the lid studs only encounter axial (tensile) loads. The in-plane load is resisted by the shear ring as it bears against the top plate. The HI-STORM 100S and the HI-STORM 100S, Version B has only one lid design, which utilizes a shear ring. Calculations have been performed for both HI-STORM 100 lid configurations, as well as the HI-STORM 100S and the HI-STORM 100S, Version B lid geometry, to demonstrate that the lid can withstand a non-mechanistic tip-over.

The deceleration level for the non-mechanistic tip-over bounds all other decelerations, directed in the plane of the lid, experienced under other accident conditions such as flood or earthquake as can be demonstrated by evaluating the loads resulting from these natural phenomena events.

It is shown that the weight of the HI-STORM 100 lid, amplified by the design basis deceleration, can be supported entirely by the shear capacity available in the four studs<sup>†</sup>. If only a single stud is loaded initially during a tipover (because of tolerances), the stud hole will enlarge rather than the stud fail in shear. Therefore, it is assured that all four bolts will resist the tipover load regardless of the initial position of the HI-STORM 100 lid.

The following tables summarize the limiting results obtained from the detailed analyses, and from the similar detailed analysis for the HI-STORM 100 lid with shear ring, for the HI-STORM 100S(243), and for the HI-STORM 100S, Version B(229). The results for the longer HI-STORM 100S and HI-STORM 100S, Version B bound the corresponding results for the shorter versions of these units.

---

<sup>†</sup> The tip-over event is non-mechanistic by definition since the HI-STORM 100 System is designed to preclude tip-over under all normal, off-normal, and accident conditions of storage, including extreme natural phenomena events. Thus, the tip-over event cannot be categorized as an operating or test condition as contemplated by ASME Section III, Article NCA-2141. The bolted connection between the overpack top lid and the overpack body provided by the top lid studs and nuts serves no structural function during normal or off-normal storage conditions, or for credible accident events. Therefore, the ASME Code does not apply to the construction of the HI-STORM top plate-to-overpack connection (the lid studs, nuts, and the through holes in the top plate). However, for conservatism, the stress limits from ASME III, Subsection NF are used for the analysis of the lid bolts.

<b>HI-STORM 100 Top Lid Integrity (No Shear Ring)</b>			
<b>Item</b>	<b>Value (ksi)</b>	<b>Allowable (ksi)</b>	<b>Safety Factor</b>
Lid Shell-Lid Top Plate Weld Shear Stress	6.733	29.4	4.367
Lid Shell-Lid Top Plate Combined Stress	9.11	29.4	3.226
Attachment Bolt Shear Stress	44.82	60.9	1.359
Attachment Bolt Combined Shear and Tension Interaction at Interface with Anchor Block	-----	-----	1.21

<b>HI-STORM 100 Top Lid Integrity (With Shear Ring)</b>			
<b>Item</b>	<b>Value (ksi)</b>	<b>Allowable (ksi)</b>	<b>Safety Factor</b>
Lid Top Plate-to-Lid Shell Weld Combined Stress	7.336	29.4	4.007
Shield Block Shells-to-Lid Top Plate Weld Combined Stress	1.768	29.4	16.63
Attachment Bolt Tensile Stress	28.02	107.13	3.823
Shear Ring-to-Lid Top Plate Weld Stress	32.11	40.39	1.258
Shear Ring Bearing Stress	25.43	63.0	2.477
Top Plate-to-Outer Shell Weld Stress	35.61	40.39	1.134

<b>HI-STORM 100S(243) Top Lid Integrity<sup>†</sup></b>			
<b>Item</b>	<b>Value (ksi)</b>	<b>Allowable (ksi)</b>	<b>Safety Factor</b>
Inner and Outer Shell Weld to Base	17.61	29.4	1.669
Shield Block Shell-to-Lid Weld Shear Stress	7.692	29.4	3.822
Attachment Bolt Tensile Stress	37.38	107.13	2.866
Shear Ring-to-Overpack Shell Weld Stress	33.24	42.0	1.264
Shear Ring Bearing Stress	19.36	63.0	3.254
Lid Shield Ring-to-Shear Ring Weld Stress	20.95	42.0	2.004

<sup>†</sup> Results are based on a bounding weight of 28,000 lb for the HI-STORM 100S top lid.

<b>HI-STORM 100S, Version B(229) Top Lid Integrity<sup>†</sup></b>			
<b>Item</b>	<b>Value (ksi)</b>	<b>Allowable (ksi)</b>	<b>Safety Factor</b>
Lid Outer Ring to Lid Shield Ring Weld	26.15	30.3	1.159
Shield Block Shell-to-Lid Weld Shear Stress	26.94	30.3	1.125
Attachment Bolt Tensile Stress	41.563	107.13	2.578
Shear Ring-to-Overpack Shell Weld Stress	30.57	42.0	1.374
Shear Ring Bearing Stress	20.59	63.0	3.06
Lid Shield Ring-to-Shear Ring Weld Stress	32.36	42.0	1.298

<sup>†</sup> Results are based on a bounding weight of 29,000 lb for the HI-STORM 100S, Version B top lid.

#### 3.4.4.3.2.3 Vertical Drop of HI-STORM 100 Storage Overpack (Load Case 02.a of Table 3.1.5)

A loaded HI-STORM 100, with the top lid in place, drops vertically and impacts the ISFSI. Figure 3.4.20 illustrates the drop scenario. The regions of the structure that require detailed examination are the storage overpack top lid, the inlet vent horizontal plate, the pedestal shield, the inlet vent vertical plate, and all welds in the load path. These components are examined for the Level D event of a HI-STORM 100 drop developing the design basis deceleration.

The table provided below summarizes the results of the analyses for the weight and configuration of the HI-STORM 100. The results for the HI-STORM 100S are bounded by the results given below. Any calculation pertaining to the pedestal is bounding since the pedestal dimensions and corresponding weights are less in the HI-STORM 100S. The HI-STORM 100S, Version B, however, has sufficient differences in configuration to merit a separate evaluation using similar analyses; therefore, a separate summary table of results is provided for the HI-STORM 100S, Version B.



<b>HI-STORM 100 Load Case 02.a Evaluation</b>			
<b>Item</b>	<b>Value (ksi)</b>	<b>Allowable (ksi)</b>	<b>Safety Factor</b>
Lid Bottom Plate Bending Stress Intensity	6.00	58.7	9.777 <sup>†</sup>
Lid Bottom Plate Collapse Load	10450x1.06 (in.*lb./in.)	12730 (in.*lb./in.)	1.15 <sup>†</sup>
Weld- lid bottom plate-to-lid shell	10.91	29.4	2.695
Lid Shell – Membrane Stress Intensity	1.90	39.1	20.58
Lid Top (2" thick) Plate Bending Stress Intensity	11.27	58.7	5.208*
Inner Shell –Membrane Stress Intensity	11.46	39.1	3.41
Outer Shell –Membrane Stress Intensity	3.401	39.1	11.495
Inlet Vent Horizontal Plate Bending Stress Intensity	46.20	58.7	1.271
Inlet Vent Vertical Plate Membrane Stress Intensity	12.86	39.1	3.04
Pedestal Shield – Compression	1.252	1.266	1.011
Weld – outer shell-to-baseplate	2.569	29.4	11.443
Weld – inner shell-to-baseplate	6.644	29.4	4.425
Weld-Pedestal shell-to-baseplate	2.281	29.4	12.887

- <sup>†</sup> Note that the dynamic load factor for the lid top plate is negligible and for the lid bottom plate is 1.06. This dynamic load factor has been incorporated in the above table.
- \* For the HI-STORM 100S, this safety factor is conservatively evaluated to be 1.357 because of increased load on the upper of the two lid plates.

Applicable analyses are performed for the HI-STORM 100S, Version B for the amplified loads resulting from the vertical drop of a fully loaded cask with the top lid in place.

<b>HI-STORM 100S, Version B Load Case 02.a Evaluation</b>			
<b>Item</b>	<b>Value (ksi)</b>	<b>Allowable (ksi)</b>	<b>Safety Factor</b>
Lid Vent Shield Bending Stress Intensity	13.09	36.0	2.75
Lid Inner Ring Compression	16.80	24.0	1.43
Inner Shell Compression	8.180	35.94	4.39
Outer Shell Compression	2.604	35.94	13.8
Weld – outer shell-to-baseplate	5.404	29.4	5.44
Weld – inner shell-to-baseplate	7.183	29.4	4.093

An assessment of the potential for instability of the compressed inner and outer shells under the compressive loading during the drop event has also been performed. The methodology is from ASME Code Case N-284 (Metal Containment Shell Buckling Design Methods, Division I, Class MC (8/80)). This Code Case has been previously accepted by the NRC as an acceptable method for evaluation of stability in vessels. The results obtained are conservative in that the loading in the shells is assumed to be uniformly distributed over the entire length of the shells. In reality, the component due to the amplified weight of the shell varies from zero at the top of the shell to the maximum value at the base of the shell. It is concluded that large factors of safety exist so that elastic or plastic instability of the inner and outer shells does not provide a limiting condition. The results for the HI-STORM 100 bound similar results for the HI-STORM 100S since the total weight of the “S” configuration is decreased (see Subsection 3.2). The same methodology has been used for an assessment of the HI-STORM 100S Version B with the same conclusion; namely, that elastic or plastic instability of the inner and outer shells is not a concern under the postulated design basis load cases.

The results do not show any gross regions of stress above the material yield point that would imply the potential for gross deformation of the storage overpack subsequent to the handling accident. MPC stability has been evaluated in the HI-STAR 100 FSAR for a drop event with 60g deceleration and shown to satisfy the Code Case N-284 criteria. Therefore, ready retrievability of the MPC is maintained as well as the continued performance of the HI-STORM 100 storage overpack as the primary shielding device.

#### 3.4.4.3.3 HI-TRAC Transfer Cask Stress Calculations

The structural functions of the transfer cask are stated in Section 3.1. The analyses presented here demonstrate the ability of components of the HI-TRAC transfer cask to perform their structural functions in the transfer mode. Load Cases considered are given in Table 3.1.5.

The purpose of the analyses is to provide the necessary assurance that there will be no unacceptable release of radioactive material, unacceptable radiation levels, or impairment of ready retrievability.

#### 3.4.4.3.3.1 Analysis of Pocket Trunnions (Load Case 01 of Table 3.1.5)

The HI-TRAC 125 and HI-TRAC 100 transfer casks have pocket trunnions attached to the outer shell and to the water jacket. During the rotation of HI-TRAC from horizontal to vertical or vice versa (see Figure 3.4.18), these trunnions serve to define the axis of rotation. The HI-TRAC is also supported by the lifting trunnions during this operation. Two load conditions are considered: Level A when all four trunnions support load during the rotation; and, Level B when the hoist cable is assumed slack so that the entire load is supported by the rotation trunnions. A dynamic amplification of 15% is assumed in both cases appropriate to a low-speed operation. Figure 3.4.23 shows a free body of the trunnion and shows how the applied force and moment are assumed to be resisted by the weld group that connects the trunnion to the outer shell. Drawings 1880 (sheet 10) and 2145 (sheet 10) show the configuration. An optional construction for the HI-TRAC 100 permits the pocket trunnion base to be split to reduce the “envelope” of the HI-TRAC. For that construction, bolts and dowel pins are used to insure that the force and moment applied to the pocket trunnions are transferred properly to the body of the transfer cask. The analysis also evaluates the bolts and dowel pins and demonstrates that safety factors greater than 1.0 exist for bolt loads, dowel bearing and tear-out, and dowel shear. Allowable strengths and loads are computed using applicable sections of ASME Section III, Subsection NF.

Unlike the HI-TRAC 125 and the HI-TRAC 100, the HI-TRAC 125D and HI-TRAC 100D are designed and fabricated without pocket trunnions. An L-shaped rotation frame is used to upend and downend the HI-TRAC 125D and HI-TRAC 100D, instead of pocket trunnions. Thus, a pocket trunnion analysis is not applicable to the HI-TRAC 125D or the HI-TRAC 100D.

The table below summarizes the results for the HI-TRAC 125 and the HI-TRAC 100:

Pocket Trunnion Weld Evaluation Summary			
Item	Value (ksi)	Allowable (ksi) <sup>†</sup>	Safety Factor
HI-TRAC 125 Pocket Trunnion-Outer Shell Weld Group Stress	7.979	23.275	2.917
HI-TRAC 125 Pocket Trunnion-Water Jacket Weld Group Stress	5.927	23.275	3.9
HI-TRAC 100 Pocket Trunnion-Outer Shell Weld Group Stress	6.603	23.275	3.525
HI-TRAC 100 Pocket Trunnion-Water Jacket Weld Group Stress	5.244	23.275	4.438
HI-TRAC 100 Pocket Trunnion-Bolt Tension at Optional Split	45.23	50.07	1.107
HI-TRAC 100 Pocket Trunnion-Bearing Stress on Base Surfaces at Dowel	6.497	32.7	5.033
HI-TRAC 100 Pocket Trunnion-Tear-out Stress on Base Surfaces at Dowel	2.978	26.09	8.763
HI-TRAC 100 Pocket Trunnion-Shear Stress on Dowel Cross Section at Optional Split	29.04	37.93	1.306

<sup>†</sup> Allowable stress is reported for the Level B loading, which results in the minimum safety factor.

To provide additional information on the local stress state adjacent to the rotation trunnion, a new finite element analysis is undertaken to provide details on the state of stress in the metal structure surrounding the rotation trunnions for the HI-TRAC 125. The finite element analysis has been based on a model that includes major structural contributors from the water jacket enclosure shell panels, radial channels, end plates, outer and inner shell, and bottom flange. In the finite element analysis, the vertical trunnion load has been oriented in the direction of the HI-TRAC 125 longitudinal axis. The structural model has been confined to the region of the HI-TRAC adjacent to the rotation trunnion block; the extent of the model in the longitudinal direction has been determined by calculating the length of the “bending boundary layer” associated with a classical shell analysis. This was considered to be a sufficient length to capture maximum shell stresses arising from the Level B (off-normal) rotation trunnion loading. The local nature of the stress around the trunnion block is clearly demonstrated by the finite element results.

Consistent with the requirements of ASME Section III, Subsection NF, for Class 3 components, safety factors for primary membrane stress have been computed. Primary stresses are located away from the immediate vicinity of the trunnion; although the NF Code sets no limits on primary plus secondary stresses that arise from the gross structural discontinuity immediately adjacent to the trunnion, these stresses are listed for information. The results are summarized in the table below for the Level B load distribution for the HI-TRAC 125.

ITEM –HI-TRAC 125	CALCULATED VALUE	ALLOWABLE VALUE
Longitudinal Stress - (ksi) (Primary Stress – Inner Shell)	-0.956	23.275
Tangential Stress (ksi) (Primary Stress - Inner Shell)	-1.501	23.275
Longitudinal Stress (ksi) (Primary Stress – Outer Shell)	-0.830	23.275
Tangential Stress (ksi) (Primary Stress - Outer Shell)	-0.436	23.275
Longitudinal Stress - (ksi) (Primary Stress – Radial Channels)	2.305	23.275
Tangential Stress (ksi) (Primary Stress - Radial Channels)	-0.631	23.275
Longitudinal Stress - (ksi) (Primary plus Secondary Stress -Inner Shell)	1.734	No Limit (34.9)*
Tangential Stress (ksi) (Primary plus Secondary Stress - Inner Shell)	-1.501	NL
Longitudinal Stress (ksi) (Primary plus Secondary Stress - Outer Shell)	2.484	NL
Tangential Stress (ksi) (Primary plus Secondary Stress - Outer Shell)	-2.973	NL
Longitudinal Stress - (ksi) (Primary plus Secondary Stress - Radial Channels)	-13.87	NL
Tangential Stress (ksi) (Primary plus Secondary Stress - Radial Channels)	-2.303	NL

\* The NF Code sets no limits (NL) for primary plus secondary stress (see Table 3.1.17). Nevertheless, to demonstrate the robust design with its large margins of safety, we list here, for information only, the allowable value for Primary Membrane plus Primary Bending Stress appropriate to temperatures up to 650 degrees F.

The only stress of any significance is the longitudinal stress in the radial channels. This stress occurs immediately adjacent to the trunnion block/radial channel interface and by its localized nature is identifiable as a stress arising at the gross structural discontinuity (secondary stress).

The finite element analysis has also been performed for the HI-TRAC 100 transfer cask. The following table summarizes the results:

ITEM –HI-TRAC 100	CALCULATED VALUE	ALLOWABLE VALUE
Longitudinal Stress - (ksi) (Primary Stress –Inner Shell)	-0.756	23.275
Tangential Stress (ksi) (Primary Stress - Inner Shell)	-2.157	23.275
Longitudinal Stress (ksi) (Primary Stress – Outer Shell)	-0.726	23.275
Tangential Stress (ksi) (Primary Stress - Outer Shell)	-0.428	23.275
Longitudinal Stress - (ksi) (Primary Stress – Radial Channels)	2.411	23.275
Tangential Stress (ksi) (Primary Stress - Radial Channels)	-0.5305	23.275
Longitudinal Stress - (ksi) (Primary plus Secondary Stress - Inner Shell)	2.379	NL
Tangential Stress (ksi) (Primary plus Secondary Stress - Inner Shell)	-2.157	NL
Longitudinal Stress (ksi) (Primary plus Secondary Stress - Outer Shell)	3.150	NL
Tangential Stress (ksi) (Primary plus Secondary Stress - Outer Shell)	-3.641	NL
Longitudinal Stress - (ksi) (Primary plus Secondary Stress - Radial Channels)	-15.51	NL
Tangential Stress (ksi) (Primary plus Secondary Stress - Radial Channels)	-2.294	NL

The finite element analyses of the metal structure adjacent to the trunnion block did not include the state of stress arising from the water jacket internal pressure. These stresses are conservatively computed based on a two-dimensional strip model that neglects the lower annular plate. The water jacket bending stresses are summarized below:

<b>Tangential Bending Stress in Water Jacket Outer Panel from Water Pressure (including hydrostatic and inertia effects)</b>	<b>Calculated Value (ksi)</b>
HI-TRAC 125	14.18
HI-TRAC 100	13.63

To establish a minimum safety factor for the outer panels of the water jacket for the Level A condition, we must add primary membrane circumferential stress from the trunnion load analysis to primary circumferential bending stress from the water jacket bending stress. Then, the safety factors may be computed by comparison to the allowable limit for primary membrane plus primary bending stress. The following results are obtained:

<b>Results for Load Case 01 in Water Jacket (Load Case 01) – Level A Load</b>			
<b>Circumferential Stress in Water Jacket Outer Enclosure</b>	<b>CALCULATED VALUE (ksi)</b>	<b>ALLOWABLE VALUE (ksi)</b>	<b>SAFETY FACTOR (allowable value/calculated value)</b>
HI-TRAC 125	14.57	26.25	1.80
HI-TRAC 100	13.94	26.25	1.88

To arrive at minimum safety factors for primary membrane plus bending stress in the outer panel of the water jacket for the Level B condition, we amplify the finite element results the trunnion load analysis, add the appropriate stress from the two-dimensional water jacket calculation, and compare the results to the increased Level B allowable. The following results are obtained:

<b>Results for Load Case 01 in Water Jacket (Load Case 01) – Level B Load</b>			
<b>Circumferential Stress in Water Jacket Outer Enclosure</b>	<b>CALCULATED VALUE (ksi)</b>	<b>ALLOWABLE VALUE (ksi)</b>	<b>SAFETY FACTOR (allowable value/calculated value)</b>
HI-TRAC 125	14.81	35.0	2.36
HI-TRAC 100	14.16	35.0	2.47

All safety factors are greater than 1.0; the Level A load condition governs.

#### 3.4.4.3.3.2 Lead Slump in HI-TRAC 125 - Horizontal Drop Event (Case 02.b in Table 3.1.5)

During a side drop of the HI-TRAC 125 transfer cask, the lead shielding must be shown not to slump and cause significant amounts of shielding to be lost in the top area of the lead annulus. Slumping of the lead is not considered credible in the HI-TRAC transfer cask because of:

- a. the shape of the interacting surfaces
- b. the ovalization of the shell walls under impact
- c. the high coefficient of friction between lead and steel
- d. The inertia force from the MPC inside the HI-TRAC will compress the inner shell at the impact location and locally “pinch” the annulus that contains the lead; this opposes the tendency for the lead to slump and open up the annulus at the impact location.

Direct contact of the outer shell of the HI-TRAC with the ISFSI pad is not credible since there is a water jacket that surrounds the outer shell. The water jacket metal shell will experience most of the direct impact. Nevertheless, to conservatively analyze the lead slump scenario, it is assumed that there is no water jacket, the impact occurs far from either end of the HI-TRAC so as to ignore any strengthening of the structure due to end effects, the impact occurs directly on the outer shell of the HI-TRAC, and the contact force between HI-TRAC and the MPC is ignored. All of these assumptions are conservative in that their imposition magnifies any tendency for the lead to slump.

To confirm that lead slump is not credible, a finite element analysis of the lead slump problem, incorporating the conservatisms listed above, during a postulated HI-TRAC 125 horizontal drop (see Figure 3.4.22) is carried out. The HI-TRAC 125 cask body modeled consists only of an inner steel shell, an outer steel shell, and a thick lead annulus shield contained between the inner and outer shell.

A unit length of HI-TRAC is modeled and the contact at the lead/steel interface is modeled as a compression-only interface. Interface frictional forces are conservatively neglected. As the HI-TRAC 125 has a greater lead thickness, analysis of the HI-TRAC 125 is considered to bound the HI-TRAC 100 and the HI-TRAC 100D. Furthermore, since there are no differences between the HI-TRAC 125 and the HI-TRAC 125D with respect to the finite element model, the results are valid for both 125-Ton transfer casks.

The analysis is performed in two parts:

First, to maximize the potential for lead/steel separation, the shells are ignored and the gap elements grounded. This has the same effect as assuming the shells to be rigid and maximizes the potential and magnitude of any separation at the lead/steel interface (and subsequent slump). This also maximizes the contact forces at the portion of the interface that continues to have compression forces developed. The lead annulus is subjected to a 45g deceleration and the deformation, stress field, and interface force solution developed. This solution establishes a conservative result for the movement of the lead relative to the metal shells.

In the second part of the analysis, the lead is removed and replaced by the conservative (high)



interface forces from the first part of the analysis. These interface forces, together with the 45g deceleration-induced inertia forces from the shell self weight are used to obtain a solution for the stress and deformation field in the inner and outer metal shells.

The results of the analysis are as follows:

- a. The maximum predicted lead slump at a location 180 degrees from the impact point is 0.1". This gap decreases gradually to 0.0" after approximately 25 degrees from the vertical axis. The decrease in the diameter of the inner shell of the transfer cask (in the direction of the deceleration) is approximately 0.00054". This demonstrates that ovalization of the HI-TRAC shells does not occur. Therefore, the lead shielding deformation is confined to a local region with negligible deformation of the confining shells.
- b. The stress intensity distribution in the shells demonstrates that high stresses are concentrated, as anticipated, only near the assumed point of impact with the ISFSI pad. The value of the maximum stress intensity (51,000 psi) remains below the allowable stress intensity for primary membrane plus primary bending for a Level D event (58,700 psi). Thus, the steel shells continue to perform their function and contain the lead. The stress distribution, obtained using the conservatively large interface forces, demonstrates that permanent deformation could occur only in a localized region near the impact point. Since the "real" problem precludes direct impact with the outer shell, the predicted local yielding is simply a result of the conservatism imposed in the model.

It is concluded that a finite element analysis of the lead slump under a 45g deceleration in a side drop clearly indicates that there is no appreciable change in configuration of the lead shielding and no overstress of the metal shell structure. Therefore, retrievability of the MPC is not compromised and the HI-TRAC transfer cask continues to provide shielding.

#### 3.4.4.3.3.3 HI-TRAC Lid Stress Analysis During HI-TRAC Drop Accident (Load Case 02.b in Table 3.1.5)

The stress in the HI-TRAC 125 transfer lid is analyzed when the lid is subject to the deceleration loads of a side drop Figure 3.4.22 is a sketch of the scenario. The analysis shows that the cask body, under a deceleration of 45g's, will not separate from the transfer lid during the postulated side drop. This event is considered a Level D event in the ASME parlance.

The bolts that act as doorstops to prevent opening of the doors are also checked for their load capacity. It is required that sufficient shear capacity exists to prevent both doors from opening and exposing the MPC.

The only difference between the HI-TRAC 100 and the HI-TRAC 125 transfer lid doors is that the HI-TRAC 100 has less lead and has no middle steel plate. A similar analysis of the HI-TRAC 100

shows that all safety factors are greater than 1.0. The table given below summarizes the results for both units:

<b>Transfer Lid Attachment Integrity Under Side Drop</b>			
<b>Item – Shear Capacity</b>	<b>Value (kip) or (ksi)</b>	<b>Capacity (kip) or (ksi)</b>	<b>Safety Factor= Capacity/Value</b>
HI-TRAC 125 Attachment (kip)	1,272.0	1,475.0	1.159
HI-TRAC 125 Door Lock Bolts (ksi)	20.24	48.3	2.387
HI-TRAC 100 Attachment (kip)	1,129.0	1,503.0	1.331
HI-TRAC 100 Door Lock Bolts (ksi)	13.81	48.3	3.497

All safety factors are greater than 1.0 and are based on actual interface loads. For the HI-TRAC 125 and the HI-TRAC 100, the interface load (primary impact at transfer lid) computed from the handling accident analysis is bounded by the values given below:

<b>BOUNDING INTERFACE LOADS COMPUTED FROM HANDLING ACCIDENT ANALYSES</b>	
<b>Item</b>	<b>Bounding Value (kip)</b>
HI-TRAC 125	1,300
HI-TRAC 100	1,150

The HI-TRAC 125D and HI-TRAC 100D transfer casks do not utilize a transfer lid. Instead, the MPC is transferred to or from a storage overpack using the HI-TRAC pool lid and a special mating device. Therefore, an analysis is performed to demonstrate that the pool lid will not separate from the cask body during the postulated side drop. The results of the analyses are summarized in the following tables for the HI-TRAC 125D and the HI-TRAC 100D.

<b>HI-TRAC 125D Pool Lid Attachment Integrity Under Side Drop</b>			
<b>Item</b>	<b>Calculated Value</b>	<b>Allowable Limit</b>	<b>Safety Factor</b>
Lateral Shear Force (kips)	562.5	1085	1.929
Maximum Bolt Tensile Stress (ksi)	2.548	116.7	45.8
Combined Tension and Shear Interaction	0.269	1.00	3.72

HOLTEC INTERNATIONAL COPYRIGHTED MATERIAL

<b>HI-TRAC 100D Pool Lid Attachment Integrity Under Side Drop</b>			
<b>Item</b>	<b>Calculated Value</b>	<b>Allowable Limit</b>	<b>Safety Factor</b>
Lateral Shear Force (kips)	360.0	1085	3.015
Maximum Bolt Tensile Stress (ksi)	1.477	116.7	79.0
Combined Tension and Shear Interaction	0.11	1.00	9.08

#### 3.4.4.3.3.4 Stress Analysis of the HI-TRAC Water Jacket (Load Case 03 in Table 3.1.5)

The water jacket is assumed subject to internal pressure from pressurized water and gravity water head. Calculations are performed for the HI-TRAC 125, the HI-TRAC 125D, the HI-TRAC 100, and the HI-TRAC 100D to determine the water jacket stress under internal pressure plus hydrostatic load. Results are obtained for the water jacket configuration and the connecting welds for all HI-TRAC transfer casks. The table below summarizes the results of the analyses.

<b>Water Jacket Stress Evaluation</b>			
<b>Item</b>	<b>Value (ksi)</b>	<b>Allowable (ksi)</b>	<b>Safety Factor</b>
HI-TRAC 125 Water Jacket Enclosure Shell Panel Bending Stress	14.18	26.25	1.851
HI-TRAC 100 Water Jacket Enclosure Shell Panel Bending Stress	13.63	26.25	1.926
HI-TRAC 125 Water Jacket Bottom Flange Bending Stress	18.3	26.25	1.434
HI-TRAC 100 Water Jacket Bottom Flange Bending Stress	16.92	26.25	1.551
HI-TRAC 125 Weld Stress – Bottom Flange to Outer Shell Double Fillet Weld	14.79	21.0	1.42
HI-TRAC 125 - Radial Rib Direct Stress	2.198	17.5	7.961
HI-TRAC 100 - Radial Rib Direct Stress	1.975	17.5	8.861
HI-TRAC 125D Water Jacket Bottom Flange Bending Stress	18.88	26.25	1.39
HI-TRAC 125D Water Jacket Enclosure Shell Panel Bending Stress	10.80	26.25	2.43
HI-TRAC 125D Weld Stress – Enclosure Panel to Radial Rib Plug Welds	1.093	17.5	16.01
HI-TRAC 125D Weld Stress – Bottom Flange to Outer Shell Single Fillet Weld	3.133	21.0	6.70
HI-TRAC 100D Water Jacket Bottom Flange Bending Stress	16.69	26.25	1.57
HI-TRAC 100D Water Jacket Enclosure Shell Panel Bending Stress	12.75	26.25	2.06

HOLTEC INTERNATIONAL COPYRIGHTED MATERIAL

HI-STORM FSAR

REPORT HI-2002444

HI-STORM 100 FSAR, NON-PROPRIETARY

REVISION 12

MARCH 12, 2014

3.4-59

Rev. 10

HI-TRAC 100D Weld Stress – Enclosure Panel to Radial Rib Plug Welds	0.680	17.5	25.7
HI-TRAC 100D Weld Stress – Bottom Flange to Outer Shell Single Fillet Weld	2.836	21.0	7.40

#### 3.4.4.3.3.5 HI-TRAC Top Lid Separation (Load Case 02.b in Table 3.1.5)

The potential of top lid separation under a 45g deceleration side drop event requires evaluation. It is concluded by analysis that the connection provides acceptable protection against top lid separation. It is also shown that the bolts and the lid contain the MPC within the HI-TRAC cavity during and after a drop event. The results from the HI-TRAC 125 bound the corresponding results from the HI-TRAC 100 because the top lid bolts are identical in the two units and the HI-TRAC 125 top lid weighs more. The analysis also bounds the HI-TRAC 125D and the HI-TRAC 100D because the postulated side drop of the HI-TRAC 125, during which the transfer lid impacts the target surface, produces a larger interface load between the MPC and the top lid of the HI-TRAC than the nearly horizontal drop of the HI-TRAC 125D and the HI-TRAC 100D. The table below provides the results of the bounding analysis.

<b>HI-TRAC Top Lid Separation Analysis</b>			
<b>Item</b>	<b>Value</b>	<b>Capacity</b>	<b>Safety Factor= Capacity/Value</b>
Attachment Shear Force (lb.)	123,750	957,619	7.738
Tensile Force in Stud (lb.)	132,000	1,117,222	8.464
Bending Stress in Lid (ksi)	35.56	58.7	1.65
Shear Load per unit Circumferential Length in Lid (lb./in)	533.5	29,400	55.10

#### 3.4.4.4 Comparison with Allowable Stresses

Consistent with the formatting guidelines of Reg. Guide 3.61, calculated stresses and stress intensities from the finite element and other analyses are compared with the allowable stresses and stress intensities defined in Subsection 3.1.2.2 per the applicable sections of [3.4.2] and [3.4.4] for defined normal and off-normal events and [3.4.3] for accident events (Appendix F).

##### 3.4.4.4.1 MPC

In Amendment #5 to the HI-STORM CoC, the weight limits for fuel assemblies to be stored in the MPCs were increased from 1,680 lbs to 1,720 lbs per assembly for PWR fuel and from 700 lbs to 730 lbs per assembly for BWR fuel. In order to account for this small increase in fuel weight, the

results of the MPC stress analysis under lateral loading, which is described in Subsection 3.4.4.3.1.1, are uniformly scaled based on the percentage weight increase. Specifically, the results for the MPC-68 are scaled by a factor of 1.043 ( $=730/700$ ) and results for the other MPCs are scaled by a factor of 1.024 ( $=1720/1680$ ). This approach is acceptable because (i) the finite element analysis results are based on linear elastic material properties and (ii) the percentage increases in total weight, considering the stored fuel, fuel basket, and MPC shell, are less than the factors above. Finally, since the stresses associated with closing the support clearance gaps between the fuel basket and the MPC shell and between the MPC shell and the overpack are secondary stress components, as explained in Subsection 3.4.4.3.1.1, the use of a linear scale factor is an appropriate means of computing the primary stresses in the fuel basket and MPC shell.

Table 3.4.6 provides summary data extracted from the numerical analysis results for the fuel basket, enclosure vessel, and fuel basket supports after scaling to adjust for the increased fuel assembly weights. The results presented in Table 3.4.6 are based on the design basis deceleration and do not include any dynamic amplification due to internal elasticity of the structure (i.e., local inertia effects). Calculations suggest that a uniform conservative dynamic amplifier for the fuel basket would be 1.08 independent of the duration of impact. If we recognize that the tip-over event for HI-STORM 100 is a long duration event, then a dynamic amplifier of 1.04 is appropriate. The summary data provided in Table 3.4.3 and 3.4.4 gives the lowest safety factor computed for the fuel basket and for the MPC, respectively. Safety factors reported for the MPC shell in Table 3.4.4 are based on allowable strengths at 500 deg. F. Modification of the fuel basket safety factor for dynamic amplification leaves considerable margin. Factors of safety greater than 1 indicate that calculated results are less than the allowable strengths.

A perusal of the results in Tables 3.4.3 and 3.4.4 under different load combinations for the fuel basket and the enclosure vessel reveals that all factors of safety are above 1.0 even if we use the most conservative value for dynamic amplification factor. The relatively modest factor of safety in the fuel basket under side drop events (Load Case F3.b and F3.c) in Table 3.4.3 warrants further explanation since a very conservative finite element model of the structure has been utilized in the analysis.

The wall thickness of the storage cells, which is by far the most significant variable in a fuel basket's structural strength, is significantly greater in the MPCs than in comparable fuel baskets licensed in the past. For example, the cell wall thickness in the TN-32 basket (Docket No. 72-1021, M-56), is 0.1 inch and that in the NAC-STC basket (Docket No. 71-7235) is 0.048 inch. In contrast, the cell wall thickness in the MPC-68 is 0.25 inch. In spite of their relatively high flexural rigidities, computed margins in the fuel baskets are rather modest. This is because of some assumptions in the analysis that lead to an overstatement of the state of stress in the fuel basket. For example:

- i. The section properties of longitudinal fillet welds that attach contiguous cell walls to each other are completely neglected in the finite element model (Figure 3.4.7). The fillet welds strengthen the cell wall section modulus at the very locations where maximum stresses develop.
- ii. The radial gaps at the fuel basket-MPC shell and at the MPC shell-storage overpack

interface are explicitly modeled. As the applied loading is incrementally increased, the MPC shell and fuel basket deform until a "rigid" backing surface of the storage overpack is contacted, making further unlimited deformation under lateral loading impossible. Therefore, some portion of the fuel basket and enclosure vessel (EV) stress has the characteristics of secondary stresses (which by definition, are self-limited by deformation in the structure to achieve compatibility). For conservativeness in the incremental analysis, we make no distinction between deformation controlled (secondary) stress and load controlled (primary) stress in the stress categorization of the MPC-24, 32, and 68 fuel baskets. We treat all stresses, regardless of their origin, as primary stresses. Such a conservative interpretation of the Code has a direct (adverse) effect on the computed safety factors. As noted earlier, the results for the MPC-24E are properly based only on primary stresses to illustrate the conservatism in the reporting of results for the MPC-24, 32, and 68 baskets.

- iii. A uniform pressure simulates the SNF inertia loading on the cell panels, which is a most conservative approach for incorporating the SNF/cell wall structure interaction.

The above assumptions act to depress the computed values of factors of safety in the fuel basket finite element analysis and render conservative results.

The reported factors of safety do not include the effect of dynamic load amplifiers. The duration of impact and the predominant natural frequency of the basket panels under drop events result in the dynamic load factors that do not exceed 1.08. Therefore, since all reported factors of safety for all fuel basket types are greater than the DLF, the MPC is structurally adequate for its intended functions.

Tables 3.4.7 and 3.4.8 report stress intensities and safety factors for the confinement boundary subject to internal pressure alone and internal pressure plus the normal operating condition temperature with the most severe thermal gradient. The final values for safety factors in the various locations of the confinement boundary provide assurance that the MPC enclosure vessel is a robust pressure vessel.

#### 3.4.4.4.2 Storage Overpack and HI-TRAC

The result from analyses of the storage overpack and the HI-TRAC transfer cask is shown in Table 3.4.5. The location of each result is indicated in the table. Safety factors for lifting operations where three times the lifted load is applied are reported in Section 3.4.3.

The table shows that all allowable stresses are much greater than their associated calculated stresses and that safety factors are above the limit of 1.0.

#### 3.4.4.5 Elastic Stability Considerations

##### 3.4.4.5.1 MPC Elastic Stability

Stability calculations for the MPC have been carried out in the HI-STAR 100 FSAR, Docket Number 72-1008. Using identical methodology with input loads and decelerations appropriate to the HI-STORM, safety factors  $> 1.0$  are obtained for all relevant load cases. Note that for HI-STORM, the design external pressure differential is reduced to 0.0 psi, and the peak deceleration under accident events is reduced from 60g's (HI-STAR) to 45g's.

##### 3.4.4.5.2 HI-STORM 100 Storage Overpack Elastic Stability

HI-STORM 100 (and 100S and the 100S Version B) storage overpack shell buckling is not a credible scenario since the two steel shells plus the entire radial shielding act to resist vertical compressive loading. Subsection 3.4.4.3.2.3 develops values for compressive stress in the steel shells of the storage overpack. Because of the low value for compressive stress coupled with the fact that the concrete shielding backs the steel shells, we can conclude that instability is unlikely. Note that the entire weight of the storage overpack can also be supported by the concrete shielding acting in compression. Therefore, in the unlikely event that a stability limit in the steel was approached, the load would simply shift to the massive concrete shielding. Notwithstanding the above comments, stability analyses of the storage overpack have been performed for bounding cases of longitudinal compressive stress with nominal circumferential compressive stress and for bounding circumferential compressive stress with nominal axial compressive stress. This latter case is for a bounding all-around external pressure on the HI-STORM 100 outer shell. The latter case is listed as Load Case 05 in Table 3.1.5 and is performed to demonstrate that explosions or other environmental events that could lead to an all-around external pressure on the outer shell do not cause a buckling instability. ASME Code Case N-284, a methodology accepted by the NRC, has been used for this analysis. The storage overpack shells for the HI-STORM 100 are examined individually assuming that the four radial plates provide circumferential support against a buckling deformation mode. The analysis of the storage overpack outer shell for a bounding external pressure of

$$p_{\text{ext}} = 30 \text{ psi}$$

together with a nominal compressive axial load that bounds the dead weight load at the base of the outer shell, gives a safety factor against an instability of:

$$\text{Safety Factor} = (1/0.466) \times 1.34 = 2.88$$

The factor 1.34 is included in the above result since the analysis methodology of Code Case N-284 builds in this factor for a stability analysis for an accident condition. The suite of stability analyses have also been performed for the HI-STORM 100S Version B. No credit is taken for any support provided by the concrete shielding and the effect of support by radial ribs is conservatively neglected (since the ribs in the HI-STORM 100S Version B do not extend the full height of the overpack). It is shown that the safety factor computed for the classic HI-STORM 100 is a lower bound for all of the

HI-STORM 100S versions.

The external pressure for the overpack stability considered here significantly bounds the short-time 10-psi differential pressure (between outer shell and internal annulus) specified in Table 2.2.1.

The same postulated external pressure condition can also act on the HI-TRAC during movement from the plant to the ISFSI pad. In this case, the lead shielding acts as a backing for the outer shell of the HI-TRAC transfer cask just as the concrete does for the storage overpack. The water jacket metal structure provides considerable additional structural support to the extent that it is reasonable to state that instability under external pressure is not credible. If it is assumed that the all-around water jacket support is equivalent to the four locations of radial support provided in the storage overpack, then it is clear that the instability result for the storage overpack bounds the results for the HI-TRAC transfer cask. This occurs because the R/t ratio (mean radius-to-wall thickness) of the HI-TRAC outer shell is less than the corresponding ratio for the HI-STORM storage overpack. Therefore, no HI-TRAC analysis is performed.

#### 3.4.5 Cold

A discussion of the resistance to failure due to brittle fracture is provided in Subsection 3.1.2.3.

The value of the ambient temperature has two principal effects on the HI-STORM 100 System, namely:

- i. The steady-state temperature of all material points in the cask system will go up or down by the amount of change in the ambient temperature.
- ii. As the ambient temperature drops, the absolute temperature of the contained helium will drop accordingly, producing a proportional reduction in the internal pressure in accordance with the Ideal Gas Law.

In other words, the temperature gradients in the system under steady-state conditions will remain the same regardless of the value of the ambient temperature. The internal pressure, on the other hand, will decline with the lowering of the ambient temperature. Since the stresses under normal storage condition arise principally from pressure and thermal gradients, it follows that the stress field in the MPC under -40 degree F ambient would be smaller than the "heat" condition of storage, treated in the preceding subsection. Additionally, the allowable stress limits tend to increase as the component temperatures decrease.

Therefore, the stress margins computed in Section 3.4.4 can be conservatively assumed to apply to the "cold" condition as well.

Finally, it can be readily shown that the HI-STORM 100 System is engineered to withstand "cold" temperatures (-40 degrees F), as set forth in the Technical Specification, without impairment of its storage function.



Unlike the MPC, the HI-STORM 100 storage overpack is an open structure; it contains no pressure. Its stress field is unaffected by the ambient temperature, unless low temperatures produce brittle fracture due to the small stresses which develop from self-weight of the structure and from the minute difference in the thermal expansion coefficients in the constituent parts of the equipment (steel and concrete). To prevent brittle fracture, all steel material in HI-STORM 100 is qualified by impact testing as set forth in the ASME Code (Table 3.1.18).

The structural material used in the MPC (Alloy X) is recognized to be completely immune from brittle fracture in the ASME Codes.

As no liquids are included in the HI-STORM 100 storage overpack design, loads due to expansion of freezing liquids are not considered. The HI-TRAC transfer cask utilizes demineralized water in the water jacket. However, the specified lowest service temperature for the HI-TRAC is 0 degrees F and a 25% ethylene glycol solution is required for the temperatures from 0 degrees F to 32 degrees F. Therefore, loads due to expansion of freezing liquids are not considered.

There is one condition, however, that does require examination to insure ready retrievability of the fuel. Under a postulated loading of an MPC from a HI-TRAC transfer cask into a cold HI-STORM 100 storage overpack, it must be demonstrated that sufficient clearances are available to preclude interference when the "hot" MPC is inserted into a "cold" storage overpack. To this end, a bounding analysis for free thermal expansions has been performed in Subsection 4.4.6, wherein the MPC shell is postulated at its maximum design basis temperature and the thermal expansion of the overpack is ignored. The results from the evaluation of free thermal expansion are summarized in Table 4.4.10. The final radial clearance (greater than 0.25" radial) is sufficient to preclude jamming of the MPC upon insertion into a cold HI-STORM 100 storage overpack.

#### 3.4.6 HI-STORM 100 Kinematic Stability under Flood Condition (Load Case A in Table 3.1.1)

The flood condition subjects the HI-STORM 100 System to external pressure, together with a horizontal load due to water velocity. Because the HI-STORM 100 storage overpack is equipped with ventilation openings, the hydrostatic pressure from flood submergence acts only on the MPC. As stated in subsection 3.1.2.1.1.3, the design external pressure for the MPC bounds the hydrostatic pressure from flood submergence. Subsection 3.4.4.5.2 has reported a positive safety factor against instability from external pressure in excess of that expected from a complete submergence in a flood. The analysis performed below is also valid for the HI-STORM 100S and the HI-STORM 100S, Version B.

The water velocity associated with flood produces a horizontal drag force, which may act to cause sliding or tip-over. In accordance with the provisions of ANSI/ANS 57.9, the acceptable upper bound flood velocity,  $V$ , must provide a minimum factor of safety of 1.1 against overturning and sliding. For HI-STORM 100, we set the upper bound flood velocity design basis at 15 feet/sec. Subsequent

calculations conservatively assume that the flow velocity is uniform over the height of the storage overpack.

The overturning horizontal force,  $F$ , due to hydraulic drag, is given by the classical formula:

$$F = C_d A V^*$$

where:

$V^*$  is the velocity head =  $\frac{\rho V^2}{2g}$ ; ( $\rho$  is water weight density, and  $g$  is acceleration due to gravity).

$A$ : projected area of the HI-STORM 100 cylinder perpendicular to the fluid velocity vector.

$C_d$ : drag coefficient

The value of  $C_d$  for flow past a cylinder at Reynolds number above  $5E+05$  is given as 0.5 in the literature (viz. Hoerner, Fluid Dynamics, 1965).

The drag force tending to cause HI-STORM 100's sliding is opposed by the friction force, which is given by

$$F_f = \mu K W$$

where:

$\mu$  = limiting value of the friction coefficient at the HI-STORM 100/ISFSI pad interface (conservatively taken as 0.25, although literature citations give higher values).

$K$  = buoyancy coefficient (documented in HI-981928, Structural Calculation Package for HI-STORM 100 (see citation in Subsection 3.6.4).

$W$ : Minimum weight of HI-STORM 100 with an empty MPC.

### Sliding Factor of Safety

The factor of safety against sliding,  $\beta_1$ , is given by

$$\beta_1 = \frac{F_f}{F} = \frac{\mu K W}{C_d A V^*}$$

It is apparent from the above equation,  $\beta$ , will be minimized if the empty weight of HI-STORM 100

is used in the above equation.

As stated previously,  $\mu = 0.25$ ,  $C_d = 0.5$ .

$V^*$  corresponding to 15 ft./sec. water velocity is 218.01 lb per sq. ft.

$A = \text{length} \times \text{diameter of HI-STORM 100} = 132.5" \times 231.25"/144 \text{ sq. in./sq.ft.} = 212.78 \text{ sq. ft.}$

$K = \text{buoyancy factor} = 0.64$  (per calculations in HI-981928)

$W = \text{empty weight of overpack w/ lid} = 270,000 \text{ lbs.}$  (Table 3.2.1)

Substituting in the above formula for  $\beta$ , we have

$$\beta_1 = 1.86 > 1.1 \text{ (required)}$$

Since the weight of the HI-STORM 100S or HI-STORM 100S, Version B, plus the weight of an empty MPC-32 (i.e., the lightest MPC) is greater than 270,000 lb, the above calculation is also valid for these two units for the entire range of concrete densities.

#### Overturning Factor of Safety

For determining the margin of safety against overturning  $b_2$ , the cask is assumed to pivot about a fixed point located at the outer edge of the contact circle at the interface between HI-STORM 100 and the ISFSI. The overturning moment due to a force  $F_T$  applied at height  $H^*$  is balanced by a restoring moment from the reaction to the cask buoyant force  $KW$  acting at radius  $D/2$ .

$$F_T H^* = KW \frac{D}{2}$$

$$F_T = \frac{K W D}{2 H^*}$$

$W$  is the empty weight of the storage overpack.

We have,

$$W = 270,000 \text{ lb. (Table 3.2.1)}$$

$$H^* = 119.2" \text{ (maximum height of mass center per Table 3.2.3)}$$

$$D = 132.5" \text{ (Holtec Drawing 1495)}$$

$$K = 0.64 \text{ (calculated in HI-981928)}$$

$$F_T = 96,040 \text{ lb.}$$

$F_T$  is the horizontal drag force at incipient tip-over.

$$F = C_d A V^* = 23,194 \text{ lbs. (drag force at 15 feet/sec)}$$

The safety factor against overturning,  $\beta_2$ , is given as:

$$\beta_2 = \frac{F_T}{F} = 4.14 > 1.1 \text{ (required)}$$

This result bounds the result for the HI-STORM 100S, for the HI-STORM 100S Version B, as well as for the densified concrete shielding option, since the calculation uses a conservative lower bound weight and a bounding height for the center of gravity.

In the next subsection, results are presented to show that the load  $F$  (equivalent to an inertial deceleration of  $F/360,000 \text{ lb} = 0.0644 \text{ g's}$  applied to the loaded storage overpack) does not lead to large global circumferential stress or ovalization of the storage overpack that could prevent ready retrievability of the MPC. It is shown in Subsection 3.4.7 that a horizontal load equivalent to  $0.47\text{g's}$  does not lead to circumferential stress levels and ovalization of the HI-STORM storage overpack to prevent ready retrievability of the MPC. The load used for that calculation clearly bounds the side load induced by flood.

### 3.4.7 Seismic Event and Explosion - HI-STORM 100

#### 3.4.7.1 Seismic Event (Load Case C in Table 3.1.1)

##### Overturning Analysis

The HI-STORM 100 System plus its contents may be assumed to be subject to a seismic event consisting of three orthogonal statistically independent acceleration time-histories. For the purpose of performing a conservative analysis to determine the maximum ZPA that will not cause incipient tipping, the HI-STORM 100 System is considered as a rigid body subject to a net horizontal quasi-static inertia force and a vertical quasi-static inertia force. This is consistent with the approach used in previously licensed dockets. The vertical seismic load is conservatively assumed to act in the most unfavorable direction (upwards) at the same instant. The vertical seismic load is assumed to be equal to or less than the net horizontal load with  $\epsilon$  being the ratio of vertical component to one of the horizontal components. For use in calculations, define  $D_{\text{BASE}}$  as the contact patch diameter, and  $H_{\text{CG}}$  as the height of the centroid of an empty HI-STORM 100 System (no fuel). Conservatively, assume

$$D_{\text{BASE}} = 132.5" \text{ (Drawing 1495, Sheet 1 specifies 133.875" including overhang for welding)}$$

Tables 3.2.1 and 3.2.3 give HI-STORM 100 weight data and center-of-gravity heights.

The weights and center-of-gravity heights are reproduced here for calculation of the composite center-of-gravity height of the storage overpack together with an empty MPC.

<u>Weight (pounds)</u>	<u>C.G. Height (Inches); H</u>
Overpack - $W_o = 270,000$	116.8
MPC-24 - $W_{24} = 42,000$	$109.0 + 24 = 133.0^\dagger$
MPC-68 - $W_{68} = 39,000$	$111.5 + 24 = 135.5$
MPC-32 - $W_{32} = 36,000$	$113.2 + 24 = 137.2$
MPC-24E - $W_{24E} = 45,000$	$108.9 + 24 = 132.9$

The height of the composite centroid,  $H_{CG}$ , is determined from the equation

$$H_{cg} = \frac{W_o \times 116.8 + W_{MPC} \times H}{W_o + W_{MPC}}$$

Performing the calculations for all of the MPCs gives the following results:

<u><math>H_{cg}</math> (inches)</u>	
MPC-24 with storage overpack	118.98
MPC-68 with storage overpack	119.16
MPC-32 with storage overpack	119.20
MPC-24E with storage overpack	119.10

A conservative overturning stability limit is achieved by using the largest value of  $H_{CG}$  (call it  $H$ ) from the above. Because the HI-STORM 100 System is a radially symmetric structure, the two horizontal seismic accelerations can be combined vectorially and applied as an overturning force at the C.G. of the cask. The net overturning static moment is

$$WG_H H$$

where  $W$  is the total system weight and  $G_H$  is the resultant zero period acceleration seismic loading (vectorial sum of two orthogonal seismic loads) so that  $WG_H$  is the inertia load due to the resultant horizontal acceleration. The overturning moment is balanced by a vertical reaction force, acting at the outermost contact patch radial location  $r = D_{BASE}/2$ . The resistive moment is minimized when the vertical zero period acceleration  $G_V$  tends to reduce the apparent weight of the cask. At that instant,

<sup>†</sup> From Table 3.2.3, it is noted that MPC C.G. heights are measured from the base of the MPC. Therefore, the thickness of the overpack baseplate and the concrete MPC pedestal must be added to determine the height above ground.

the moment that resists "incipient tipping" is:

$$W (1 - G_v) r$$

Performing a static moment balance and eliminating W results in the following inequality to ensure a "no-overturning condition:

$$G_H + \frac{r}{H} G_v \leq \frac{r}{H}$$

Using the values of r and H for the HI-STORM 100 (r = 66.25", H = 119.20"), representative combinations of G<sub>H</sub> and G<sub>V</sub> that satisfy the limiting equality relation are computed and tabulated below:

Acceptable Net Horizontal G-Level (HI-STORM100), G <sub>H</sub>	Acceptable Vertical G-Level, G <sub>V</sub>
0.467	0.16
0.445	0.20
0.417	0.25
0.357	0.357

We repeat the above computations using the weight and c.g. location of the HI-STORM 100S(232). Because of the lowered center of gravity positions, the maximum net horizontal "G" levels are slightly increased.

Performing the calculations for all of the MPCs gives the following results:

H<sub>cg</sub> (inches)

MPC-24 with storage overpack	113.89
MPC-68 with storage overpack	114.07
MPC-32 with storage overpack	114.11
MPC-24E with storage overpack	114.01

Using the values of r and H for the HI-STORM 100S(232) (r = 66.25", H = 114.11"), representative combinations of G<sub>H</sub> and G<sub>V</sub> that satisfy the limiting equality relation are computed and tabulated below:

Acceptable Net Horizontal G-Level (HI-STORM 100S(232)), $G_H$	Acceptable Vertical G-Level, $G_V$
0.488	0.16
0.464	0.20
0.435	0.25
0.367	0.367

The limiting values of  $G_H$  and  $G_V$  for the HI-STORM 100S(243), which is taller than the HI-STORM 100S(232), are the same as the HI-STORM 100.

If the HI-STORM 100 or the HI-STORM 100S is fabricated using high density concrete (i.e., above 160.8 pcf dry), the C.G. height of the overpack decreases and thereby enables the cask system to withstand higher g-loads. This conclusion becomes immediately clear when the maximum acceptable vertical g-level is expressed in the following form:

$$G_V = 1 - \frac{H}{r} G_H$$

For fixed values of  $G_H$  and  $r$ , the value of  $G_V$  increases as  $H$  decreases. Therefore, the representative combinations of  $G_H$  and  $G_V$  given above for the HI-STORM 100 and the HI-STORM 100S are conservative for the densified concrete shielding option.

Since the HI-STORM 100S, Version B has further reduced the centroid of the loaded units, it is expected that acceptable G-Levels are further increased. The following calculations provide the limiting G-level combinations for the HI-STORM 100S Version B with standard weight concrete. As noted previously, the result for standard weight concrete will bound the corresponding result for the high density concrete (densified) shielding option.

We repeat the above computations using the weight and c.g. location of the HI-STORM 100S(218). Because of the lowered center of gravity positions, the maximum net horizontal "G" levels are slightly increased.

Performing the calculations for all of the MPCs gives the following results:

$H_{cg}$  (inches)

MPC-24 with storage overpack	109.88
MPC-68 with storage overpack	110.12
MPC-32 with storage overpack	110.23
MPC-24E with storage overpack	109.93

HOLTEC INTERNATIONAL COPYRIGHTED MATERIAL

Using the values of  $r$  and  $H$  for the HI-STORM 100S, Version B(218) ( $r = 66.25"$ ,  $H = 110.23"$ ), representative combinations of  $G_H$  and  $G_V$  that satisfy the limiting equality relation are computed and tabulated below:

Acceptable Net Horizontal G-Level (HI-STORM 100S, Version B(218)), $G_H$	Acceptable Vertical G-Level, $G_V$
0.505	0.16
0.481	0.20
0.451	0.25
0.376	0.375

The limiting values of  $G_H$  and  $G_V$  for the HI-STORM 100S, Version B(229), which is taller than the HI-STORM 100S, Version B(218), are bounded by the values listed for the HI-STORM 100.

#### Primary Stresses in the HI-STORM 100 Structure Under Net Lateral Load Over 180 degrees of the Periphery

Under a lateral loading, the storage overpack will experience axial primary membrane stress in the inner and outer shells as it resists bending as a "beam-like" structure. Under the same kind of lateral loading over one-half of the periphery of the cylinder, the shells will tend to ovalize under the loading and develop circumferential stress. Calculations for stresses in both the axial and circumferential direction are required to demonstrate satisfaction of the Level D structural integrity requirements and to provide confidence that the MPC will be readily removable after a seismic event, if necessary. An assessment of the stress state in the structure under the seismic induced load will be shown to bound the results for any other condition that induces a peripheral load around part of the HI-STORM 100 storage overpack perimeter. The specific analyses are performed using the geometry and loading for the HI-STORM 100; the results obtained for stress levels and the safety assessment are also applicable to an assessment of the HI-STORM 100S.

A simplified calculation to assess the flexural bending stress in the HI-STORM 100 structure under the limiting seismic event (at which tipping is incipient) is presented in the following:

A representative net horizontal acceleration of  $0.47g$  is used to determine the primary stresses in the HI-STORM 100 storage overpack. The corresponding lateral seismic load,  $F$ , is given by

$$F = 0.47 W$$

This load will be maximized if the upper bound HI-STORM 100 weight ( $W = 410,000$  lbs. (Table 3.2.1)) is used. Accordingly,



$$F = (0.47) (410,000) = 192,700 \text{ lbs.}$$

No dynamic amplification is assumed as the overpack, considered as a beam, has a natural frequency well into the rigid range.

The moment,  $M$ , at the base of the HI-STORM 100 due to this lateral force is given by

$$M = \frac{F H}{2}$$

where  $H$  = height of HI-STORM 100 (taken conservatively as 235 inches). Note that the loading has now been approximated as a uniform load acting over the full height of the cask.

The flexural stress,  $\sigma$ , is given by the ratio of the moment  $M$  to the section modulus of the steel shell structure,  $z$ , which is computed to be 12,640 in<sup>3</sup> for the HI-STORM 100 overpack with inner and outer shell thicknesses of 1-1/4" and 3/4", respectively. The use of this value is conservative since the steel section modulus associated with the optional 1" thick inner and outer shell design is slightly higher.

Therefore,

$$\sigma = \frac{(192,700) (235)}{(12,640) (2)} = 1,791 \text{ psi}$$

We note that the strength of concrete has been neglected in the above calculation.

The maximum axial stress in the storage overpack shell will occur on the "compressive" side where the flexural bending stress algebraically sums with the direct compression stress  $\sigma_d$  from vertical compression.

From the representative acceleration tables, the vertical seismic accelerations corresponding to the net 0.47g horizontal acceleration is below 0.25g.

Therefore, using the maximum storage overpack weight (bounded by 410,000 lbs. from data in Table 3.2.1)

$$\sigma_d = \frac{(410,000) (1.25)}{554.47} = 924 \text{ psi}$$

where 554.47 sq. inch is the metal area (cross section) of the steel structure in the HI-STORM 100 storage overpack as computed in Subsection 3.4.4.3.2.1. The total axial stress, therefore, is

$$\sigma_T = 1,791 + 924 = 2,715 \text{ psi}$$

Per Table 3.1.12, the allowable membrane stress intensity for a Level D event is 39,750 psi at 350 degrees F.

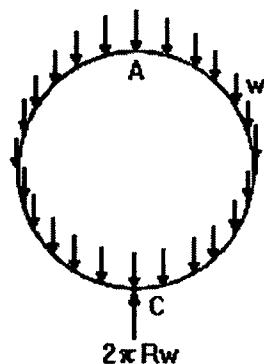
The Factor of Safety,  $\beta$ , is, therefore

$$\beta = \frac{39,750}{2,715} = 14.6$$

Examination of the stability calculations for the overpack outer shell under a 45-g vertical end drop demonstrates that no instability will result from this compressive load induced by a seismic or other environmental load leading to bending of the storage overpack as a beam.

The previous calculation has focused on the axial stress in the members developed assuming that the storage overpack does not overturn but resists the lateral load by remaining in contact with the ground and bending like a beam. Since the lateral loading is only over a portion of the periphery, there is also the potential for this load to develop circumferential stress in the inner and outer shells to resist ovalization of the shells. To demonstrate continued retrievability of the MPC after a seismic event, it must be shown that either the stresses remain in the elastic range or that any permanent deformation that develops due to plasticity does not intrude into the MPC envelope after the event is ended. In the following subsection, classical formulas for the deformation of rings under specified surface loadings are used to provide a conservative solution for the circumferential stresses in the HI-STORM 100. Specifically, the solution for a point-supported ring subject to a gravitational induced load, as depicted in the sketch below, is implemented. This solution provides a conservative estimate of the circumferential stress and the deformation of the ring that will develop under the actual applied seismic load.

Ring supported at base and loaded by its own weight,  $w$ , given per unit circumferential length.



The solution considers the geometry and load appropriate to a unit length of the inner and outer shells of the HI-STORM 100 storage overpack with a total weight equal to the overpack bounding weight (no MPC) subject to a 45g deceleration inertial loading. The numerical results for the 45g tipover event can be directly applied here by multiplying by the factor "X", where "X" reflects the differences in the deceleration and the weights used for the tipover event and for the seismic load case here in this subsection.

$$X = (0.47g/45g) \times (410,000\text{lb.}/270,000\text{lb.}) = 0.0159$$

Using this factor on the tipover solution gives the following bounding results for maximum stresses (without regard for sign and location of the stress) and deformations:

$$\text{Maximum circumferential stress due to bending moment} = (29,310 \text{ psi} \times X) = 466 \text{ psi}$$

$$\text{Maximum circumferential stress due to mean tangential force} = (18,900 \text{ lb.}/2 \text{ sq.inch}) \times X = 150.3 \text{ psi}$$

$$\text{Change in diameter in the direction of the load} = -0.11'' \times X = -0.0017''$$

$$\text{Change in diameter perpendicular to the direction of the load} = +0.06'' \times X = 0.0010''$$

From the above results, it is clear that no permanent ovalization of the storage overpack occurs during the seismic event and that circumferential stresses will remain elastic and are bounded by the stresses computed based on considering the storage overpack as a simple beam. Therefore, the safety factors based on maximum values of axial stress are appropriate. The magnitudes of the diameter changes that are suggested by the ring solution clearly demonstrate that ready retrievability of the MPC is maintained after the seismic event.

Because of the low values for the calculated axial stress, the conclusions of the previous section are also valid for the HI-STORM 100S, and for the HI-STORM 100S, Version B.

#### Potential for Concrete Cracking

It can be readily shown that the concrete shielding material contained within the HI-STORM 100 structure will not crack due to the flexuring action of HI-STORM 100 during a bounding seismic event that leads to a maximum axial stress in the storage overpack. For this purpose, the maximum axial strain in the steel shell is computed by dividing the tensile stress developed by the seismic G forces (for the HI-STORM 100, for example) by the Young's Modulus of steel.

$$\zeta = \frac{1,791 - 858}{28 \text{ E}+06} = 33.3 \text{ E}-06$$

where the Young's Modulus of steel is taken from Table 3.3.2 at 350 degrees F.

The acceptable concrete strain in tension is estimated from information in ACI-318.1 for plain concrete. The ratio of allowable tensile stress to concrete Young' Modulus is computed as

$$\text{Allowable Concrete Strain} = (5 \times (0.75) \times (f)^{1/2}) / (57,000(f)^{1/2}) = 65.8\text{E-}06$$

In the above expression,  $f$  is the concrete compressive strength.

Therefore, we conclude that considerable margins against tensile cracking of concrete under the bounding seismic event exist.

### Sliding Analysis

An assessment of sliding of the HI-STORM 100 System on the ISFSI pad during a postulated seismic event is performed using a one-dimensional "slider block on friction supported surface" dynamic model. The results for the shorter HI-STORM 100S are comparable. The HI-STORM 100 is simulated as a rigid block of mass ' $m$ ' placed on a surface, which is subject to a sinusoidal acceleration of amplitude ' $a$ '. The coefficient of friction of the block is assumed to be reduced by a factor  $\alpha$  to recognize the contribution of vertical acceleration in the most adverse manner (vertical acceleration acts to reduce the downward force on the friction interface). The equation of motion for such a "slider block" is given by:

$$m\ddot{x} = R + m a \sin \omega t$$

where:

$\ddot{x}$ : relative acceleration of the slider block (double dot denotes second derivative of displacement ' $x$ ' in time)

$a$ : amplitude of the sinusoidal acceleration input

$\omega$ : frequency of the seismic input motion (radians/sec)

$t$ : time coordinate

$R$  is the resistive Coulomb friction force that can reach a maximum value of  $\mu(mg)$  ( $\mu$  = coefficient of friction) and which always acts in the direction of opposite to  $\dot{x}(t)$ .

Solution of the above equation can be obtained by standard numerical integration for specified values of  $m$ ,  $a$ ,  $\alpha$  and  $\mu$ . The calculation is performed for representative horizontal and vertical accelerations of 0.47g and 0.16g, respectively. The input values are summarized below.

$$a = 0.47g$$

---

HOLTEC INTERNATIONAL COPYRIGHTED MATERIAL

$$\alpha = 0.84 = 1 - \text{vertical acceleration } (= 0.16g)$$

$$m = 360,000 \text{ lbs/g}$$

$$\mu = 0.25$$

For establishing the appropriate value of  $\omega$ , reference is made to the USAEC publication TID-7024, "Nuclear Reactor and Earthquakes", page 35, 1963, which states that the significant energy of all seismic events in the U.S. essentially lies in the range of 0.4 to 10 Hz. Taking the mid-point value

$$\omega = (6.28) (0.5) (0.4+10) = 32.7 \text{ rad/sec.}$$

The numerical solution of the above equation yields the maximum excursion of the slider block  $x_{\max}$  as 0.12 inches, which is negligible compared to the spacing between casks.

Calculations performed at lower values of  $\omega$  show an increase in  $x_{\max}$  with reducing  $\omega$ . At 1 Hz, for example,  $x_{\max} = 3.2$  inches. It is apparent from the above that there is a large margin of safety against inter-module collision within the HI-STORM 100 arrays at an ISFSI, where the minimum installed spacing is over 2 feet (Table 1.4.1).

The above dynamic analysis indicates that the HI-STORM 100 System undergoes minimal lateral vibration under a seismic input with net horizontal ZPA g-values as high as 0.47 even under a bounding (from below) low interface surface friction coefficient of 0.25. Data reported in the literature (ACI-349R (97), Commentary on Appendix B) indicates that values of the coefficient of friction,  $\mu$ , as high as 0.7 are obtained at steel/concrete interfaces.

To ensure against unreasonably low coefficients of friction, the ISFSI pad design may require a "broom finish" at the user's discretion. The bottom surface of the HI-STORM 100 is manufactured from plate stock (i.e. non-machine finish). A coefficient of friction value of 0.53 is considered to be a conservative numerical value for the purpose of ascertaining the potential for incipient sliding of the HI-STORM 100 System. If a higher value is used, the coefficient of friction is required to be verified by test (see Table 2.2.9).

The relationship between the vertical ZPA,  $G_V$ , (conservatively assumed to act opposite to the normal gravitational acceleration), and the resultant horizontal ZPA  $G_H$  to insure against incipient sliding is given from static equilibrium considerations as:

$$G_H + \mu G_V \leq \mu$$

Using a conservative value of  $\mu$  equal to 0.53, the above relationship provides governing ZPA limits for a HI-STORM 100 (or 100S) System arrayed in a freestanding configuration. The table below gives representative combinations that meet the above limit.

$G_H$ (in g's)	$G_V$ (in g's)
0.445	0.16
0.424	0.20
0.397	0.25
0.350	0.34

Since the sliding inequality is independent of the weight and centroid of the cask system, the results above remain valid for HI-STORM overpacks with high density concrete and with different heights.

If the values for the DBE event at an ISFSI site satisfy the above inequality relationship for incipient sliding with coefficient of friction equal to 0.53, then the non-sliding criterion set forth in NUREG-1536 is assumed to be satisfied a priori. However, if the ZPA values violate the inequality by a small amount, then it is permissible to satisfy the non-sliding criterion by implementing measures to roughen the HI-STORM 100/ISFSI pad interface to elevate the value of  $\mu$  to be used in the inequality relation. To demonstrate that the value of  $\mu$  for the ISFSI pad meets the required value implied by the above inequality, a series of Coulomb friction tests (under the QA program described in Chapter 13) shall be performed as follows:

Pour a concrete block with horizontal dimensions no less than 2' x 2' and a block thickness no less than 0.5'. Finish the top surface of the block in the same manner as the ISFSI pad surface will be prepared.

Prepare a 6" x 6" x 2" SA516 Grade 70 plate specimen (approximate weight = 20.25 lb.) to simulate the bottom plate of the HI-STORM 100 overpack. Using a calibrated friction gage attached to the steel plate, perform a minimum of twenty (20) pull tests to measure the static coefficient of friction at the interface between the concrete block and the steel plate. The pull tests shall be performed on at least ten (10) different locations on the block using varying orientations for the pull direction.

The coefficient of friction to be used in the above sliding inequality relationship will be set as the average of the results from the twenty tests.

The satisfaction of the "no-sliding" criterion set down in the foregoing shall be carried out along with the "no-overturning" qualification (using the static moment balance method in the manner described at the beginning of this subsection) and documented as part of the ISFSI facility's 10CFR72.212 evaluation.

#### Alternative Evaluation of Overturning and Sliding

In this subsection, an evaluation of the propensity for the free standing cask to be in a state of either incipient overturning or incipient sliding has been performed using a simple static analysis that is independent of time phasing of the input acceleration time histories and considers only the Zero Period Acceleration (ZPA) obtained from the response spectra. For both incipient overturning and incipient sliding, the following inequality must be satisfied to ensure satisfaction of the static criteria.

$$G_H + \mu G_V \leq \mu$$

For the incipient overturning evaluation,  $\mu$ =(radius of cask base/height to loaded cask center-of-gravity). For the incipient sliding evaluation,  $\mu$ = Coulomb coefficient of friction =0.53 at the cask/ISFSI pad interface (unless testing justifies use of a higher value). The inequality has been derived assuming that the cask is resting on a flat and level surface that is subject to a seismic event characterized by a response spectra set with the net horizontal and vertical Zero Period Acceleration (ZPA) denoted by  $G_H$  and  $G_V$ , respectively.

This “screening” evaluation provides a conservative criterion to insure that top-of-pad acceleration time histories from the aggregate effect of soil structure interaction and free field acceleration would not predict initiation of overturning or sliding. If on-the-pad acceleration time histories are available, the applicable inequality (for overturning and sliding) may be satisfied at each time instant during the Design Basis Earthquake with  $G_H$  and  $G_V$  representing coincident values of the magnitude of the net horizontal and vertical acceleration vectors.

#### 3.4.7.2 Explosion (Load Case 05 in Table 3.1.5)

In the preceding subsection, it has been demonstrated that incipient tipping of the storage overpack will not occur under a side load equal to 0.47 times the weight of the cask. For a fully loaded cask with high density concrete, this side load is equal to

$$F = 192,700 \text{ lb.}$$

If it is assumed that this side load is uniformly distributed over the height of the cask and that the cask centroid is approximately at the half-height of the overpack, then an equivalent pressure,  $P$ , acting over 180 degrees of storage overpack periphery, can be defined as follows:

$$P \times (DH) = F$$

Where  $D$  = overpack outside diameter, and  $H$  = minimum height of a storage overpack (HI-STORM 100S Version B(218)).

For  $D = 132.5''$  and  $H = 218''$ , the equivalent pressure is

$$P = 192,700 \text{ lb}/(132.5'' \times 218'') = 6.67 \text{ psi}$$

Therefore, establishing 5 psi as the design basis steady state pressure differential (Table 2.2.1) across the overpack diameter is reasonable.

Since the actual explosion produces a transient wave, the use of a static incipient tip calculation is very conservative. To evaluate the margin against tip-over from a short-time pressure pulse, a Working Model analysis of the two-dimensional dynamic motion of the HI-STORM subject to a given initial angular velocity is carried out. Figures 3.4.25 and 3.4.26 provide details of the model and the solution for a HI-STORM 100 System (simulated as a rigid body) having a weight and inertia property appropriate to a minimum weight cask of height  $H=235''$ . The results show that an initial angular velocity of 0.626 radians/second does not lead to a tipover of the storage overpack. The results bound those obtained for the HI-STORM 100S(232) and for the HI-STORM 100S Version B (229) since the overall cask height is reduced. The results for the HI-STORM 100S(243) are roughly equal to the results for the HI-STORM 100 since the differences in height and weight are negligible. The results for the HI-STORM 100S Version B will be bounded by the results presented because of lower centroid location.

Continuing, the initial angular velocity can be related to a square wave pressure pulse of magnitude  $P$  and time duration  $T$  by the following formula:

$$I\omega = (P \times D \times H) \times (0.5 \times H) \times T$$

The above formula relates the change in angular motion resulting from an impulsive moment about the base of the overpack.  $D$  is the diameter of the outer shell,  $H$  is the height of the storage overpack, and  $I$  is the mass moment of inertia of the storage overpack about the mass center (assumed to be at half-height). For  $D=132.5''$ ,  $H=235''$ ,  $P=10$  psi,  $T=1$  second, and  $I=64,277,000$  lb.inch sec<sup>2</sup>, the resulting initial angular velocity is:

$$\omega = 0.569 \text{ radians/second}$$

Therefore, an appropriate short time pressure limit is 10 psi with pulse duration less than or equal to 1 second. Table 2.2.1 sets this as the short-time external pressure differential.

The overpack is also qualified to sustain without tip-over a lateral impulse load of 60 psi (differential pressure for 85 milliseconds maximum) [3.4.5].

The analysis in Subsection 3.4.7.1 evaluates ovalization of the shell by considering the seismically applied load as a line loading along the height of the overpack that is balanced by inertial body forces in the metal ring. The same solutions can be used to examine the circumferential stress state that would be induced to resist an external pressure that developed around one-half of the periphery. Such a pressure distribution may be induced by a pressure wave crossing the cask from a nearby explosion. It is shown here that a uniform pressure load over one-half of the overpack outer shell gives rise to an elastic stress state and deformation state that is bounded by a large margin by the results just presented for the seismic event in Subsection 3.4.7.1.

The case of an external pressure load from an explosion pressure wave (Load Case 05 in Table 3.1.5) is examined by combining the solutions for two different load cases. The combined case that results is a balance of pressure load over one-half the perimeter and inertial body forces. The sketch below

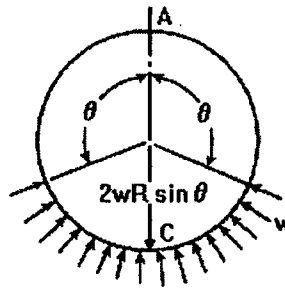
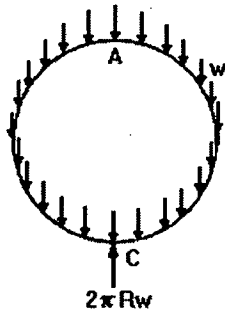


describes this:

Case 1

+

Case 3



Both cases are considered under identical total loads (with the angle in case 3 set to 90 degrees). Therefore, adding the results from the two cases results in the desired combined case; namely, the balance of a peripheral external pressure with internal all around loading simulating an inertia load (since the reactions are identical in magnitude and opposite in direction, there is a complete cancellation of the concentrated loads).

Examination of the results shows that the algebraic sum of the two solutions gives results that are smaller in magnitude than the case 1 solution for a line loading balanced by inertially induced body forces. The applied loading used to develop the solution for case 1 is 56,180 lb. per inch of storage overpack axial length. This load is equivalent to an external pressure  $P = 424$  psi applied over one-half of the outer perimeter of the shell as is shown below:

$$P \times D = 56,180 \text{ lb./inch} \quad D = 132.5'' \quad \text{Therefore, } P = 424 \text{ psi}$$

Since this is higher by a large margin than any postulated external pressure load, circumferential stresses induced by the differential pressure specified in Table 2.2.1 are insignificant. Specifically, by adding the results from the two solutions (ring load case 1 for a point support reaction to a body force + ring load case 3 for a point support reaction to a lateral pressure over one-half of the perimeter), it is determined that the circumferential bending stress from case 1 is reduced by the factor "R" to obtain the corresponding stress from the combined case. R is computed as the ratio of moment magnitudes from the combined case to the results of case 1 alone.

$$R = (\text{maximum bending moment from case 1} + \text{case 3}) / (\text{maximum bending moment from case 1}) \\ = 0.75/6.197 = 0.12$$

Examination of the graphs from the moment distribution from the two solutions shows that the

individual terms always subtract and nearly cancel each other at every location.

Therefore, it is concluded that the maximum circumferential stress that develops under a pressure of 424 psi applied over one-half of the perimeter, and conservatively assumed balanced by inertia loading, is

$$\text{Stress} = 29,310 \text{ psi} \times 0.12 = 3517 \text{ psi}$$

The stress due to a differential pressure of 10 psi (Table 2.2.1) is only 2.36% of the above value and needs no further evaluation for stress limits or deformation to demonstrate retrievability of the MPC. Because of the large margin obtained for a specific set of values appropriate to the HI-STORM 100, the same conclusion is reached for the HI-STORM 100S and the HI-STORM 100S, Version B; that is, differential pressures of the postulated magnitude will not affect retrievability of the stored MPC.

#### 3.4.7.3 Anchored HI-STORM Systems Under High-Seismic DBE (Load Case C in Table 3.1.1)

The anchored HI-STORM System (Figures 1.1.4 and 1.1.5) is assumed to be subjected to quasi-static inertial seismic loads corresponding to the ZPA design basis limits given in Table 2.2.8. The results from this quasi-static analysis are used to evaluate structural margins for the preloaded anchor studs and the sector lugs. In the quasi-static evaluation, the effect of the “rattling” of the MPC inside of the overpack is accounted for by the imposition of a dynamic load factor of 2.0 on the incremental stresses that arise during the seismic event. In addition to the quasi-static analysis, confirmatory 3-D dynamic analyses are performed using base acceleration excitation histories developed from two sets of response spectra. Figure 3.4.30 shows the two sets of response spectra that are assumed to be imposed at the top of the ISFSI pad. One set of response spectra is the Regulatory Guide 1.60 spectra for 5% damping with zero period acceleration conservatively amplified to 1.5 in each direction. This spectra set has been used as the input spectra at many nuclear plants in the U.S. (although generally, the ZPA was much below 1.0). Three statistically independent acceleration time histories (two horizontal labeled as “H1”, “H2”) and one vertical (labeled as “VT”) have been developed. A twenty-second duration event was considered. Figures 3.4.31 to 3.4.33 show the time histories. The second set of response spectra used for time history analysis has similar levels of zero period acceleration but has higher peak spectral acceleration values in the low frequency range (2-3 Hz). This spectra set is the design basis set for a Pacific coast U.S. plant. Figures 3.4.34 to 3.4.36 (labeled as “FN”, “FP” for the two horizontal acceleration histories and “FV” for the vertical acceleration time history), show the corresponding time histories simulating a long duration seismic event (170 seconds).

The objectives of the quasi-static and dynamic seismic analyses are the following:

- i. Quantify the structural safety factor in the anchor studs and in the sector lugs that constitute the fastening system for the loaded HI-STORM 100A overpack. The structural safety factor is defined as the ratio of the permitted stress (stress intensity) per Subsection “NF” of the ASME Code to the maximum stress (stress intensity)

developed in the loaded component.

- ii. Compute the safety factor against fatigue failure of the anchor studs from a single seismic event.
- iii. Quantify the interface loads applicable to the ISFSI pad to enable the ISFSI owner to design the ISFSI pad under the provisions of ACI-349 (85). The bounding interface loads computed for the maximum intensity seismic event (ZPA) and for extreme environmental loads may be used in pad design instead of the site-specific loads calculated for the loadings applicable to the particular ISFSI.

The above design objectives are satisfied by performing analyses of a loaded HI-STORM 100A System using a conservative set of input data and a conservative dynamic model. Calculations using the quasi-static model assume that the net horizontal inertia loads and the vertical inertia load correspond to the weight of the loaded cask times the appropriate ZPA. The results from the analyses are set down as the interface loads, and may be used in the ISFSI pad design work effort by the ISFSI owner. The information on the seismic analysis is presented in five paragraphs as follows:

Input data for analysis  
Quasi-static model and results  
Dynamic model and modeling assumptions.  
Results of dynamic analysis  
Summary of interface loads

a. Input Data for Analysis:

Key input data for the seismic analysis of a loaded HI-STORM 100A System is summarized in Table 3.4.10. As can be seen from Table 3.4.10, the input data used in the analysis is selected to bound the actual data, wherever possible, so as to maximize the seismic response. For example, a bounding weight of the loaded MPC and HI-STORM 100A overpack is used because an increase in the weight of the system directly translates into an increased inertial loading on the structure.

For quasi-static analysis, bounding ZPA values of 1.5 in all three directions are used with the vertical event directed upward to maximize the stud tension. The resulting ZPAs are then further amplified by the dynamic load factor (DLF=2.0) to reflect "rattling" of the MPC within the overpack. Input data for anchor stud lengths are representative. We consider long and short studs in order to evaluate the effect of stud spring rate.

For the confirmatory dynamic analyses, the time history base excitations are shown in Figures 3.4.31 through 3.4.36 and the propensity for "rattling" is included in the model.

b. Quasi-Static Model and Results:

We consider the HI-STORM100A baseplate as a rigid plate resting on the ISFSI pad with the twenty-

eight studs initially preloaded so as to impart a compressive load at the baseplate pad interface that is balanced by a tensile load in the studs prior to the seismic event occurring. The discrete studs are replaced by a thin ring located at the stud circle radius for analysis purposes. The thickness of the thin ring is set so that the ring area is equal to the total stress area of the twenty-eight studs. Figure 3.4.37 shows a view of a segment of the baseplate with the outline of the ring. The ISFSI pad is represented by a linear spring and a rotational spring with spring constants determined from the exact solution for a rigid circular punch pressed into a elastic half-space. We assume that subsequent to pre-tensioning the studs, the seismic event occurs, represented by a net horizontal load DH and a net vertical load DV. In the analysis, the input loads DH and DV are:

$$G_H = (1.5^2 \times 2)^{1/2} \times DLF = 4.242 ; \quad G_V = 1.5 \times DLF = 3.0$$

$$DH = G_H \times 360,000 \text{ lb.} ; \quad DV = -G_V \times 360,000 \text{ lb}$$

DH is the magnitude of the vector sum of the two horizontal ZPA accelerations multiplied by the bounding HI-STORM 100A weight. Similarly, DV is an upward directed load due to the vertical ZPA acceleration. The upward direction is chosen in order to maximize the stud tension as the assemblage of studs and foundation resists overturning from the moment induced by DH applied at the centroid of the cask. Figure 3.4.38 shows the free-body diagram associated with the seismic event. Essentially, we consider an analysis of a pre-compressed interface and determine the interface joint behavior under the imposition of an external loading (note that this kind of analysis is well established in the pressure vessel and piping area where it is usually associated with establishing the effectiveness of a gasketed joint). An analysis is performed to determine the maximum stud tension that results if the requirement of no separation between baseplate and pad is imposed under the imposed loading. The following result is obtained from static equilibrium, for a preload stress of 60 ksi, when the “no separation condition” is imposed:

$$\frac{2a/3h_{cg} (F_{\text{preload}}/W + 1)(1 + \alpha_1)}{G_H - 2a/3h_{cg} (G_V(1 + \alpha_1)/(1 + \alpha))} = 1.016$$

In the above equation,

$$F_{\text{preload}} = (\text{Total stress area of twenty-eight, 2" diameter studs}) \times 60 \text{ ksi} = 4,200,000 \text{ lb.}$$

$$W = \text{Bounding weight of loaded HI-STORM 100A} = 360,000 \text{ lb.}$$

$$a = 73.25 \text{ inches,}$$

$$h_{cg} = 118.5 \text{ inches}$$

The coefficients  $\alpha$  and  $\alpha_1$  relate the stiffness of the totality of studs to the stiffness of the foundation under direct loading and under rotation. The result given above is for the representative case of stud free length “L”, equal to

L= 42 inches, which gives  $\alpha$  and  $\alpha_1$  equal to 0.089 and 0.060, respectively.

A simplified confirmatory analysis of the above problem can be performed by considering the limiting case of a rigid baseplate and a rigid ISFSI pad. In the limit of a rigid ISFSI pad (foundation), the coefficients  $\alpha$  and  $\alpha_1$  go to zero. A related solution for the case of a rigid baseplate and a rigid foundation can be obtained when the criteria is not incipient separation, but rather, a more “liberal” incipient rotation about a point on the edge of the baseplate. That solution is given in “Mechanical Design of Heat Exchangers and Pressure Vessel Components”, by Singh and Soler (Arcturus Publishers, 1984). The result is (for 60 ksi pre-stress in each stud):

$$\frac{a/h_{cg} (F_{preload}/W + 1)}{G_H - a/h_{cg} (G_V)} = 1.284$$

Although not a requirement of any design code imposed herein, the right hand side of the previous relationships can be viewed as the safety factor against incipient separation (or rotation about an edge) at the radius “a”. Note that since we have assumed a bounding event, there is an additional margin of 1.5 in results since the Reg. Guide 1.60 event has not been applied with a ZPA in excess of 1.0.

For the real seismic event associated with a western U.S. plant having a slightly lower horizontal ZPA and a reduced vertical ZPA (see Figure 3.4.30). Using the same DLF =2.0 to account for “rattling” of the confined MPC:

$$G_H = 4.1 \quad ; \quad G_V = 2.6,$$

the aforementioned safety factors are:

$$\begin{aligned} \text{SF (incipient separation)} &= 1.076 \\ \text{SF (incipient edging)} &= 1.372 \end{aligned}$$

The increment of baseplate displacement and rotation, up to incipient separation, is computed from the equilibrium and compatibility equations associated with the free body in Figure 3.4.38 and the change in stud tension computed. The following formula gives the stud tensile stress in terms of the initial preload and the incremental change from the application of the horizontal and vertical seismic load.

$$\sigma_{stud} = \sigma_{preload} + \alpha \frac{W}{NA_{stress}} \left( \frac{-G_V}{1 + \alpha} + \left( \frac{3h_{cg}}{2a} \right) \left( \frac{c}{a} \right) \left( \frac{G_H}{1 + \alpha_1} \right) \right)$$

In the above formula,

N = number of studs = 28 (maximum number based on HI-STORM dimensions). For lower seismic inputs, this might be reduced (in groups of 4 to retain symmetry).

$A_{\text{stress}}$  = tensile stress area of a 2" diameter stud

2c = stud circle diameter

The results demonstrate that there is a relatively small change in stud stress from the initial pre-tension condition with the ISFSI pad foundation resisting the major portion of the overturning moment. For the geometry considered (maximum stud free length and nominal pre-stress), the maximum tensile stress in the stud increases by 9.1%. The following table summarizes the results from the quasi-static analysis using minimum ultimate strength for the stud to compute the safety factors. Note that under the seismic load, the direct stress in the stud is limited to 70% of the stud ultimate strength (per Appendix F of the ASME Code Section III). The allowable pad compressive stress is determined from the ACI Code assuming confined concrete and the minimum concrete compressive strength from Table 2.0.4. Because of the large compressive load at the interface from the pre-tensioning operation, the large frictional resistance inhibits sliding of the cask. Consequently, there will be no significant shear stress in the studs. Safety factors for sliding are obtained by comparing the ratio of horizontal load to vertical load with the coefficient of friction between steel and concrete (0.53). Values in parenthesis represent results obtained using ZPA values associated with the real seismic event for the western U.S. plant instead of the bounding Reg. Guide 1.60 event.

<b>SUMMARY OF RESULTS FOR STUDS AND INTERFACE FROM QUASI-STATIC SEISMIC EVALUATION WITH DLF = 2.0, Stud Prestress = 60 ksi</b>			
<b>Item</b>	<b>Calculated Value</b>	<b>Allowable Value</b>	<b>Safety Factor = (Allowable Value/Calculated Value)</b>
Stud Stress(ksi) (42" stud free length)	65.48 (65.18)	87.5	1.336 (1.343)
Maximum Pad Pressure (ksi)(42" stud free length)	3.126 (3.039)	4.76	1.52 (1.57)
Stud Stress (ksi)(16" stud free length)	73.04 (72.34)	87.5	1.20 (1.21)
Maximum Pad Pressure(ksi) (16" stud free length)	2.977 (2.898)	4.76	1.60 (1.64)
Overpack Sliding	0.439 (0.407)	0.53	1.21 (1.31)

The effect of using a minimum stud free length in the embedment design is to increase the values of the coefficients  $\alpha$  and  $\alpha_1$  because the stud stiffness increases. The increase in stud stiffness, relative to the foundation stiffness results in an increase in incremental load on the studs. This is a natural and expected characteristic of preloaded configurations. It is noted that the stud safety factors are based on minimum ultimate strength and can be increased, without altering the calculated results, by changing the stud material.

The quasi-static analysis methodology has also been employed to evaluate the effects of variation in the initial pre-stress on the studs. The following tables reproduce the results above for the cases of lower bound stud pre-stress (55 ksi) and upper bound stud pre-stress (65 ksi) on the studs. Only the

results using the values associated with the Reg. Guide 1.60 bounding event are reported.

<b>SUMMARY OF RESULTS FOR STUDS AND INTERFACE FROM QUASI- STATIC SEISMIC EVALUATION WITH DLF = 2.0, Stud Prestress = 55 ksi</b>			
<b>Item</b>	<b>Calculated Value</b>	<b>Allowable Value</b>	<b>Safety Factor = (Allowable Value/Calculated Value)</b>
Stud Stress(ksi) (42" stud free length)	60.48	87.5	1.45
Maximum Pad Pressure (ksi)(42" stud free length)	3.012	4.76	1.58
Stud Stress (ksi)(16" stud free length)	68.07	87.5	1.29
Maximum Pad Pressure(ksi) (16" stud free length)	2.862	4.76	1.663
Overpack Sliding	0.488	0.53	1.09

<b>SUMMARY OF RESULTS FOR STUDS AND INTERFACE FROM QUASI- STATIC SEISMIC EVALUATION WITH DLF = 2.0, Stud Prestress = 65 ksi</b>			
<b>Item</b>	<b>Calculated Value</b>	<b>Allowable Value</b>	<b>Safety Factor = (Allowable Value/Calculated Value)</b>
Stud Stress(ksi) (42" stud free length)	70.48	87.5	1.24
Maximum Pad Pressure (ksi)(42" stud free length)	3.24	4.76	1.47
Stud Stress (ksi)(16" stud free length)	78.07	87.5	1.12
Maximum Pad Pressure(ksi) (16" stud free length)	3.091	4.76	1.54
Overpack Sliding	0.399	0.53	1.33

The results above confirm the expectations that an increase in preload increases the safety factor against sliding. The calculated coefficient of friction in the above tables is computed as the ratio of applied horizontal load divided by available vertical load. For all combinations examined, ample margin against incipient separation at the interface exists.

Based on the results from the quasi-static analysis, an assessment of the safety factors in the sector lugs is obtained by performing a finite element analysis of a repeated element of one of the sector lugs. Figure 3.4.39 shows the modeled section and the finite element mesh. The stud load is conservatively applied as a uniform downward pressure applied over a 5"x5" section of the extended baseplate simulating the washer between two gussets. This is conservative as the rigidity of the washer is neglected. The opposing pressure loading from the interface pressure is applied as a pressure over the entire extended baseplate flat plate surface. Only one half the thickness of each gusset plate is included in the model. The outer shell is modeled as 3/4" thick, which corresponds to

the minimum thickness option per Bill of Material 1575.

Two cases are considered: (1) the pre-loaded state (a Normal Condition of Storage-Level A stress limits apply); and, (2), the seismic load condition at the location of the maximum tensile load in a stud (an Accident Condition of Storage – Level D stress intensity limits apply). Figures 3.4.40 and 3.4.41 present the stress results for the following representative input conditions:

Level A analysis - Preload stress/bolt = 60 ksi

Level D analysis - Maximum Bolt stress (includes seismic increment) = 65.5 ksi

In the Level A analysis, the resisting local foundation pressure exactly balances the preload. For the Level D analysis, the opposing local foundation pressure = 190 psi (average over the area between gussets). This represents the reduced pressure under the highest loaded stud under the induced rotation of the storage system.

The most limiting weld stress is obtained by evaluating the available load capacity of the fillet weld attaching the extended baseplate annulus region to the gussets (approximately 25 inches of weld per segment) using a limit strength equal to 42% of the ultimate strength of the base material.

The following table summarizes the limiting safety factors for the sector lugs. Allowable values for primary bending stress and stress intensity are from Tables 3.1.10 and 3.1.12 for SA-516 Grade 70 at 300 degrees F.

SUMMARY OF RESULTS FOR SECTOR LUGS FROM QUASI-STATIC SEISMIC EVALUATION			
Item	Calculated Value	Allowable Value	Safety Factor = (Allowable Value/Calculated Value)
Maximum Primary Membrane + Bending Stress Away From Loaded Region and Discontinuity (ksi) – Case 1 - Preload	15.62	26.3	1.68
Maximum Primary Membrane + Bending Stress Intensity Away From Loaded Region and Discontinuity (ksi) – Case 2 - Preload + Seismic	36.67	60.6	1.65
Maximum Weld Shear Load (kips)	150.8	194.9	1.29

c. Dynamic Model and Modeling Assumptions:

The dynamic model of the HI-STORM 100A System consists of the following major components.



- i. The HI-STORM 100 overpack is modeled as a six degree-of-freedom (rigid body) component.
- ii. The loaded MPC is also modeled as a six degree-of-freedom (rigid body) component that is free to rattle inside the overpack shell. Gaps between the two bodies reflect the nominal dimensions from the drawings.
- iii. The contact between the MPC and the overpack is characterized by a coefficient of restitution and a coefficient of friction. For the dynamic analysis, the coefficient of restitution is set to 0.0, reflecting the large areas of nearly flat surface that come into contact and have minimal relative rebound. The coefficient of friction is set to 0.5 between all potentially contacting surfaces of the MPC/overpack interface.
- iv. The anchor studs, preloaded to axial stress  $\sigma_i$  (Table 3.4.10), induce a contact stress between the overpack base and the ISFSI pad. The loaded cask-pad interface can support a certain amount of overturning moment before an uplift (loss of circularity of the contact patch) occurs. The anchor studs are modeled as individual linear springs connecting the periphery of the extended baseplate to the ISFSI pad section. The resistance of the foundation is modeled by a vertical linear spring and three rotational springs connected between the cask baseplate center point and the surface of the flat plate modeling the driven ISFSI pad. The ISFSI pad is driven with the three components of acceleration time history applied simultaneously.

The HI-STORM 100A dynamic model described above is implemented on the public domain computer code WORKING MODEL (also known as VisualNastran) (See Subsection 3.6.2 for a description of the algorithm).

Figures 3.4.42 and 3.4.43 show the rigid body components of the dynamic model before and after assembly. The linear springs are not shown. Mass and inertia properties of the rigid bodies are consistent with the bounding property values in Table 3.4.10.

d. Results of Dynamic Analysis:

Figures 3.4.44 –3.4.47 show results of the dynamic analysis using the Reg. Guide 1.60 seismic time histories as input accelerations to the ISFSI pad. Figure 3.4.44 shows variation in the vertical foundation compressive force. Figure 3.4.45 shows the corresponding load variation over time for the stud having the largest instantaneous tensile load. An initial preload of approximately 150,000 lb is applied to each stud (corresponding to 60,160 psi stud tensile stress). This induces an initial compression load at the interface approximately equal to 571,000 lb. (including the dead weight of the loaded HI-STORM). Figures 3.4.44 and 3.4.45 clearly demonstrate that the foundation resists the majority of the oscillatory and impactive loading as would be expected of a preloaded configuration. Figure 3.4.46 shows the impulse (between the MPC and HI-STORM 100A) as a function of time. It is clear that the “spikes” in both the foundation reaction and the stud load over the total time of the event are related to the impacts of the rattling MPC. The results provide a graphic demonstration that

the rattling of the MPC inside the overpack must be accounted for in any quasi-static representation of the event. The quasi-static results presented herein for the anchored system, using a DLF = 2.0, are in excellent agreement with the dynamic simulation results.

We note that the dynamic simulation, which uses an impulse-momentum relationship to simulate the rattling contact, leads to results having a number of sharp peaks. Given that the stress intensity limits in the Code assume static analyses, filtering of the dynamic results is certainly appropriate prior to comparing with any static allowable strength. We conservatively do not perform any filtering of the results prior to comparison with the quasi-static analysis; we note only that any filtering of the dynamic results to eliminate high-frequency effects resulting from the impulse-momentum contact model would increase the safety factors. Finally, Figure 3.4.47 shows the ratio of the net interface horizontal force (needed to maintain equilibrium) to the instantaneous compression force at the ISFSI pad interface with the base of the HI-STORM 100A. This ratio, calculated at each instant of time from the dynamic analysis results using the Reg. Guide 1.60 event, represents an instantaneous coefficient of friction that is required to ensure no interface relative movement. Figure 3.4.47 demonstrates that the required coefficient of friction is below the available value 0.53. Thus, the dynamic analysis confirms that the foundation interface compression, induced by the preloading action, is sufficient to maintain a positive margin against sliding without recourse to any resistance from the studs.

The results of the dynamic analysis using acceleration time histories from the Reg. Guide 1.60 response spectra (grounded at 1.5 g's) confirm the ability of the quasi-static solution, coupled with a dynamic load factor, to correctly establish structural safety factors for the anchored cask. The dynamic analysis confirms that stud stress excursions from the preload value are minimal despite the large overturning moments that need to be balanced.

A second dynamic simulation has been performed using the seismic time histories appropriate to a pacific coast U.S. nuclear plant (Figures 3.4.34-3.4.36). The ZPA of these time histories are slightly less than the Reg. Guide 1.60 time histories but the period of relatively strong motion extends over a longer time duration. The results from this second simulation exhibit similar behavior as those results presented above and provide a second confirmation of the validity of the safety factors predicted by the quasi-static analysis. Reference [3.4.14] (see Subsection 3.8) provides archival information and backup calculations for the results summarized here.

Stress cycle counting using Figure 3.4.45 suggests 5 significant stress cycles per second provides a bounding number for fatigue analysis. A fatigue reduction factor of 4 is appropriate for the studs (per ASME Code rules). Therefore, a conservative analysis of fatigue for the stud is based on an alternating stress range of:

$S(\text{alt}) = .5 \times (22,300 \text{ psi}) \times 4 = 44,600 \text{ psi}$  for 5 cycles per second. The value for the stress range is obtained as the difference between the largest tensile stress excursions from the mean value as indicated in the figure.

To estimate fatigue life, we use a fatigue curve from the ASME Code for high strength steel bolting

materials (Figure I.9.4 in Appendix I, ASME Code Section III Appendices) For an amplified alternating stress intensity range of 44,600 psi, Figure I.9.4 predicts cyclic life of 3,000 cycles. Therefore, the safety factor for failure of a stud by fatigue during one Reg. Guide 1.60 seismic event is conservatively evaluated as:

$$SF(\text{stud fatigue}) = 3,000/100 = 30.$$

For the long duration event, even if we make the conservative assumption of a nine-fold increase in full range stress cycles, the safety factor against fatigue failure of an anchor stud from a single seismic event is 3.33. Recognizing that the fatigue curve itself is developed from test data with a safety factor of 20 on life and 4 on stress, the results herein demonstrate that fatigue failure of the anchor stud, from a single seismic event, is not credible.

e. Summary of Interface Loads for ISFSI Pad Design:

Bounding interface loads are set down for use by the ISFSI pad designer and are based on the validated quasi-static analysis and a dynamic load factor of 2.0:

BOUNDING INTERFACE LOADS FOR ISFSI PAD STRUCTURAL/SEISMIC DESIGN	
D (Cask Weight)	360 kips
D (Anchor Preload @ 65 ksi)	4,550 kips
E (Vertical Load)	1,080 kips
E (Net Horizontal Surface ShearLoad)	1,527.35 kips
E (Overturning Moment)	15,083 kip-ft.

3.4.8 Tornado Wind and Missile Impact (Load Case B in Table 3.1.1 and Load Case 04 in Table 3.1.5)

During a tornado event, the HI-STORM 100 System is assumed to be subjected to a constant wind force. It is also subject to impacts by postulated missiles. The maximum wind speed is specified in Table 2.2.4 and the three missiles, designated as large, intermediate, and small, are described in Table 2.2.5.

In contrast to a freestanding HI-STORM 100 System, the anchored overpack is capable of withstanding much greater lateral pressures and impulsive loads from large missiles. The quasi-static analysis result, presented in the previous subsection, can be used to determine a maximum permitted base overturning moment that will provide at least the same stud safety factors. This is accomplished by setting  $G_v = 0.0$ ,  $DLF = 1$  and finding an appropriate  $G_H$  that gives equal or better stud safety factors. The resulting value of  $G^*_H$  establishes the limit overturning moment for combined tornado missile plus wind.,  $M_L$ . ( $G^*_H \times \text{Weight} \times h_{cg}$ ) is conservatively set as the maximum permissible moment at the base of the cask due to combined action of lateral wind and tornado missile loading. Thus, if the lateral force from a tornado missile impact is  $F$  at height  $h$  and that from steady tornado wind action is a resultant force  $W$  acting at cask mid-height ( $0.5H$ ), and the two loads are acting synergistically to overturn the cask, then their magnitudes must satisfy the inequality

$$0.5WH + Fh \leq M_L$$

where the limit moment is established to ensure that the safety factors for seismic load remain bounding.

$$M_L = 18,667 \text{ kip-ft.}$$

Tornado missile impact factors should be factored into “F” prior to determining the validity of the above inequality for any specific site.

In the case of a freestanding system, the post impact response of the HI-STORM 100 System is required to assess stability. Both the HI-STORM 100 storage overpack, and the HI-TRAC transfer cask are assessed for missile penetration.

The results for the post-impact response of the HI-STORM 100 storage overpack demonstrate that the combination of tornado missile plus either steady tornado wind or instantaneous tornado pressure drop causes a rotation of the HI-STORM 100 to a maximum angle of inclination less than 3 degrees from vertical. This is much less than the angle required to overturn the cask. The results for the HI-STORM 100 are bounding since the HI-STORM 100S and the HI-STORM 100S Version B have a lower center of gravity when loaded. Since Appendix C uses a lower bound cask weight of 302,000 lb, the results are also bounding for HI-STORM overpacks that utilize high density concrete.

The maximum force (not including the initial pulse due to missile impact) acting on the projected area of the storage overpack is computed to be:

$$F = 91,920 \text{ lbs.}$$

The instantaneous impulsive force due to the missile strike is not computed here; its effect is felt as an initial angular velocity imparted to the storage overpack at time equal to zero. The net resultant force due to the simultaneous pressure drop is not an all-around distributed loading that has a net resultant, but rather is more likely to be distributed only over 180 degrees (or less) of the storage overpack periphery. The circumferential stress and deformation field will be of the same order of magnitude as that induced by a seismic loading. Since the magnitude of the force due to F is less than the magnitude of the net seismically induced force considered in Subsection 3.4.7, the storage overpack global stress analysis performed in Subsection 3.4.7 remains governing. In the next subsection, results are provided for the circumferential stress and ovalization of the portion of the storage overpack due to the bounding estimate for the impact force of the intermediate missile.

#### 3.4.8.1 HI-STORM 100 Storage Overpack

This subsection considers the post impact behavior of the HI-STORM 100 System after impact from tornado missiles. During an impact, the system consisting of missile plus storage overpack and MPC satisfies conservation of linear and angular momentum. The large missile impact is assumed to be

inelastic. This assumption conservatively transfers all of the momentum from the missile to the system. The intermediate missile and the small missile are assumed to be unyielding and hence the entire initial kinetic energy is assumed to be absorbed by motion of the cask and local yielding and denting of the storage overpack surface. It is shown that cask stability is maintained under the postulated wind and large missile loads. The conclusion is also valid for the HI-STORM 100S and for the HI-STORM 100S Version B with or without the densified concrete shielding option since their lower centers of gravity inherently provide additional stability margin.

The penetration potential of the missile strikes (Load Case 04 in Table 3.1.5) is examined first. The detailed calculations show that there will be no penetration through the concrete surrounding the inner shell of the storage overpack or penetration of the top closure plate. Therefore, there will be no impairment to the confinement boundary due to missile strikes during a tornado. Since the inner shell is not compromised by the missile strike, there will be no permanent deformation of the inner shell. Therefore, ready retrievability is assured after the missile strike. The following paragraphs summarize the analysis work for the HI-STORM 100.

- a. The small missile will dent any surface it impacts, but no significant puncture force is generated. The 1" missile can enter the air ducts, but geometry prevents a direct impact with the MPC.
- b. The following table summarizes the denting and penetration analysis performed for the intermediate missile. Denting is used to connote a local deformation mode encompassing material beyond the impacting missile envelope, while penetration is used to connote a plug type failure mechanism involving only the target material immediately under the impacting missile. The results are applicable to the HI-STORM 100 and to the HI-STORM 100S. The HI-STORM 100S version B has a thicker outer shell than the classic HI-STORM 100, and a lid configuration that consists of a 1" lid cover plate backed by concrete and a 3" thick lid vent shield plate that acts as a barrier to a top lid missile strike. Therefore, the tabular results presented below are bounding for the HI-STORM 100S Version B.

Location	Denting (in.)	Thru-Thickness Penetration
Storage overpack outer Shell	6.87 <sup>†</sup>	Yes (>0.75 in.)
Radial Concrete	9.27	No (<27.25 in.)
Storage overpack Top Lid	0.4	No (<4 in.)

<sup>†</sup> Based on minimum outer shell thickness of 3/4". Penetration is less for HI-STORM 100 and 100S overpacks with 1" thick outer shell.

The primary stresses that arise due to an intermediate missile strike on the side of the storage

overpack and in the center of the storage overpack top lid are determined next. The analysis of the storage lid for the HI-STORM 100 bounds that for the HI-STORM 100S; because of the additional energy absorbing material (concrete) in the direct path of a potential missile strike on the top lid of the HI-STORM 100S lid, the energy absorbing requirements of the circular plate structure are much reduced. The analysis demonstrates that Level D stress limits are not exceeded in either the overpack outer shell or the top lid. The safety factor in the storage overpack, considered as a cantilever beam under tip load, is computed, as is the safety factor in the top lids, considered as two centrally loaded plates. The applied load, in each case, is the missile impact load. Similar calculations are performed for the HI-STORM 100S Version B using the same model and methodology. A summary of the results for axial stress in the storage overpack is given in the table below with numbers in parentheses representing the results of calculations for the geometry of the HI-STORM 100S Version B:

<b>HI-STORM 100 MISSILE IMPACT - Global Axial Stress Results</b>			
<b>Item</b>	<b>Value (ksi)</b>	<b>Allowable (ksi)</b>	<b>Safety Factor</b>
Outer Shell – Side Strike	14.35 <sup>†</sup> (15.17)	39.75	2.77 <sup>†</sup> (2.62)
Top Lid - End Strike	44.14(47.57)	57.0 (50.65)	1.29(1.065)

<sup>†</sup> Based on HI-STORM 100 overpack with inner and outer shell thicknesses of 1-1/4" and 3/4", respectively. Result is bounding for HI-STORM 100 overpacks made with 1" thick inner and outer shells because the section modulus of the steel structure is greater.

To demonstrate ready retrievability of the MPC, we must show that the storage overpack suffers no permanent deformation of the inner shell that would prevent removal of the MPC after the missile strike. To demonstrate ready retrievability (for both HI-STORM 100 and for HI-STORM 100S) a conservative evaluation of the circumferential stress and deformation state due to the missile strike on the outer shell is performed. A conservative estimate for the 8" diameter missile impact force, "Pi", on the side of the storage overpack is calculated as:

$$P_i = 843,000 \text{ lb.}$$

This force is conservative in that the target overpack is assumed rigid; any elasticity serves to reduce the peak magnitude of the force and increase the duration of the impact. The use of the upper bound value is the primary reason for the high axial stresses resulting from this force. To demonstrate continued ability to retrieve the MPC subsequent to the strike, circumferential stress and deformation that occurs locally in the ring section near the location of the missile strike are investigated.

Subsection 3.4.7 presents stress and displacement results for a composite ring of unit width consisting of the inner and outer shells of the storage overpack. The solution assumes that the net loading is 56,184 lb. applied on the 1" wide ring (equivalent to a 45g deceleration applied uniformly along the height on a storage overpack weight of 270,000 lb.). This solution can be applied directly

to evaluate the circumferential stress and deformation caused by a tornado missile strike on the outer shell. Using the results for the 45g tipover event, an attenuation factor to adjust the results is developed that reflects the difference in load magnitude and the width of the ring that is effective in resisting the missile strike force. The strike force  $P_i$  is resisted by a combination of inertia force and shear resistance from the portion of the storage overpack above and below the location of the strike. The ring theory solution to determine the circumferential stress and deformation conservatively assumes that inertia alone, acting on an effective length of ring, balances the applied point load  $P_i$ . The effective width of ring that balances the impact load is conservatively set as the diameter of the impacting missile (8") plus the effect of the "bending boundary layer" length. This boundary layer length is conservatively set as a multiple of twice the square root of the product of mean radius times the average thickness of two shells making up the cylindrical body of the storage overpack. The mean radius of the composite cylinder and the average thickness of the inner and outer shells are

$$R_{\text{mean}} = 48''$$

$$T = .5 \times (.75'' + 1.25'') = 1''$$

The bending boundary layer " $\beta$ " in a shell is generally accepted to be given as  $(2(R_{\text{mean}}T)^{1/2}) = 13.85''$  for this configuration. That is, the effect of a concentrated load is resisted mainly in a length along the shell equal to the bending boundary layer. For a strike away from the ends of the shell, a boundary layer length above and below the strike location would be effective (i.e., double the boundary layer length). However, to conservatively account for resistance above and below the location of the strike, this calculated result is only increased by 1.5 in the following analysis (rather than 2). Therefore, the effective width of ring is assumed as:

$$13.85'' \times 1.5 + 8'' = 28.78''$$

The solution for the 45g tipover event (performed for a unit ring width and a load of 56,184 lb.) is directly applicable if we multiply all stress and displacement results by the factor "Y" where

$$Y = (1''/28.78'') \times (843,000 \text{ lb.}/56,184 \text{ lb.}) = 0.521$$

Using this factor gives the following bounding results for maximum circumferential stresses (without regard for sign and location of the stress) and deformations due to the postulated tornado missile strike on the side of the storage overpack outer shell:

$$\text{Maximum circumferential stress due to bending moment} = (29,310 \text{ psi} \times Y) = 15,271 \text{ psi}$$

$$\text{Maximum circumferential stress due to mean tangential force} = (18,900 \text{ lb.}/2 \text{ sq.inch}) \times Y = 4,923 \text{ psi}$$

$$\text{Change in diameter in the direction of the load} = -0.11'' \times Y = -0.057''$$

$$\text{Change in diameter perpendicular to the direction of the load} = +0.06'' \times Y = 0.031''$$

Based on the above calculation, the safety factor on maximum stress for this condition is

$$SF = 39,750\text{psi}/15,271 \text{ psi} = 2.60$$

The allowable stress for the above calculation is the Level D membrane stress intensity limit from Table 3.1.12. This is a conservative result since the stress intensity is localized and need not be compared to primary membrane stress intensity. Even with the overestimate of impact strike force used in the calculations here, the stresses remain elastic and the calculated diameter changes are small and do not prevent ready retrievability of the MPC. Note that because the stresses remain in the elastic range, there will be no post-strike permanent deformation of the inner shell.

The above calculations remain valid for the HI-STORM 100S, Version B using normal weight concrete and are bounding for the case where densified concrete is used.

#### 3.4.8.2 HI-TRAC Transfer Cask

##### 3.4.8.2.1 Intermediate Missile Strike

HI-TRAC is always held by the handling system while in a vertical orientation completely outside of the fuel building (see Chapter 2 and Chapter 8). Therefore, considerations of instability due to a tornado missile strike are not applicable. However, the structural implications of a missile strike require consideration.

The penetration potential of the 8" missile strike on HI-TRAC (Load Case 04 in Table 3.1.5) is examined at two locations:

1. the lead backed outer shell of HI-TRAC.
2. the flat transfer lid consisting of multiple steel plates with a layer of lead backing.

In each case, it is shown that there is no penetration consequence that would lead to a radiological release. The following paragraphs summarize the analysis results.

- a. The small missile will dent any surface it impacts, but no significant puncture force is generated.
- b. The following table summarizes the denting and penetration analysis performed for the intermediate missile. Denting connotes a local deformation mode encompassing material beyond the impacting missile envelope, while penetration connotes a plug type failure mechanism involving only the target material immediately under the impacting missile. Where there is through-thickness penetration, the lead and the inner plate absorb any residual energy remaining after penetration of the outer plate in the 100 Ton HI-TRAC transfer lid. The table summarizes the bounding results for both transfer casks.



Location	Denting (in.)	Thru-Thickness Penetration
Outer Shell - lead backed	0.498	No (<1.0 in.)
Outer Transfer Lid Door	0.516	No (<0.75 in.) (HI-TRAC 125) Yes (>0.5 in.) (HI-TRAC 100)

Based on the above results, the intermediate missile will penetrate the ½" thick bottom plate of the HI-TRAC 100D pool lid. However, the lead and the pool lid top plate will absorb any residual energy remaining after penetration of the bottom plate. The 8" missile will not penetrate the pool lid for the HI-TRAC 125D because it has a thicker bottom plate than the HI-TRAC 125 transfer lid door. In addition, the results for the 8" missile strike on the HI-TRAC outer shell are valid for the HI-TRAC 125D and the HI-TRAC 100D since all four transfer casks have the same outer shell thickness.

While the transfer cask is being transported in a horizontal orientation, the MPC lid is exposed. We conservatively assume no protective plate in place during this transport operation and evaluate the capacity of the lid peripheral groove weld to resist the impact load. The calculated result is as follows:

HI-TRAC MISSILE IMPACT - Capacity Results			
Item	Value (lb)	Capacity (lb)	Safety Factor = Capacity/Value
Top Lid Weld	2,262,000	2,789,000	1.23

The final calculation in this subsection is an evaluation of the circumferential stress and deformation consequences of the horizontal missile strike on the periphery of the HI-TRAC shell. It is assumed that the HI-TRAC is simply supported at its ends (while in transit) and is subject to a direct impact from the 8" diameter missile. To compute stresses, an estimate of the peak impact force is required. The effect of the water jacket to aid in the dissipation of the impact force is conservatively neglected. The only portion of the HI-TRAC cylindrical body that is assumed to resist the impact load is the two metal shells. The lead is assumed only to act as a separator to maintain the spacing between the shells. The previous results from the lead slump analysis demonstrate that this conservative assumption on the behavior of the lead is valid. The peak value of the impact force is a function of the stiffness of the target. The target stiffness in this postulated event has the following contributions to the stiffness of the structure.

- a. a global stiffness based on a beam deformation mode, and
- b. a local stiffness based on a shell deformation mode

The global spring constant (i.e., the inverse of the global deflection of the cask body as a beam under a unit concentrated load) is a function of location of the strike along the length of the cask. The spring constant value varies from a minimum for a strike at the half-height to a maximum value for a strike near the supports (the trunnions). Since the peak impact force is larger for larger stiffness, it is conservative to maximize the spring constant value. Therefore, in the calculation, we neglect this spring constant for the computation of peak impact force and focus only on the spring constant arising from the local deformation as a shell, in the immediate vicinity of the strike. To this end, the spring constant is estimated by considering the three-dimensional effects of the shell solution to be replaced by the two-dimensional action of a wide ring. The width of the ring is equal to the “bending boundary layer” length on either side of the strike location plus the diameter of the striking missile. Following the analysis methodology already utilized subsection 3.4.8.1, the following information is obtained:

The mean radius of the composite cylinder and the average thickness of the inner and outer shells, are (use the 100 Ton HI-TRAC data since it provides an upper bound on stress and deformation):

$$R_{\text{mean}} = 36.893$$

$$T = .5 \times (.75'' + 1.00'') = 0.875''$$

The bending boundary layer “ $\beta$ ” in a shell is generally accepted to be given as  $(2(R_{\text{mean}}T)^{1/2})$ . To account for resistance above and below the location of the strike, this calculated result is conservatively increased by multiplying by 1.5. Therefore, the effective width of ring is:

$$11.22'' \times 1.5 + 8'' = 24.84''$$

The missile impact is modeled as a point load, acting on the ring, of magnitude equal to  $P_i = 20,570$  lb. The use of a point load in the analysis is conservative in that it overemphasizes the local stress. The actual strike area is an 8” diameter circle (or larger, if the effect of the water jacket were included).

The force is assumed resisted by inertia forces in the ring section. From the results, a spring constant can be defined as the applied load divided by the change in diameter of the ring section in the direction of the applied load. Based on this approach, the following local spring constant is obtained:

$$K = P_i/D1_H = P_i/0.019'' = 1,083,000 \text{ lb./inch}$$

To determine the peak impact force, a dynamic analysis of a two-body system has been performed using the “Working Model” dynamic simulation code. A two mass-spring damper system is considered with the defined spring constant representing the ring deformation effect. Figure 3.4.24 shows the results from the dynamic analysis of the impact using the computer code “Working Model”. The small square mass represents the missile, while the larger mass represents the portion of the HI-TRAC “ring” assumed to participate in the local impact. The missile weight is 275.5 lb. and

the participating HI-TRAC weight is set to the weight of the equivalent ring used to determine the spring constant.

The peak impact force that results in each of the two springs used to simulate the local elasticity of the HI-TRAC (ring) is:

$$F(\text{spring}) = 124,400 \text{ lb.}$$

Since there are two springs in the model, the total impact force is:

$$P(\text{impact}) = 248,800 \text{ lb.}$$

To estimate circumferential behavior of the ring under the impact, the previous solution (using a load of 20,570 lb.) is used and amplified by the factor “Z”, where:

$$Z = 248,800 \text{ lb.}/20,570 \text{ lb.} = 12.095$$

Consequently, the maximum circumferential stress due to the ring moment, away from the impact location, is:

$$3,037 \text{ psi} \times (69,260 \text{ in-lb}/180,900 \text{ in-lb}) \times Z = 14,230 \text{ psi}$$

At the same location, the mean stress adds an additional component (the ring area is computed based on the effective width of the ring).

$$(5,143 \text{ lb.}/43.47 \text{ sq.in}) \times Z = 1431 \text{ psi}$$

Therefore, the safety factor on circumferential stress causing ovalization of an effective ring section that is assumed to resist the impact is:

$$SF(\text{ring stress}) = 39,750 \text{ psi}/(1431 \text{ psi} + 14,230 \text{ psi}) = 2.54$$

The allowable stress for this safety factor calculation is obtained from Table 3.1.12 for primary membrane stress intensity for a Level D event at 350 degrees F material temperature. Noting that the actual circumferential stress in the ring remains in the elastic range, it is concluded that the MPC remains readily retrievable after the impact since there is no permanent ovalization of the cavity after the event. As noted previously, the presence of the water jacket adds an additional structural barrier that has been conservatively neglected in this analysis.

#### 3.4.8.2.2 Large Missile Strike

The effects of a large tornado missile strike on the side (water jacket outer enclosure) of a loaded HI-TRAC has been simulated using a transient finite element model of the transfer cask and loaded MPC. The transient finite element code LSDYNA3D has been used (approved by the NRC for use in

impact analysis (see Appendix 3.A, reference [3.A.4] for the benchmarking of this computer code)). An evaluation of MPC retrievability and global stress state (away from the impact area) are of primary interest. The finite element model includes the loaded MPC, the HI-TRAC inner and outer shells, the HI-TRAC water jacket, the lead shielding, and the appropriate HI-TRAC lids. The water in the water jacket has been neglected for conservatism in the results. The large tornado missile has been simulated by an impact force-time pulse applied on an area representing the frontal area of an 1800-kg. vehicle. The force-time data used has been previously approved by the USNRC (Bechtel Topical Report BC-TOP-9A, "Design of Structures for Missile Impact", Revision 2, 9/1974). The frontal impact area used in the finite element analysis is that area recommended in NUREG-0800, SRP 3.5.1.4, Revision 2, 1981).

A summary of the results is presented below for the HI-TRAC 100 and HI-TRAC 125 transfer casks. Since the dimensions of the inner shell, the outer shell, the lead shielding, and the water jacket enclosure panels are the same in both the HI-TRAC 125 and the HI-TRAC 125D, the results from the HI-TRAC 125 are considered accurate for the HI-TRAC 125D. Likewise, the results from the HI-TRAC 100 are valid for the HI-TRAC 100D. The allowable value listed for the stress intensity for this Level D event comes from Table 3.1.17.

The results from the dynamic analysis have been summarized below.

<b>SUMMARY OF RESULTS FROM LARGE TORNADO MISSILE IMPACT ANALYSIS</b>		
<b>ITEM – HI-TRAC 100</b>	<b>CALCULATED VALUE</b>	<b>ALLOWABLE VALUE</b>
Maximum Stress Intensity in Water Jacket (ksi)	33.383	58.7
Maximum Stress Intensity in Inner Shell (ksi)	15.6	58.7
Maximum Plastic Strain in Water Jacket	0.0	-
Maximum Plastic Strain in Inner Shell	0.0	-

<b>ITEM – HI-TRAC 125</b>	<b>CALCULATED VALUE</b>	<b>ALLOWABLE VALUE</b>
Maximum Stress Intensity in Water Jacket (ksi)	33.697	58.7
Maximum Stress Intensity in Inner Shell (ksi)	18.669	58.7
Maximum Plastic Strain in Water Jacket	0.0	-
Maximum Plastic Strain in Inner Shell	0.0	-

The above results demonstrate that:

1. The retrievability of the MPC in the wake of a large tornado missile strike is not adversely affected since the inner shell does not experience any plastic deformation.
2. The maximum primary stress intensity, away from the impact interface on the HI-TRAC water jacket, is below the applicable ASME Code Level D allowable limit for NF, Class 3 structures.

#### 3.4.9 HI-TRAC Drop Events (Load Case 02.b in Table 3.1.5)

During transit, the HI-TRAC 125 or HI-TRAC 100 transfer cask may be carried horizontally with the transfer lid in place. Analyses have been performed to demonstrate that under a postulated carry height; the design basis 45g deceleration is not exceeded. The analyses have been performed using two different simulation models. A simplified model of the drop event is performed using the computer simulation code "Working Model 2D". The analysis using "Working Model 2D" assumed the HI-TRAC and the contained MPC acted as a single rigid body. A second model of the drop event uses DYNA3D, considers the multi-body analysis of HI-TRAC and the contained MPC as individual bodies, and is finite element based. In what follows, we outline the problem and the results obtained using each solution methodology.

##### 3.4.9.1 Working Model 2D Analysis of Drop Event

The analysis model conservatively neglects all energy absorption by any component of HI-TRAC; all kinetic energy is transferred to the ground through the spring-dampers that simulate the foundation (ground). If the HI-TRAC suffers a handling accident causing a side drop to the ground, impact will only occur at the top and bottom ends of the vessel. The so-called "hard points" are the top end lifting trunnions, the bottom end rotation trunnions, and the projecting ends of the transfer lid. Noting that the projecting hard points are of different dimensions and will impact the target at different times because of the HI-TRAC geometry, any simulation model must allow for this possibility.

A dynamic analysis of a horizontal drop, with the lowest point on the HI-TRAC assumed 50" above the surface of the target (larger than the design basis limit of 42"), is considered for the HI-TRAC 125 and for the HI-TRAC 100. Figure 3.4.22 shows the transfer cask orientation. The HI-TRAC is considered as a rigid body (calculations demonstrate that the lowest beam mode frequency is well above 33 Hz so that no dynamic amplification need be included). The effects of the ISFSI pad and the underlying soil are included using a simple spring-damper model based on a static classical Theory of Elasticity solution. The "worst" orientation of a horizontally carried HI-TRAC with the transfer cask impacting an elastic surface is considered. The HI-TRAC is assumed to initially impact the target with the impact force occurring over the rectangular surface of the transfer lid (11.875" x 81"). "Worst" is defined here as meaning an impact at a location having the maximum value of an elastic spring constant simulating the resistance of the target interface. The geometry and material properties reflect the USNRC accepted reference pad and soil (Table 2.2.9 - the pad thickness used is 36" and the Young's Modulus of the elastic soil is the upper limit value  $E=28,000$  psi). The use of an elastic representation of the target surface is conservative as it minimizes the energy absorption

capacity of the target and maximizes the deceleration loads developed during the impact. The spring constant is also calculated based on an assumption that impact at the lower end of HI-TRAC first occurs at the pocket trunnion. The results demonstrate that this spring constant is lower and therefore would lead to a lower impact force. Therefore, the dynamic analysis of the handling accident is performed assuming initial impact with the flat rectangular short end of the transfer lid. Subsequent to the initial impact, the HI-TRAC rotates in accordance with the dynamic equations of equilibrium and a secondary impact at the top of the transfer cask occurs. The impact is at the edge of the water jacket.

The following table summarizes the results from the dynamic analyses (using the Working Model 2D computer code):

<b>HI-TRAC Handling Analysis – Working Model Analysis of Horizontal Drop</b>			
<b>Item</b>	<b>Value</b>	<b>Allowable</b>	<b>Safety Factor</b>
HI-TRAC 125 – Primary Impact Deceleration (g's)	32.66	45	1.38
HI-TRAC 125 – Secondary Impact Deceleration (g's)	26.73	45	1.68
HI-TRAC 100 – Primary Impact Deceleration (g's)	33.18	45	1.36
HI-TRAC 100 – Secondary Impact Deceleration (g's)	27.04	45	1.66
Axial Membrane Stress Due to HI-TRAC 125 Bending as a Beam - Level D Drop (psi)	19.06	39.75	2.085
Axial Membrane Stress Due to HI-TRAC 100 Bending as a Beam - Level D Drop (psi)	15.77	39.75	2.52

In the table above, the decelerations are measured at points corresponding to the base and top of the fuel assemblies contained inside the MPC. The dynamic drop analysis reported above, using the Working Model 2D rigid body-spring model proved that decelerations are below the design basis value and that global stresses were within allowable limits.

#### 3.4.9.2 DYNA3D Analysis of Drop Event

An independent evaluation of the drop event to delineate the effect of target non-linearity and the flexibility of the transfer cask has been performed using DYNA3D. Both the HI-TRAC 125 and HI-TRAC 100 transfer casks are modeled as part of the cask-pad-soil interaction finite element model set forth in NUREG/CR-6608 and validated by an NRC reviewed and approved Holtec topical report (see reference [3.A.4] in Appendix 3.A). The model uses the identical MPC and target pad/soil models employed in the accident analyses of the HI-STORM 100 overpack. The HI-TRAC inner and outer shells, the contained lead, the transfer lid, the water jacket metal structure, and the top lids are included in the model. The water jacket is assumed empty for conservatism.

---

HOLTEC INTERNATIONAL COPYRIGHTED MATERIAL

Two side drop orientations are considered (see Figures 3.4.27 and 3.4.28). The first drop assumes that the plane of the lifting and rotation trunnions is horizontal with primary impact on the short side of the transfer lid. This maximizes the angle of slapdown, and represents a credible drop configuration where the HI-TRAC cask is dropped while being carried horizontally. The second drop orientation assumes primary impact on the rotation trunnion and maximizes the potential for the lifting trunnion to participate in the secondary impact. This is a non-credible event that assumes complete separation from the transfer vehicle and a ninety-degree rotation prior to impact. Nevertheless, it is the only configuration where the trunnions could be involved in both primary and secondary impacts.

For each simulation performed, the lowest point on the HI-TRAC cask (either the transfer lid edge or the rotation trunnion) is set at 42" above the target interface. Decelerations are measured at the top lid, the cask centroidal position, and the transfer lid. Normal forces were measured at the primary impact interface, at the secondary impact interface, and at the top lid/MPC interface. Decelerations are filtered at 350 Hz.

The following key results summarize the analyses:

ITEM	HI-TRAC 125		HI-TRAC 100		ALLOWABLE
	Horizontal	Vertical	Horizontal	Vertical	
Initial Orientation of Trunnions					
Max. Top Lid Vertical Deceleration – Secondary Impact (g's)	25.5	32	36.5	45 <sup>†</sup>	45
Centroid Vertical Deceleration – at Time of Secondary Impact (g's)	9.0	13.0	10.0	17.5	45
Max. Transfer Lid Vertical Deceleration – Primary Impact (g's)	30.8	23.5	35.0	31.75	45
Maximum Normal Force at Primary Impact Site (kips)	1,950.	1,700	1,700	1,700	-
Maximum Normal Force at Secondary Impact Site (kips)	1,300.	1,850.	1,500.	1,450.	-
Maximum MPC/Top Lid Interface Force (kips)	132.	-	39.	-	-
Maximum Diametral Change of Inner Shell (inch)	0.228	0.113	Not Computed	0.067	0.3725
Maximum Von Mises Stress (ksi)	37.577	38.367	40.690	40.444	58.7*

<sup>†</sup> The deceleration at the top of the basket is estimated at 41 g's

\* Allowable Level D Stress Intensity for Primary Plus Secondary Stress Intensity

HOLTEC INTERNATIONAL COPYRIGHTED MATERIAL

HI-STORM FSAR

REPORT HI-2002444

3.4-103

Rev. 10

HI-STORM 100 FSAR, NON-PROPRIETARY

REVISION 12

MARCH 12, 2014

The results summarized above demonstrate that both the HI-TRAC 125 and HI-TRAC 100 transfer casks are sufficiently robust to perform their function during and after the postulated handling accidents. We also note that the results, using the Working Model single rigid body dynamic model (see Subsection 3.4.9.1), are in reasonable agreement with the results predicted by the DYNA3D multi-body finite element dynamic model although performed for a different drop height with deceleration measurements at different locations on the HI-TRAC.

The results reported above for maximum interface force at the top lid/MPC interface are used as input to a separate analysis, which demonstrates that the top lid contains the MPC during and after a handling accident. The results reported above for the maximum normal force at the primary impact site (the transfer lid) have been used to calculate the maximum interface force at the bottom flange/transfer lid interface. This result is needed to insure that the interface forces used to evaluate transfer lid separation are indeed bounding. To obtain the interface force between the HI-TRAC transfer lid and the HI-TRAC bottom flange, it is sufficient to take a free-body of the transfer lid and write the dynamic force equilibrium equation for the lid. Figure 3.4.29 shows the free body with appropriate notation. The equation of equilibrium is:

$$M_{TL} a_{TL} = F_I - G_I$$

where

$M_{TL}$  = the mass of the transfer lid

$a_{TL}$  = the time varying acceleration of the centroid of the transfer lid

$F_I$  = the time varying contact force at the interface with the target

$G_I$  = the time varying interface force at the bottom flange/transfer lid interface

Solving for the interface force give the result

$$G_I = F_I - M_{TL} a_{TL}$$

Using the appropriate transfer lid mass and acceleration, together with the target interface force at the limiting time instant, provides values for the interface force. The table below provides the results of this calculation for the HI-TRAC 125 and HI-TRAC 100 transfer casks.



Item	Calculated from Equilibrium (kips)
HI-TRAC 125 – Trunnions Horizontal	1,183.
HI-TRAC 125 – Trunnions Vertical	1,272.
HI-TRAC 100 – Trunnions Horizontal	1,129.
HI-TRAC 100 – Trunnions Vertical	1,070.

#### 3.4.9.3 Horizontal Drop of HI-TRAC 125D

The previous subsection addressed the 42” horizontal drop of the HI-TRAC 125 and HI-TRAC 100, including an evaluation of the bolted connection between the transfer lid, which sustains the primary impact, and the cylindrical body of the loaded HI-TRAC. The HI-TRAC 125D does not have a bolted connection between the bottom flange and the cylindrical body of the cask. However, the transverse protrusions (bottom flange, lifting trunnions, and optional attachment lugs/support tabs at the top of the cask) spawn different impact scenarios. The uncontrolled lowering of the cask is assumed to occur from a height of 42” measured to the lowest location on the HI-TRAC 125D in the horizontal orientation.

The maximum decelerations for the HI-TRAC 125D are comparable to the drop results for the HI-TRAC 125 when the plane of the lifting and rotation trunnions is vertical. Although the HI-TRAC 125D has no rotation trunnions, its bottom flange extends radially beyond the water jacket shell by approximately the same amount as the HI-TRAC 125 rotation trunnions and thereby establishes a similar “hard point” for primary impact in terms of distance from the cask centerline. More important, because the bottom flange is positioned closer to the base of the HI-TRAC 125D than the rotation trunnions are in the HI-TRAC 125, the slap-down angle for the HI-TRAC 125D is less. The shallower angle decreases the participation of the lifting trunnion during the secondary impact, and increases the participation of the water jacket shell. Since the water jacket shell is a more flexible structure than the lifting trunnion, the deceleration of the HI-TRAC 125D cask during secondary impact is slightly less than the calculated deceleration of the HI-TRAC 125. In the HI-TRAC 125D, there is no bolted connection at the bottom flange/cask body interface that is active in load transfer from the flange to the cask body. It is therefore concluded that this drop scenario for the HI-TRAC 125D is bounded by the similar evaluation for the HI-TRAC 125. The same rationale applies to the HI-TRAC 100D versus the HI-TRAC 100. In fact, the protruding segments of the HI-TRAC 100D bottom flange are not in the same impact plane as the lifting trunnions; therefore, a secondary impact involving a lifting trunnion is not possible. Therefore, the drop scenarios analyzed for the HI-TRAC 100 bound any 42” horizontal drop of a HI-TRAC 100D.

A second HI-TRAC 125D drop scenario, where the two attachment lugs/support tabs are oriented in

a vertical plane, is the most limiting scenario. This drop event is unique to HI-TRAC 125D serial numbers 3 and 4, since these are the only two transfer casks fabricated with attachment lugs/support tabs. The tab dimensions are such that primary impact occurs at the top end of the cask when the support tabs impact the target surface, followed by a slap-down and a secondary impact at the bottom flange. Note that this drop scenario does not exist for the HI-TRAC 100D since it has no attachment lugs/support tabs.

The evaluation of the limiting HI-TRAC 125D drop scenario is performed using the computer code Working Model 3D (WM) (now known as Visual Nastran Desktop). First, the WM code is used to simulate the "Scenario A" drop of the HI-TRAC 125 in order to establish appropriate parameters to "benchmark" WM against the DYNA3D solution. The table below summarizes the results of the Working Model/DYNA3D benchmark comparison. Figure 3.4.48 shows the benchmark configuration after the drop event.

Comparison of HI-TRAC 125 Drop Results (Scenario A)		
	DYNA3D	Working Model
Vertical Deceleration of Top Lid (secondary impact) g's	32	33.49
Vertical Deceleration at Bottom Lid (primary impact on rotation trunnion) g's	23.5	23.59

The benchmarked Working Model simulation was then modified to simulate the second drop scenario of the HI-TRAC 125D with support tabs in a vertical plane; primary impact now occurred at the top end with secondary impact at the bottom flange. Figure 3.4.49 shows the configuration of the HI-TRAC 125D after this scenario. The impact parameters were unchanged from the benchmark model except for location. The acceleration results from the 42" horizontal drop of the HI-TRAC 125D in this second drop scenario are summarized below.

Results From HI-TRAC 125D 42" Drop	
Vertical Deceleration of Top Lid (primary impact on support tab) g's	36.75
Vertical Deceleration of Pool Lid (secondary impact on bottom flange) g's	29.27

The resulting g loads at the top of the active fuel region for the HI-TRAC 125D, with primary impact on the support tabs, are increased over the loads computed for the HI-TRAC 125 but remain well below the design basis limit.

Finally, stress calculations similar to those presented in Subsection 3.4.9.1 for the HI-TRAC 125 have also been performed for the HI-TRAC 125D using the above maximum decelerations. The table below summarizes the results:

Item	Value	Allowable	Safety Factor
Axial Membrane Stress Due to HI-TRAC 125D Bending as a Beam - Level D Drop (psi)	26.13	39.75	1.521
Shear Stress in Outer Shell Circumferential Weld Due to HI-TRAC 125D Bending as a Beam - Level D Drop (psi)	27.43	29.40	1.072

#### 3.4.10 HI-STORM 100 Non-Mechanistic Tip-over and Vertical Drop Event (Load Cases 02.a and 02.c in Table 3.1.5)

Pursuant to the provision in NUREG-1536, a non-mechanistic tip-over of a loaded HI-STORM 100 System on to the ISFSI pad is considered in this report. Analyses are also performed to determine the maximum deceleration sustained by a vertical free fall of a loaded HI-STORM 100 System from an 11" height onto the ISFSI pad. The objective of the analyses is to demonstrate that the plastic deformation in the fuel basket is sufficiently limited to permit the stored SNF to be retrieved by normal means, does not have a adverse effect on criticality safety, and that there is no significant loss of radiation shielding in the system.

Ready retrievability of the fuel is presumed to be ensured: if global stress levels in the MPC structure meet Level D stress limits during the postulated drop events; if any plastic deformations are localized; and if no significant permanent ovalization of the overpack into the MPC envelope space, remains after the event.

Subsequent to the accident events, the storage overpack must be shown to contain the shielding so that unacceptable radiation levels do not result from the accident.

Appendix 3.A provides a description of the dynamic finite element analyses undertaken to establish the decelerations resulting from the postulated event. A non-mechanistic tip-over is considered together with an end drop of a loaded HI-STORM 100 System. A dynamic finite element analysis of each event is performed using a commercial finite element code well suited for such dynamic analyses with interface impact and non-linear material behavior. This code and methodology have been fully benchmarked against Lawrence Livermore Laboratories test data and correlation [3.4.12].

The table below provides the values of computed peak decelerations at the top of the fuel basket for the vertical drop and the non-mechanistic tipover scenarios. It is seen that the peak deceleration is below 45 g's.

### Filtered Results for Drop and Tip-Over Scenarios for HI-STORM

Drop Event	Max. Deceleration at the Top of the Basket (g's)	
	Set A(36" Thick Pad)	Set B(28" Thick Pad)
End Drop for 11 Inches	43.98	41.53
Non-Mechanistic Tip-over	42.85	39.91

The tipover analysis performed in Appendix 3.A is based on the HI-STORM 100 geometry and a bounding weight. The fact that the HI-STORM 100S(232) is shorter and has a lower center of gravity suggests that the impact kinetic energy is reduced so that the target would absorb the energy with a lower maximum deceleration. However, since the actual weight of a HI-STORM 100S(232) is less than that of a HI-STORM 100 by a significant amount, the predicted maximum rigid body deceleration would tend to increase slightly. Since there are two competing mechanisms at work, it is not a foregone conclusion that the maximum rigid body deceleration level is, in fact, reduced if a HI-STORM 100S(232) suffers a non-mechanistic tipover onto the identical target as the HI-STORM 100. The situation is clearer for the HI-STORM 100S(243), which is virtually equal in weight to the HI-STORM 100, yet its center of gravity when loaded is almost one inch lower. In what follows, we present a summary of the analysis undertaken to demonstrate conclusively that the result for maximum deceleration level in the HI-STORM 100 tipover event does bound the corresponding value for the HI-STORM 100S(232), and, therefore, we need only perform a detailed dynamic finite element analysis for the HI-STORM 100.

Appendix 3.A presents a result for the angular velocity of the cylindrical body representing a HI-STORM 100 just prior to impact with the defined target. The result is expressed in Subsection 3.A.6 in terms of the cask geometry, and the ratio of the mass divided by the mass moment of inertia about the corner point that serves as the rotation origin. Since the mass moment of inertia is also linearly related to the mass, the angular velocity at the instant just prior to target contact is independent of the cask mass. Subsequent to target impact, we investigate post-impact response by considering the cask as a cylinder rotating into a target that provides a resistance force that varies linearly with distance from the rotation point. We measure "time" as starting at the instant of impact, and develop a one-degree-of freedom equation for the post-impact response (for the rotation angle into the target) as:

$$\ddot{\theta} + \omega^2 \theta = 0$$

where

$$\omega^2 = \frac{kL^3}{3I_A}$$

The initial conditions at time=0 are: the initial angle is zero and the initial angular velocity is equal to the rigid body angular velocity acquired by the tipover from the center-of-gravity over corner position. In the above relation, L is the length of the overpack, I is the mass moment of inertia defined in Appendix 3.A, and k is a “spring constant” associated with the target resistance. If we solve for the maximum angular acceleration subsequent to time = 0, we obtain the result in terms of the initial angular velocity as:

$$\ddot{\theta}_{\max} = \omega \dot{\theta}_0$$

If we form the maximum linear acceleration at the top of the four-inch thick lid of the overpack, we can finally relate the decelerations of the HI-STORM 100 and the HI-STORM 100S(232) solely in terms of their geometry properties and their mass ratio. The value of “k”, the target spring rate is the same for both overpacks so it does not appear in the relationship between the two decelerations. After substituting the appropriate geometry and calculated masses, we determine that the ratio of maximum rigid body decelerations at the top surface of the four-inch thick top lid plates is:

$$A_{\text{HI-STORM 100S(232)}}/A_{\text{HI-STORM 100}} = 0.946$$

Therefore, as postulated, there is no need to perform a separate DYNA3D analysis for the HI-STORM 100S hypothetical tipover.

Moreover, according to Appendix 3.A, analysis of a single mass impacting a spring with a given initial velocity shows that the maximum deceleration “ $a_M$ ” of the mass is related to the dropped weight “w” and the drop height “h” as follows:

$$a_M \sim \frac{\sqrt{h}}{\sqrt{w}}$$

In other words, as the dropped weight increases, the maximum deceleration of the mass decreases. Therefore, the rigid body decelerations calculated in Appendix 3.A serve as a conservative upper bound for the densified concrete shielding option.

The same considerations apply to the HI-STORM 100S Version B. The overall lengths are reduced from the classic HI-STORM 100, but the actual weights may be reduced. Therefore, calculations similar to those given above for the HI-STORM 100S are needed to conclusively demonstrate that the non-mechanistic tipover analysis of the classic HI-STORM 100 remains bounding. The results of the calculations, which demonstrate that the design basis limits are met, are presented below together with maximum G levels computed for the 11” vertical drop:

ITEM	A HI-STORM 100S VERSION B(218)/A HI-STORM 100	A HI-STORM 100S VERSION B(229)/A HI-STORM 100	Max. Calculated G Level 11" Drop
HI-STORM 100S Version B(218)	0.91	-	44.378
HI-STORM 100S Version B(229)	-	0.98	43.837

A simple elastic strength of materials calculation is performed to demonstrate that the cylindrical storage overpack will not permanently deform to the extent that the MPC cannot be removed by normal means after a tip-over event. The results demonstrate that the maximum diametrical closure of the cylindrical cavity is less than the initial clearance between the overpack MPC support channels and the MPC canister. Primary circumferential membrane stresses in the MPC shell remain in the elastic range during a tip-over (see Table 3.4.6 summary safety factors); therefore, no permanent global ovalization of the MPC shell occurs as a result of the drop.

To demonstrate that the shielding material will continue to perform its function after a tip-over accident, the stress and strain levels in the metal components of the storage overpack are examined at the end of the tip-over event. The results obtained in Appendix 3.A for impact decelerations conservatively assumed a rigid storage overpack model to concentrate nearly all energy loss in the target. However, to assess the state of stress and strain in the storage overpack after an accident causing a tip-over, the tip-over analysis was also performed using a non-rigid storage overpack model using overpack material properties listed in Appendix 3.A. Figure 3.4.13 shows the calculated von Mises stress in the top lid and outer shell at 0.08 seconds after the initiation of impact. Figure 3.4.14 shows the residual plastic strains in the same components. Figures 3.4.15 and 3.4.16 provide similar results for the inner shell, the radial plates, and the support channels<sup>†</sup>. The results show that while some plastic straining occurs, accompanied by stress levels above the yield stress of the material, there is no tearing in the metal structure which confines the radiation shielding (concrete). Therefore, there is no gross failure of the metal shells enclosing the concrete. The shielding concrete will remain inside the confines of the storage overpack and maintain its performance after the tipover event. Although the preceding results are based on an overpack model having inner and outer shell thicknesses of 1-1/4" and 3/4", respectively, the conclusion holds for the optional HI-STORM design with 1" thick inner and outer shells since having a thicker steel shell at the primary point of impact provides more strength and greater protection against a cavity breach. The results from these analyses are also applicable to the HI-STORM 100S and the HI-STORM 100S, Version B since the structural material at the top of the cask that would be locally deformed after a tipover event is essentially the same.

<sup>†</sup> During fabrication the channels are attached to the inner shell by one of two methods, either the channels are welded directly to the inner shell or they are welded to a pair of L-shaped angles (i.e., channel mounts) that are pre-fastened to the inner shell. The results presented in Figures 3.4.16a and 3.4.16b bound the results from both methods of attachment.

### 3.4.11 Storage Overpack and HI-TRAC Transfer Cask Service Life

The term of the 10CFR72, Subpart L C of C, granted by the NRC is 20 years; therefore, the License Life (please see glossary) of all components is 20 years. Nonetheless, the HI-STORM 100 and 100S Storage overpacks and the HI-TRAC transfer cask are engineered for 40 years of design life, while satisfying the conservative design requirements defined in Chapter 2, including the regulatory requirements of 10CFR72. In addition, the storage overpack and HI-TRAC are designed, fabricated, and inspected under the comprehensive Quality Assurance Program discussed in Chapter 13 and in accordance with the applicable requirements of the ACI and ASME Codes. This assures high design margins, high quality fabrication, and verification of compliance through rigorous inspection and testing, as describe in Chapter 9 and the design drawings in Section 1.5. Technical Specifications defined in Chapter 12 assure that the integrity of the cask and the contained MPC are maintained throughout the components' design life. The design life of a component, as defined in the Glossary, is the minimum duration for which the equipment or system is engineered to perform its intended function if operated and maintained in accordance with the FSAR. The design life is essentially the lower bound value of the service life, which is the expected functioning life of the component or system. Therefore, component longevity should be: licensed life < design life < service life. (The licensed life, enunciated by the USNRC, is the most pessimistic estimate of a component's life span.) For purposes of further discussion, we principally focus on the service life of the HI-STORM 100 System components that, as stated earlier, is the reasonable expectation of equipment's functioning life span.

The service life of the storage overpack and HI-TRAC transfer cask is further discussed in the following sections.

#### 3.4.11.1 Storage Overpack

The principal design considerations that bear on the adequacy of the storage overpack for the service life are addressed as follows:

##### Exposure to Environmental Effects

In the following text, all references to HI-STORM 100 also apply to HI-STORM 100S and to the HI-STORM 100S Version B. All exposed surfaces of HI-STORM 100 are made from ferritic steels that are readily painted. Concrete, which serves strictly as a shielding material, is completely encased in steel. Therefore, the potential of environmental vagaries such as spalling of concrete, are ruled out for HI-STORM 100. Under normal storage conditions, the bulk temperature of the HI-STORM 100 storage overpack will, because of its large thermal inertia, change very gradually with time. Therefore, material degradation from rapid thermal ramping conditions is not credible for the HI-STORM 100 storage overpack. Similarly, corrosion of structural steel embedded in the concrete structures due to salinity in the environment at coastal sites is not a concern for HI-STORM 100 because HI-STORM 100 does not rely on rebars (indeed, it contains no rebars). As discussed in Appendix 1.D, the aggregates, cement and water used in the storage cask concrete are carefully controlled to provide high durability and resistance to temperature effects. The configuration of the

storage overpack assures resistance to freeze-thaw degradation. In addition, the storage overpack is specifically designed for a full range of enveloping design basis natural phenomena that could occur over the 40-year design life of the storage overpack as defined in Subsection 2.2.3 and evaluated in Chapter 11.

#### Material Degradation

The relatively low neutron flux to which the storage overpack is subjected cannot produce measurable degradation of the cask's material properties and impair its intended safety function. Exposed carbon steel components are coated to prevent corrosion. The controlled environment of the ISFSI storage pad mitigates damage due to direct exposure to corrosive chemicals that may be present in other industrial applications.

#### Maintenance and Inspection Provisions

The requirements for periodic inspection and maintenance of the storage overpack throughout the 40-year design life are defined in Chapter 9. These requirements include provisions for routine inspection of the storage overpack exterior and periodic visual verification that the ventilation flow paths of the storage overpack are free and clear of debris. ISFSIs located in areas subject to atmospheric conditions that may degrade the storage cask or canister should be evaluated by the licensee on a site-specific basis to determine the frequency for such inspections to assure long-term performance. In addition, the HI-STORM 100 System is designed for easy retrieval of the MPC from the storage overpack should it become necessary to perform more detailed inspections and repairs on the storage overpack.

The above findings are consistent with those of the NRC's Waste Confidence Decision Review [3.4.11], which concluded that dry storage systems designed, fabricated, inspected, and operate in accordance with such requirements are adequate for a 100-year service life while satisfying the requirements of 10CFR72.

#### 3.4.11.2 Transfer Cask

The principal design considerations that bear on the adequacy of the HI-TRAC Transfer Cask for the service life are addressed as follows:

##### Exposure to Environmental Effects

All transfer cask materials that come in contact with the spent fuel pool are coated to facilitate decontamination. The HI-TRAC is designed for repeated normal condition handling operations with high factor of safety, particularly for the lifting trunnions, to assure structural integrity. The resulting cyclic loading produces stresses that are well below the endurance limit of the trunnion material, and therefore, will not lead to a fatigue failure in the transfer cask. All other off-normal or postulated accident conditions are infrequent or one-time occurrences that do not contribute significantly to fatigue. In addition, the transfer cask utilizes materials that are not susceptible to brittle fracture



during the lowest temperature permitted for loading, as discussed in Chapter 12.

### Material Degradation

All transfer cask materials that are susceptible to corrosion are coated. The controlled environment in which the HI-TRAC is used mitigates damage due to direct exposure to corrosive chemicals that may be present in other industrial applications. The infrequent use and relatively low neutron flux to which the HI-TRAC materials are subjected do not result in radiation embrittlement or degradation of the HI-TRAC's shielding materials that could impair the HI-TRAC's intended safety function. The HI-TRAC transfer cask materials are selected for durability and wear resistance for their deployment.

### Maintenance and Inspection Provisions

The requirements for periodic inspection and maintenance of the HI-TRAC transfer cask throughout the 40-year design life are defined in Chapter 9. These requirements include provisions for routine inspection of the HI-TRAC transfer cask for damage prior to each use, including an annual inspection of the lifting trunnions. Precautions are taken during lid handling operations to protect the sealing surfaces of the pool lid. The leak tightness of the liquid neutron shield is verified periodically. The water jacket pressure relief valves and other fittings used can be easily removed.

#### 3.4.12 MPC Service Life

The term of the 10CFR72, Subpart L C of C, granted by the NRC (i.e., licensed life) is 20 years. Nonetheless, the HI-STORM 100 MPC is designed for 40 years of design life, while satisfying the conservative design requirements defined in Chapter 2, including the regulatory requirements of 10CFR72. Additional assurance of the integrity of the MPC and the contained SNF assemblies throughout the 40-year life of the MPC is provided through the following:

- Design, fabrication, and inspection in accordance with the applicable requirements of the ASME Code as described in Chapter 2 assures high design margins.
- Fabrication and inspection performed in accordance with the comprehensive Quality Assurance program discussed in Chapter 13 assures competent compliance with the fabrication requirements.
- Use of materials with known characteristics, verified through rigorous inspection and testing, as described in Chapter 9, assures component compliance with design requirements.
- Use of welding procedures in full compliance with Section III of the ASME Code ensures high-quality weld joints.

Technical Specifications, as defined in Chapter 12, have been developed and imposed on the MPC that assure that the integrity of the MPC and the contained SNF assemblies are maintained throughout the 40-year design life of the MPC.

The principal design considerations bearing on the adequacy of the MPC for the service life are summarized below.

### Corrosion

All MPC materials are fabricated from corrosion-resistant austenitic stainless steel and passivated aluminum. The corrosion-resistant characteristics of such materials for dry SNF storage canister applications, as well as the protection offered by these materials against other material degradation effects, are well established in the nuclear industry. The moisture in the MPC is removed to eliminate all oxidizing liquids and gases and the MPC cavity is backfilled with dry inert helium at the time of closure to maintain an atmosphere in the MPC that provides corrosion protection for the SNF cladding throughout the dry storage period. The preservation of this non-corrosive atmosphere is assured by the inherent sealworthiness of the MPC confinement boundary integrity (there are no gasketed joints in the MPC).

### Structural Fatigue

The passive non-cyclic nature of dry storage conditions does not subject the MPC to conditions that might lead to structural fatigue failure. Ambient temperature and insolation cycling during normal dry storage conditions and the resulting fluctuations in MPC thermal gradients and internal pressure is the only mechanism for fatigue. These low-stress, high-cycle conditions cannot lead to a fatigue failure of the MPC that is made from stainless alloy stock (endurance limit well in excess of 20,000 psi). All other off-normal or postulated accident conditions are infrequent or one-time occurrences, which cannot produce fatigue failures. Finally, the MPC uses materials that are not susceptible to brittle fracture.

### Maintenance of Helium Atmosphere

The inert helium atmosphere in the MPC provides a non-oxidizing environment for the SNF cladding to assure its integrity during long-term storage. The preservation of the helium atmosphere in the MPC is assured by the robust design of the MPC confinement boundary described in Section 7.1. Maintaining an inert environment in the MPC mitigates conditions that might otherwise lead to SNF cladding failures. The required mass quantity of helium backfilled into the canister at the time of closure and the associated fabrication and closure requirements for the canister are specifically set down to assure that an inert helium atmosphere is maintained in the canister throughout the 40-year design life.

### Allowable Fuel Cladding Temperatures

The helium atmosphere in the MPC promotes heat removal and thus reduces SNF cladding temperatures during dry storage. In addition, the SNF decay heat will substantially attenuate over a 40-year dry storage period. Maintaining the fuel cladding temperatures below allowable levels during long-term dry storage mitigates the damage mechanism that might otherwise lead to SNF cladding

failures. The allowable long-term SNF cladding temperatures used for thermal acceptance of the MPC design are conservatively determined, as discussed in Section 4.3.

#### Neutron Absorber Boron Depletion

The effectiveness of the fixed borated neutron absorbing material used in the MPC fuel basket design requires that sufficient concentrations of boron be present to assure criticality safety during worst case design basis conditions over the 40-year design life of the MPC. Information on the characteristics of the borated neutron absorbing material used in the MPC fuel basket is provided in Subsection 1.2.1.3.1. The relatively low neutron flux, which will continue to decay over time, to which this borated material is subjected, does not result in significant depletion of the material's available boron to perform its intended safety function. In addition, the boron content of the material used in the criticality safety analysis is conservatively based on the minimum specified boron areal density (rather than the nominal), which is further reduced by 25% for analysis purposes, as described in Section 6.1. Analysis discussed in Section 6.3.2 demonstrates that the boron depletion in the neutron absorber material is negligible over a 50-year duration. Thus, sufficient levels of boron are present in the fuel basket neutron absorbing material to maintain criticality safety functions over the 40-year design life of the MPC.

The above findings are consistent with those of the NRC's Waste Confidence Decision Review, which concluded that dry storage systems designed, fabricated, inspected, and operated in the manner of the requirements set down in this document are adequate for a 100-year service life, while satisfying the requirements of 10CFR72.

#### 3.4.13 Design and Service Life

The discussion in the preceding sections seeks to provide the logical underpinnings for setting the design life of the storage overpacks, the HI-TRAC transfer cask, and the MPCs as forty years. Design life, as stated earlier, is a lower bound value for the expected performance life of a component (service life). If operated and maintained in accordance with this Final Safety Analysis Report, Holtec International expects the service life of its HI-STORM 100 and HI-STORM 100S Version's components to substantially exceed their design life values.

Table 3.4.1

## FINITE ELEMENTS IN THE MPC STRUCTURAL MODELS

<b>MPC Type</b>	<b>Model Type</b>		
<b>Element Type</b>	<b>Basic</b>	<b>0 Degree Drop</b>	<b>45 Degree Drop</b>
<b>MPC-24</b>	1068	1114	1113
BEAM3	1028	1028	1028
PLANE82	0	0	0
CONTAC12	40	38	38
CONTAC26	0	45	45
COMBIN14	0	3	2
<b>MPC-32</b>	1374	1604	1603
BEAM3	1346	1346	1346
CONTAC12	28	27	24
CONTAC26	0	229	228
COMBIN14	0	2	5
<b>MPC-68</b>	1842	2066	2063
BEAM3	1782	1782	1782
PLANE82	16	16	16
CONTAC12	44	43	40
CONTAC26	0	223	222
COMBIN14	0	2	3
<b>MPC-24E</b>	1070	1124	1122
BEAM3	1030	1030	1030
PLANE82	0	0	0
CONTAC12	40	38	38
CONTAC26	0	53	52
COMBIN14	0	3	2

HOLTEC INTERNATIONAL COPYRIGHTED MATERIAL

**TABLE 3.4.2**  
**HI-STORM 100 SYSTEM MATERIAL COMPATIBILITY**  
**WITH OPERATING ENVIRONMENTS**

<b>Material/Component</b>	<b>Fuel Pool (Borated and Unborated Water)<sup>†</sup></b>	<b>ISFSI Pad (Open to Environment)</b>
<u>Alloy X:</u> <ul style="list-style-type: none"> <li>- MPC Fuel Basket</li> <li>- MPC Baseplate</li> <li>- MPC Shell</li> <li>- MPC Lid</li> <li>- MPC Fuel Spacers</li> </ul>	Stainless steels have been extensively used in spent fuel storage pools with both borated and unborated water with no adverse reactions or interactions with spent fuel.	The MPC internal environment will be an inert (helium) atmosphere and the external surface will be exposed to ambient air. No adverse interactions identified.
<u>Aluminum:</u> <ul style="list-style-type: none"> <li>- Heat Conduction Elements</li> </ul>	Aluminum and stainless steel form a galvanic couple. However, aluminum will be used in a passivated state. Upon passivation, aluminum forms a thin ceramic (Al <sub>2</sub> O <sub>3</sub> ) barrier. Therefore, during the short time they are exposed to pool water, significant corrosion of aluminum or production of hydrogen is not expected (see operational requirements under "Neutron Absorber Material" below).	In a non-aqueous atmosphere, galvanic corrosion is not expected.
<u>Neutron Absorber Material:</u>	Extensive in-pool experience on spent fuel racks with no adverse reactions. See Chapter 8 for additional requirements for combustible gas monitoring and required actions for control of combustible gas accumulation under the MPC lid.	No adverse potential reactions identified.

<sup>†</sup> HI-TRAC/MPC short-term operating environment during loading and unloading.

**TABLE 3.4.2 (CONTINUED)**  
**HI-STORM 100 SYSTEM MATERIAL COMPATIBILITY**  
**WITH OPERATING ENVIRONMENTS**

<b>Material/Component</b>	<b>Fuel Pool (Borated and Unborated Water)<sup>†</sup></b>	<b>ISFSI Pad (Open to Environment)</b>
<u>Steels:</u> - SA350-LF2 - SA350-LF3 - SA203-E - SA515 Grade 70 - SA516 Grade 70 - SA193 Grade B7 - SA106 (HI-TRAC)	All exposed steel surfaces (except seal areas, and pocket trunnions) will be coated with paint specifically selected for performance in the operating environments. Even without coating, no adverse reactions (other than nominal corrosion) have been identified. Lid bolts are plated and the threaded portion of the bolt anchor blocks is coated to seal the threaded area.	Internal surfaces of the HI-TRAC will be painted and maintained. Exposed external surfaces (except those listed in fuel pool column) will be painted and will be maintained with a fully painted surface. No adverse reactions identified.
<u>Steels:</u> - SA516 Grade 70 - SA203-E - SA350-LF3 - A36 Storage Overpack	HI-STORM 100 storage overpack is not exposed to fuel pool environment.	Internal and external surfaces will be painted (except for bolt locations that will have protective coating). External surfaces will be maintained with a fully painted surface. No adverse reaction identified.
<u>Stainless Steels:</u> - SA240 304 - SA193 Grade B8 - 18-8 S/S  Miscellaneous Components	Stainless steels have been extensively used in spent fuel storage pools with both borated and unborated water with no adverse reactions.	Stainless steel has a long proven history of corrosion resistance when exposed to the atmosphere. These materials are used for bolts and threaded inserts. No adverse reactions with steel have been identified. No impact on performance.

<sup>†</sup> HI-TRAC/MPC short-term operating environment during loading and unloading.

**TABLE 3.4.2 (CONTINUED)**  
**HI-STORM 100 SYSTEM MATERIAL COMPATIBILITY**  
**WITH OPERATING ENVIRONMENTS**

<b>Material/Component</b>	<b>Fuel Pool (Borated and Unborated Water)<sup>†</sup></b>	<b>ISFSI Pad (Open to Environment)</b>
<u>Nickel Alloy:</u> - SB637-NO7718 - SA564-630 H1100 (for HI-TRAC 125D only)  Lifting Trunnion	No adverse reactions with borated or unborated water.	Exposed to weathering effects. No adverse reactions with storage overpack closure plate. No impact on performance.
<u>Brass/Bronze:</u> - Pressure Relief Valve HI-TRAC	Small surface of pressure relief valve will be exposed. No significant adverse impact identified.	Exposed to external weathering. No loss of function expected.
<u>Holtite-A:</u> - Solid Neutron Shield	The neutron shield is fully enclosed. No adverse reaction identified. No adverse reactions with thermal expansion foam or steel.	The neutron shield is fully enclosed in the outer enclosure. No adverse reaction identified. No adverse reactions with thermal expansion foam or steel.

<sup>†</sup> HI-TRAC/MPC short-term operating environment during loading and unloading.

**TABLE 3.4.2 (CONTINUED)**  
**HI-STORM 100 SYSTEM MATERIAL COMPATIBILITY**  
**WITH OPERATING ENVIRONMENTS**

Material/Component	Fuel Pool (Borated and Unborated Water) <sup>†</sup>	ISFSI Pad (Open to Environment)
<u>Paint:</u> - as per Appendix 1.C	<p>Paint used for the HI-TRAC exterior surface has acceptable performance for short-term exposure in mild borated pool water.</p> <p>Paint selected for HI-TRAC internal surfaces has excellent high temperature resistance properties. Will only be exposed to demineralized water during in-pool operations as annulus is filled prior to placement in the spent fuel pool and the inflatable seal prevents fuel pool water in-leakage. No adverse interaction identified which could affect MPC/fuel assembly performance.</p>	<p>Good performance on surfaces. Discoloration is not a concern.</p>
<u>Elastomer Seals:</u>	<p>No adverse reactions identified.</p>	<p>Only used during fuel pool operations.</p>
<u>Lead:</u>	<p>Enclosed by carbon steel. Lead is not exposed to fuel pool water. Lead has no interaction with carbon steel.</p>	<p>Enclosed by carbon steel. Lead is not exposed to ambient environment. Lead has no interaction with carbon steel.</p>
<u>Concrete:</u>	<p>Storage overpack is not exposed to fuel pool water.</p>	<p>Concrete is enclosed by carbon steel and not exposed to ambient environment. Concrete has no interaction with carbon steel.</p>

<sup>†</sup> HI-TRAC/MPC short-term operating environment during loading and unloading.



**TABLE 3.4.3**  
**FUEL BASKET RESULTS - MINIMUM SAFETY FACTORS**

Load Case I.D.	Loading <sup>†</sup>	Safety Factor	Location in FSAR
F1	T, T'	No interference	Subsection 3.4.4.2
F2	D + H	2.87	Table 3.4.9 of Docket 72-1008
F3			
F3.a	D + H' (end drop)	3.6	3.4.4.3.1.3
F3.b	D + H' (side drop 0 deg.)	1.29	Table 3.4.6
F3.c	D + H' (side drop 45 deg.)	1.25	Table 3.4.6

---

<sup>†</sup> The symbols used for the loadings are defined in Table 2.2.13.

**TABLE 3.4.4**  
**MPC RESULTS - MINIMUM SAFETY FACTOR**

Load Case I.D.	Load Combination <sup>†,††</sup>	Safety Factor	Location in FSAR Where the Analysis is Performed	
E1				
E1.a	Design internal pressure, $P_i$	4.30 <sup>†††</sup> 1.326 1.20 N/A	E1.a	Lid Table 3.4.7 Baseplate 3.1.8.1 of Docket 72-1008 Shell Table 3.4.7 Supports
E1.b	Design external pressure, $P_o$	4.30 <sup>†††</sup> 1.326 23.3  N/A	E1.b	Lid $P_i$ bounds Baseplate $P_i$ bounds Shell 3.4.4.3.1.7 (buckling methodology in 3.H of Docket 72-1008)  Supports
E1.c	Design internal pressure, $P_i$ , plus Temperature T	1.09	E1.c	Shell Table 3.4.8
E2	D + H + ( $P_i$ , $P_o$ )	1.8 <sup>†††</sup> 1.08 2.64*0.967(stress), 45.5  5.85	Lid	3.E.8.1.2 of Docket 72-1008
			Baseplate	3.4.3.6
			Shell	Table 3.4.9 of Docket 72-1008 Buckling methodology in 3.H of Docket 72-1008
			Supports	Table 3.4.9 of Docket 72-1008

Note: 0.967 multiplier reflects increase in MPC shell design temperature to 500 deg. F.

<sup>†</sup> The symbols used for the loadings are defined in Table 2.2.13

<sup>††</sup> Note that in analyses, bounding pressures are applied, i.e., in buckling calculations  $P_o$  is used, and in stress evaluations either  $P_o$  or  $P_i$  is appropriate

<sup>†††</sup> Minimum safety factor is based on the dual lid configuration.

HOLTEC INTERNATIONAL COPYRIGHTED MATERIAL

**TABLE 3.4.4 (CONTINUED)**  
**MPC RESULTS - MINIMUM SAFETY FACTOR**

Load Case I.D.	Load Combination <sup>†,††</sup>	Safety Factor	Location in FSAR
E3 E3.a	(P <sub>i</sub> ,P <sub>o</sub> ) + D + H', end drop	1.4 <sup>†††</sup> 1.87 1.72  N/A	E3.a    Lid            3.E.8.2.1.2 of Docket 72-1008 Baseplate    3.I.8.3 of Docket 72-1008 Shell        Buckling methodology in 3.H of Docket 72-1008 Supports
E3.b	(P <sub>i</sub> ,P <sub>o</sub> ) + D + H', side drop 0 deg.	1.4 <sup>†††</sup> 1.87 1.02 1.13	E3.b    Lid            end drop bounds Baseplate    end drop bounds Shell        Table 3.4.6 Supports    Table 3.4.6
E3.c	(P <sub>i</sub> ,P <sub>o</sub> ) + D + H', side drop 45 deg.	1.4 <sup>†††</sup> 1.87 1.38 1.50	E3.c    Lid            end drop bounds Baseplate    end drop bounds Shell        Table 3.4.6 Supports    Table 3.4.6

†        The symbols used for the loadings are defined in Table 2.2.13

††       Note that in analyses, bounding pressures are applied, i.e., in buckling calculations P<sub>o</sub> is used, and in stress evaluations either P<sub>o</sub> or P<sub>i</sub> is appropriate

†††      Minimum safety factor is based on the dual lid configuration.

HOLTEC INTERNATIONAL COPYRIGHTED MATERIAL

**TABLE 3.4.4 (CONTINUED)**  
**MPC RESULTS - MINIMUM SAFETY FACTOR**

Load Case I.D.	Load Combination <sup>†, ††</sup>	Safety Factor	Location in FSAR
E4	T	Subsection 3.4.4.2 shows there are no primary stresses from thermal expansion.	Subsection 3.4.4.2
E5	D + T* + (P <sub>i</sub> *, P <sub>o</sub> *)	8.6 <sup>†††</sup> 1.17 1.15 (buckling)  2.60 (stress)  N/A	Lid 3.4.4.3.1.10 Baseplate 3.4.4.3.1.10 Shell Buckling methodology in 3.H of Docket 72-1008 3.4.4.3.1.2 (stress)  Supports N/A

† The symbols used for the loadings are defined in Table 2.2.13.

†† Note that in analyses, bounding pressures are applied, i.e., in buckling calculations P<sub>o</sub> is used, and in stress evaluations either P<sub>o</sub> or P<sub>i</sub> is appropriate.

††† Minimum safety factor is based on the dual lid configuration.

HOLTEC INTERNATIONAL COPYRIGHTED MATERIAL

**TABLE 3.4.5**  
**HI-STORM 100 STORAGE OVERPACK AND HI-TRAC RESULTS - MINIMUM SAFETY FACTORS**

Load Case I.D.	Loading <sup>†</sup>	Safety Factor	Location in FSAR
01	D + H + T + (P <sub>o</sub> , P <sub>i</sub> )	1.33 N/A  2.69(125); 2.17(100) 2.604 (ASME Code limit) 2.61 (ASME Code limit) 2.91; 1.11(optional bolts)	Overpack Shell (inlet vent)/Base 3.4.3.5 Top Lid N/A  HI-TRAC Shell 3.4.3.3; 3.4.3.4 Pool Lid 3.4.3.8 Top Lid N/A Pocket Trunnion 3.4.4.3.3.1
02			
02.a	D + H' + (P <sub>o</sub> , P <sub>i</sub> ) (end drop/tip-over)	1.271 1.125	Overpack Shell 3.4.4.3.2.3 Top Lid 3.4.4.3.2.2
02.b	D + H' + (P <sub>o</sub> , P <sub>i</sub> ) (side drop)	1.52 1.159 1.651	HI-TRAC Shell 3.4.9.3 Transfer Lid 3.4.4.3.3.3 Top Lid 3.4.4.3.3.5
03	D (water jacket)	1.39	3.4.4.3.3.4
04	M (small and medium penetrant missiles)	2.60 (Side Strike); 1.065(End strike)  1.23 (End Strike)	Overpack 3.4.8.1  HI-TRAC 3.4.8.2.1

<sup>†</sup> The symbols used for the loadings are defined in Table 2.2.13.

**TABLE 3.4.6**  
**MINIMUM SAFETY FACTORS FOR MPC COMPONENTS DURING TIP-OVER**  
**45g DECELERATIONS**

Component - Stress Result	MPC-24		MPC-68	
	0 Degrees	45 Degrees	0 Degrees	45 Degrees
Fuel Basket - Primary Membrane ( $P_m$ )	3.38 (1134)	4.72 (396)	2.89 (1603)	4.18 (1603)
Fuel Basket - Local Membrane Plus Primary Bending ( $P_L+P_b$ )	1.29 (1065)	1.30 (577)	2.09 (1590)	1.38 (774)
Enclosure Vessel - Primary Membrane ( $P_m$ )	6.39*.967 (1354)	6.46*.967 (1370)	6.29*.967 (2393)	6.58*.967 (2377)
Enclosure Vessel - Local Membrane Plus Primary Bending ( $P_L+P_b$ )	2.46*.967 (1278)	2.92*.967 (1247)	1.05*.967 (1925)	1.50*.967 (1925)
Basket Supports - Primary Membrane ( $P_m$ )	N/A	N/A	6.86 (1710)	8.98 (1699)
Basket Supports - Local Membrane Plus Primary Bending ( $P_L+P_b$ )	N/A	N/A	1.13 (1715)	1.50 (1704)

Notes:

1. Corresponding ANSYS element number shown in parentheses.
2. Multiplier of 0.967 reflects increase in Enclosure Vessel Design Temperature from 450 deg. F to 500 deg. F (Table 2.2.3).
3. Safety factors for the MPC-24 and MPC-68 have been reduced (divided by factors of 1.024 and 1.043, respectively) to adjust for the fuel assembly weight increase (see Subsection 3.4.4.4.1)

**TABLE 3.4.6 (CONTINUED)**  
**MINIMUM SAFETY FACTORS FOR MPC COMPONENTS DURING TIP-OVER**  
**45g DECELERATIONS**

Component - Stress Result	MPC-32	
	0 Degrees	45 Degrees
Fuel Basket - Primary Membrane ( $P_m$ )	3.43 (715)	4.84 (366)
Fuel Basket - Local Membrane Plus Primary Bending ( $P_L+P_b$ )	1.47 (390)	1.25 (19)
Enclosure Vessel - Primary Membrane ( $P_m$ )	4.01*.967 (1091)	5.46*.967 (1222)
Enclosure Vessel - Local Membrane Plus Primary Bending ( $P_L+P_b$ )	1.08*.967 (1031)	1.43*.967 (1288)
Basket Supports - Primary Membrane ( $P_m$ )	3.36 (905)	4.74 (905)
Basket Supports - Local Membrane Plus Primary Bending ( $P_L+P_b$ )	1.27 (901)	1.67 (908)

Notes:

1. Corresponding ANSYS element number shown in parentheses.
2. Multiplier of 0.967 reflects increase in Enclosure Vessel Design Temperature from 450 deg. F to 500 deg. F (Table 2.2.3).
3. Safety factors for the MPC-32 has been reduced (divided by factor of 1.024) to adjust for the fuel assembly weight increase (see Subsection 3.4.4.4.1)

**TABLE 3.4.6 (CONTINUED)**  
**MINIMUM SAFETY FACTORS FOR MPC-24E COMPONENTS DURING TIP-OVER**  
**45g DECELERATIONS**

<b>Components – Stress Result</b>	<b>0 Degrees</b>	<b>45 Degrees</b>
Fuel Basket – Primary Membrane ( $P_m$ )	-10,554 (3.50)	-7,608 (4.86)
Fuel Basket – Primary Membrane plus Primary Bending ( $P_L + P_b$ )	38,029 (1.46)	32,745 (1.70)
Enclosure Vessel – Primary Membrane ( $P_m$ )	6,611 (6.57*.967)	6,612 (6.57*.967)
Enclosure Vessel – Primary Membrane plus Primary Bending ( $P_L + P_b$ )	23,680 (2.75*.967)	16,868 (3.87*.967)

Notes:

1. All stresses are reported in psi units and are based on closed gaps (primary stresses only).
2. The numbers shown in parentheses are the corresponding safety factors.
3. Multiplier of 0.967 reflects the increase in Enclosure Vessel Design Temperature from 450 deg. F to 500 deg. F (Table 2.2.3).
4. Stress results/safety factors for the MPC-24E have been multiplied/divided by a factor of 1.024 to adjust for the fuel assembly weight (See subsection 3.4.4.4.1).



**TABLE 3.4.7**  
**STRESS INTENSITY RESULTS FOR CONFINEMENT BOUNDARY -**  
**INTERNAL PRESSURE ONLY**

Locations (Per Fig. 3.4.11)	Calculated Value of Stress Intensity (psi)	Category	Table 3.1.13 Allowable Value (psi) <sup>†</sup>	Safety Factor (Allowable/Calculated)
<u>Top Lid</u> <sup>††</sup>				
A	1,633	$P_L + P_b$	25,450	15.6
Neutral Axis	21.9	$P_m$	16,950	774
B	1,604	$P_L + P_b$	25,450	15.9
C	695	$P_L + P_b$	25,450	36.6
Neutral Axis	732	$P_m$	16,950	23.2
D	2,962	$P_L + P_b$	25,450	8.59
<u>Baseplate</u>				
E	19,773	$P_L + P_b$	28,100	1.42
Neutral Axis	415	$P_m$	18,700	45.1
F	20,601	$P_L + P_b$	28,100	1.36
G	9,610	$P_L + P_b$	28,100	2.92
Neutral Axis	2,268	$P_m$	18,700	8.25
H	8,279	$P_L + P_b$	28,100	3.39

<sup>†</sup> Allowable stress intensities are evaluated at 550 degrees F (lid), 400 degrees F (baseplate), and 500 degrees F (canister).

<sup>††</sup> Stresses for the top lid are reported for the single lid configuration; a doubling of the calculated stress values (and a halving of the top lid safety factors) results when the dual lid configuration is considered.

**TABLE 3.4.7 (CONTINUED)**  
**STRESS INTENSITY RESULTS FOR CONFINEMENT BOUNDARY -**  
**INTERNAL PRESSURE ONLY**

Locations (Per Fig. 3.4.11)	Calculated Value of Stress Intensity (psi)	Category	Table 3.1.13 Allowable Value (psi) <sup>†</sup>	Safety Factor (Allowable/Calculated)
<u>Canister</u>				
I	6,788	$P_m$	17,500	2.58
Upper Bending Boundary Layer Region	7,202 7,014	$P_L + P_b + Q$ $P_L$	52,500 26,300	7.29 3.75
Lower Bending Boundary Layer Region	43,645 11,349	$P_L + P_b + Q$ $P_L$	52,500 26,300	1.20 2.32

<sup>†</sup> Allowable stress intensities are evaluated at 550 degrees F (lid), 400 degrees F (baseplate), and 500 degrees F (canister).

**TABLE 3.4.8**  
**PRIMARY AND SECONDARY STRESS INTENSITY RESULTS FOR**  
**CONFINEMENT BOUNDARY - PRESSURE PLUS THERMAL LOADING**

Locations (Per Fig. 3.4.11)	Calculated Value of Stress Intensity (psi)	Category	Allowable Stress Intensity (psi) <sup>†</sup>	Safety Factor (Allowable/Calculated)
<u>Top Lid</u> <sup>††</sup>				
A	7,866	$P_L + P_b + Q$	50,850	6.46
Neutral Axis	6,553	$P_m + P_L$	25,450	3.88
B	3,409	$P_L + P_b + Q$	50,850	14.9
C	13,646	$P_L + P_b + Q$	50,850	3.73
Neutral Axis	12,182	$P_m + P_L$	25,450	2.09
D	11,145	$P_L + P_b + Q$	50,850	4.56
<u>Baseplate</u>				
E	19,417	$P_L + P_b + Q$	56,100	2.89
Neutral Axis	223.1	$P_m + P_L$	28,100	126
F	19,860	$P_L + P_b + Q$	56,100	2.82
G	4,836	$P_m + P_L + Q$	56,100	11.6
Neutral Axis	1,201	$P_m + P_L$	28,100	23.4
H	4,473	$P_L + P_b + Q$	56,100	12.5

<sup>†</sup> Allowable stress intensities are evaluated at 550 degrees F (lid), 400 degrees F (baseplate), and 500 degrees F (canister).

<sup>††</sup> Stresses for the top lid are reported for the single lid configuration; a doubling of the calculated stress values (and a halving of the top lid safety factors) results when the dual lid configuration is considered.

HOLTEC INTERNATIONAL COPYRIGHTED MATERIAL

**TABLE 3.4.8 (CONTINUED)**  
**PRIMARY AND SECONDARY STRESS INTENSITY RESULTS FOR**  
**CONFINEMENT BOUNDARY - PRESSURE PLUS THERMAL LOADING**

Locations (Per Fig. 3.4.11)	Calculated Value of Stress Intensity (psi)	Category	Allowable Stress Intensity (psi) <sup>†</sup>	Safety Factor (Allowable/Calculated)
<u>Canister</u>				
I	6,799	$P_L$	26,300	3.87
Upper Bending Boundary Layer Region	12,813	$P_L + P_b + Q$	52,500	4.10
	12,185	$P_L$	26,300	2.16
Lower Bending Boundary Layer Region	48,378	$P_L + P_b + Q$	52,500	1.09
	12,028	$P_L$	26,300	2.19

<sup>†</sup> Allowable stress intensities are evaluated at 550 degrees F (lid), 400 degrees F (baseplate), and 500 degrees F (canister).

HOLTEC INTERNATIONAL COPYRIGHTED MATERIAL

**TABLE 3.4.9**  
**SAFETY FACTORS FROM SUPPLEMENTARY CALCULATIONS**

Item	Loading	Safety Factor	FSAR Location Where Details are Provided
HI-STORM Top Lid Weld Shear	Tipover	3.22	3.4.4.3.2.2
HI-STORM Lid Bottom Plate	End Drop	9.777	3.4.4.3.2.3
HI-STORM Lid Bottom Plate Welds	End Drop	2.695	3.4.4.3.2.3
Pedestal Shield Compression	End Drop	1.011	3.4.4.3.2.3
HI-STORM Inlet Vent Plate Bending Stress	End Drop	1.271	3.4.4.3.2.3
HI-STORM Lid Top Plate Bending	End Drop –100 100S	5.208 1.357	3.4.4.3.2.3
HI-TRAC Pocket Trunnion Weld	HI-TRAC Rotation	2.92	3.4.4.3.3.1
HI-TRAC 100 Optional Bolts - Tension	HI-TRAC Rotation	1.11	3.4.4.3.3.1
HI-STORM 100 Shell	Seismic Event	14.6	3.4.7
HI-TRAC Transfer Lid Door Lock Bolts	Side Drop	2.387	3.4.4.3.3.3
HI-TRAC Transfer Lid Separation	Side Drop	1.159	3.4.4.3.3.3
HI-STORM 100 Top Lid	Missile Impact	1.20	3.4.8.1
HI-STORM 100 Shell	Missile Impact	2.77	3.4.8.1
HI-TRAC Water Jacket –Enclosure Shell Bending	Pressure	1.85	3.4.4.3.3.4
HI-TRAC Water Jacket – Enclosure Shell Bending	Pressure plus Handling	1.80	3.4.4.3.3.1
HI-TRAC Water Jacket – Bottom Flange Bending	Pressure	1.39	3.4.4.3.3.4
HI-TRAC Water Jacket – Weld	Pressure	1.42	3.4.4.3.3.4
Fuel Basket Support Plate Bending	Side Drop	1.82	3.4.4.3.1.8
Fuel Basket Support Leg Stability	Side Drop	4.07	3.4.4.3.1.8
Fuel Basket Support Welds	Side Drop	1.35	3.4.4.3.1.8
MPC Cover Plates in MPC Lid	Normal Condition Internal Pressure	1.81	3.4.4.3.1.8
MPC Cover Plate Weld	Accident Condition Internal Pressure	2.52	3.4.4.3.1.8
HI-STORM Storage Overpack	External Pressure	2.88	3.4.4.5.2
HI-STORM Storage Overpack Circumferential Stress	Missile Strike	2.60	3.4.8.1
HI-TRAC Transfer Cask Circumferential Stress	Missile Strike	2.61	3.4.8.2
HI-TRAC Transfer Cask Axial Membrane Stress	Side Drop	1.52	3.4.9.3

HOLTEC INTERNATIONAL COPYRIGHTED MATERIAL

**TABLE 3.4.10**  
**INPUT DATA FOR SEISMIC ANALYSIS OF ANCHORED HI-STORM 100 SYSTEM**

Item	Data Used	Actual Value and Reference
Cask height, inch	231.25	231.25" (Dwg. 1495)
Contact diameter at ISFSI pad, inch	146.5	146.5 (Dwg. 3187)
Overpack empty, wt. Kips	270	267.87 (Table 3.2.1)
Bounding wt. of loaded MPC, kips	90	88.135 (Table 3.2.1)
Overpack-to-MPC radial gap (inch)	2.0	2.0' (Dwg. 1495, Sheets 2 and 5)
Overpack C.G. height above ISFSI pad, inch	117.0	116.8 (Table 3.2.3)
Overpack with Loaded MPC - C.G. height above ISFSI pad	118.5	118.5 (Table 3.2.3)
Applicable Response Spectra	Fig. 3.4-31 to 3.4-36	Figure 3.4-30
ZPA:	RG 1.60      Western Plant	
Horizontal 1	1.5              1.45	
Horizontal 2	1.5              1.45	Site-Specific
Vertical	1.5              1.3	
No. of Anchor Studs	28	Up to 28
Anchor Stud Diameter		
Inch	2.0	2.0 (BOM 3189)
Yield stress, ksi	80 (minimum)	Table 1.2.7
Ultimate stress, ksi	125 (minimum)	Table 1.2.7
Free length, inch*	16-42	Site-specific
Pre-load tensile stress, ksi*	55-65	55-65

\*For the confirmatory dynamic analyses, bolt spring rates were computed using the maximum length, and the preload stress was slightly above 60.1 ksi. For the static analysis, all combinations were evaluated.

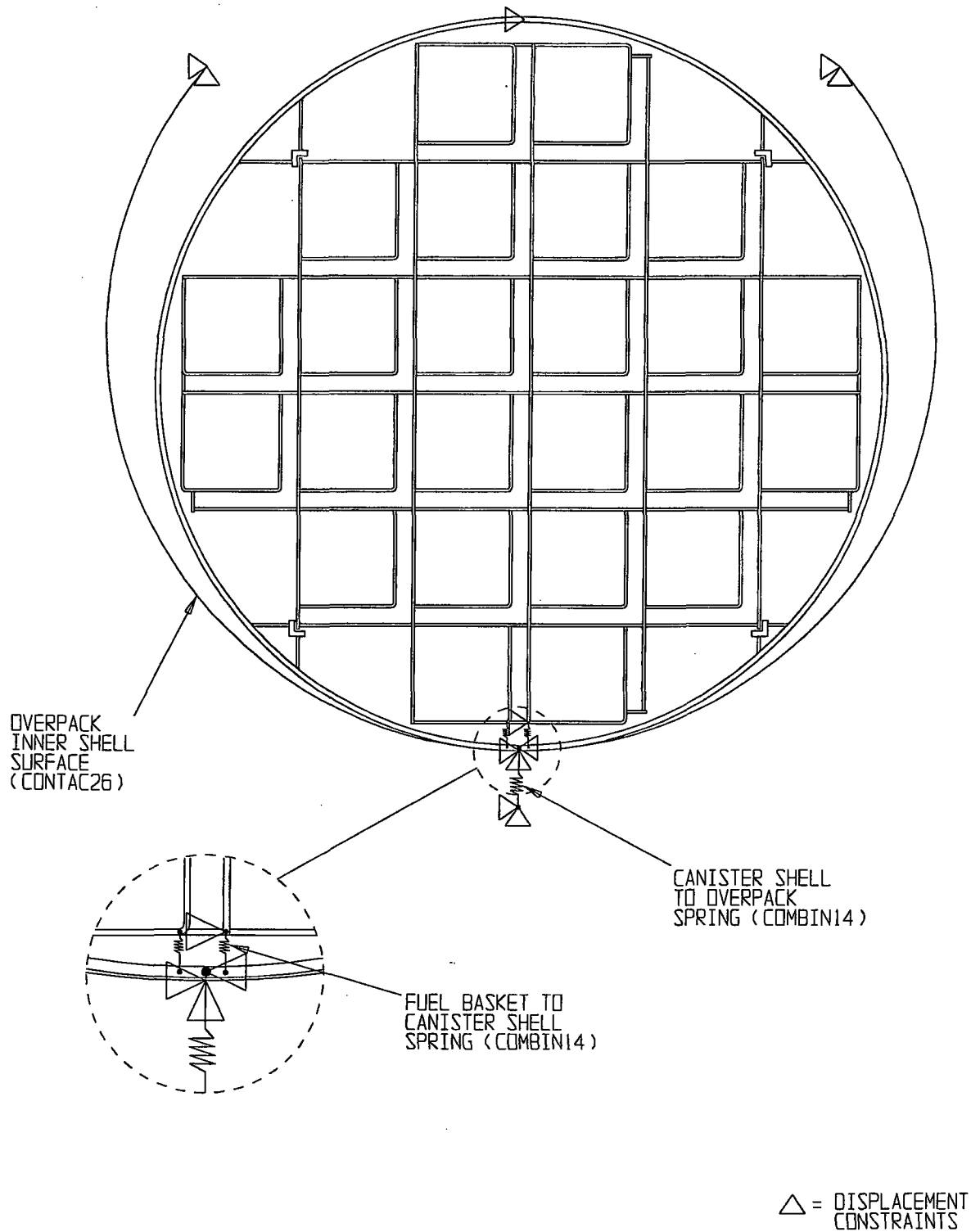


**FIGURE 3.4.1; FINITE ELEMENT MODEL OF MPC-24**

REPORT HI-2002444

( 0 DEGREE DROP MODEL )

REVISION 0

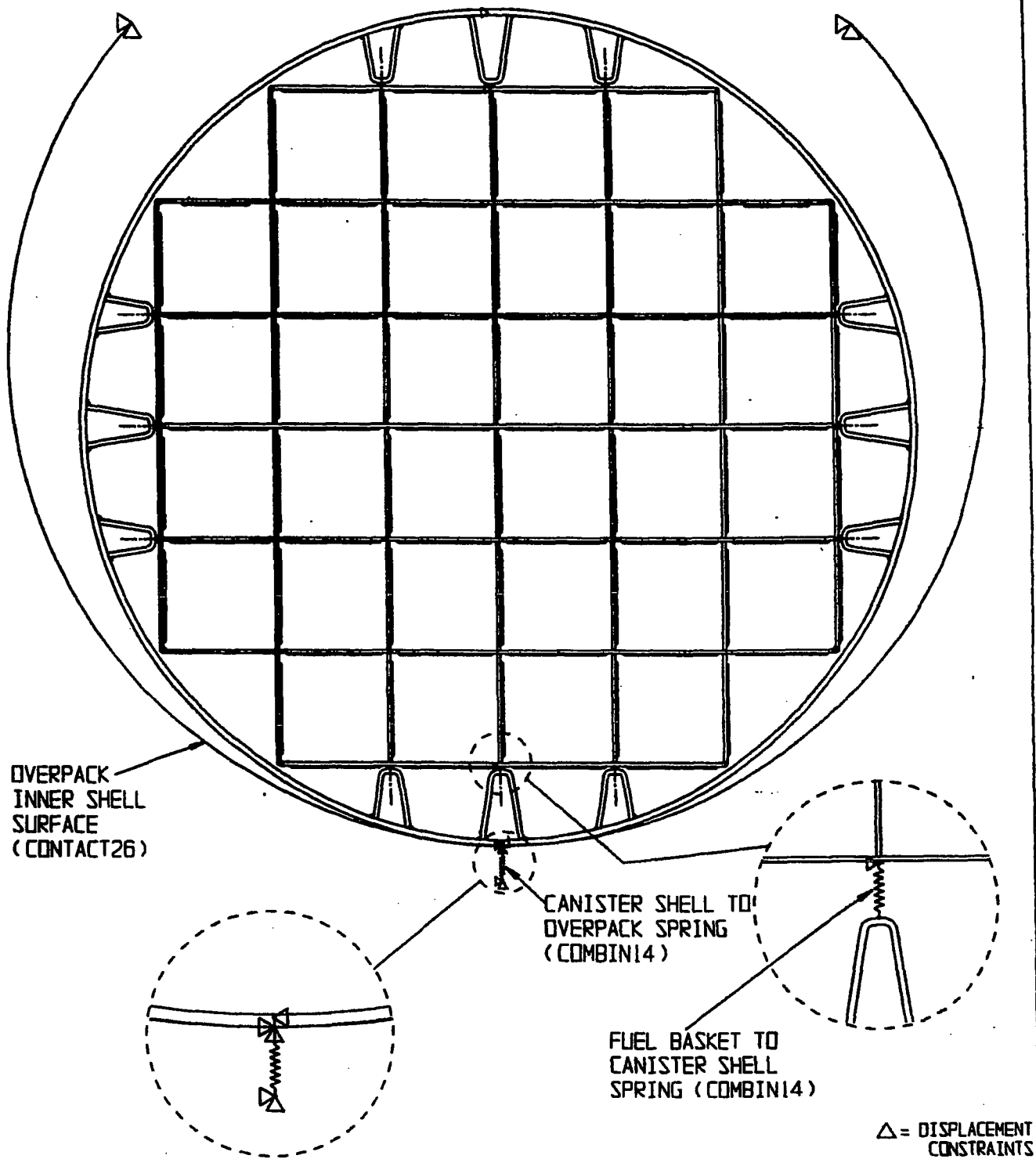


**FIGURE 3.4.2; FINITE ELEMENT MODEL OF MPC-32**

(0 DEGREE DROP MODEL)

REPORT HI-2002444

REVISION 1



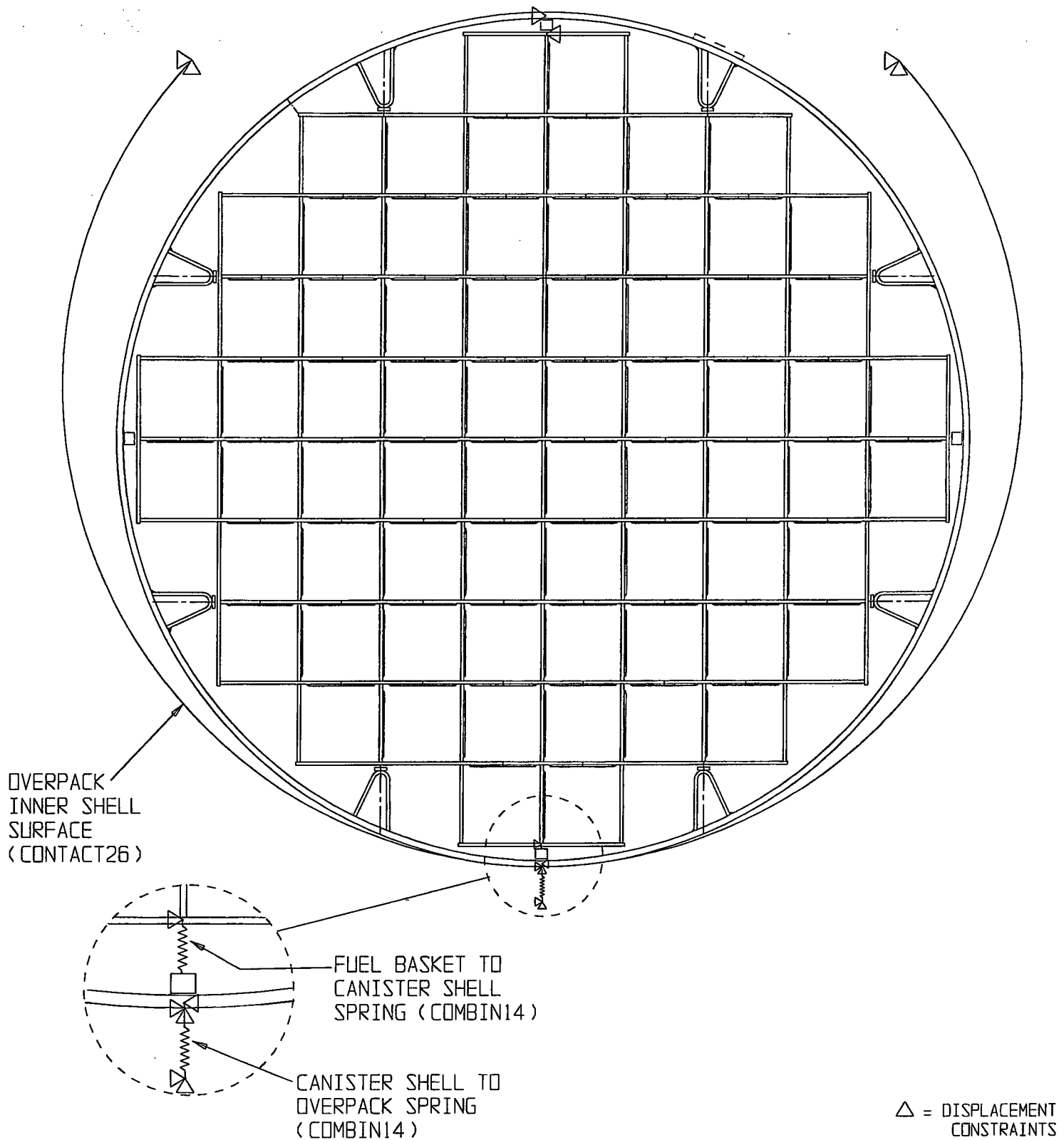


FIGURE 3.4.3; FINITE ELEMENT MODEL OF MPC-68

(0 DEGREE DROP MODEL)

REPORT HI-2002444

REVISION 0

HI-STORM 100 FSAR, NON-PROPRIETARY  
REVISION 12  
MARCH 12, 2014

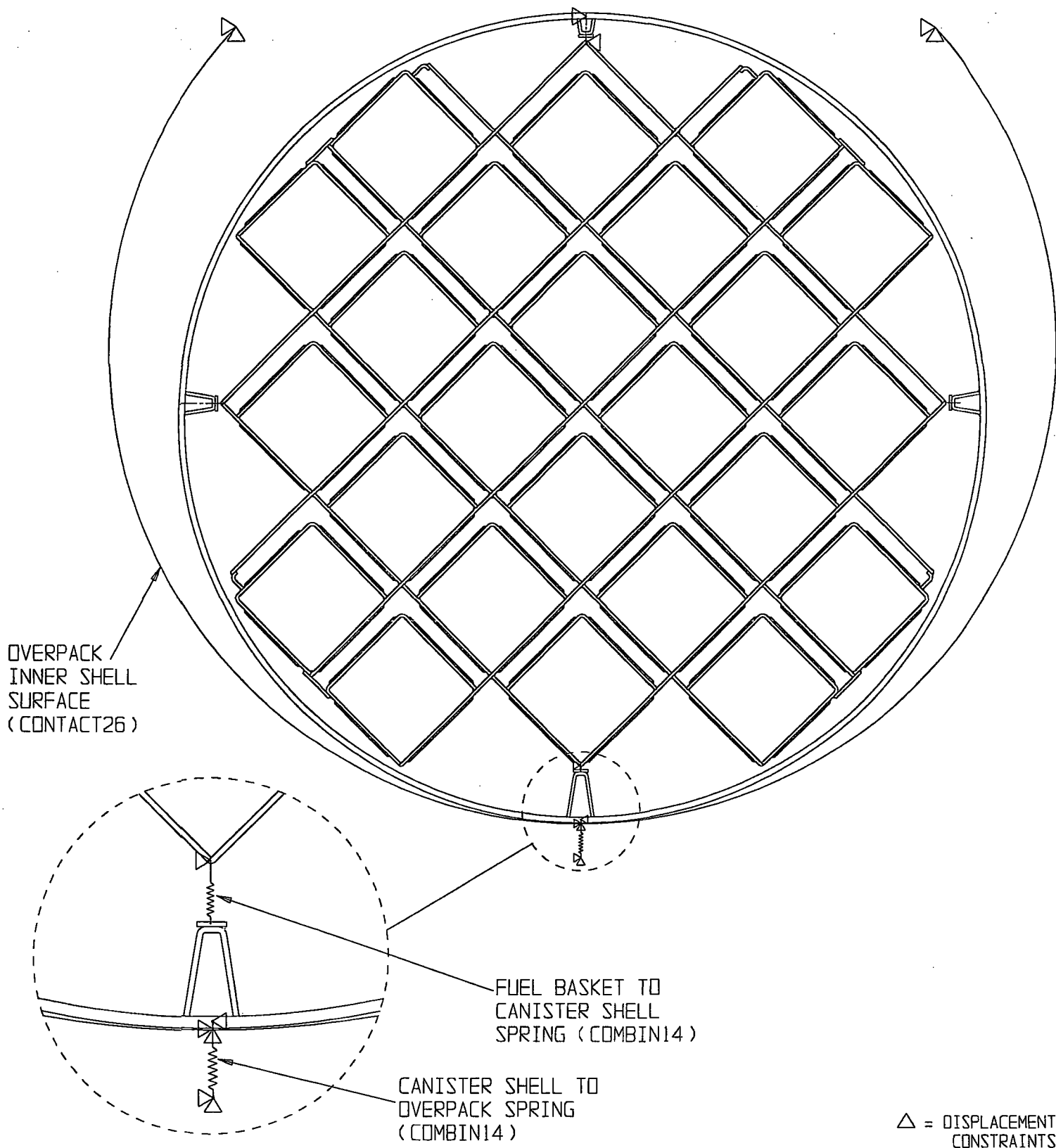


FIGURE 3.4.4; FINITE ELEMENT MODEL OF MPC-24

(45 DEGREE DROP MODEL)

REPORT HI-2002444

REVISION 0

HI-STORM 100 FSAR, NON-PROPRIETARY  
REVISION 12  
MARCH 12, 2014

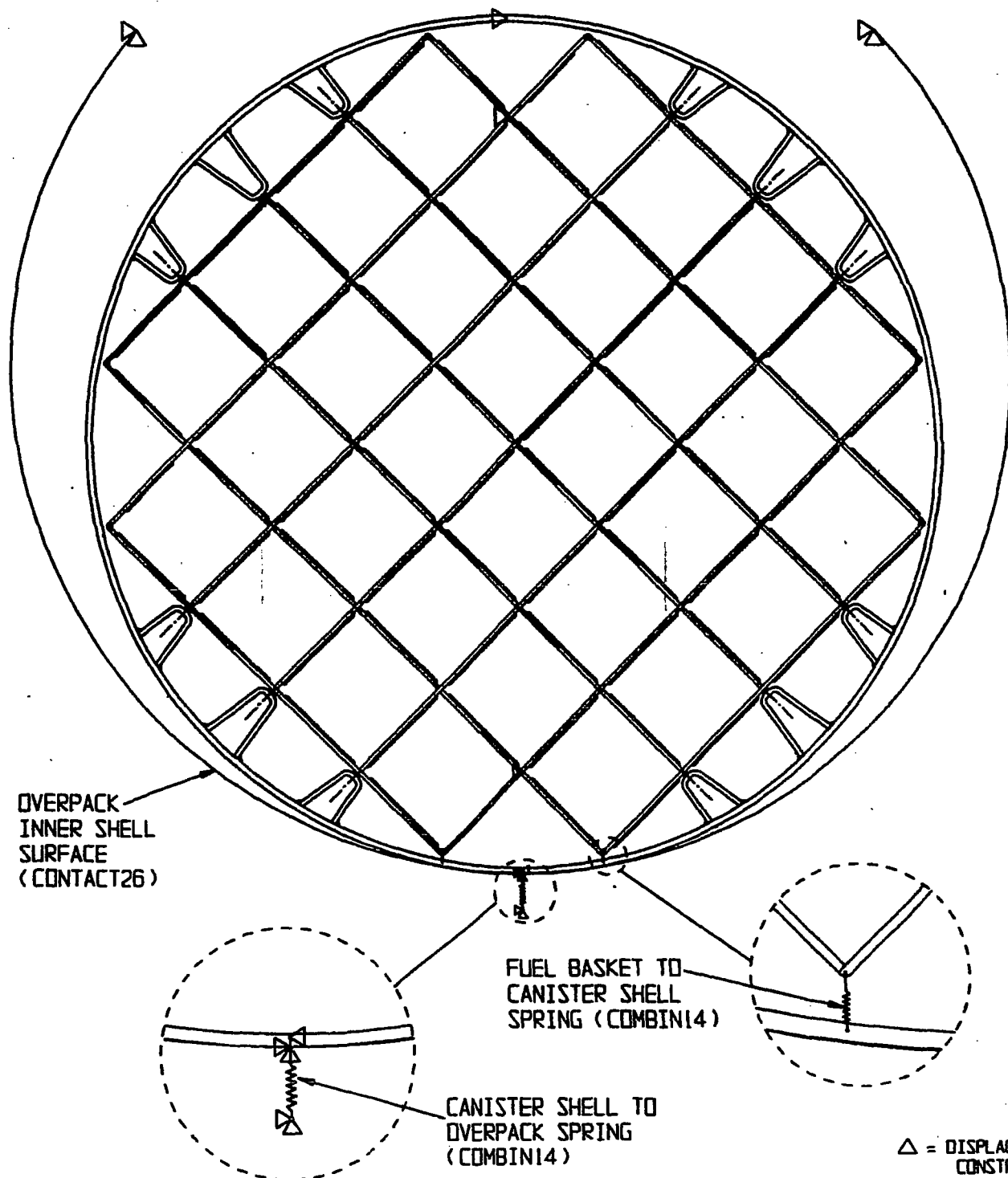


**FIGURE 3.4.5; FINITE ELEMENT MODEL OF MPC-32**

(45 DEGREE DROP MODEL)

REPORT HI-2002444

REVISION 1

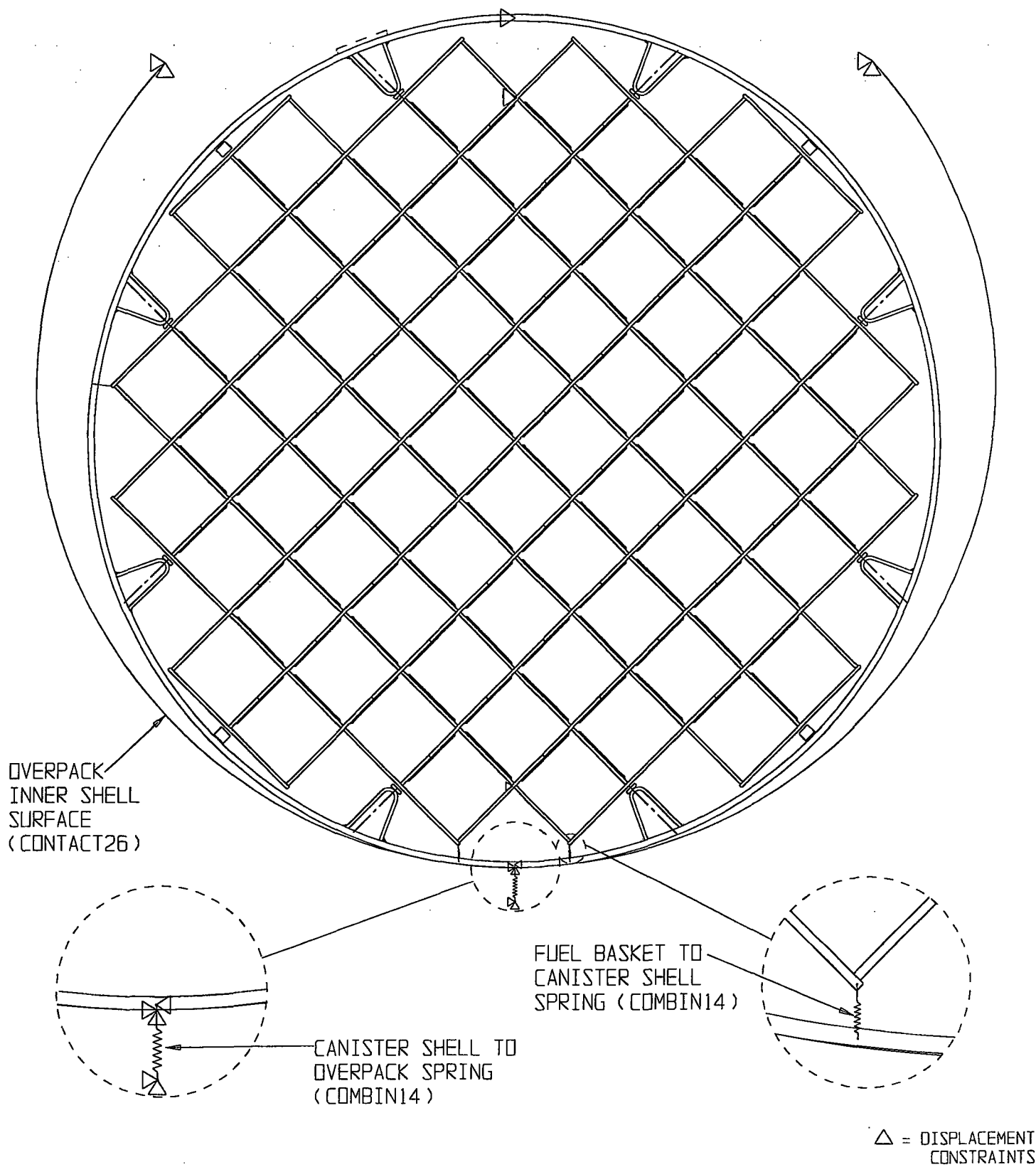


FIGURE 3.4.6; FINITE ELEMENT MODEL OF MPC-68

(45 DEGREE DROP MODEL)

REPORT HI-2002444

REVISION 0

HI-STORM 100 FSAR, NON-PROPRIETARY  
REVISION 12  
MARCH 12, 2014

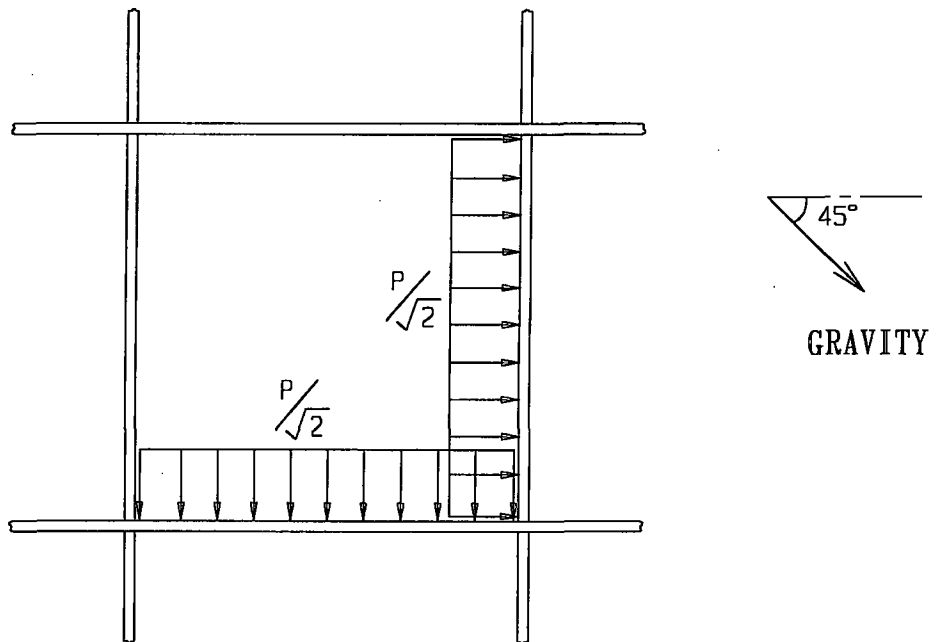
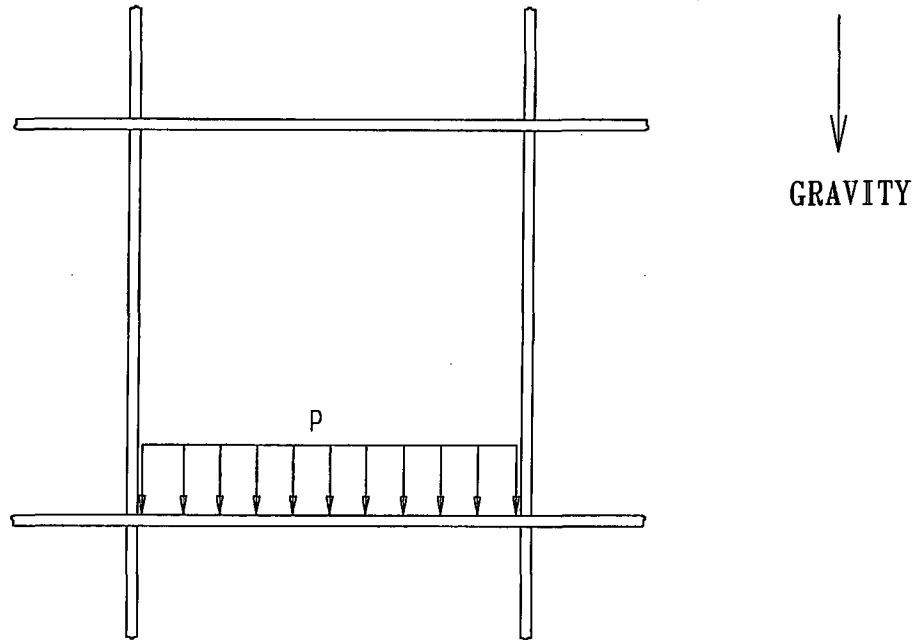


**FIGURE 3.4.7; DETAIL OF FUEL ASSEMBLY PRESSURE  
LOAD ON MPC BASKET**

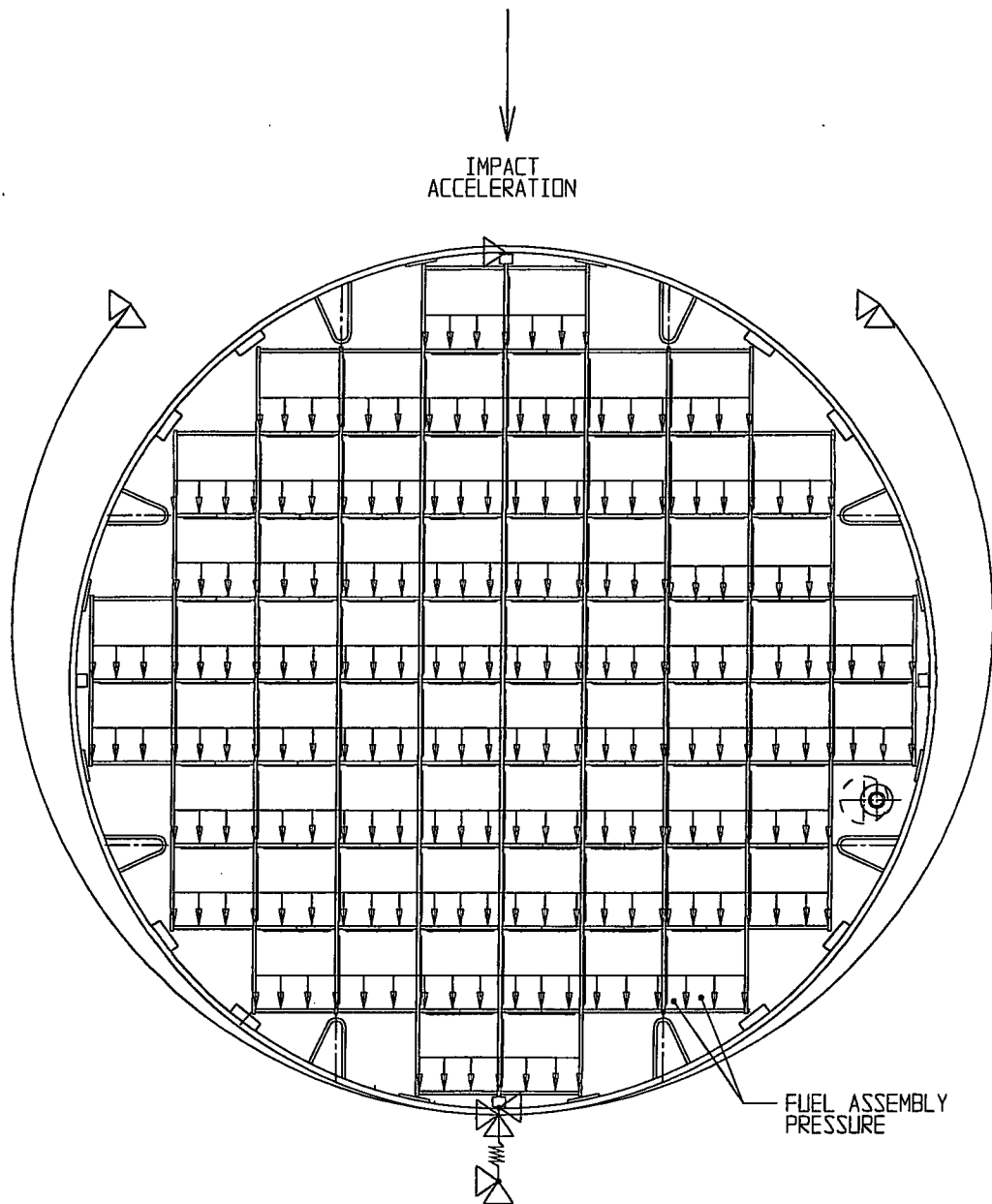


*FIGURE 3.4.8; 0 DEGREE SIDE DROP OF MPC*

REPORT HI-2002444

REVISION 0

\\5014\HI2002444\CH\_3\3\_4\_8

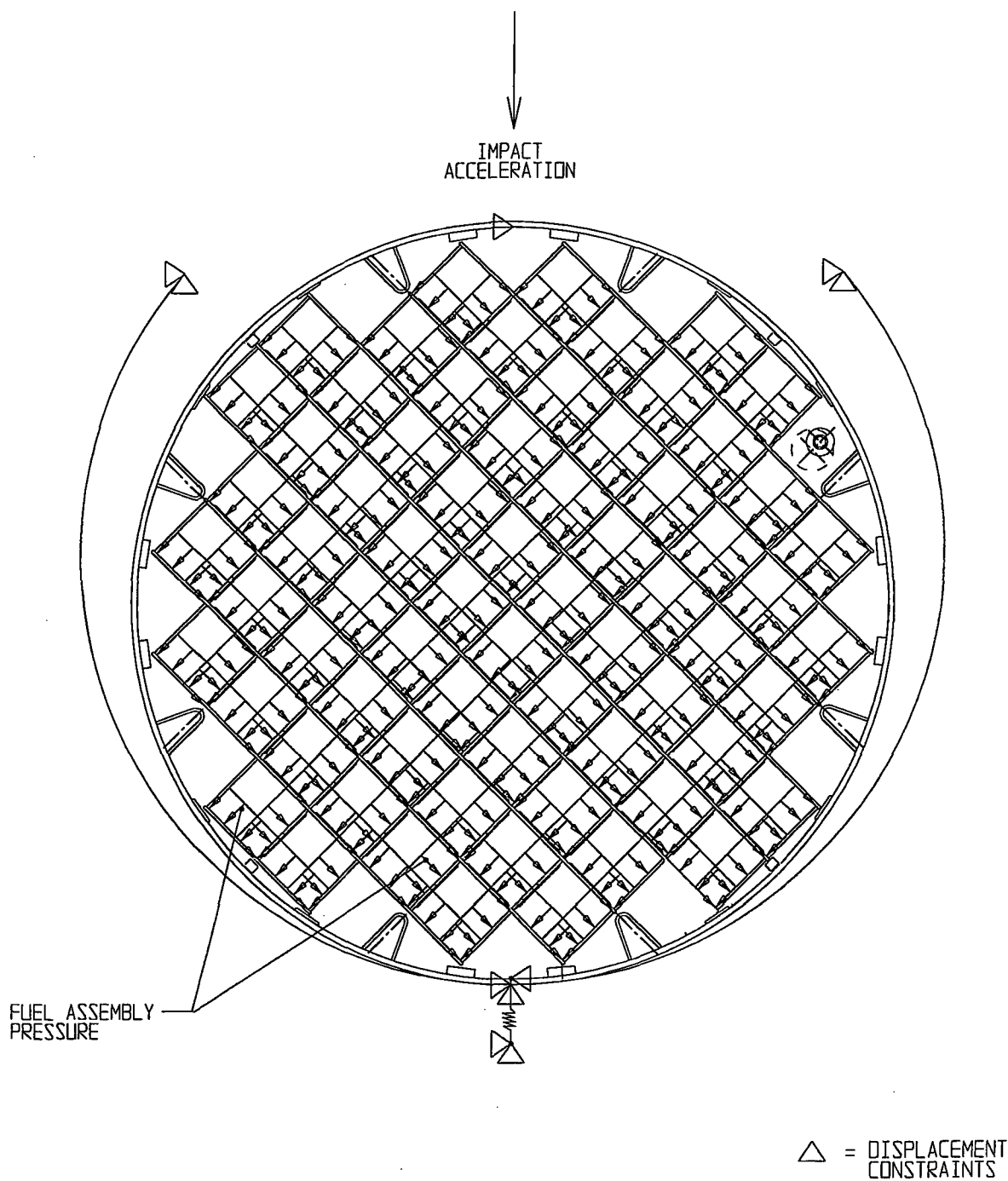


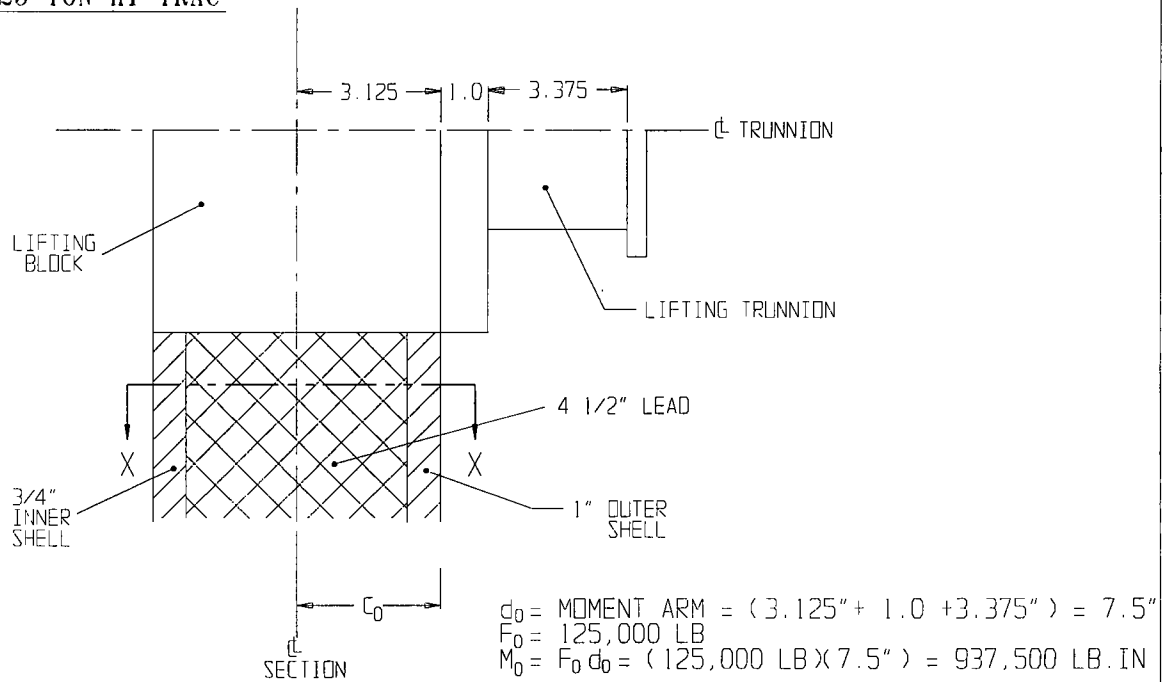
*FIGURE 3.4.9; 45 DEGREE SIDE DROP OF MPC*

REPORT HI-2002444

REVISION 0

\\5014\HI2002444\CH\_3\3\_4\_9

### 125 TON HI-TRAC



### 100 TON HI-TRAC

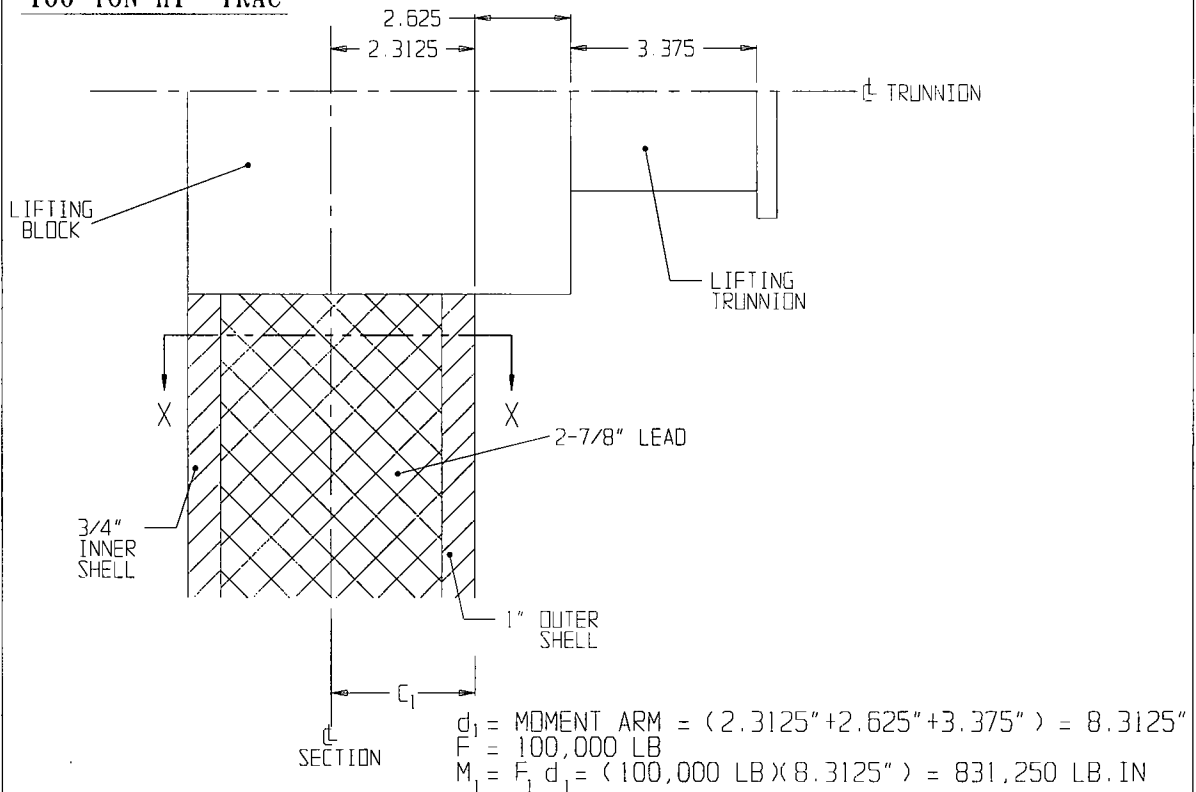


FIGURE 3.4.10; COMPARISON OF 125 TON AND 100 TON HI-TRAC LIFTING TRUNNION CONNECTION

REPORT HI-2002444

REVISION 1

G:\SAR DOCUMENTS\HI-STORM F-SAR\FIGURES\UFSAR-REV. 1\CHP.3\FIG 3\_4\_10R1



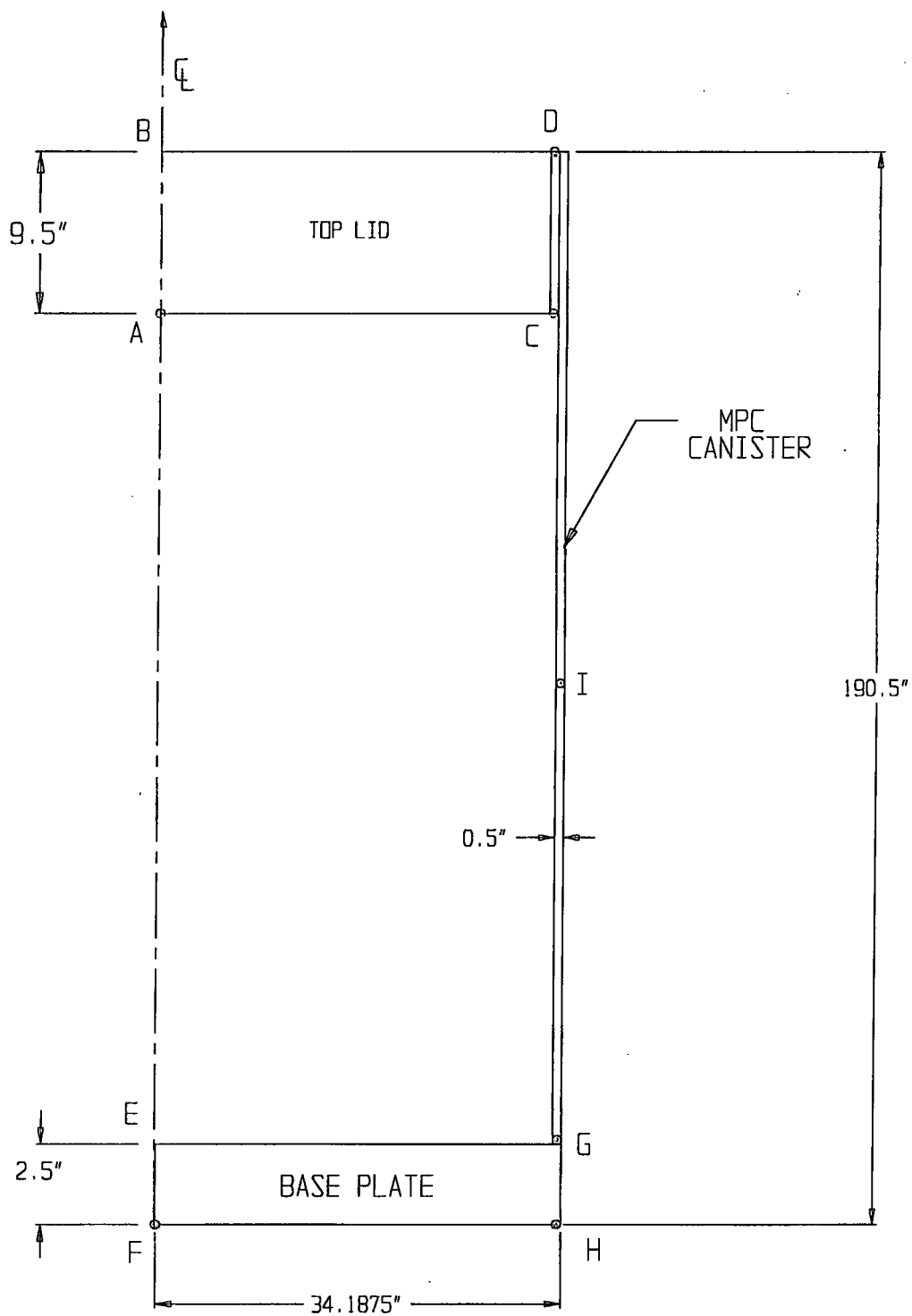


FIGURE 3.4.11 CONFINEMENT BOUNDARY MODEL SHOWING TEMPERATURE DATA POINTS

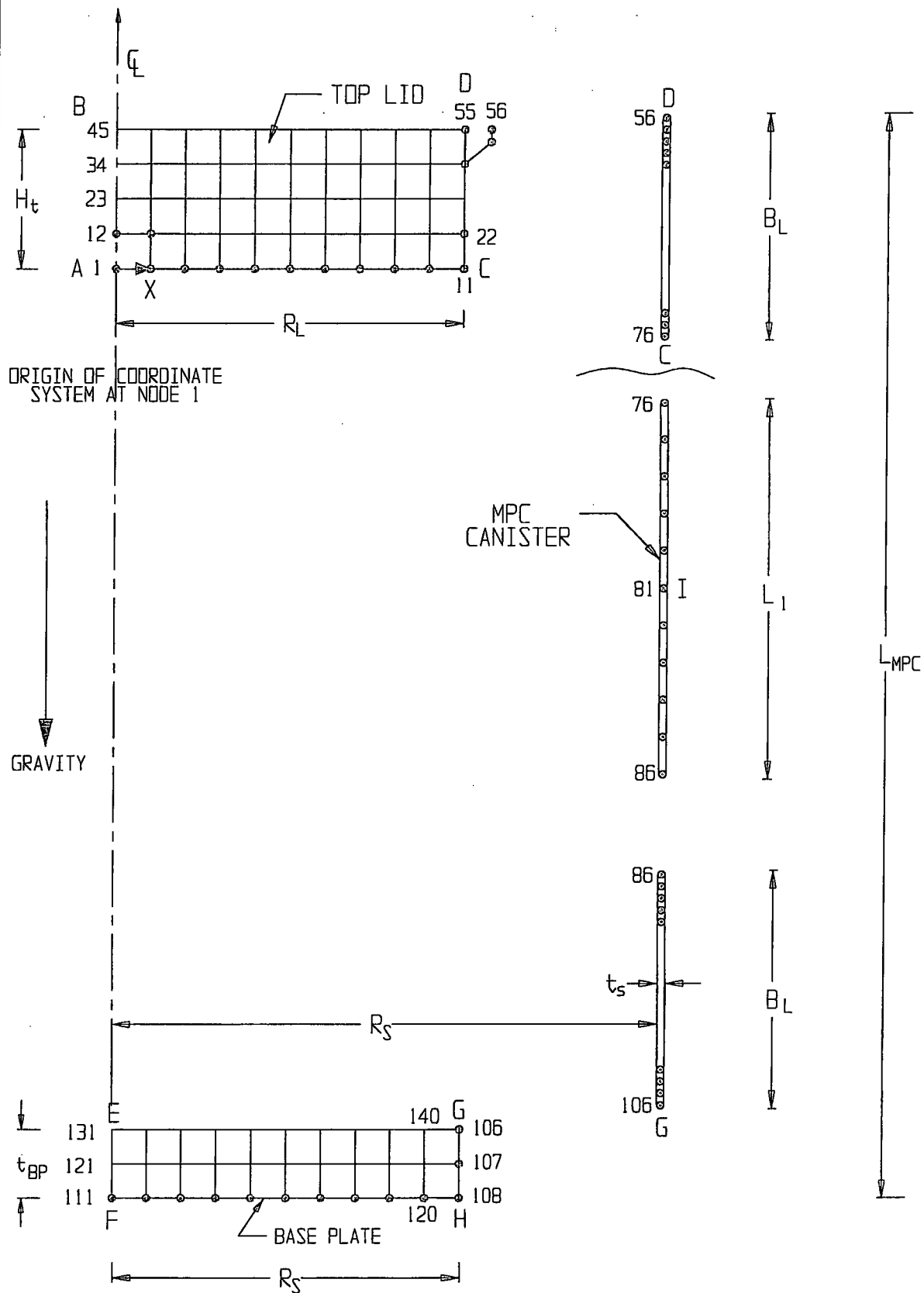


FIGURE 3.4.12 MPC - CONFINEMENT BOUNDARY  
FINITE ELEMENT GRID (EXPLODED VIEW)

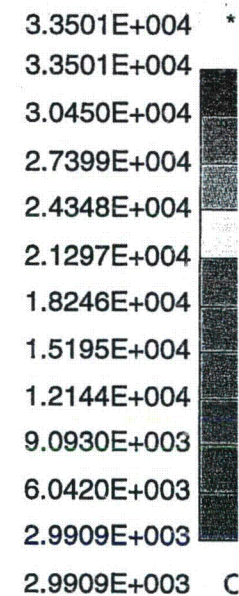
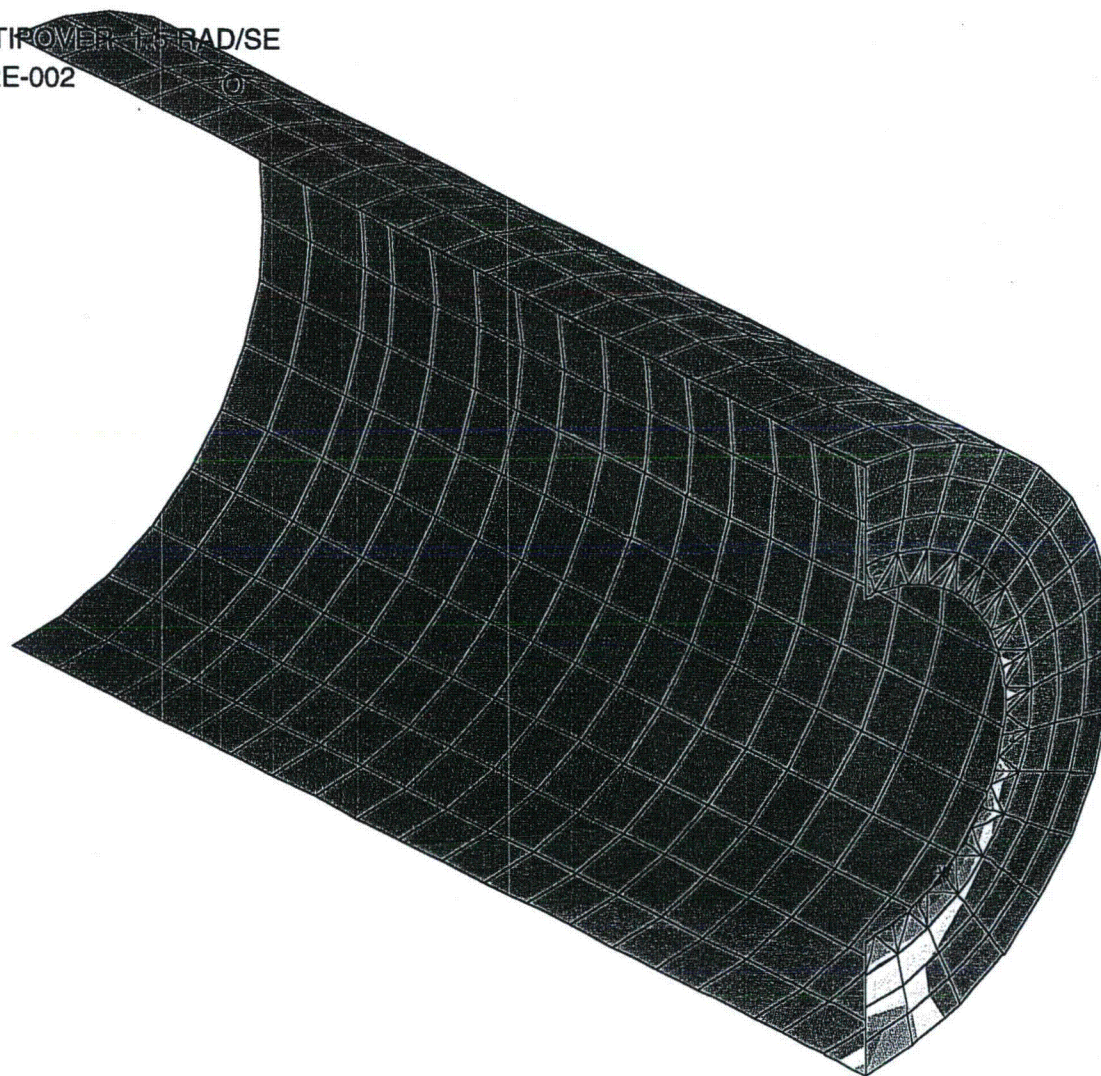
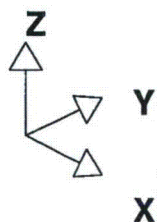
REPORT HI-2002444

REVISION 0

\\5014\\HI2002444\\CH\_3\\3\_4\_12

HI-STORM 100 FSAR, NON-PROPRIETARY  
REVISION 12  
MARCH 12, 2014

HISTORM DEFORMABLE TIP OVER 1.5 RAD/SE  
STEP 80 TIME = 7.9997852E-002  
MAX\_VONMISES



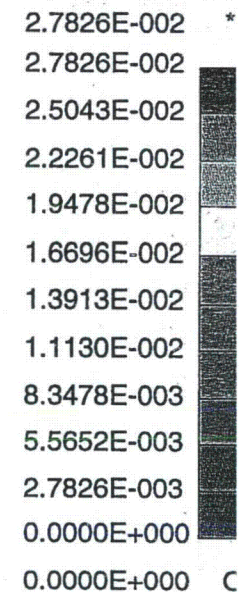
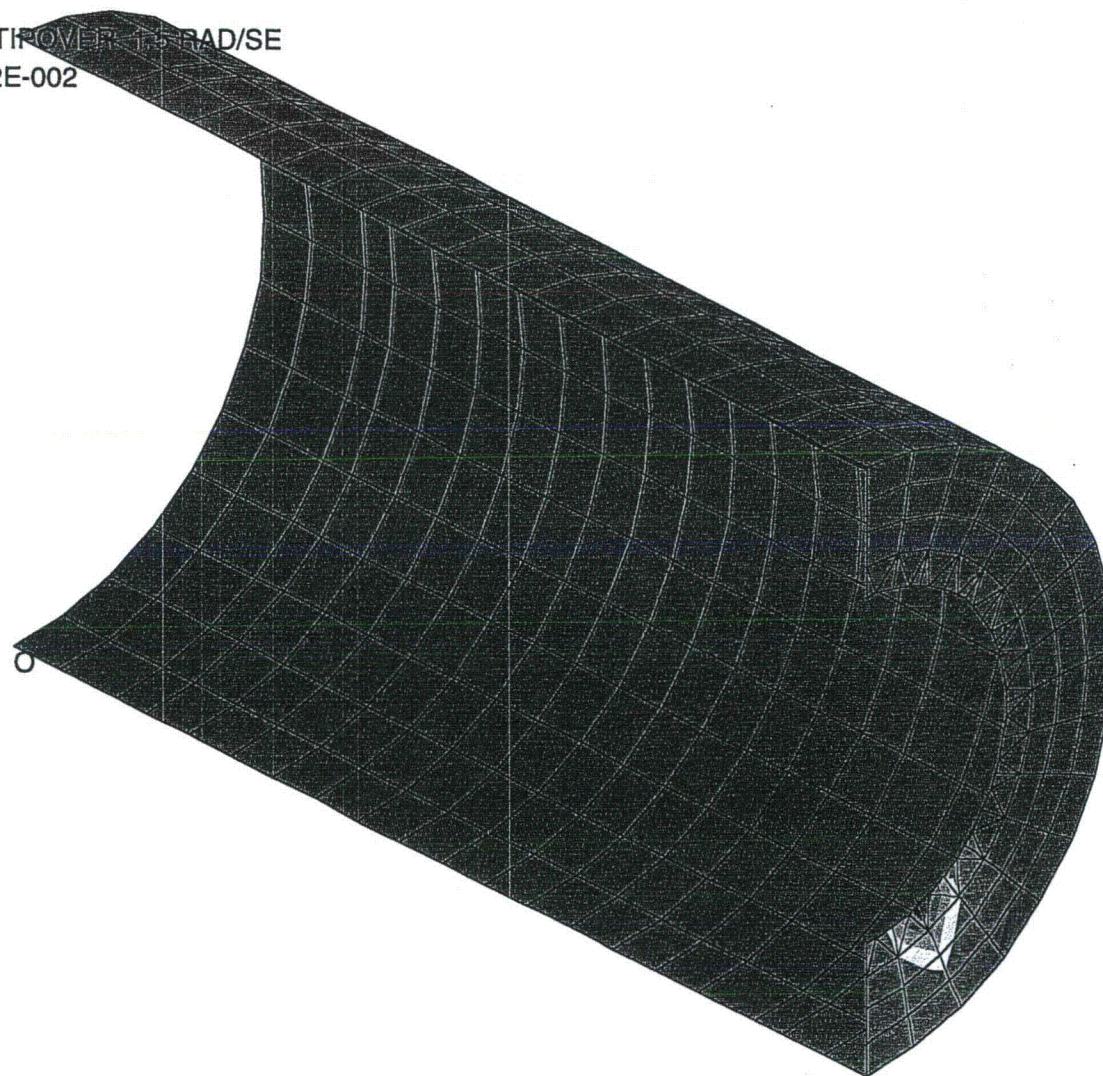
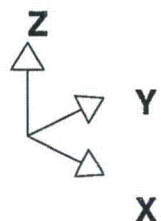
HI-STORM FSAR  
HI-2002444

Fig. 3.4.13 Von Mises Stress Outer Shell

REV. 0

HI-STORM 100 FSAR, NON-PROPRIETARY  
REVISION 12  
MARCH 12, 2014

HISTORM DEFORMABLE TIP OVER: 1.5 RAD/SE  
STEP 80 TIME = 7.9997852E-002  
PSTN(TOP)



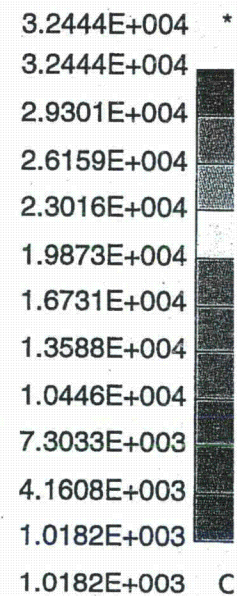
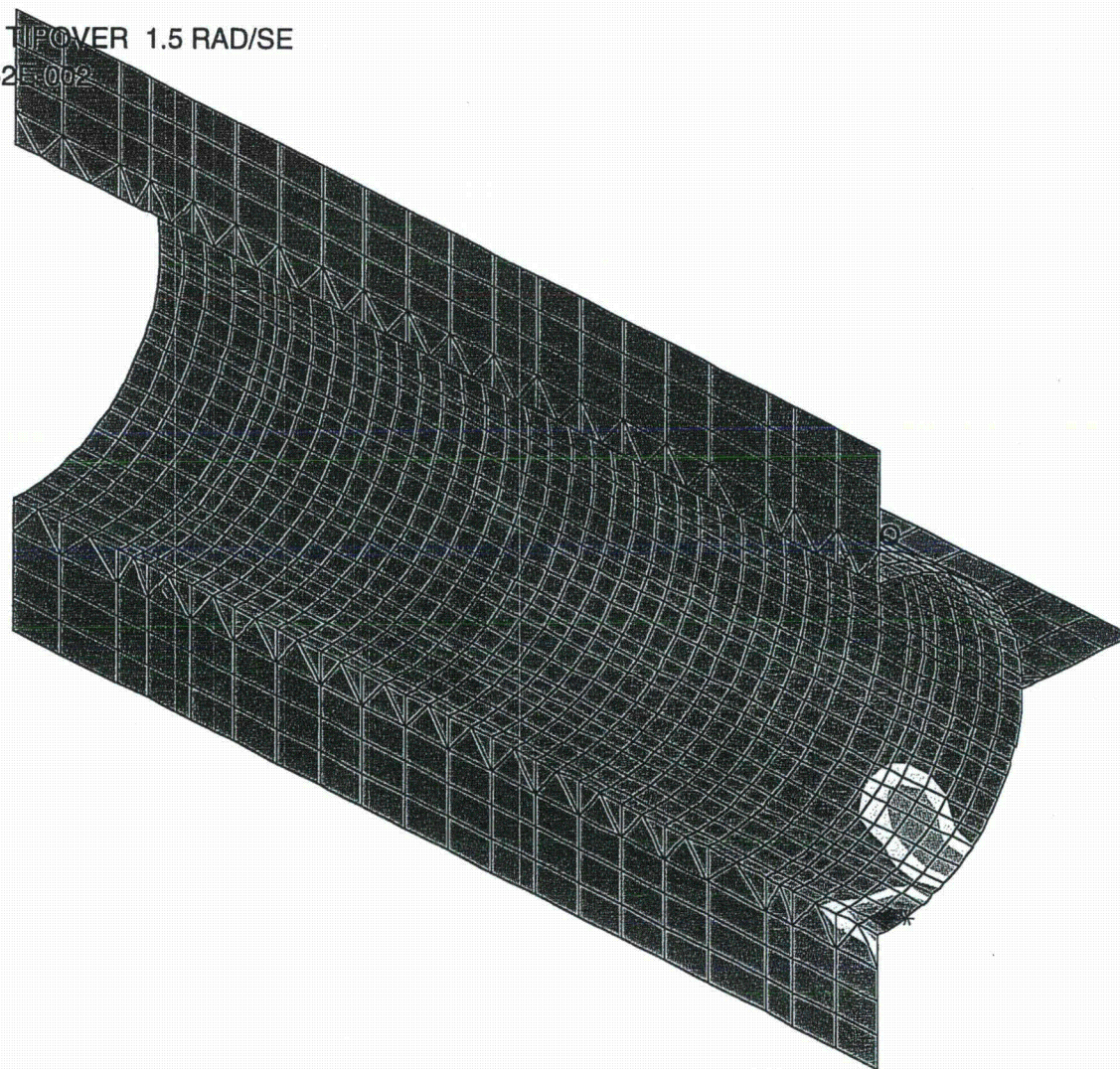
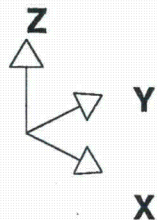
HI-2002444  
HI-STORM FSAR

Fig. 3.4.14 Plastic Strain Outer Shell

Rev. 0



HISTORM DEFORMABLE TIP OVER 1.5 RAD/SE  
 STEP 80 TIME = 7.9997852E-002  
 MAX\_VONMISES



HI-2002444

Fig. 34.15 Von Mises Stress - Inner Shell

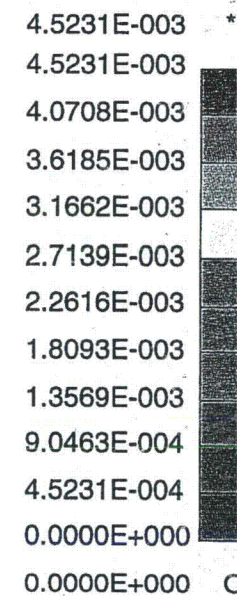
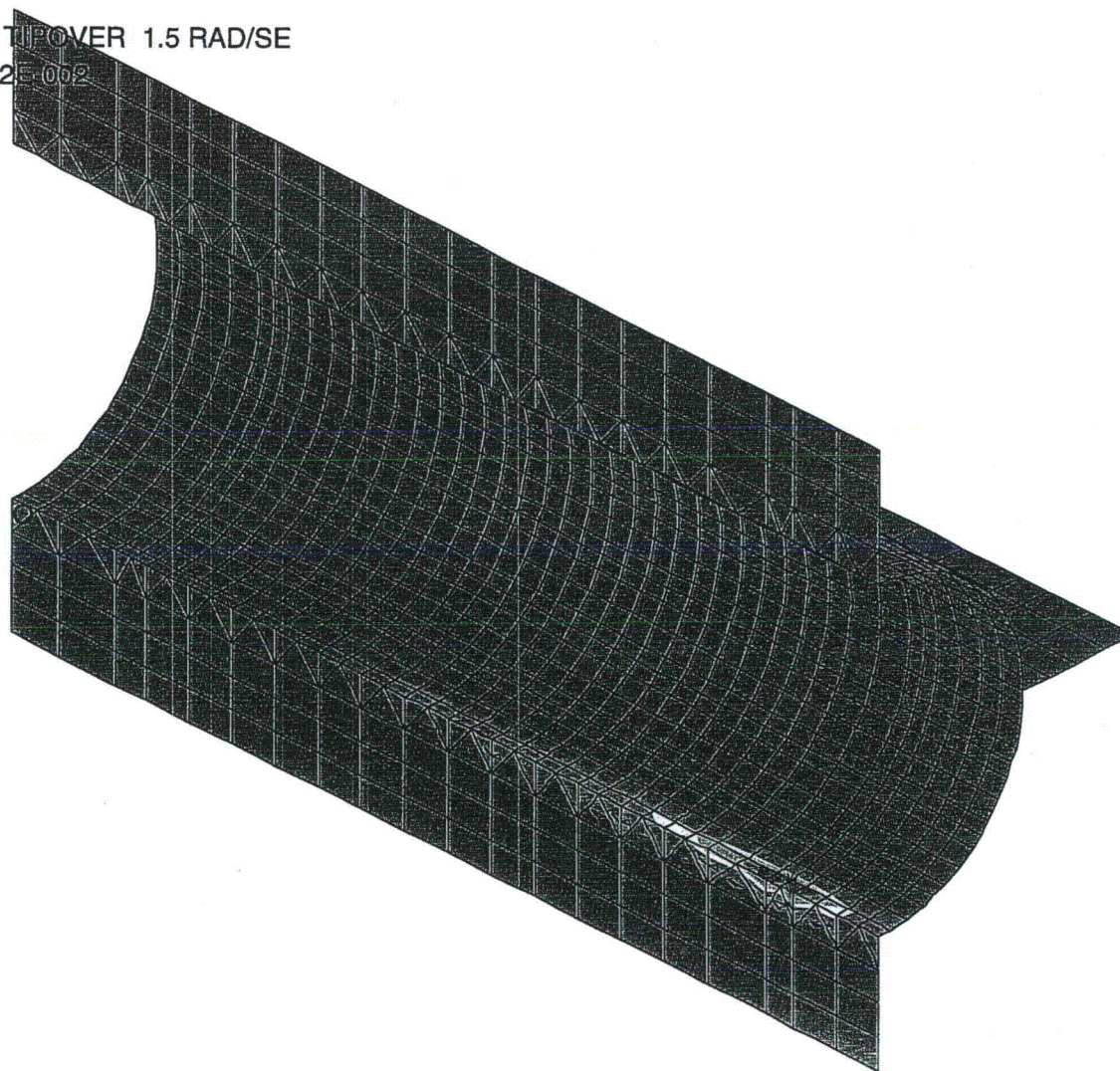
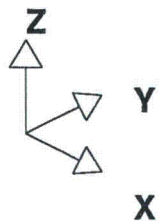
REV. 0

HI-STORM FSAR



HI-STORM 100 FSAR, NON-PROPRIETARY  
REVISION 12  
MARCH 12, 2014

HISTORM DEFORMABLE TIPOVER 1.5 RAD/SE  
STEP 80 TIME = 7.9997852E-002  
PSTN(TOP)

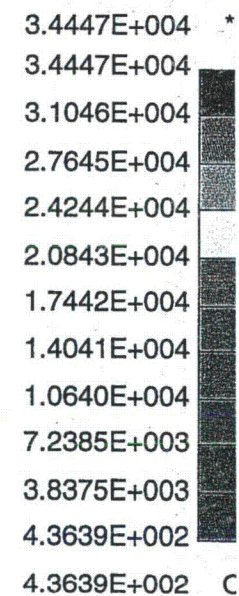
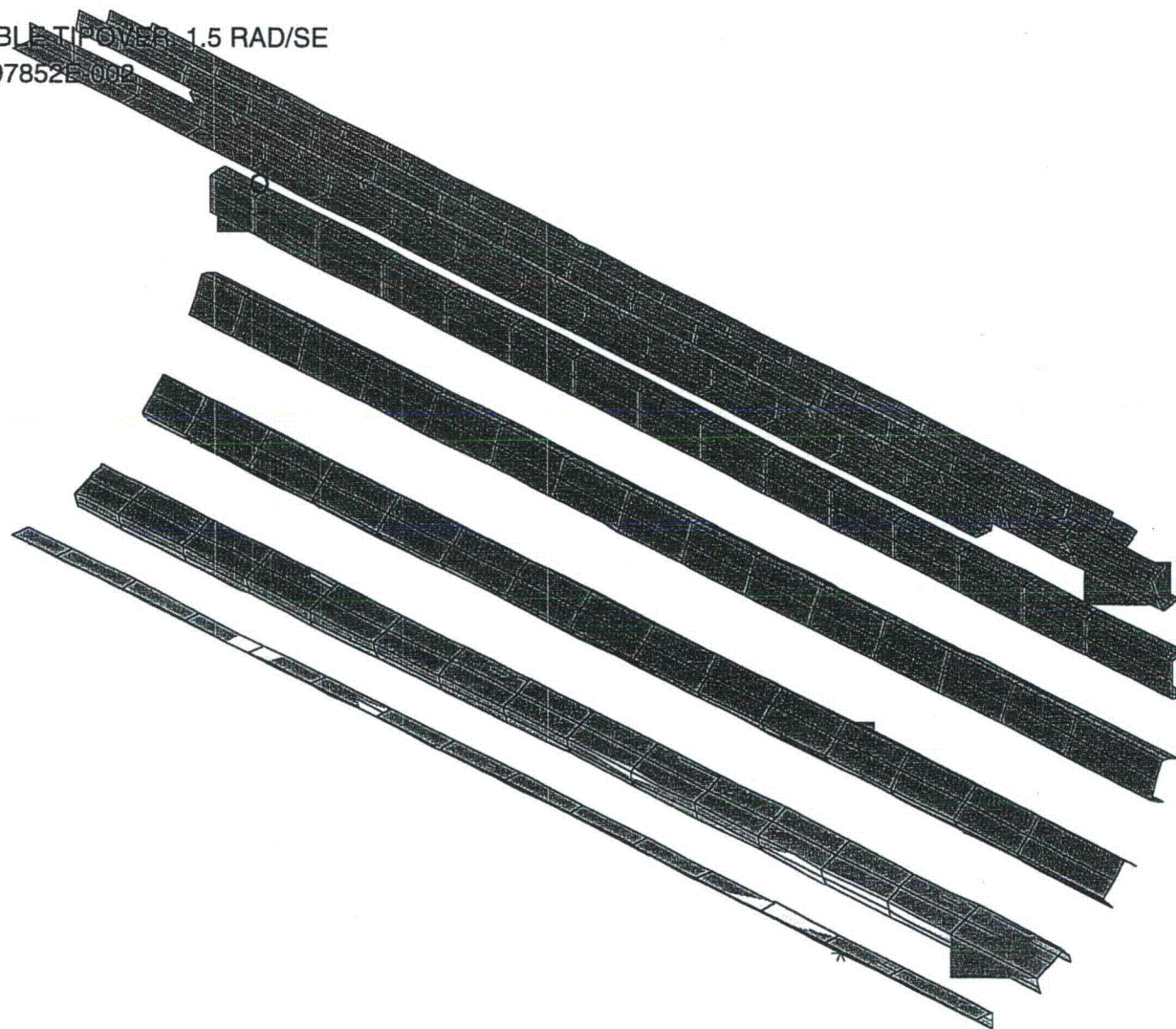
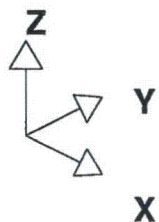


HI-2002444  
HI-STORM FSAR

Fig. 3.4.16 Plastic Strain Inner Shell

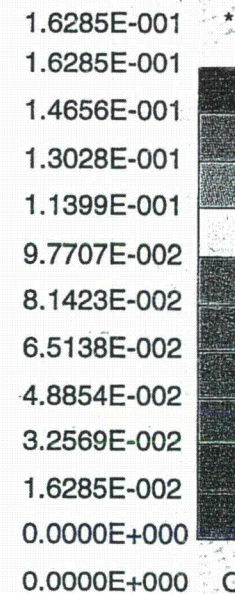
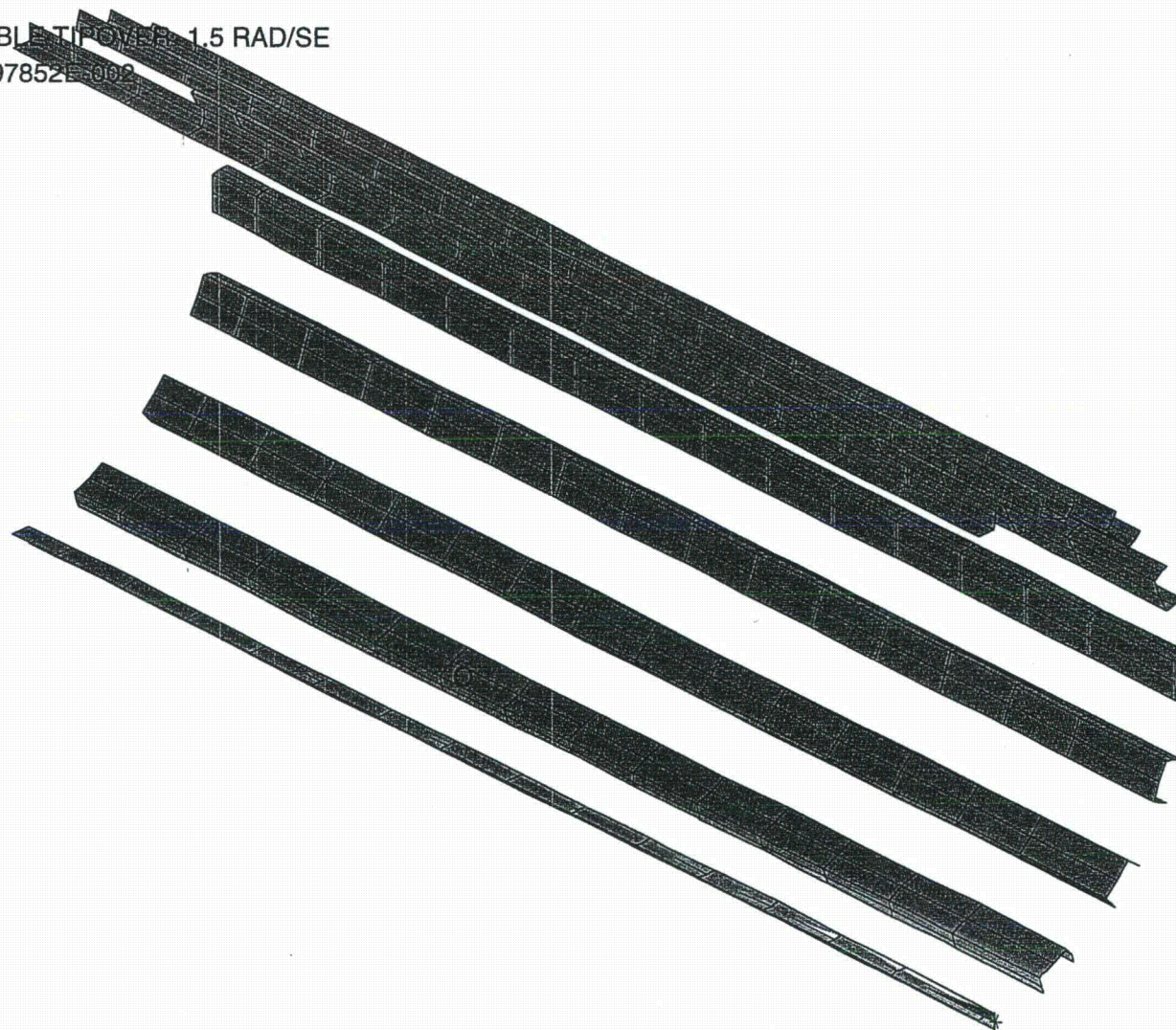
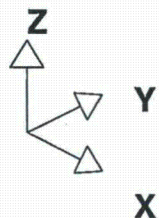
Rev. 0

HISTORM DEFORMABLE TIPON-3 1.5 RAD/SE  
 STEP 80 TIME = 7.9997852E-002  
 MAX\_VONMISES





HISTORM DEFORMABLE TYPICAL 1.5 RAD/SE  
 STEP 80 TIME = 7.9997852E-002  
 PSTN(MID)





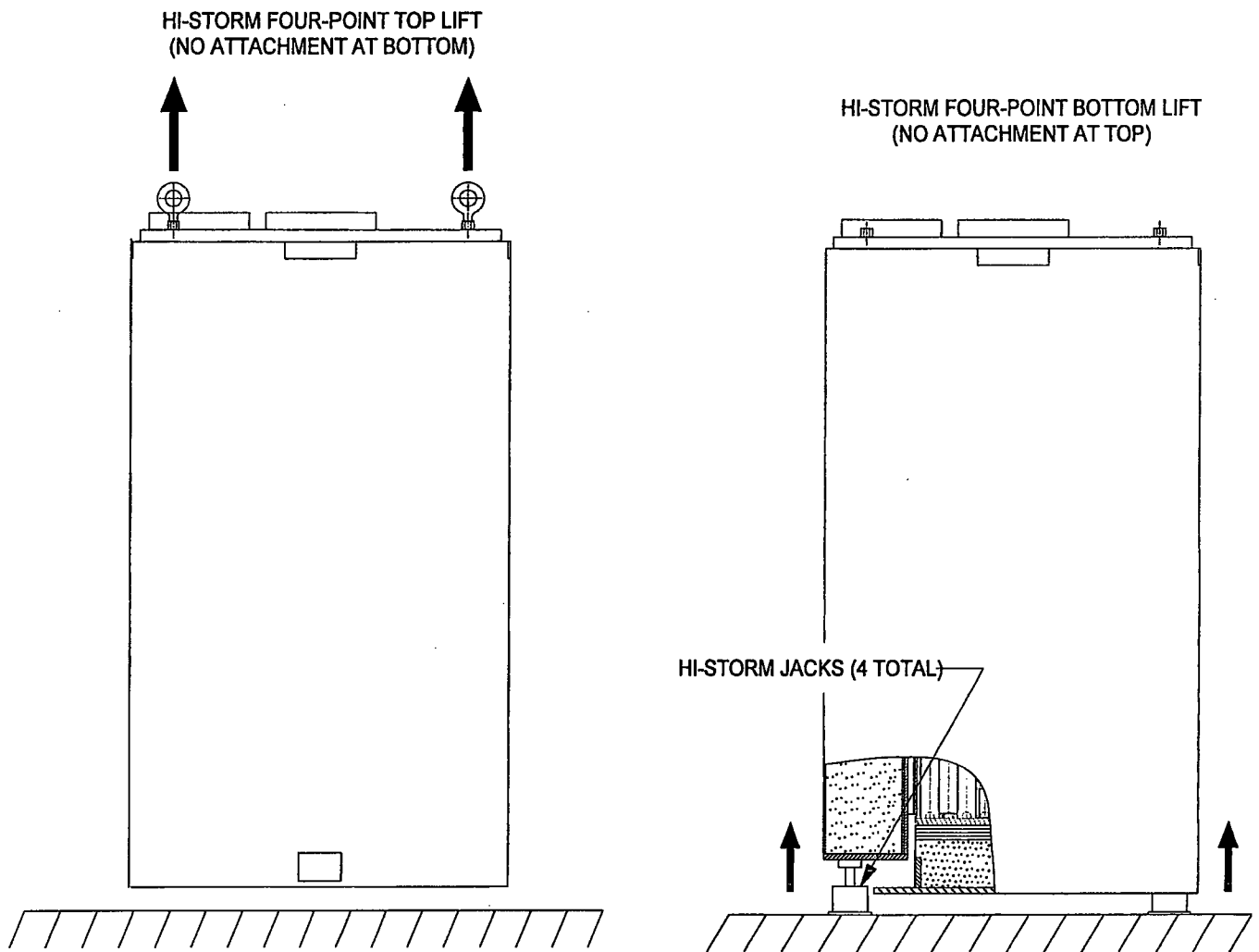


**Figure 3.4.17; Top and Bottom Lifting of the Loaded HI-STORM 100**

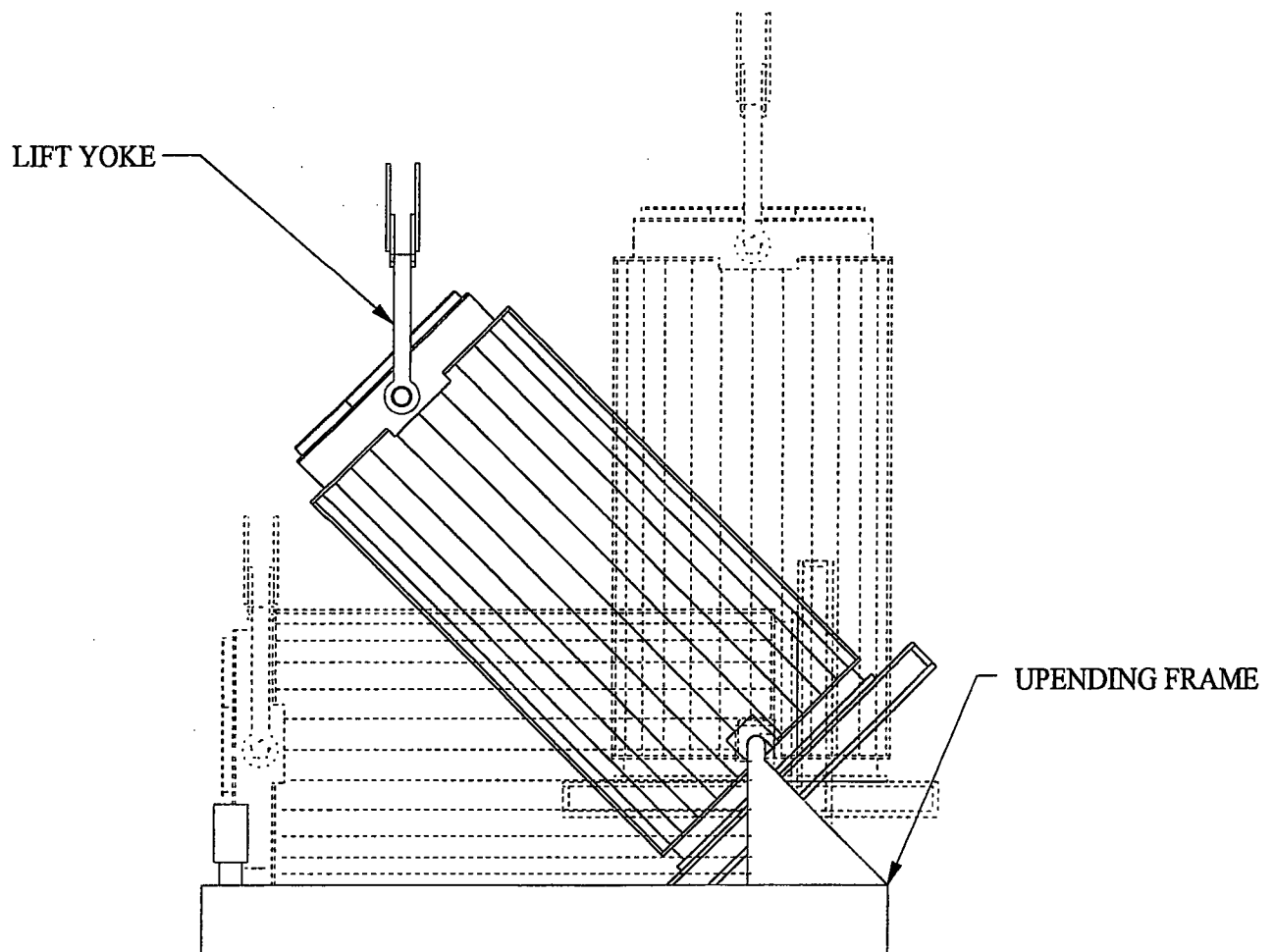


**Figure 3.4.18; HI-TRAC Upending in the Upending Frame**

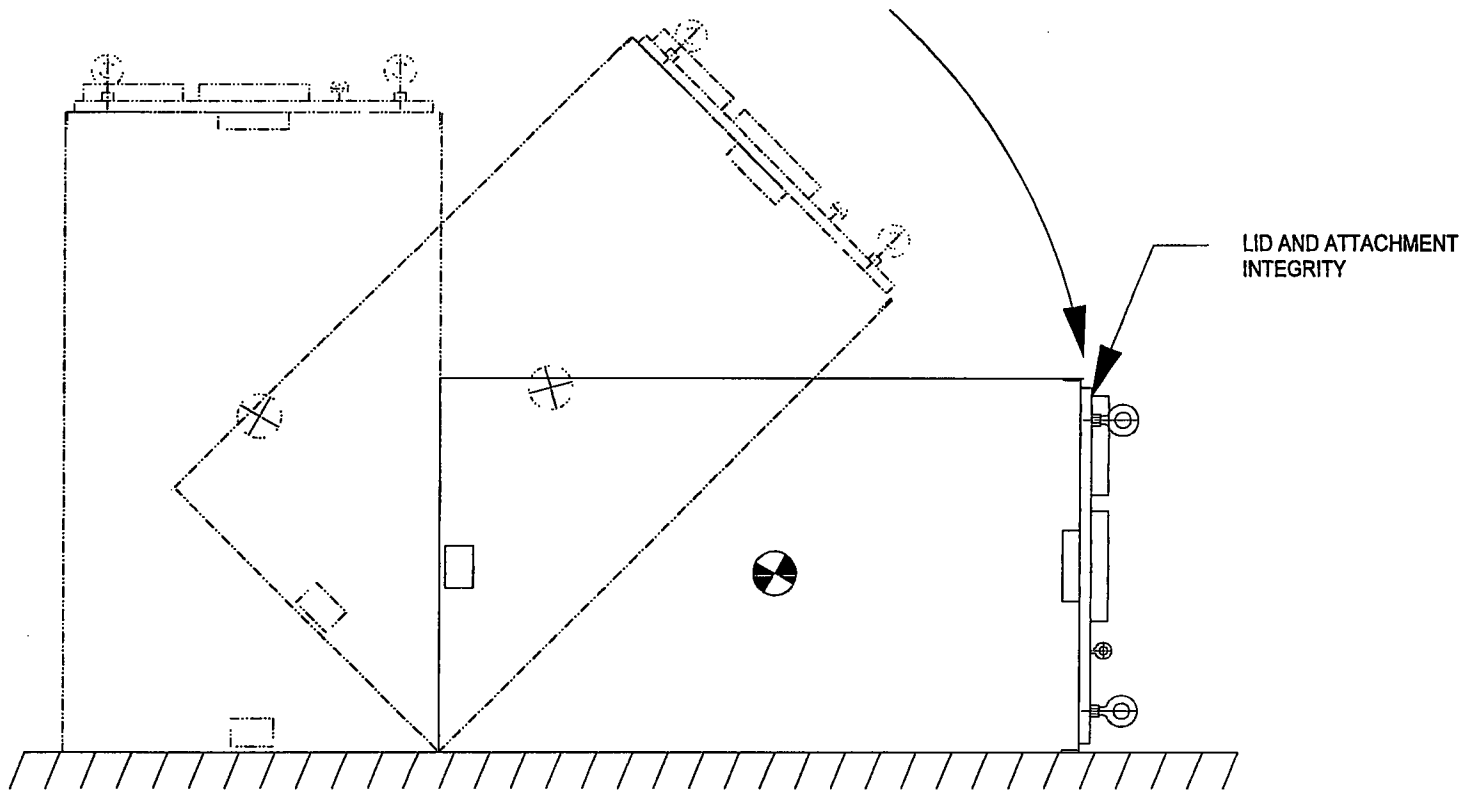


**Figure 3.4.19; HI-STORM 100 Tip-Over Event**

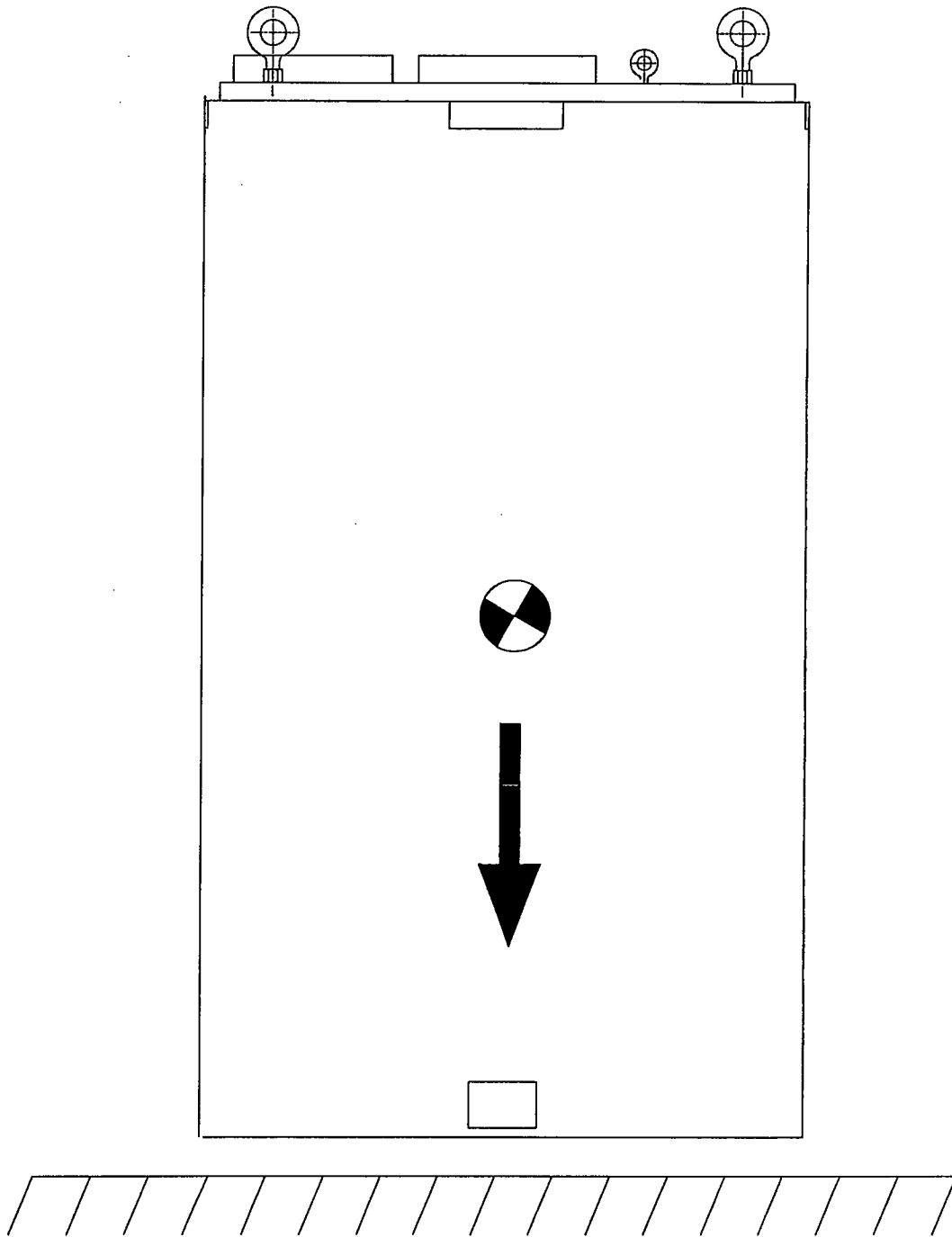
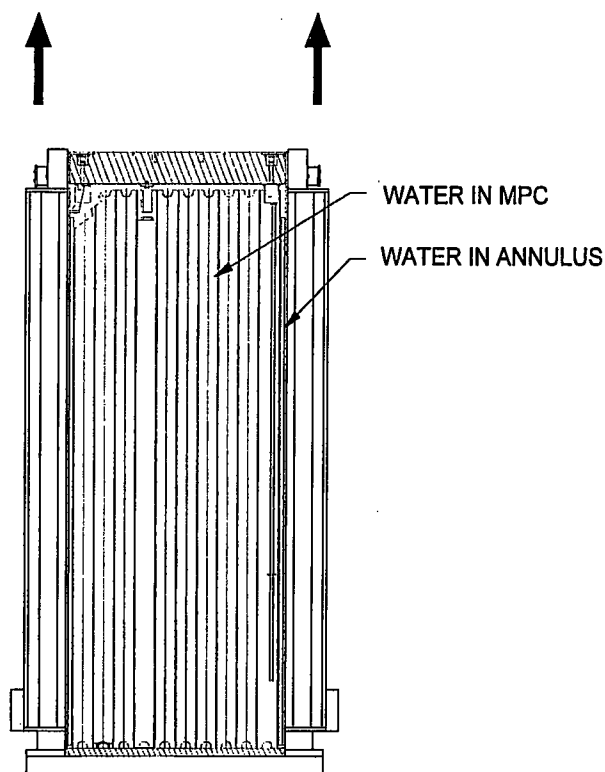
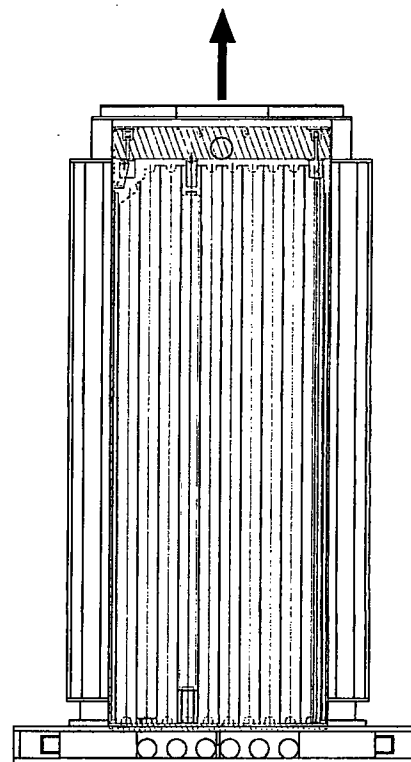


**Figure 3.4.20; HI-STORM 100 End Drop Event**



HI-TRAC LIFTING WITH  
THE POOL LID



HI-TRAC LIFTING WITH  
THE TRANSFER LID

**Figure 3.4.21; HI-TRAC Lifting with the Pool and Transfer Lids**

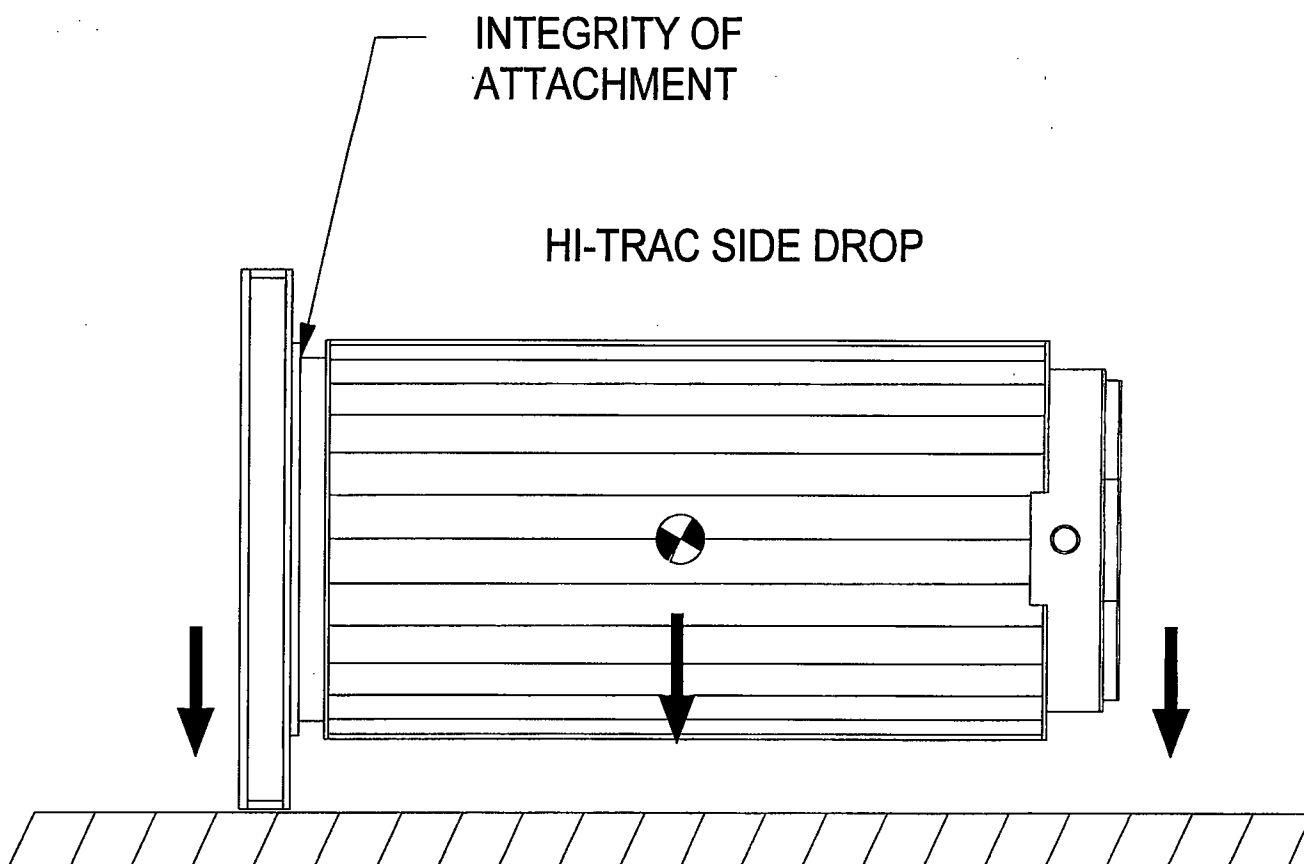


**Figure 3.4.22; HI-TRAC Side Drop Event**

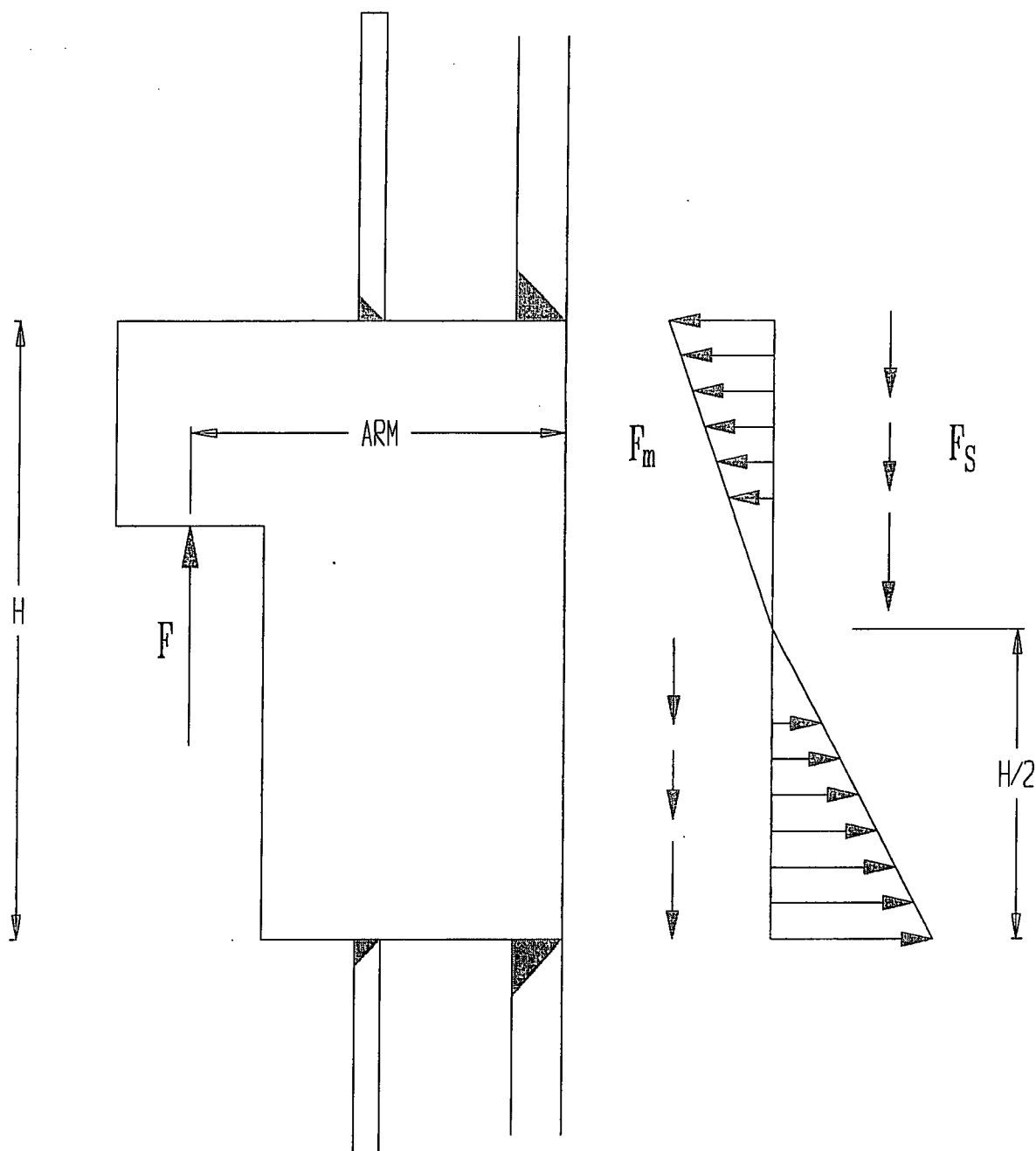


FIGURE 3.4.23 FORCES AND MOMENTS ON  
125 TON ROTATION TRUNNION WELD

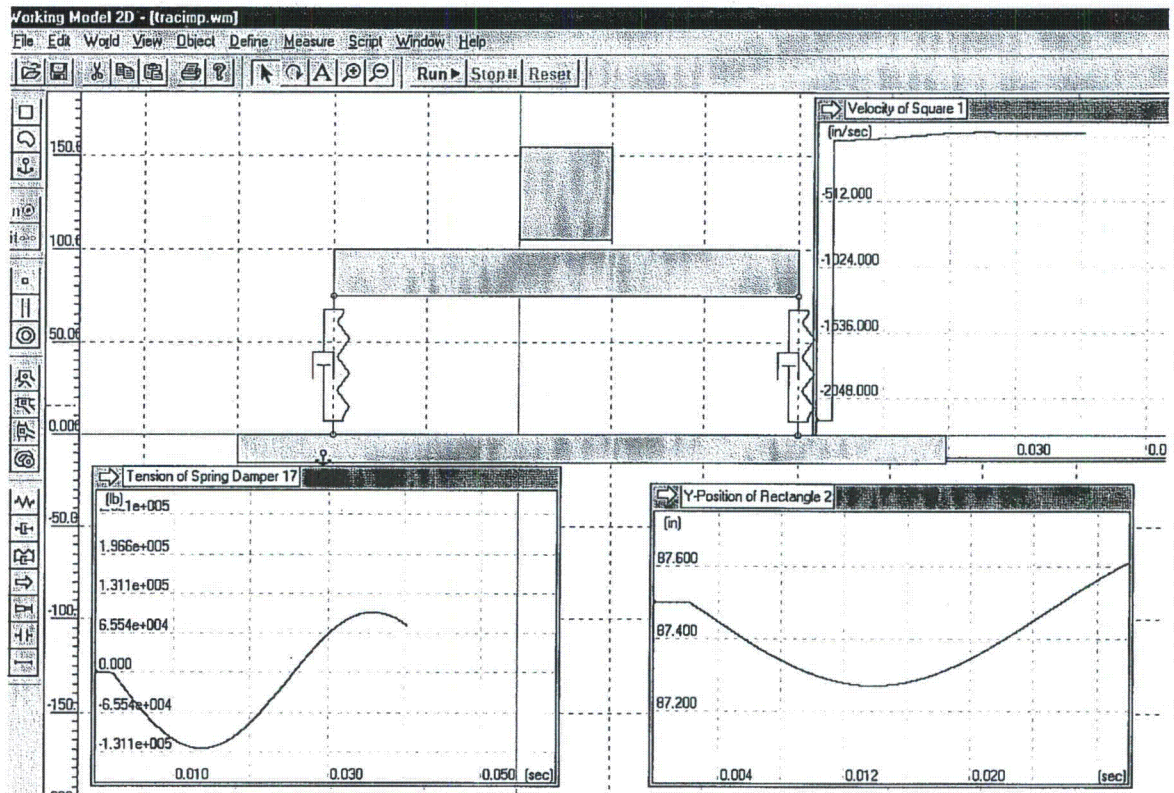


FIGURE 3.4.24 WORKING MODEL SOLUTION FOR IMPACT FORCE ON HI-TRAC 100 TRANSFER CASK OUTER SHELL



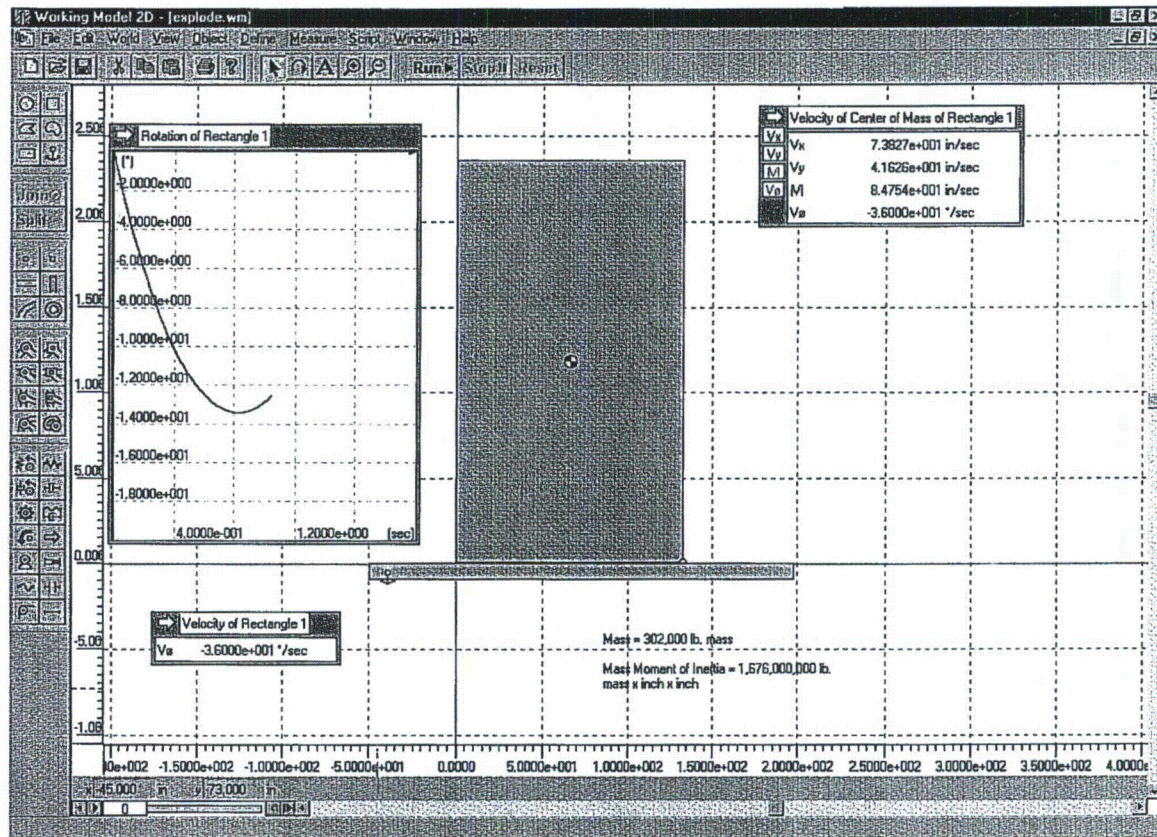


FIGURE 3.4.25: HI-STORM 100 OVERTURNING SCENARIO - INITIAL ANGULAR VELOCITY = 0.628 RADIANS/SECOND ASSUMED CAUSED BY A PRESSURE PULSE

HI-2002444

Revision 0

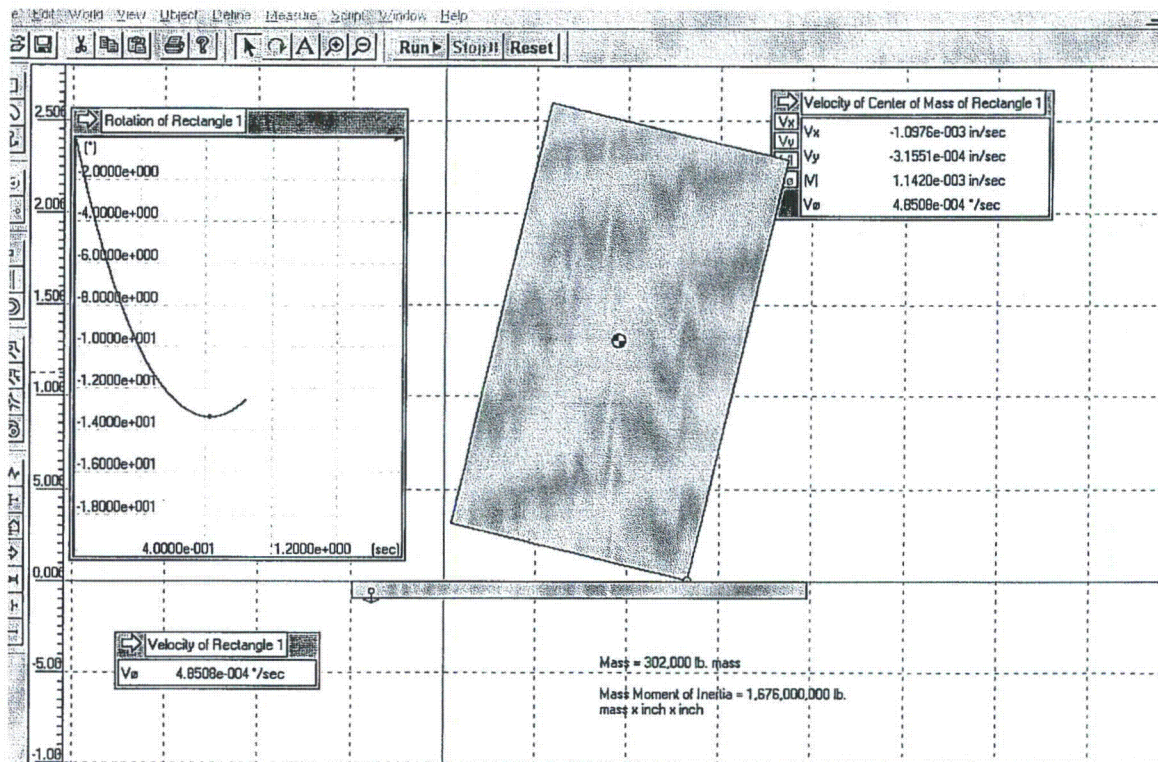
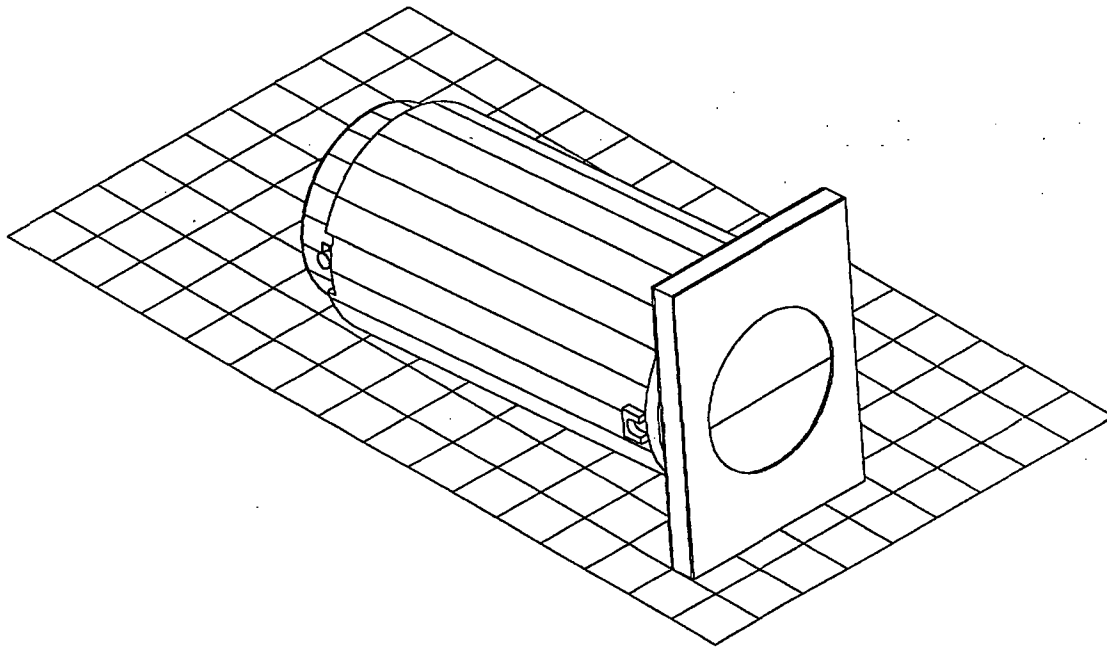
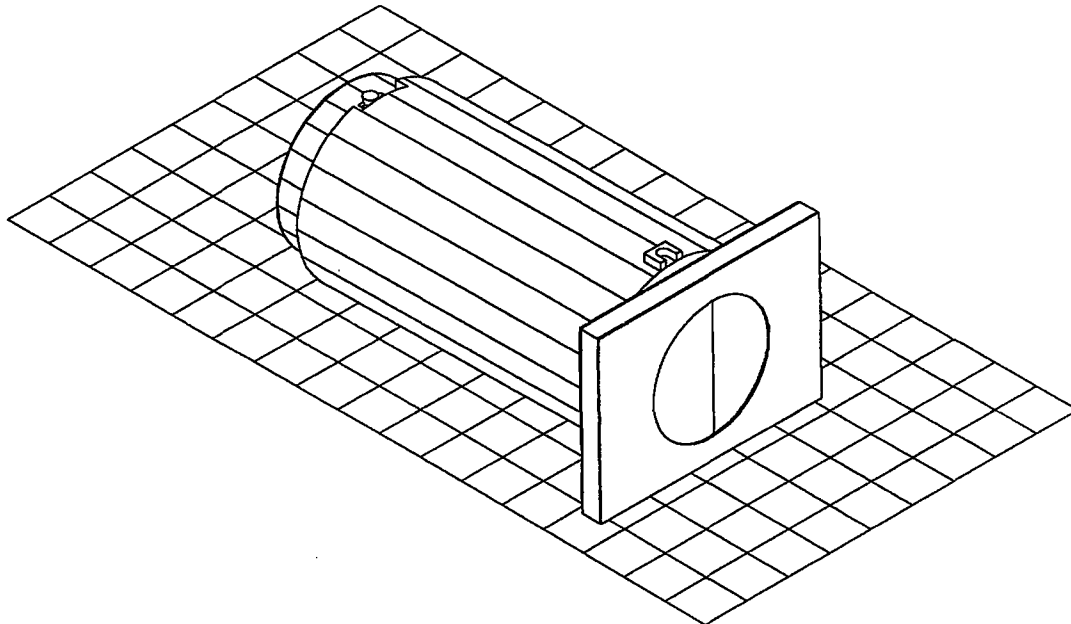


FIGURE 3.4.26: HI-STORM 100 OVERTURNING SCENARIO -  
INITIAL ANGULAR VELOCITY = 0.628 RADIANS/SECOND  
MAXIMUM ANGULAR EXCURSION



**FIGURE 3.4.27; HI-TRAC TRANSFER CASK IN SHORT-SIDE IMPACT  
(CASK RESTS AT A POSITION OF  $-5^{\circ}$  FROM HORIZONTAL)**



**FIGURE 3.4.28; HI-TRAC TRANSFER CASK IN LONG-SIDE IMPACT  
(CASK RESTS AT A POSITION OF  $-1^{\circ}$  FROM HORIZONTAL)**

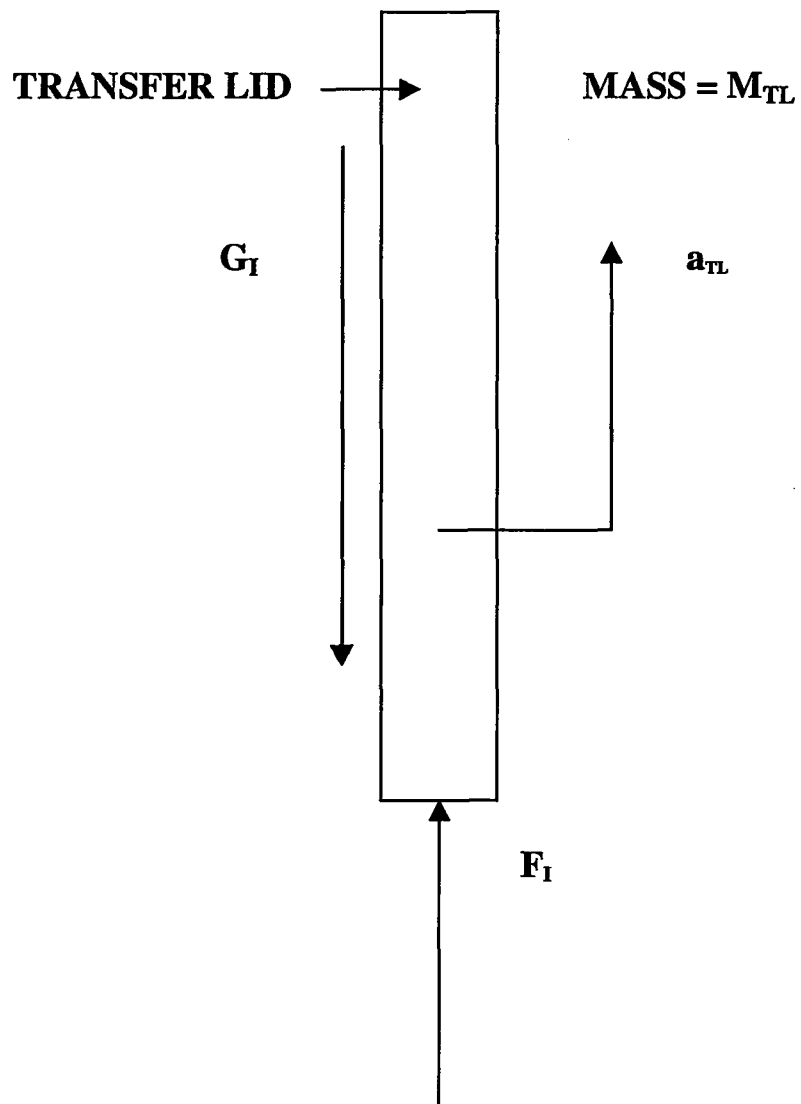


**FIGURE 3.4.29; FREE-BODY OF TRANSFER LID DURING PRIMARY IMPACT WITH TARGET**



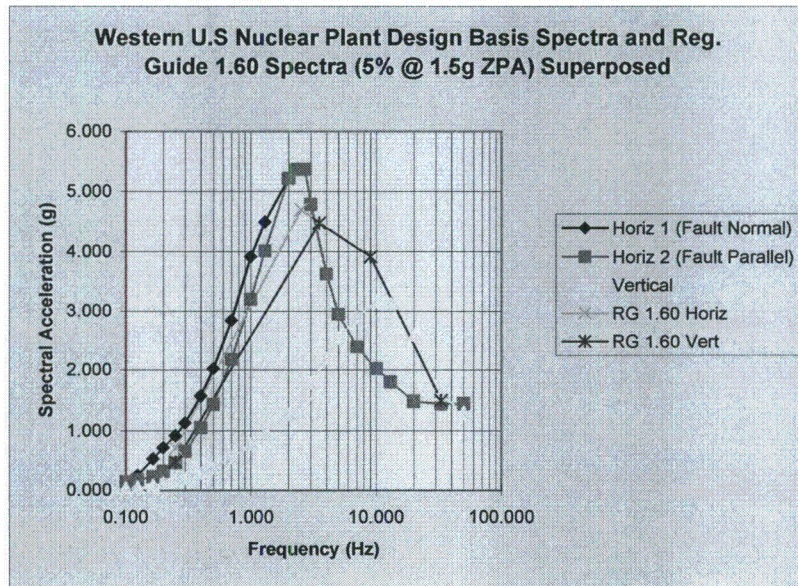


FIGURE 3.4.30 SEISMIC SPECTRA SETS USED FOR TIME HISTORY ANALYSIS OF HI-STORM 100A ON ISFSI PAD

HI-STORM FSAR  
HI-2002444

HOLTEC PROPRIETARY INFORMATION

Rev. 1

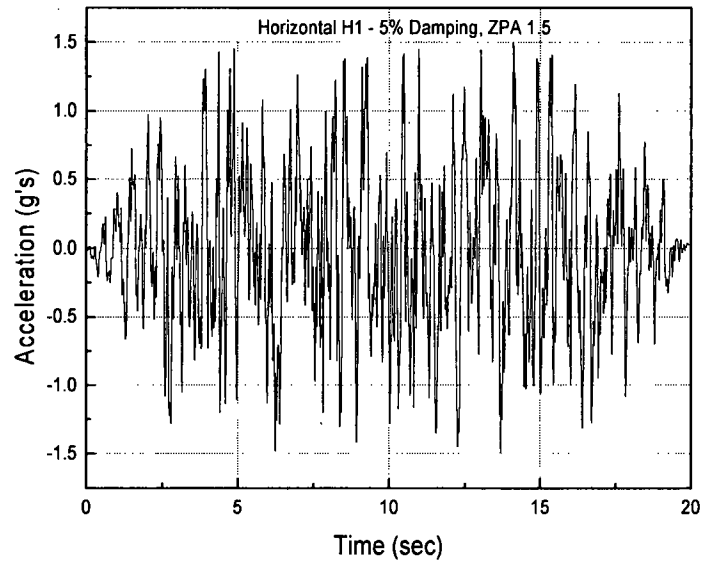


FIGURE 3.4.31 – RG 1.60 “H1”

HI-STORM FSAR  
HI-2002444

HOLTEC PROPRIETARY INFORMATION

Rev. 1

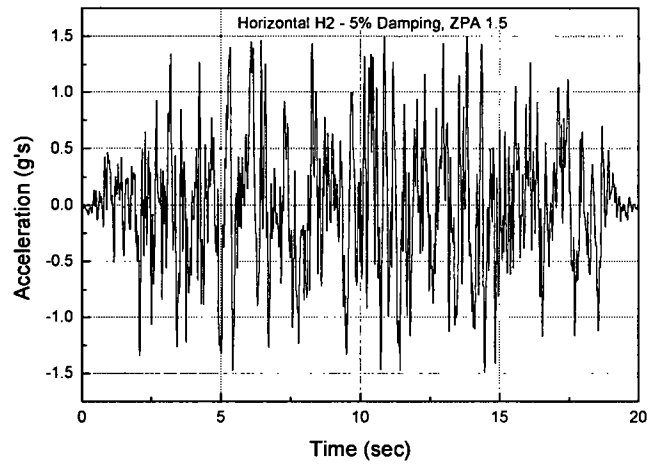


FIGURE 3.4.32 – RG 1.60 “H2”

HI-STORM FSAR  
HI-2002444

HOLTEC PROPRIETARY INFORMATION

Rev. 1

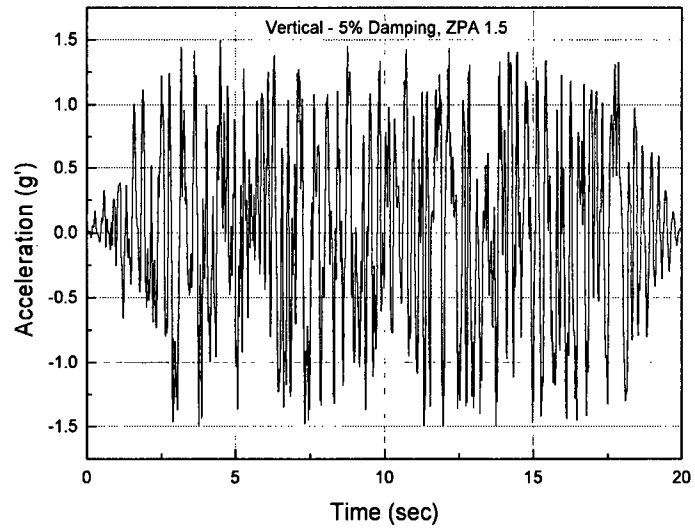


FIGURE 3.4.33 – RG 1.60 “VT”

HI-STORM FSAR  
HI-2002444

HOLTEC PROPRIETARY INFORMATION

Rev. 1



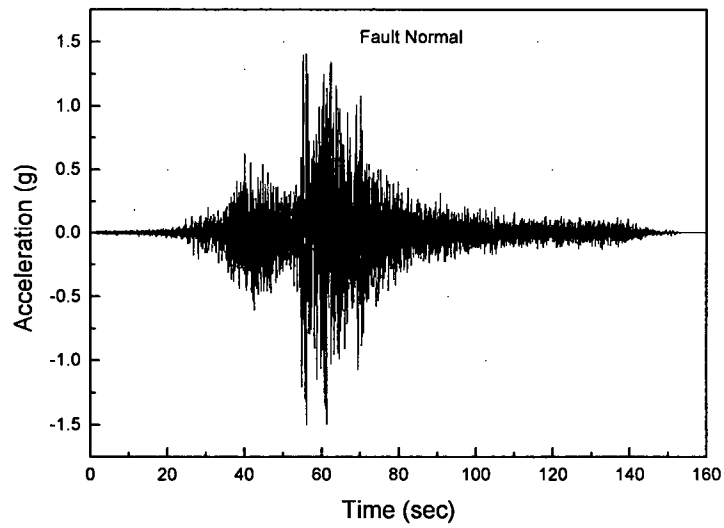


FIGURE 3.4.34 Horizontal Acceleration Time history "FN"

HI-STORM FSAR  
HI-2002444

HOLTEC PROPRIETARY INFORMATION

Rev. I

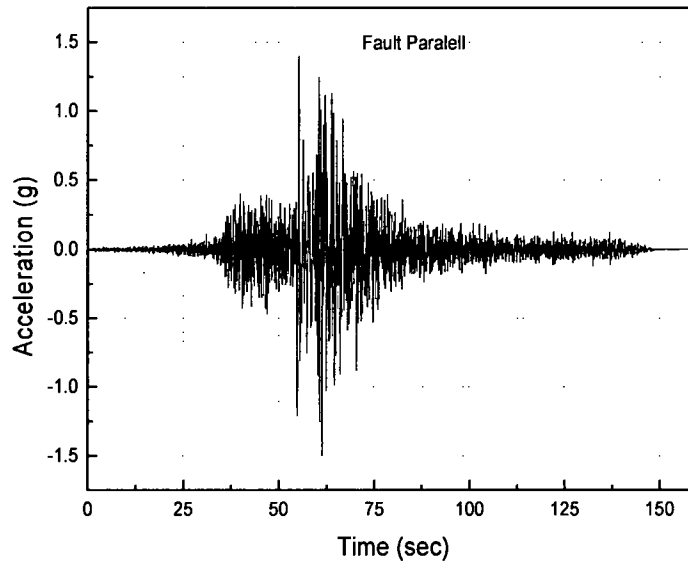


FIGURE 3.4.35 Horizontal Acceleration Time history "FP"

HI-STORM FSAR  
HI-2002444

HOLTEC PROPRIETARY INFORMATION

Rev. 1

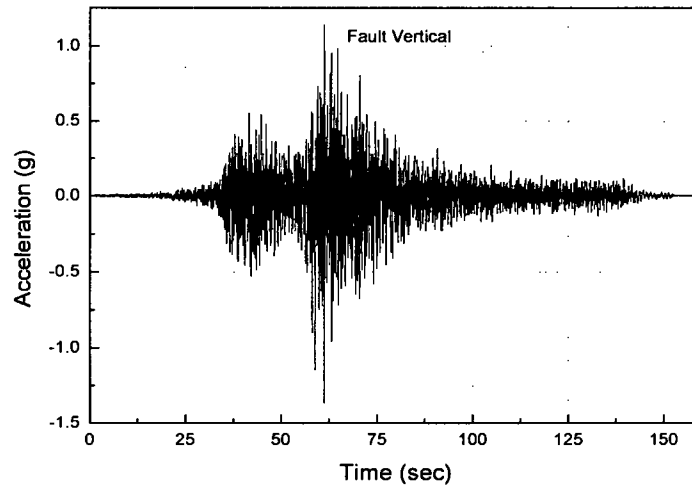


FIGURE 3.4.36 Vertical Acceleration Time history “FV”

HI-STORM FSAR  
HI-2002444

HOLTEC PROPRIETARY INFORMATION

Rev. 1

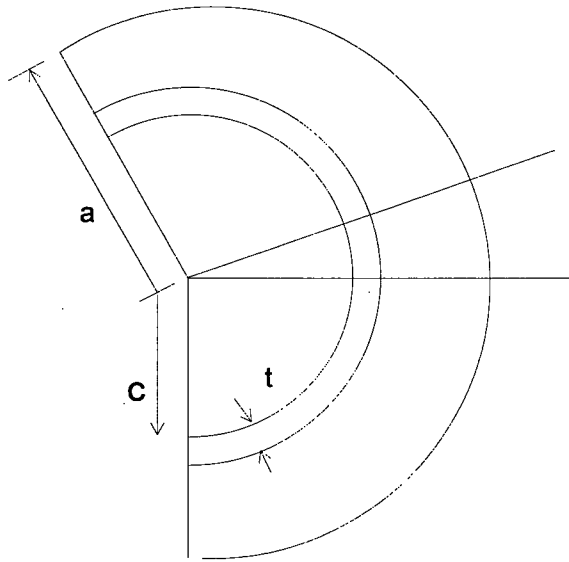


FIGURE 3.4.37 GEOMETRY FOR QUASI-STATIC ANALYSIS

HI-STORM FSAR  
HI-2002444

HOLTEC PROPRIETARY INFORMATION

Rev. 1

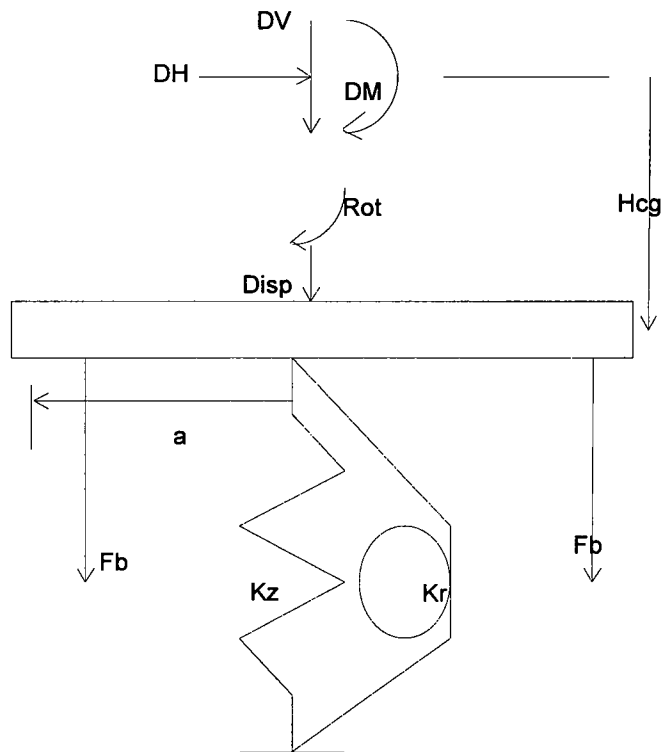


FIGURE 3.4.38 FREE BODY FOR QUASI-STATIC ANALYSIS

HI-STORM FSAR  
HI-2002444

HOLTEC PROPRIETARY INFORMATION

Rev. 1

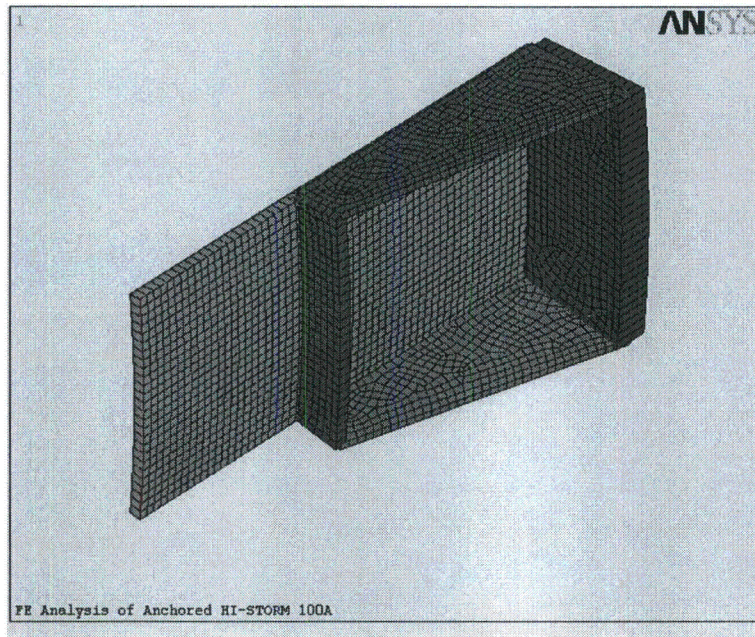


FIGURE 3.4.39 Sector Lug Finite Element Mesh

HI-STORM FSAR  
HI-2002444

HOLTEC PROPRIETARY INFORMATION

Rev. 1

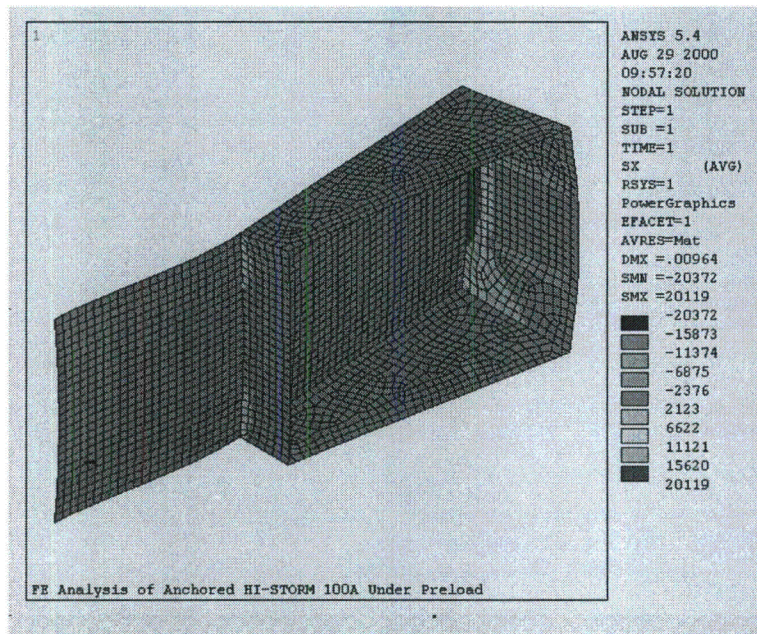


FIGURE 3.4.40 Sector Lug Stress – Case 1 Preload

HI-STORM FSAR  
 HI-2002444

HOLTEC PROPRIETARY INFORMATION

Rev. 1



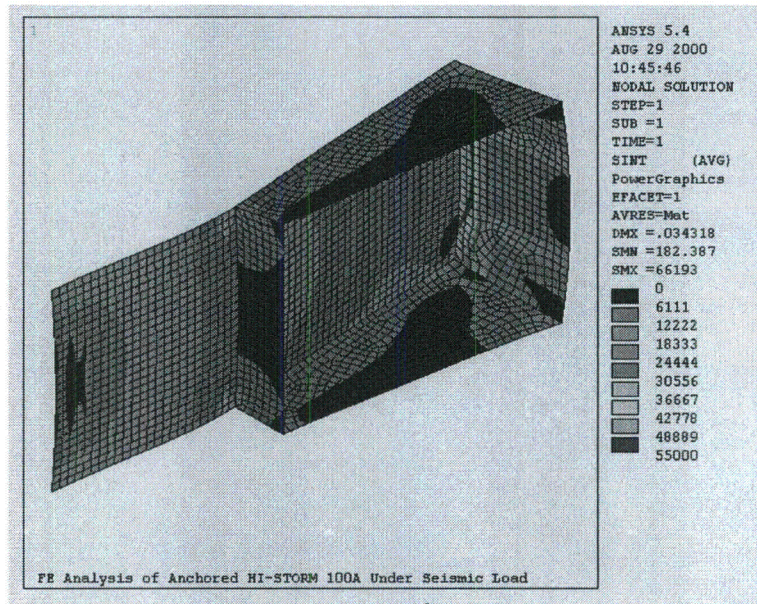


FIGURE 3.4.41 Sector Lug Stress Intensity – Case 2 Preload + Seismic

HI-STORM FSAR  
HI-2002444

HOLTEC PROPRIETARY INFORMATION

Rev. 1



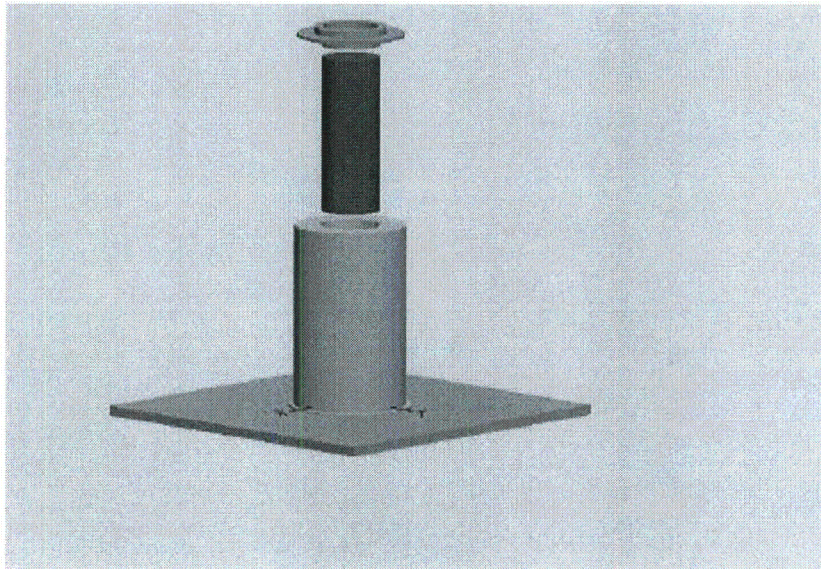


FIGURE 3.4.42: EXPLODED VIEW SHOWING GROUND PLANE, OVERPACK, MPC, AND OVERPACK TOP LID

HI-STORM FSAR  
HI-2002444

HOLTEC PROPRIETARY INFORMATION

Rev. 1

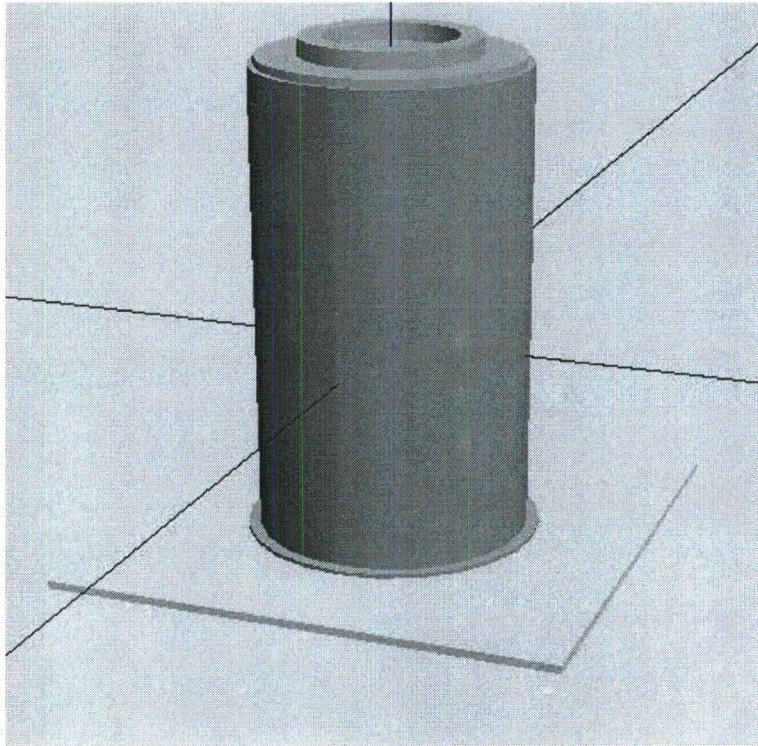


FIGURE 3.4.43: VIEW OF ASSEMBLED HI-STORM ON PAD-MPC  
INSIDE AND TOP LID ATTACHED (Note Extended Baseplate for  
Anchor Connections)

HI-STORM FSAR  
HI-2002444

HOLTEC PROPRIETARY INFORMATION

Rev. 1



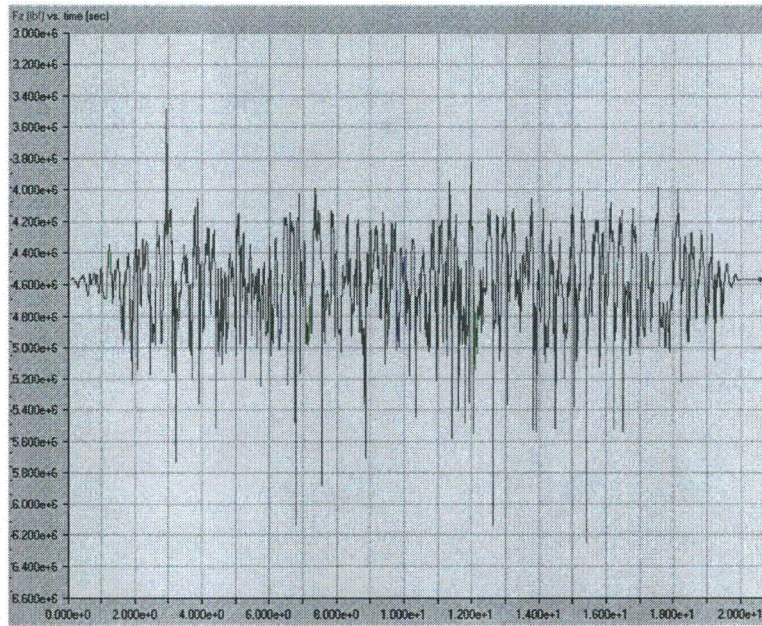


FIGURE 3.4.44 Variation of Foundation Resistance Force vs. Time for Reg. Guide 1.60 Seismic Input

HI-STORM FSAR  
HI-2002444

HOLTEC PROPRIETARY INFORMATION

Rev. 1

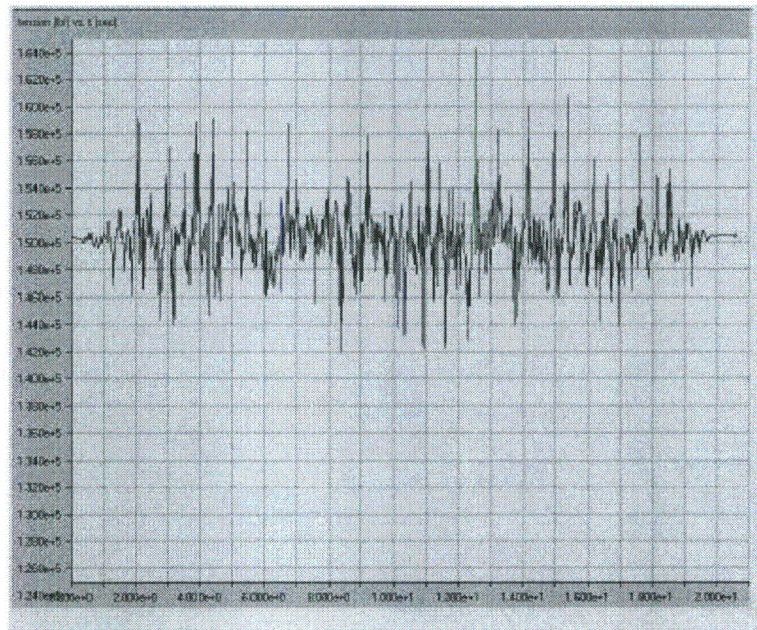


FIGURE 3.4.45 Variation of Representative Stud Tensile Force vs. Time for Reg. Guide 1.60 Seismic Input

HI-STORM FSAR  
HI-2002444

HOLTEC PROPRIETARY INFORMATION

Rev. 1



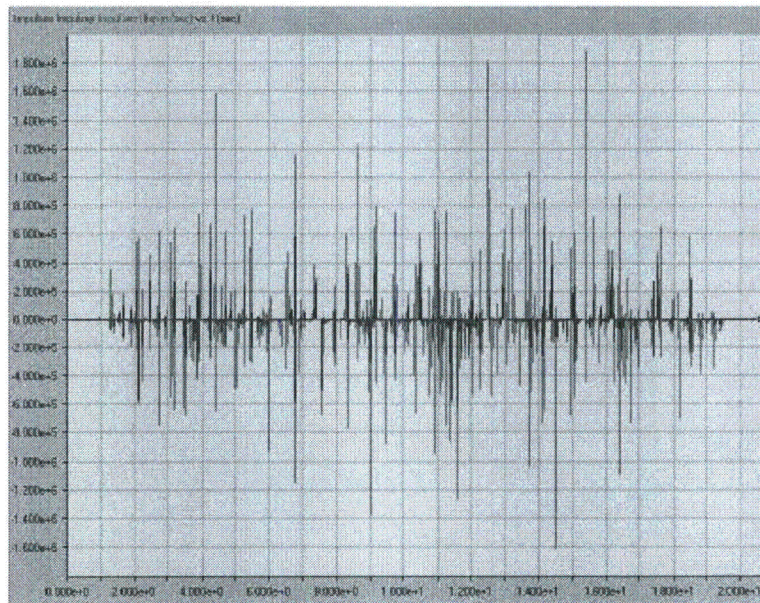


FIGURE 3.4.46 MPC/HI-STORM 100A Impulse vs. Time – Reg. Guide 1.60 Event

HI-STORM FSAR  
HI-2002444

HOLTEC PROPRIETARY INFORMATION

Rev. 1

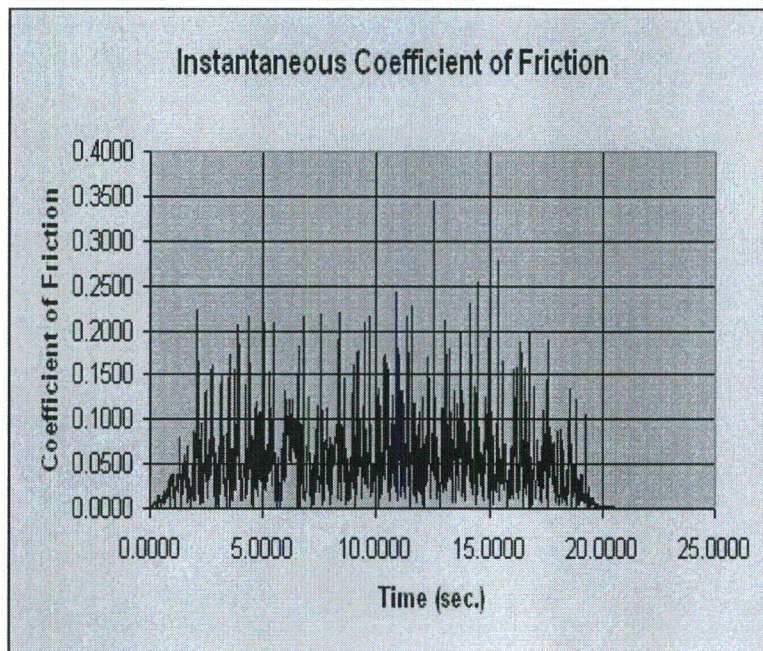


FIGURE 3.4.47 Instantaneous Calculated Coefficient of Friction – Reg. Guide 1.60 Event

HI-STORM FSAR  
HI-2002444

HOLTEC PROPRIETARY INFORMATION

Rev. 1



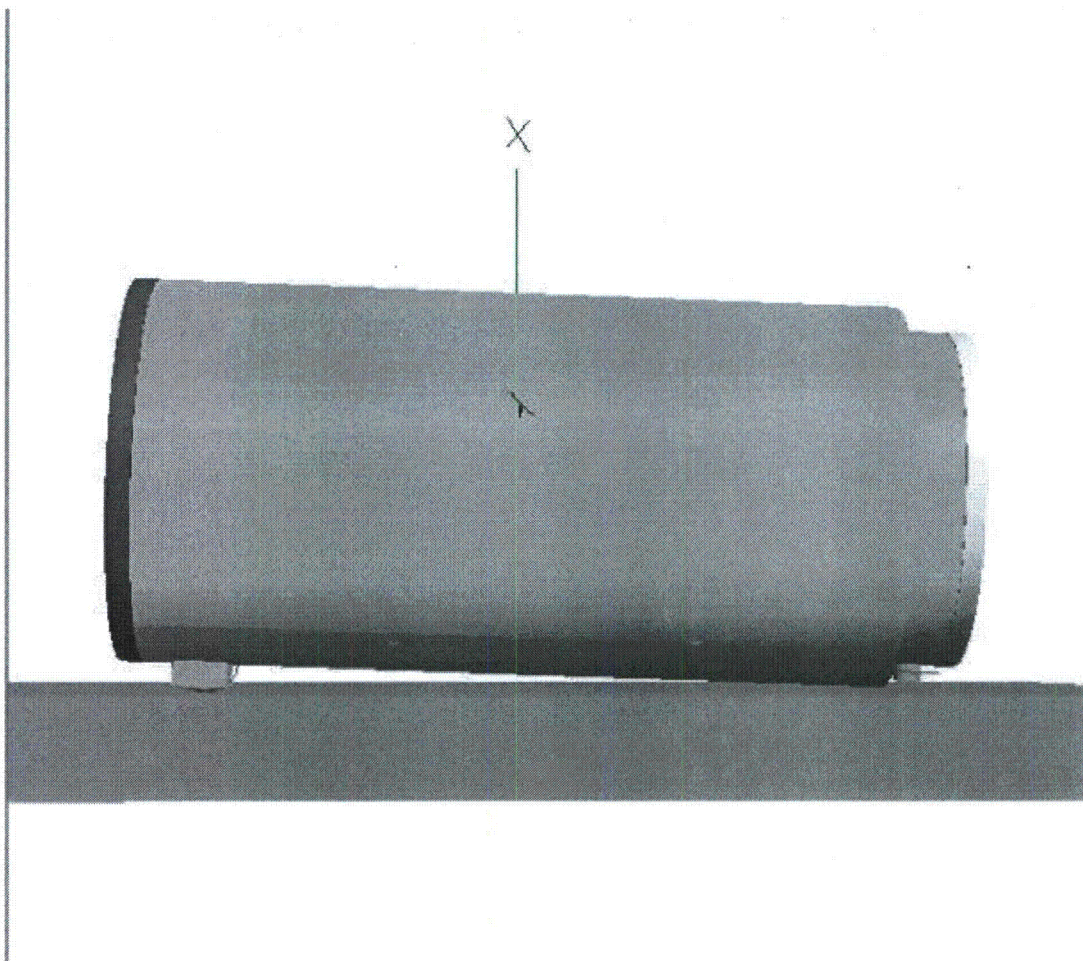


**FIGURE 3.4.48; HI-TRAC 125 BENCHMARK SIMULATION OF DROP SCENARIO A**

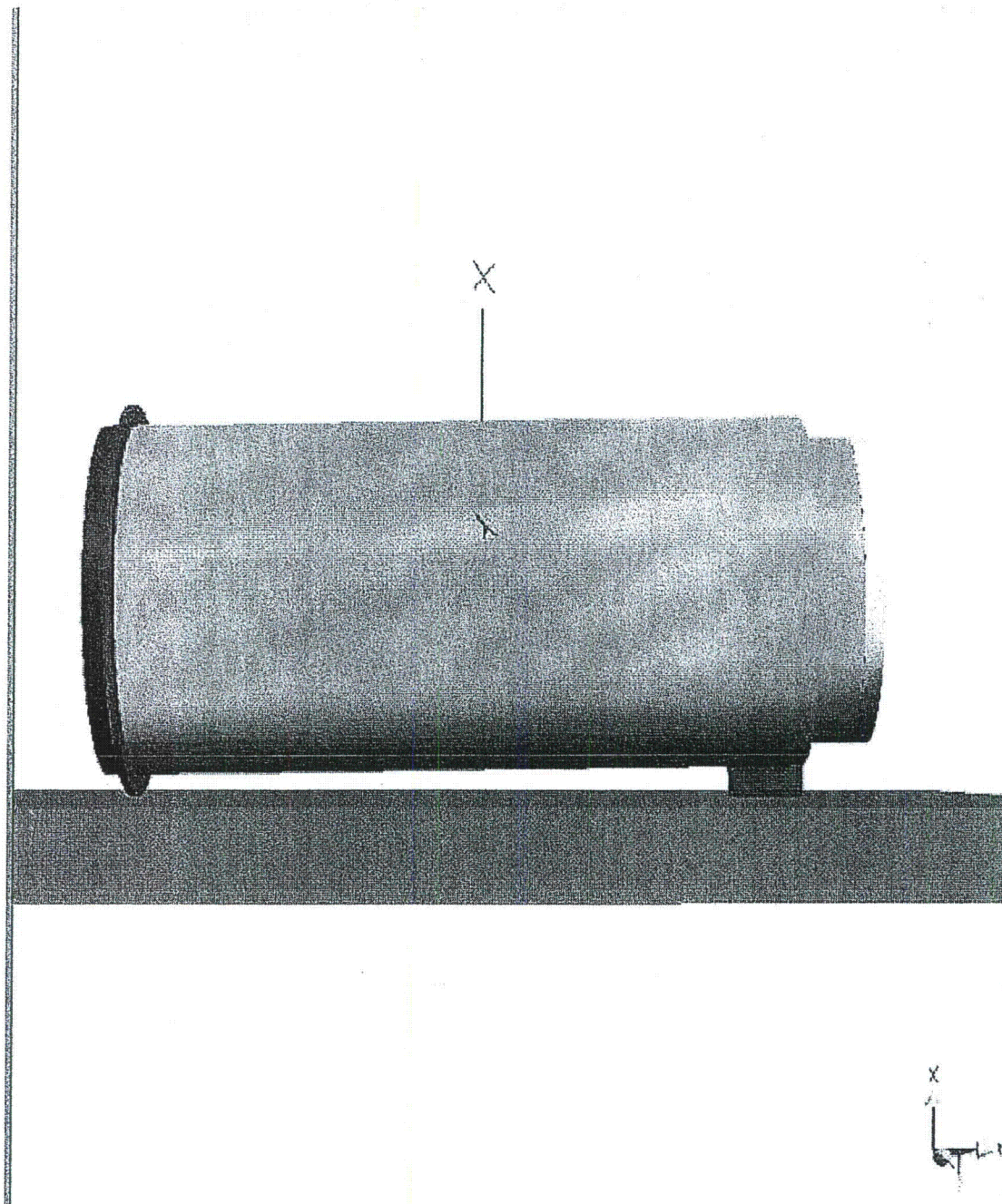


**FIGURE 3.4.49; SIMULATION OF HI-TRAC 125D 42"  
HORIZONTAL DROP WITH PRIMARY IMPACT  
AT TOP END RADIAL SUPPORT TAB**



### 3.5 FUEL RODS

The regulations governing spent fuel storage cask approval and fabrication (10 CFR 72.236) require that a storage cask system “will reasonably maintain confinement of radioactive material under normal, off-normal, and credible accident conditions” (§72.236(l)). Per Regulatory Guide 3.61, Section 3.5, “When fuel cladding is considered in the design criteria for confinement of radioactive material under normal or accident condition, provide an analysis or test results showing that the cladding will maintain its integrity.” Although the cladding of intact fuel rods does provide a barrier against the release of radioactive fission products, the confinement evaluation for the HI-STORM System (Chapter 7) takes no credit for fuel cladding integrity in satisfying the regulatory confinement requirement.

As described in Section 7.1, the confinement boundary in the HI-STORM System consists of the MPC Enclosure Vessel. The Enclosure Vessel is designed and, to the extent practicable, manufactured in accordance with the most stringent ASME B&PV Code (Section III, Subsection NB). As required by NB, all materials are 100% UT inspected and all butt welds are subjected to 100% volumetric inspection. The field closure features redundant barriers (the MPC lid and port cover plates are the primary barriers, the closure ring is the secondary barrier). Section 7.1 further describes that the MPC design, welding, testing and inspection requirements meet the guidance of ISG-18 [7.1.2] such that leakage from the confinement boundary may be considered non-credible. Section 7.2 addresses confinement for normal and off-normal conditions, and states “Since the MPC confinement vessel remains intact, and the design bases temperatures and pressure are not exceeded, leakage from the MPC confinement boundary is not credible”. Confinement for accident conditions is addressed in Section 7.3, which states “there is no mechanistic failure that results in a breach of, and associated leakage of radioactive material from the MPC confinement boundary”.

The assured integrity of the MPC Confinement Boundary eliminates the reliance on the fuel cladding to prevent release of radiological matter to the environment. Since the cladding is not considered as part of the confinement during normal, off-normal, or accident conditions, there is no need for providing an analysis for computing the allowable g-load for the fuel rods to demonstrate cladding integrity and none is included in this FSAR.

FIGURES 3.5.1 THROUGH 3.5.9

INTENTIONALLY DELETED

### 3.6 SUPPLEMENTAL DATA

#### 3.6.1 Additional Codes and Standards Referenced in HI-STORM 100 System Design and Fabrication

The following additional codes, standards and practices were used as aids in developing the design, manufacturing, quality control and testing methods for HI-STORM 100 System:

##### a. Design Codes

- (1) AISC Manual of Steel Construction, 1964 Edition and later.
- (2) ANSI N210-1976, "Design Requirements for Light Water Reactor Spent Fuel Storage Facilities at Nuclear Power Stations".
- (3) American Concrete Institute Building Code Requirements for Structural Concrete, ACI-318-95.
- (4) Code Requirements for Nuclear Safety Related Concrete Structures, ACI349-85/ACI349R-85, ACI349.1R-80, and ACI 349-97.
- (5) ASME NQA-1, Quality Assurance Program Requirements for Nuclear Facilities.
- (6) ASME NQA-2-1989, Quality Assurance Requirements for Nuclear Facility Applications.
- (7) ANSI Y14.5M, Dimensioning and Tolerancing for Engineering Drawings and Related Documentation Practices.
- (8) ACI Detailing Manual - 1980.
- (9) Crane Manufacturer's Association of America, Inc., CMAA Specification #70, Specifications for Electric Overhead Traveling Cranes, Revised 1988.

##### b. Material Codes - Standards of ASTM

- (1) E165 - Standard Methods for Liquid Penetrant Inspection.
- (2) A240 - Standard Specification for Heat-Resisting Chromium and Chromium-Nickel Stainless Steel Plate, Sheet and Strip for Fusion-Welded Unfired Pressure Vessels.

- (3) A262 - Detecting Susceptibility to Intergranular Attack in Austenitic Stainless Steel.
  - (4) A276 - Standard Specification for Stainless and Heat-Resisting Steel Bars and Shapes.
  - (5) A479 - Steel Bars for Boilers & Pressure Vessels.
  - (6) A564, Standard Specification for Hot-Rolled and Cold-Finished Age-Hardening Stainless and Heat-Resisting Steel Bars and Shapes.
  - (7) C750 - Standard Specification for Nuclear-Grade Boron Carbide Powder.
  - (8) A380 - Recommended Practice for Descaling, Cleaning and Marking Stainless Steel Parts and Equipment.
  - (9) C992 - Standard Specification for Boron-Based Neutron Absorbing Material Systems for Use in Nuclear Spent Fuel Storage Racks.
  - (10) E3, Preparation of Metallographic Specimens.
  - (11) E190, Guided Bend Test for Ductility of Welds.
  - (12) NCA3800 - Metallic Material Manufacturer's and Material Supplier's Quality System Program.
- c. Welding Codes: ASME Boiler and Pressure Vessel Code, Section IX - Welding and Brazing Qualifications, 1995 Edition.
- d. Quality Assurance, Cleanliness, Packaging, Shipping, Receiving, Storage, and Handling Requirements
- (1) ANSI 45.2.1 - Cleaning of Fluid Systems and Associated Components during Construction Phase of Nuclear Power Plants.
  - (2) ANSI N45.2.2 - Packaging, Shipping, Receiving, Storage and Handling of Items for Nuclear Power Plants (During the Construction Phase).
  - (3) ANSI - N45.2.6 - Qualifications of Inspection, Examination, and Testing Personnel for Nuclear Power Plants (Regulatory Guide 1.58).

- (4) ANSI-N45.2.8, Supplementary Quality Assurance Requirements for Installation, Inspection and Testing of Mechanical Equipment and Systems for the Construction Phase of Nuclear Power Plants.
- (5) ANSI - N45.2.11, Quality Assurance Requirements for the Design of Nuclear Power Plants.
- (6) ANSI-N45.2.12, Requirements for Auditing of Quality Assurance Programs for Nuclear Power Plants.
- (7) ANSI N45.2.13 - Quality Assurance Requirements for Control of Procurement of Equipment Materials and Services for Nuclear Power Plants (Regulatory Guide 1.123).
- (8) ANSI N45.2.15-18 - Hoisting, Rigging, and Transporting of Items for Nuclear Power Plants.
- (9) ANSI N45.2.23 - Qualification of Quality Assurance Program Audit Personnel for Nuclear Power Plants (Regulatory Guide 1.146).
- (10) ASME Boiler and Pressure Vessel, Section V, Nondestructive Examination, 1995 Edition.
- (11) ANSI - N16.9-75 Validation of Calculation Methods for Nuclear Criticality Safety.

e. Reference NRC Design Documents

- (1) NUREG-0800, Radiological Consequences of Fuel Handling Accidents.
- (2) NUREG-0612, "Control of Heavy Loads at Nuclear Power Plants", USNRC, Washington, D.C., July, 1980.
- (3) NUREG-1536, "Standard Review Plan for Dry Cask Storage Systems", USNRC, January 1997, Final Report.

f. Other ANSI Standards (not listed in the preceding)

- (1) 8.1 (N16.1) - Nuclear Criticality Safety in Operations with Fissionable Materials Outside Reactors.
- (2) 8.17, Criticality Safety Criteria for the Handling, Storage, and Transportation of LWR Fuel Outside Reactors.
- (3) N45.2 - Quality Assurance Program Requirements for Nuclear Facilities - 1971.

- (4) N45.2.9 - Requirements for Collection, Storage and Maintenance of Quality Assurance Records for Nuclear Power Plants - 1974.
- (5) N45.2.10 - Quality Assurance Terms and Definitions - 1973.
- (6) 57.2 (N210) - Design Requirements for Light Water Reactor Spent Fuel Storage Facilities at Nuclear Power Plants.
- (7) N14.6 (1993) - American National Standard for Special Lifting Devices for Shipping Containers Weighing 10,000 pounds (4500 kg) or more for Nuclear Materials.
- (8) N626-3, Qualification and Duties of Personnel Engaged in ASME Boiler and Pressure Vessel Code Section III, Div. 1, Certifying Activities.

g. Code of Federal Regulations

- (1) 10CFR20 - Standards for Protection Against Radiation.
- (2) 10CFR21 - Reporting of Defects and Non-compliance.
- (3) 10CFR50 - Appendix A - General Design Criteria for Nuclear Power Plants.
- (4) 10CFR50 - Appendix B - Quality Assurance Criteria for Nuclear Power Plants and Fuel Reprocessing Plants.
- (5) 10CFR61 - Licensing Requirements for Land Disposal of Radioactive Material.
- (6) 10CFR71 - Packaging and Transportation of Radioactive Material.

h. Regulatory Guides

- (1) RG 1.13 - Spent Fuel Storage Facility Design Basis (Revision 2 Proposed).
- (2) RG 1.25 - Assumptions Used for Evaluating the Potential Radiological Consequences of a Fuel Handling Accident in the Fuel Handling and Storage Facility of Boiling and Pressurized Water Reactors.
- (3) RG 1.28 - (ANSI N45.2) - Quality Assurance Program Requirements.
- (4) RG 1.29 - Seismic Design Classification (Rev. 3).
- (5) RG 1.31 - Control of Ferrite Content in Stainless Steel Weld Material.
- (6) RG 1.38 - (ANSI N45.2.2) Quality Assurance Requirements for Packaging, Shipping, Receiving, Storage and Handling of Items for Water-Cooled Nuclear

Power Plants.

- (7) RG 1.44 - Control of the Use of Sensitized Stainless Steel.
- (8) RG 1.58 - (ANSI N45.2.6) Qualification of Nuclear Power Plant Inspection, Examination, and Testing Personnel.
- (9) RG 1.61 - Damping Values for Seismic Design of Nuclear Power Plants, Rev. 0, 1973.
- (10) RG 1.64 - (ANSI N45.2.11) Quality Assurance Requirements for the Design of Nuclear Power Plants.
- (11) RG 1.71 - Welder Qualifications for Areas of Limited Accessibility.
- (12) RG 1.74 - (ANSI N45.2.10) Quality Assurance Terms and Definitions.
- (13) RG 1.85 - Materials Code Case Acceptability - ASME Section 3, Div. 1.
- (14) RG 1.88 - (ANSI N45.2.9) Collection, Storage and Maintenance of Nuclear Power Plant Quality Assurance Records.
- (15) RG 1.92 - Combining Modal Responses and Spatial Components in Seismic Response Analysis.
- (16) RG 1.122 - Development of Floor Design Response Spectra for Seismic Design of Floor-Supported Equipment or Components.
- (17) RG 1.123 - (ANSI N45.2.13) Quality Assurance Requirements for Control of Procurement of Items and Services for Nuclear Power Plants.
- (18) RG 1.124 - Service Limits and Loading Combinations for Class 1 Linear-Type Component Supports, Revision 1, 1978.
- (19) Reg. Guide 3.4 - Nuclear Criticality Safety in Operations with Fissionable Materials at Fuels and Materials Facilities.
- (20) RG 3.41 - Validation of Calculational Methods for Nuclear Criticality Safety, Revision 1, 1977.
- (21) Reg. Guide 8.8 - Information Relative to Ensuring that Occupational Radiation Exposure at Nuclear Power Plants will be as Low as Reasonably Achievable (ALARA).
- (22) DG-8006, "Control of Access to High and Very High Radiation Areas in Nuclear

---

HOLTEC INTERNATIONAL COPYRIGHTED MATERIAL

Power Plants".

i. Branch Technical Position

- (1) CPB 9.1-1 - Criticality in Fuel Storage Facilities.
- (2) ASB 9-2 - Residual Decay Energy for Light-Water Reactors for Long-Term Cooling.

j. Standard Review Plan (NUREG-0800)

- (1) SRP 3.2.1 - Seismic Classification.
- (2) SRP 3.2.2 - System Quality Group Classification.
- (3) SRP 3.7.1 - Seismic Design Parameters.
- (4) SRP 3.7.2 - Seismic System Analysis.
- (5) SRP 3.7.3 - Seismic Subsystem Analysis.
- (6) SRP 3.8.4 - Other Seismic Category I Structures (including Appendix D), Technical Position on Spent Fuel Rack.
- (7) SRP 3.8.5 - Foundations
- (8) SRP 9.1.2 - Spent Fuel Storage, Revision 3, 1981.
- (9) SRP 9.1.3 - Spent Fuel Pool Cooling and Cleanup System.
- (10) SRP 9.1.4 - Light Load Handling System.
- (11) SRP 9.1.5 - Overhead Heavy Load Handling System.
- (12) SRP 15.7.4 - Radiological Consequences of Fuel Handling Accidents.

k. AWS Standards

- (1) D1.1 - Structural Welding Code, Steel.
- (2) A2.4 - Standard Symbols for Welding, Brazing and Nondestructive Examination.
- (3) A3.0 - Standard Welding Terms and Definitions.
- (4) A5.12 - Tungsten Arc-welding Electrodes.



- (5) QC1 - Standards and Guide for Qualification and Certification of Welding Inspectors.

1. Others

- (1) ASNT-TC-1A - Recommended Practice for Nondestructive Personnel Qualification and Certification.
- (2) SSPC SP-2 - Surface Preparation Specification No. 2 Hand Tool Cleaning.
- (3) SSPC SP-3 - Surface Preparation Specification No. 3 Power Tool Cleaning.
- (4) SSPC SP-10 - Near-White Blast Cleaning.

3.6.2 Computer Programs

Three computer programs, all with a well established history of usage in the nuclear industry, have been utilized to perform structural and mechanical analyses documented in this report. These codes are ANSYS, DYNA3D, and WORKING MODEL. ANSYS is a public domain code which utilizes the finite element method for structural analyses.

WORKING MODEL, Version V.3.0/V.4.0

This code is used in this 10CFR72 submittal to compute the dynamic load resulting from intermediate missile impact on the overpack closure and to evaluate the maximum elastic spring rate associated with the target during a HI-TRAC handling accident event.

WORKING MODEL has been previously utilized in similar dynamic analyses of the HI-STAR 100 system (Docket No. 72-1008).

"WORKING MODEL" (V3.0/V4.0) is a Computer Aided Engineering (CAE) tool with an integrated user interface that merges modeling, simulation, viewing, and measuring. The program includes a dynamics algorithm that provides automatic collision and contact handling, including detection, response, restitution, and friction.

Numerical integration is performed using the Kutta-Merson integrator which offers options for variable or fixed time-step and error bounding.

The Working Model Code is commercially available. Holtec has performed independent QA validation of the code (in accordance with Holtec's QA requirements) by comparing the solution of several classical dynamics problems with the numerical results predicted by Working Model. Agreement in all cases is excellent.

Additional theoretical material is available in the manual: "Users Manual, Working Model, Version 3", Knowledge Revolution, 66 Bovet Road, Suite 200, San Mateo, CA, 94402.

---

HOLTEC INTERNATIONAL COPYRIGHTED MATERIAL

This code has been acquired by MSC Software and has now been designated "VisualNastran Desktop". The most current version, which has been used in this revision, is VN 2003. The descriptions given above are still valid.

### DYNA3D

"DYNA3D" is a nonlinear, explicit, three-dimensional finite element code for solid and structural mechanics. It was originally developed at Lawrence Livermore Laboratories and is ideally suited for study of short-time duration, highly nonlinear impact problems in solid mechanics. DYNA3D is commercially available for both UNIX work stations and Pentium class PCs running Windows 95 or Windows NT. The PC version has been fully validated at Holtec following Holtec's QA procedures for commercial computer codes. This code is used to analyze the drop accidents and the tip-over scenario for the HI-STORM 100. Benchmarking of DYNA3D for these storage analyses is discussed and documented in Appendix 3.A. DYNA3D is also known as LS-DYNA and is currently supported and distributed by Livermore Software. Each update is independently subject to QA validation.

#### 3.6.3 Appendices Included in Chapter 3

##### 3.A HI-STORM Deceleration Under Postulated Vertical Drop Event and Tipover

#### 3.6.4 Calculation Packages

In addition to the calculations presented in Chapter 3, supporting calculation packages have been prepared to document other information pertinent to the analyses. As new components are added (e.g., the HI-STORM 100S versions and additional MPC's), supporting calculation packages back up the summary results reported herein.

The calculation packages contain additional details on component weights, supporting calculations for some results summarized in the chapter, and miscellaneous supporting data that supplements the results summarized in Chapter 3 of the FSAR. All of the finite element tabular data, node and element data, supporting figures, and numerical output for all fuel baskets are contained in the calculation package supplement supporting Revision 1 of the FSAR.

### 3.7 COMPLIANCE WITH NUREG-1536

Supporting information to provide reasonable assurance with respect to the adequacy of the HI-STORM 100 System to store spent nuclear fuel in accordance with the stipulations of the Technical Specifications (Chapter 12) is provided throughout this FSAR. An itemized table (Table 3.0.1 at the beginning of this chapter) has been provided to locate and collate the substantiating material to support the technical evaluation findings listed in NUREG-1536 Chapter 3, Article VI.

The following statements are germane to an affirmative safety evaluation:

- The design and structural analysis of the HI-STORM 100 System is in full compliance with the provisions of Chapter 3 of NUREG-1536 except as listed in the Table 1.0.3 (list of code compliance exceptions).
- The list of Regulatory Guides, Codes, and standards presented in Section 3.6 herein is in full compliance with the provisions of NUREG-1536.
- All HI-STORM 100 structures, systems, and components (SSC) that are important to safety (ITS) are identified in Table 2.2.6. Section 1.5 contains the design drawings that describe the HI-STORM 100 SSCs in complete detail. Explanatory narrations in Subsections 3.4.3 and 3.4.4 provide sufficient textual details to allow an independent evaluation of their structural effectiveness.
- The requirements of 10CFR72.24 with regard to information pertinent to structural evaluation is provided in Chapters 2, 3, and 11.
- Technical Specifications pertaining to the structures of the HI-STORM 100 System have been provided in Section 12.3 herein pursuant to the requirements of 10CFR72.26.
- A series of analyses to demonstrate compliance with the requirements of 10CFR72.122(b) and (c), and 10CFR72.24(c)(3) have been performed which show that SSCs designated as ITS possess an adequate margin of safety with respect to all load combinations applicable to normal, off-normal, accident, and natural phenomenon events. In particular, the following information is provided:
  - i. Load combinations for the fuel basket, enclosure vessel, and the HI-STORM 100/HI-TRAC overpacks for normal, off-normal, accident, and natural phenomenon events are compiled in Tables 2.2.14, 3.1.1, and 3.1.3 through 3.1.5, respectively.
  - ii. Stress limits applicable to the materials are found in Subsection 3.3.

- iii. Stresses at various locations in the fuel basket, the enclosure vessel, and the HI-STORM 100/HI-TRAC overpacks have been computed by analysis.

Descriptions of stress analyses are presented in Sections 3.4.3 and 3.4.4.

- iv. Factors of safety in the components of the HI-STORM 100 System are reported as below:

a.	Fuel basket	Tables 3.4.3 and 3.4.6
b.	Enclosure vessel	Tables 3.4.4, 3.4.6, 3.4.7, and 3.4.8
c.	HI-STORM 100 overpack/ HI-TRAC	Table 3.4.5
d.	Miscellaneous components	Table 3.4.9
e.	Lifting devices	Subsection 3.4.3

- The structural design and fabrication details of the fuel baskets whose safety function in the HI-STORM 100 System is to maintain nuclear criticality safety, have been carried out to comply with the provisions of Subsection NG of the ASME Code (loc. cit.) Section III. The structural factors of safety, summarized in Tables 3.4.3 and 3.4.6 for all credible load combinations under normal, off-normal, accident, and natural phenomenon events demonstrate that the Code limits are satisfied in all cases. As the stress analyses have been performed using linear elastic methods and the computed stresses are well within the respective ASME Code limits, it follows that the physical geometry of the fuel basket will not be altered under any load combination to create a condition adverse to criticality safety. This conclusion satisfies the requirement of 10CFR72.124(a), with respect to structural margins of safety for SSCs important to nuclear criticality safety.
- Structural margins of safety during handling, packaging, and transfer operations, mandated by the provisions of 10CFR Part 72.236(b), require that the lifting and handling devices are engineered to comply with the stipulations of ANSI N14.6, NUREG-0612, Regulatory Guide 3.61, and NUREG-1536, and that the components being handled meet the applicable ASME Code service condition stress limits. The requirements of the governing codes for handling operations are summarized in Subsection 3.4.3 herein. A summary table of factors of safety for all ITS components under lifting and handling operations, presented in Subsection

3.4.3, shows that adequate structural margins exist in all cases.

- Consistent with the requirements of 10CFR72.236(i), the confinement boundary for the HI-STORM 100 System has been engineered to maintain confinement of radioactive materials under normal, off-normal, and postulated accident conditions. This assertion of confinement integrity is made on the strength of the following information provided in this FSAR.
  - i. The MPC Enclosure Vessel which constitutes the confinement boundary is designed and fabricated in accordance with Section III, Subsection NB (Class 1 nuclear components) of the ASME Code to the maximum extent practicable.
  - ii. The MPC lid of the MPC Enclosure Vessel is welded using a strength groove weld and is subjected to volumetric examination or multiple liquid penetrant examinations, pressure testing, and liquid penetrant (root and final) testing to establish a maximum confidence in weld joint integrity.
  - iii. The closure of the MPC Enclosure Vessel consists of *two* independent isolation barriers.
  - iv. The confinement boundary is constructed from stainless steel alloys with a proven history of material integrity under environmental conditions.
  - v. The load combinations for normal, off-normal, accident, and natural phenomena events have been compiled (Table 2.2.14) and applied on the MPC Enclosure Vessel (confinement boundary). The results, summarized in Tables 3.4.4 through 3.4.9, show that the factor of safety (with respect to the appropriate ASME Code limits) is greater than one in all cases. Design Basis natural phenomena events such as tornado-borne missiles (large, intermediate, or small) have also been analyzed to evaluate their potential for breaching the confinement boundary. Analyses presented in Subsection 3.4.8, and summarized in unnumbered tables in Subsection 3.4.8, show that the integrity of the confinement boundary is preserved under all design basis projectile impact scenarios.
- The information on structural design included in this FSAR complies with the requirements of 10CFR72.120 and 10CFR72.122, and can be ascertained from the information contained in Table 3.7.1.
- The provisions of features in the HI-STORM 100 structural design, listed in Table 3.7.2, demonstrate compliance with the specific requirements of 10CFR72.236(e), (f), (g), (h), (i), (j), (k), and (m).

Table 3.7.1

## NUREG –1536 COMPLIANCE MATRIX FOR 10CFR72.120 AND 10CFR72.122 REQUIREMENTS

Item	Compliance	Location of Supporting Information in This Document
i. Design and fabrication to acceptable quality standards	<p>All ITS components designed and fabricated to recognized Codes and Standards:</p> <ul style="list-style-type: none"> <li>Basket: Subsection NG, Section III</li> <li>Enclosure Vessel: Subsection NB, loc. cit.</li> <li>HI-STORM 100 Structure: Subsection NF, loc. cit.</li> <li>HI-TRAC Structure: Subsection NF, loc. cit.</li> </ul>	<p>Subsections 2.0.1 and 3.1.1 Tables 2.2.6 and 2.2.7</p> <p>Subsections 2.0.1 and 3.1.1 Tables 2.2.6 and 2.2.7</p> <p>Subsections 2.0.2 and 3.1.1</p> <p>Subsections 2.0.3 and 3.1.1</p>
ii. Erection to acceptable quality standards	<ul style="list-style-type: none"> <li>Concrete in HI-STORM 100 meets requirements of : ACI –349(85)</li> </ul>	<p>Appendix 1.D Subsection 3.3.2</p>
iii. Testing to acceptable quality standards	<ul style="list-style-type: none"> <li>All non-destructive examination of ASME Code components for provisions in the Code (see exceptions in Table 2.2.15).</li> <li>Pressure test of pressure vessel per the Code.</li> <li>Testing for radiation containment per provisions of NUREG-1536</li> <li>Concrete testing in accordance with ACI-349(85)</li> </ul>	<p>Section 9.1</p> <p>Section 9.1</p> <p>Sections 7.1 and 9.1</p> <p>Appendix 1.D</p>

HOLTEC INTERNATIONAL COPYRIGHTED MATERIAL

Table 3.7.1

## NUREG –1536 COMPLIANCE MATRIX FOR 10CFR72.120 AND 10CFR72.122 REQUIREMENTS

Item	Compliance	Location of Supporting Information in This Document
iv. Adequate structural protection against environmental conditions and natural phenomena.	Analyses presented in Chapter 3 demonstrate that the confinement boundary will preserve its integrity under all postulated off-normal and natural phenomena events listed in Chapters 2.	Section 2.2 Chapter 11
v. Adequate protection against fires and explosions	<ul style="list-style-type: none"> <li>The extent of combustible (exothermic) material in the vicinity of the cask system is procedurally controlled (the sole source of hydrocarbon energy is diesel in the tow vehicle).</li> <li>Analyses show that the heat energy released from the postulated fire accident condition surrounding the cask will not result in impairment of the confinement boundary and will not lead to structural failure of the overpack. The effect on shielding will be localized to the external surfaces directly exposed to the fire which will result in a loss of the water in the water jacket for the HI-TRAC, and no significant change in the HI-STORM 100 overpack.</li> <li>Explosion effects are shown to be bounded by the Code external pressure design basis and there is no adverse effect on ready retrievability of the MPC.</li> </ul>	Subsections 12.3.20 and 12.3.21  Subsection 11.2.4  Subsection 11.2.11 and Subsection 3.1.2.1.1.4; 3.4.7
vi. Appropriate inspection, maintenance, and testing	Inspection, maintenance, and testing requirements set forth in this FSAR are in full compliance with the governing regulations and established industry practice.	Sections 9.1 and 9.2 Chapter 12
vii. Adequate accessibility in emergencies.	<p>The HI-STORM 100 overpack lid can be removed to gain access to the multi-purpose canister.</p> <p>The HI-TRAC transfer cask has removable bottom and top lids.</p>	Chapter 8  Chapter 8

HOLTEC INTERNATIONAL COPYRIGHTED MATERIAL

Table 3.7.1

## NUREG –1536 COMPLIANCE MATRIX FOR 10CFR72.120 AND 10CFR72.122 REQUIREMENTS

Item	Compliance	Location of Supporting Information in This Document
viii. A confinement barrier that acceptably protects the spent fuel cladding during storage.	<p>The peak temperature of the fuel cladding at design basis heat duty of each MPC has been demonstrated to be maintained below the limits specified in ISG-11 [4.1.4].</p> <p>The confinement barriers consist of highly ductile stainless steel alloys. The multi-purpose canister is housed in the overpack, built from a steel structure whose materials are selected and examined to maintain protection against brittle fracture under off-normal ambient (cold) temperatures (minimum of -40°F).</p>	<p>Section 4.4</p> <p>Subsection 3.1.1 Subsection 3.1.2.3</p>
ix. The structures are compatible with the appropriate monitoring systems.	The HI-STORM 100 overpack is a thick, upright cylindrical structure with large ventilation openings near the top and bottom. These openings are designed to prevent radiation streaming while enabling complete access to temperature monitoring probes.	Section 1.5, Subsection 2.3.3.2
x. Structural designs that are compatible with ready retrievability of fuel.	<p>The fuel basket is designed to be an extremely stiff honeycomb structure such that the storage cavity dimensions will remain unchanged under all postulated normal and accident events. Therefore, the retrievability of the spent nuclear fuel from the basket will not be jeopardized.</p> <p>The MPC canister lid is attached to the shell with a groove weld which is made using an automated welding device. A similar device is available to remove the weld. Thus, access to the fuel basket can be realized.</p> <p>The storage overpack and the transfer casks are designed to withstand accident loads without suffering permanent deformations of their structures that would prevent retrievability of the MPC by normal means. It is demonstrated by analysis that there is no physical interference between the MPC and the enveloping HI-STORM storage overpack or HI-TRAC transfer cask.</p>	<p>Subsection 3.1.1</p> <p>Sections 8.1 and 8.3</p> <p>Section 3.4</p>



Table 3.7.2

## COMPLIANCE OF HI-STORM 100 SYSTEM WITH 10CFR72.236(e), ET ALS.

Item	Compliance	Location of Supporting Information in This Document
i. Redundant sealing of confinement systems.	Two physically independent lids, each separately welded to the MPC shell (Enclosure Vessel shell) provide a redundant confinement system.	Section 1.5, Drawings Section 7.1.
ii. Adequate heat removal without active cooling systems.	Thermal analyses presented in Chapter 4 show that the HI-STORM 100 System will remove the decay heat generated from the stored spent fuel by strictly passive means and maintain the system temperature within prescribed limits.	Sections 4.4 and Sections 9.1 and 9.2
iii. Storage of spent fuel for a minimum of 20 years.	The service life of the MPC, storage overpack, and HI-TRAC are engineered to be in excess of 20 years.	Subsections 3.4.11 and 3.4.12
iv. Compatibility with wet or dry spent fuel loading and unloading facilities.	<ul style="list-style-type: none"> <li>The system is designed to eliminate any material significant interactions in the wet (spent fuel pool) environment.</li> <li>The HI-TRAC transfer cask is engineered for full compatibility with the MPCs, and standard loading and unloading facilities.</li> <li>The HI-TRAC System is engineered for MPC transfer on the ISFSI pad with full consideration of ALARA and handling equipment compatibility.</li> </ul>	Subsection 3.4.1  Subsection 8.1.1  Subsection 8.1.1
v. Ease of decontamination.	<ul style="list-style-type: none"> <li>The external surface of the multi-purpose canister is protected from contamination during fuel loading through a custom designed sealing device.</li> <li>The HI-STORM storage overpack is not exposed to contamination</li> <li>All exposed surfaces of the HI-TRAC transfer cask are coated to aid in decontamination</li> </ul>	Figures 8.1.13 and 8.1.14  Chapter 8  Section 1.5, Drawings

Table 3.7.2

## COMPLIANCE OF HI-STORM 100 SYSTEM WITH 10CFR72.236(e), ET ALS.

Item	Compliance	Location of Supporting Information in This Document
vi. Inspection of defects that might reduce confinement effectiveness.	<ul style="list-style-type: none"> <li>The MPC enclosure vessel is designed and fabricated in accordance with ASME Code, Section III, Subsection NB, to the maximum extent practical.</li> <li>Pressure testing and NDE of the closure welds verify containment effectiveness.</li> </ul>	Section 9.1
vii. Conspicuous and durable marking.	<p>The stainless steel lid of each MPC will have model number and serial number engraved for ready identification.</p> <p>The exterior envelope of the cask (the storage overpack) is marked in a conspicuous manner as required by 10CFR 72.236(k).</p>	N/A
viii. Compatibility with removal of the stored fuel from the site, transportation, and ultimate disposal by the U.S. Department of Energy.	The MPC is designed to be in full compliance with the DOE's draft specification for transportability and disposal published under the now dormant "MPC" program.	Section 2.4 Subsection 1.2.1.1

REFERENCES

- [3.1.1] NUREG-0612, "Control of Heavy Loads at Nuclear Power Plants," United States Nuclear Regulatory Commission.
- [3.1.2] ANSI N14.6-1993, "American National Standard for Special Lifting Devices for Shipping Containers Weighing 10000 Pounds (4500 kg) or More for Nuclear Materials," American National Standards Institute, Inc.
- [3.1.3] D. Burgreen, "Design Methods for Power Plant Structures", Arcturus Publishers, 1975.
- [3.1.4] Deleted.
- [3.1.5] NUREG/CR-1815, "Recommendations for Protecting Against Failure by Brittle Fracture in Ferritic Steel Shipping Containers Up to Four Inches Thick"
- [3.1.6] Aerospace Structural Metals Handbook, Manson.
- [3.3.1] ASME Boiler & Pressure Vessel Code, Section II, Part D, 1995.
- [3.3.2] American Concrete Institute, "Building Code Requirements for Structural Plain Concrete (ACI 318.1-89) (Revised 1992) and Commentary - ACI 318.1R-89 (Revised 1992)".
- [3.3.3] American Concrete Institute, "Code Requirements for Nuclear Safety Related Structures" (ACI-349-85) and Commentary (ACI-349R-85)(For anchored casks, the requirements on the design of the steel embedment are ACI-349-97, including Appendix B and the Commentary (ACI-349R-97)).
- [3.3.5] J.H. Evans, "Structural Analysis of Shipping Casks, Volume 8, Experimental Study of Stress-Strain Properties of Lead Under Specified Impact Conditions", ORNL/TM-1312, Vol. 8, ORNL, Oak Ridge, TN, August, 1970.
- [3.4.1] ANSYS 5.3, ANSYS, Inc., 1996 (Current usage of ANSYS includes Versions up thru 7.0, 2003).
- [3.4.2] ASME Boiler & Pressure Vessel Code, Section III, Subsection NF, 1995.
- [3.4.3] ASME Boiler & Pressure Vessel Code, Section III, Appendices, 1995.
- [3.4.4] ASME Boiler & Pressure Vessel Code, Section III, Subsection NB, 1995.
- [3.4.5] "Evaluation of Bounding Explosion Pressure Limits for HI-STORM 100", Holtec Report HI-2063635, Revision 0.

- [3.4.6] Deleted.
- [3.4.7] NRC Bulletin 96-04: Chemical, Galvanic or Other Reactions in Spent Fuel Storage and Transportation Casks, July 5, 1996.
- [3.4.8] Theory of Elastic Stability, S.P. Timoshenko and J. Gere, McGraw Hill, 2nd Edition.
- [3.4.9] Marks Standard Handbook for Mechanical Engineering, 9th Edition.
- [3.4.10] ASME Boiler and Pressure Vessel Code, Section III, Subsection NG, 1995.
- [3.4.11] 10CFR71, Waste Confidence Decision Review, USNRC, September 11, 1990.
- [3.4.12] "Benchmarking of the Holtec LS-DYNA3D Model for Cask Drop Events", Holtec Report HI-971779, September 1997.
- [3.4.13] NUREG/CR-6322, Buckling Analysis of Spent Fuel Basket, Lawrence Livermore National Laboratory, May, 1995.
- [3.4.14] Soler, A, "Calculation Package for High Seismic Support of HI-STORM 100A", Holtec Report HI-2002465, August 2000.
- [3.5.1] Chun, Witte, Schwartz, "Dynamic Impact Effects on Spent Fuel Assemblies." UCID-21246, Lawrence Livermore National Laboratory, October 20, 1987.
- [3.5.2] NUREG-1864, "A Pilot Probabilistic Risk Assessment of a Dry Cask Storage System at a Nuclear Power Plant," USNRC, March 2007

## APPENDIX 3.A: HI-STORM DECELERATION UNDER POSTULATED VERTICAL DROP EVENT AND TIPOVER

### 3.A.1 INTRODUCTION

Handling accidents with a HI-STORM overpack containing a loaded MPC are credible events (Section 2.2.3). The stress analyses carried out in Chapter 3 of this safety analysis report assume that the inertial loading on the load bearing members of the MPC, fuel basket, and the overpack due to a handling accident are limited by the Table 3.1.2 decelerations. The maximum deceleration experienced by a structural component is the product of the rigid body deceleration sustained by the structure and the dynamic load factor (DLF) applicable to that structural component. The DLF is a function of the contact impulse and the structural characteristics of the component.

The rigid body deceleration is a strong function of the load-deformation characteristics of the impact interface, weight of the cask, and the drop height or angle of free rotation. For the HI-STORM 100 System, the weight of the structure and its surface compliance characteristics are known. However, the contact stiffness of the ISFSI pad (and other surfaces over which the HI-STORM 100 may be carried during its movement to the ISFSI) is site-dependent. The contact resistance of the collision interface, which is composed of the HI-STORM 100 and the impacted surface compliance, therefore, is not known a priori for a specific site. Analyses for the rigid body decelerations are, therefore, presented here using a reference ISFSI pad (which is the pad used in a recent Lawrence Livermore National Laboratory report and is the same reference pad used in the HI-STAR 100 FSAR). The finite element model (grid size, extent of model, soil properties, etc.) follows the LLNL report.

An in-depth investigation by the Lawrence Livermore Laboratory (LLNL) into the mechanics of impact between a cask-like impactor on a reinforced concrete slab founded on a soil-like subgrade has identified three key parameters, namely, the thickness of the concrete slab,  $t_p$ , compressive strength of the concrete  $f_c'$  and equivalent Young's Modulus of the subgrade  $E$ . These three parameters are key variables in establishing the stiffness of the pad under impact scenarios. The LLNL reference pad parameters, which we hereafter denote as Set A, provide one set of values of  $t_p$ ,  $f_c'$ , and  $E$  that are found to satisfy the deceleration criteria applicable to the HI-STORM 100 cask. Another set of parameters, referred to as Set B herein, is also shown to satisfy the g-load limit requirements. In fact, an infinite number of combinations of  $t_p$ ,  $f_c'$ , and  $E$  can be compiled that would meet the g-load limit qualification. However, in addition to satisfying the g-limit criterion, the pad must be demonstrated to possess sufficient flexural and shear stiffness to meet the ACI 318-95 strength limits under factored load combinations. The minimum strength requirement to comply with ACI 318-95 provisions places a restriction on the lower bound values of  $t_p$ ,  $f_c'$ , and  $E$  that must be met in an ISFSI pad design.

Our focus in this appendix, however, is to quantify the peak decelerations that would be experienced by a loaded HI-STORM 100 cask under the postulated impact scenarios for the two pad designs defined by parameter Sets A and B, respectively. The information presented in this appendix also serves to further authenticate the veracity of the Holtec DYNA3D model described in the 1997 benchmark report [3.A.4.]

### 3.A.2 Purpose

The purpose of this appendix is to demonstrate that the rigid body deceleration experienced by the HI-STORM 100 System during a handling accident or non-mechanistic tip-over are below the design basis deceleration of 45g's (Table 3.1.2). Two accidental drop scenarios of a loaded HI-STORM 100 cask on the ISFSI pad are considered in this appendix. They are:

- i. Tipover: A loaded HI-STORM 100 is assumed to undergo a non-mechanistic tipover event and impacting the ISFSI pad with an incipient impact angular velocity, which is readily calculated from elementary dynamics.
- ii. End drop: The loaded HI-STORM 100 is assumed to drop from a specified height  $h$ , with its longitudinal axis in the vertical orientation, such that its bottom plate impacts the ISFSI pad.

The dynamic load factors are a function of the predominant natural frequency of vibration of the component for a given input load pulse shape. Dynamic load factors are applied, as necessary, to the results of specific component analyses performed using the loading from the design basis rigid body decelerations. Therefore, for the purposes of this appendix, it is desired to demonstrate that the rigid body deceleration experienced in each of the drop scenarios is below the HI-STORM 100 45g design basis.

### 3.A.3 Background and Methodology

In 1997 Lawrence Livermore National Laboratory (LLNL) published the experimentally obtained results of the so-called fourth series billet tests [3.A.1] together with a companion report [3.A.2] documenting a numerical solution that simulated the drop test results with reasonable accuracy. Subsequently, USNRC personnel published a paper [3.A.3] affirming the NRC's endorsement of the LLNL methodology. The LLNL simulation used modeling and simulation algorithms contained within the commercial computer code DYNA3D [3.A.6].

The LLNL cask drop model is not completely set forth in the above-mentioned LLNL reports. Using the essential information provided by the LLNL [3.A.2] report, however, Holtec is able to develop a finite element model for implementation on LS-DYNA3D [3.A.5] which is fully consistent with LLNL's (including the use of the Butterworth filter for discerning rigid body deceleration from "noisy" impact data). The details of the LS-DYNA3D dynamic model, henceforth referred to as the Holtec model, are contained in the proprietary benchmark report [3.A.4] wherein it is shown that the peak deceleration in every case of billet drop analyzed by LLNL is replicated within a small tolerance by the Holtec model. The case of the so-called "generic" cask, for which LLNL provided predicted response under side drop and tipover events, is also bounded by the Holtec model. In

summary, the benchmarking effort documented in [3.A.4] is in full compliance with the guidance of the Commission [3.A.3].

Having developed and benchmarked an LLNL-consistent cask impact model, a very similar model is developed and used to prognosticate the HI-STORM drop scenarios. The reference elasto-plastic-damage characteristics of the target concrete continuum used by LLNL, and used in the HI-STAR 100 FSAR are replicated herein. The HI-STORM 100 target model is identical in all aspects to the reference pad approved for the HI-STAR 100 FSAR.

In the tipover scenario the cask surface structure must be sufficiently pliable to cushion the impact and limit the rigid body deceleration. The angular velocity at the contact time is readily calculated using planar rigid body dynamics and is used as an initial condition in the LS-DYNA3D simulation.

The end drop event produces a circular impact patch equal to the diameter of the overpack baseplate. The elasto-plastic-damage characteristics of the concrete target and the drop height determine the maximum deceleration. A maximum allowable height "h" is determined to limit the deceleration to a value below the design basis.

A description of the work effort and a summary of the results are presented in the following sections. In all cases, the reported decelerations are below the design basis of 45g's at the top of the MPC fuel basket.

### 3.A.4            Assumptions and Input Data

#### 3.A.4.1        Assumptions

The assumptions used to create the model are completely described in Reference [3.A.4] and are shown there to be consistent with the LLNL simulation. There are key aspects, however, that are restated here:

The maximum deceleration experienced by the cask during a collision event is a direct function of the structural rigidity (or conversely, compliance) of the impact surface. The compliance of the ISFSI pad is quite obviously dependent on the thickness of the pad,  $t_p$ , the compressive strength of the concrete,  $f_c'$  and stiffness of the sub-grade (expressed by its effective Young's modulus,  $E$ ). The structural rigidity of the ISFSI pad will increase if any of the three above-mentioned parameters ( $t_p$ ,  $f_c'$  or  $E$ ) is increased. For the reference pad, the governing parameters (i.e.,  $t_p$ ,  $f_c'$  and  $E$ ) are assumed to be identical to the pad defined by LLNL [3.A.2], which is also the same as the pad utilized in the benchmark report [3.A.4]. We refer to the LLNL ISFSI pad parameters as Set A. (Table 3.A.1).

As can be seen from Table 3.A.1, the nominal compressive strength  $f_c'$  in Set A is limited to 4200 psi. However, experience has shown that ISFSI owners have considerable practical difficulty in limiting the 28 day strength of poured concrete to 4200 psi, chiefly because a principal element of progress in reinforced concrete materials technology has been in realizing ever increasing concrete nominal strength. Inasmuch as a key objective of the ISFSI pad is to limit its structural rigidity (and

not  $f_c'$  per se), and limiting  $f_c'$  to 4200 psi may be problematic in certain cases, an alternative set of reference pad parameters is defined (Set B in Table 3.A.1), which permits a higher value of  $f_c'$  but much smaller values of pad thickness,  $t_p$  and sub-grade Young's modulus, E.

The ISFSI owner has the option of constructing the pad to comply with the limits of Set A or Set B without performing site-specific cask impact analyses. It is recognized that, for a specific ISFSI site, the reinforced concrete, as well as the underlying engineered fill properties, may be different at different locations on the pad or may be uniform, but non-compliant with either Set A or Set B. In that case, the site-specific conditions must be performed to demonstrate compliance with the design limits of the HI-STORM system (e.g., maximum rigid body g-load less than 45 g's). The essential data which define the pad (Set A and Set B) used to qualify the HI-STORM 100 are provided in Table 3.A.1.

The HI-STORM 100 steel structural elements (outer shell, inner shell, radial plates, lid, etc.), are fabricated from SA-516 Grade 70. The steel is described as a bi-linear elastic-plastic material with limited strain failure by five material parameters (E,  $S_y$ ,  $S_u$ ,  $\epsilon_u$ , and  $\nu$ ). The numerical values used in the finite element model are shown in Table 3.A.2. The concrete located inside of the overpack for this dynamic analysis is defined to be identical with the concrete pad. This is conservative since the concrete assumed in the reference pad is reinforced. Therefore, the strength of the concrete inside the HI-STORM 100 absorbs less energy if it is also assumed to be reinforced.

#### 3.A.4.2 Input Data

Table 3.A.1 characterizes the properties of the full-scale reference target pad used in the analysis of the full size HI-STORM 100 System. The principal strength parameters that define the stiffness of the pad, namely,  $t_p$ , E and  $f_c'$  are input in the manner described in [3.A.2] and [3.A.4].

Table 3.A.2 contains the material description parameters for the steel types; SA-516-70 used in the numerical investigation.

Table 3.A.3 details the geometry of the HI-STORM 100 used in the drop simulations. This data is taken from applicable HI-STORM 100 drawings.

#### 3.A.5 Finite Element Model

The finite-element model of the Holtec HI-STORM 100 overpack (baseplate, shells, radial plates, lid, concrete, etc.), concrete pad and a portion of the subgrade soil is constructed using the pre-processor integrated with the LS-DYNA3D software [3.A.5]. The deformation field for all postulated drop events (the end-drop and the tipover) exhibits symmetry with the vertical plane passing through the cask diameter and the concrete pad length. Using this symmetry condition of the deformation field only a half finite-element model is constructed. The finite-element model is organized into nineteen independent parts (the baseplate components, the outer shell, the inner shell, the radial plates, the channels, the lid components, the basket steel plates, the basket fuel zone, the concrete pad and the soil). The final model contains 30351 nodes, 24288 solid type finite-elements, 1531 shell type finite-elements, seven (7) materials, ten (10) properties and twenty-four (24)



interfaces. The finite-element model used for the tipover-drop event is depicted in Figures 3.A.1 through 3.A.4. Figures 3.A.5 through 3.A.8 show the end-drop finite-element model.

The soil grid, shown in Figure 3.A.9, is a rectangular prism (800 inches long, 375 inches wide and 470 inches deep), is constructed from 13294 solid type finite-elements. The material defining this part is an elastic isotropic material. The central portion of the soil (400 inches long, 150 inches wide and 170 inches deep) where the stress concentration is expected to appear is discretized with a finer mesh.

The concrete pad is 320 inches long, 100 inches wide and is 36 inches thick. This part contains 8208 solid finite-elements. A uniform sized finite-element mesh, shown in Figure 3.A.10, is used to model the concrete pad. The concrete behavior is described using a special constitutive law and yielding surface (MAT\_PSEUDO\_TENSOR) contained within LS-DYNA3D. The geometry, the material properties, and the material behavior are identical to the LLNL reference pad (Material 16 IIB).

The half portion of the steel cylindrical overpack contains 1531 shell finite-elements. The steel material description (SA-516-70) is realized using a bi-linear elasto-plastic constitutive model (MAT\_PIECEWISE\_LINEAR\_PLASTICITY). Figure 3.A.11 depicts details of the steel components of the cask finite-element mesh, with the exception of the inner shell, channels and lid components, which are shown in Figures 3.A.12 and 3.A.13. The concrete filled between the inner and the outer shells, and contained in the baseplate and lid components is modeled using 1664 solid finite-elements and is depicted in Figure 3.A.14. The concrete material is defined identical to the pad concrete.

The MPC and the contained fuel are modeled in two parts that represent the lid and baseplate, and the fuel area. An elastic material is used for both parts. The finite-element mesh pertinent to the MPC contains 1122 solid finite-elements and is shown in Figure 3.A.15. The mass density is appropriate to match a representative weight of 356,521 lb. that is approximately mid-way between the upper and lower weight estimates for a loaded HI-STORM 100.

The total weight used in the analysis is approximately 2,000 lb. lighter than the HI-STORM 100 containing the lightest weight MPC.

Analysis of a single mass impacting a spring with a given initial velocity shows that both the maximum deceleration " $a_M$ " of the mass and the time duration of contact with the spring " $t_c$ " are related to the dropped weight " $w$ " and drop height " $h$ " as follows:

$$a_M \sim \frac{\sqrt{h}}{\sqrt{w}}; t_c \sim \sqrt{w}$$

Therefore, the most conservatism is introduced into the results by using the minimum weight. It is emphasized that the finite element model described in the foregoing is identical in its approach to the "Holtec model" described in the benchmark report [3.A.4]. Gaps between the MPC and the overpack are included in the model.

### 3.A.6 Impact Velocity

#### a. Linear Velocity: Vertical Drops

For the vertical drop event, the impact velocity,  $v$ , is readily calculated from the Newtonian formula:

$$v = \sqrt{(2gh)}$$

where

$g$  = acceleration due to gravity  
 $h$  = free-fall height

#### b. Angular Velocity: Tip-Over

The tipover event is an artificial construct wherein the HI-STORM 100 overpack is assumed to be perched on its edge with its C.G. directly over the pivot point A (Figure 3.A.16). In this orientation, the overpack begins its downward rotation with zero initial velocity. Towards the end of the tip-over, the overpack is horizontal with its downward velocity ranging from zero at the pivot point (point A) to a maximum at the farthest point of impact (point E in Figure 3.A.17). The angular velocity at the instant of impact defines the downward velocity distribution along the contact line.

In the following, an explicit expression for calculating the angular velocity of the cask at the instant when it impacts on the ISFSI pad is derived. Referring to Figure 3.A.16, let  $r$  be the length AC where C is the cask centroid. Therefore,

$$r = \left( \frac{d^2}{4} + h^2 \right)^{1/2}$$

The mass moment of inertia of the HI-STORM 100 System, considered as a rigid body, can be written about an axis through point A, as

$$I_A = I_c + \frac{W}{g} r^2$$

where  $I_c$  is the mass moment of inertia about a parallel axis through the cask centroid C and  $W$  is the weight of the cask ( $W = Mg$ ).

Let  $\theta_1(t)$  be the rotation angle between a vertical line and the line AC. The equation of motion for rotation of the cask around point A, during the time interval prior to contact with the ISFSI pad, is

$$I_A \frac{d^2 \theta_1}{dt^2} = Mgr \sin \theta_1$$

This equation can be rewritten in the form

$$\frac{I_A}{2} \frac{d(\dot{\theta}_1)^2}{d\theta_1} = Mgr \sin \theta_1$$

which can be integrated over the limits  $\theta_1 = 0$  to  $\theta_1 = \theta_{2f}$  (See Figure 3.A.17).

The final angular velocity  $\dot{\theta}_1$  at the time instant just prior to contact with the ISFSI pad is given by the expression

$$\dot{\theta}_1(t_B) = \sqrt{\frac{2 Mgr}{I_A} (1 - \cos \theta_{2f})}$$

where, from Figure 3.A.17

$$\theta_{2f} = \cos^{-1} \left( \frac{d}{2r_1} \right)$$

This equation establishes the initial conditions for the final phase of the tip-over analysis; namely, the portion of the motion when the cask is decelerated by the resistive force at the ISFSI pad interface.

Using the data germane to HI-STORM 100 (Table 3.A.3), and the above equations, the angular velocity of impact is calculated as 1.49 rad/sec.

### 3.A.7 Results

#### 3.A.7.1 Set A Pad Parameters

It has been previously demonstrated in the benchmark report [3.A.4] that bounding rigid body decelerations are achieved if the cask is assumed to be rigid with only the target (ISFSI pad) considered as an energy absorbing media. Therefore, for the determination of the bounding decelerations reported in this appendix, the HI-STORM storage overpack was conservatively made rigid except for the radial channels that position the MPC inside of the overpack. The MPC material behavior was characterized in the identical manner used in the Livermore Laboratory analysis as was the target ISFSI pad and underlying soil. The LS-DYNA3D time-history results are processed using the Butterworth filter (in conformance with the LLNL methodology) to establish the rigid body motion time-history of the cask. The material points on the cask where the acceleration displacement and velocity are computed for each of the drop scenarios are shown in Figure 3.A.18.

Node 82533 (Channel A1), which is located at the center of the outer surface of the baseplate, serves as the reference point for end-drop scenarios.

Node 84392 (Channel A2), which is located at the center of the cask top lid outer surface, serves as the reference point for the tipover scenario with the pivot point indicated as Point 0 in Figure 3.A.18.

The final results are shown in Table 3.A.4.

i. Tipover:

The time-histories of the impact force, the displacement and velocity time-histories of Channel A2, and the average vertical deceleration of the overpack lid top plate have been determined for this event [3.A.7].

The deceleration at the top of the fuel basket is obtained by ratioing the average deceleration of the overpack lid top plate. The maximum filtered deceleration at the top of the fuel basket is 42.85g's, which is below the design basis limit.

ii. End Drop:

The drop height  $h = 11$ " is considered in the numerical analysis. This is considered as an acceptable maximum carry height for the HI-STORM 100 System if lifted above a surface with design values of  $t_p$ ,  $f_c'$ , and  $E$  equal to those presented in Table 3.A.1 for Parameter Set "A". The maximum filtered deceleration at the top of the fuel basket is 43.98g's, which is below the design basis limit.

The computer code utilized in this analysis is LS-DYNA3D [3.A.5] validated under Holtec's QA system. Table 3.A.4 summarizes the key results from all impact simulations for the Set A parameters discussed in the foregoing.

The filter frequencies (to remove unwanted high-frequency contributions) for the Holtec cask analyses analyzed in this TSAR is the same as used for the corresponding problem analyzed in [3.A.2] and [3.A.4]. To verify the Butterworth filter parameters (350 Hz cutoff frequency, etc.) used in processing the numerical data, a Fourier power decomposition was generated.

#### 3.A.7.2 Set B Parameters

As stated previously, Set B parameters produce a much more compliant pad than the LLNL reference pad (Set A). This fact is borne out by the tipover and end drop analyses performed on the pad defined by the Set B parameters. Table 3.A.4 provides the filtered results for the two impact scenarios. In every case, the peak decelerations corresponding to Set B parameters are less than those for Set A (also provided in Table 3.A.4).

Impact force and acceleration time history curves for Set B have the same general shape as those for Set A and are contained in the calculation package [3.A.7]. All significant results are summarized in Table 3.A.4.

#### 3.A.8 Computer Codes and Archival Information

The input and output files created to perform the analyses reported in this appendix are archived in Holtec International calculation package [3.A.7].

### 3.A.9 Conclusion

The DYNA3D analysis of HI-STORM 100 reported in this appendix leads to the following conclusion:

- a. If a loaded HI-STORM undergoes a free fall for a height of 11 inches in a vertical orientation on to a reference pad defined by Table 3.A.1, the maximum rigid body deceleration is less than 45g's for both Set A and Set B pad parameters.
- b. If a loaded HI-STORM 100 overpack pivots about its bottom edge and tips over on to a reference pad defined by Table 3.A.1, then the maximum rigid body deceleration of the cask centerline at the plane of the top of the MPC fuel basket cellular region is less than 45g's for both Set A and Set B parameters.

Table 3.A.4 provides key results for all drop cases studied herein for both pad parameter sets (A and B). If the pad designer maintains each of the three significant parameters ( $t_p$ ,  $f_c$ , and  $E$ ) below the limit for the specific set selected (Set A or Set B), then the stiffness of the pad at any ISFSI site will be lower and the computed decelerations at the ISFSI site will also be lower. Furthermore, it is recognized that a refinement of the cask dynamic model will accrue further reduction in the computed peak deceleration. For example, incorporation of the structural flexibility in the MPC enclosure vessel, fuel basket, etc., would lead to additional reductions in the computed values of the peak deceleration. These refinements, however, add to the computational complexity. Because g-limits are met without the above-mentioned and other refinements in the cask dynamic model, the simplified dynamic model described in this appendix was retained to reduce the overall computational effort.

3.A.10      References

- [3.A.1]      Witte, M., et al., "Evaluation of Low-Velocity Impacts Tests of Solid Steel Billet onto Concrete Pads.", Lawrence Livermore National Laboratory, UCRL-ID-126274, Livermore, California, March 1997.
- [3.A.2]      Witte, M., et al., "Evaluation of Low-Velocity Impacts Tests of Solid Steel Billet onto Concrete Pads, and Application to Generic ISFSI Storage Cask for Tipover and Side Drop.", Lawrence Livermore National Laboratory, UCRL-ID-126295, Livermore, California, March 1997.
- [3.A.3]      Tang, D.T., Raddatz, M.G., and Sturz, F.C., "NRC Staff Technical Approach for Spent Fuel Cask Drop and Tipover Accident Analysis", SFPO, USNRC (1997).
- [3.A.4]      Simulescu, I., "Benchmarking of the Holtec LS-DYNA3D Model for Cask Drop Events", Holtec Report HI-971779, September 1997.
- [3.A.5]      LS-DYNA3D, Version 936-03, Livermore Software Technology Corporation, September 1996.
- [3.A.6]      Whirley, R.G., "DYNA3D, A Nonlinear, Explicit, Three-Dimensional Finite element Code for Solid and Structural Mechanics - User Manual.", Lawrence Livermore National Laboratory, UCRL-MA-107254, Revision 1, 1993.
- [3.A.7]      Zhai, J. "Analysis of the Loaded HI-STORM 100 System Under Drop and Tip-Over Scenarios", Holtec Report HI-2002474, July 2000.

Table 3.A.1: Essential Variables to Characterize the ISFSI Pad (Set A and Set B)

Item	Parameter Set A	Parameter Set B
Thickness of concrete, (inches)	36	28
Nominal compressive strength of concrete at 28 days, (psi)	4,200	6,000
Max. modulus of elasticity of the subgrade (psi)	28,000	16,000

Notes:

1. The concrete Young's Modulus is derived from the American Concrete Institute recommended formula  $57,000\sqrt{f}$  where  $f$  is the nominal compressive strength of the concrete (psi).
2. The effective modulus of elasticity of the subgrade will be measured by the classical "plate test" or other appropriate means before pouring of the concrete to construct the ISFSI pad.
3. The pad thickness, concrete compressive strength, and the subgrade soil effective modulus are the upper bound values to ensure that the deceleration limits under the postulated events set forth in Table 3.1.2 are satisfied.



Table 3.A.2: Essential Steel Material Properties for HI-STORM 100 Overpack

Steel Type	Parameter	Value
SA-516-70 at T = 350 deg. F	E	2.800E + 07
	S <sub>y</sub>	3.315E+04 psi
	S <sub>u</sub>	7.000E+04 psi
	ε <sub>u</sub>	0.21
	ν	0.30

Note that the properties of the steel components, except for the radial channels used to position the MPC, do not affect the results reported herein since the HI-STORM 100 is eventually assumed to behave as a rigid body (by internal constraint equations automatically computed by DYNA3D upon issue of a “make rigid” command). In Section 3.4, however, stress and strain results for an additional tip-over analysis, performed using the actual material behavior ascribed to the storage overpack, are presented for the sole purpose of demonstrating ready retrievability of the MPC after the tip-over. As an option, the radial channels may be fabricated from SA240-304 material. The difference in material properties, however, has a negligible effect on the end results.

Table 3.A.3: Key Input Data in Drop Analyses

Overpack weight	267,664 lb
Radial Concrete weight	163,673 lb
Length of the cask	231.25 inches
Diameter of the bottom plate	132.50 inches
Inside diameter of the cask shell	72.50 inches
Outside diameter of the cask shells	132.50 inches
MPC weight (including fuel)	88,857 lb
MPC height	190.5 inches
MPC diameter	68.375 inches
MPC bottom plate thickness	2.5 inches
MPC top plate thickness	9.5 inches

Table 3.A.4: Filtered Results for Drop and Tip-Over Scenarios for HI-STORM 100<sup>†</sup>

Drop Event	Max. Displacement (inch)		Impact Velocity (in/sec)	Max. Deceleration <sup>††</sup> at the Top of the (g's) Basket		Duration of Deceleration Pulse (msec)	
	Set A	Set B		Set A	Set B	Set A	Set B
End Drop for 11 inches	0.65	0.81	92.2	43.98	41.53	3.3	3.0
Non-Mechanistic Tip-over	4.25	5.61	304.03	42.85	39.91	2.3	2.0

<sup>†</sup> The passband frequency of the Butterworth filter is 350 Hz.

<sup>††</sup> The distance of the top of the fuel basket is 206" from the pivot point. The distance of the top of the cask is 231.25" from the pivot point. Therefore, all displacements, velocities, and accelerations at the top of the fuel basket are 89.08% of those at the cask top (206"/231.25").

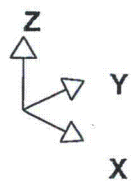
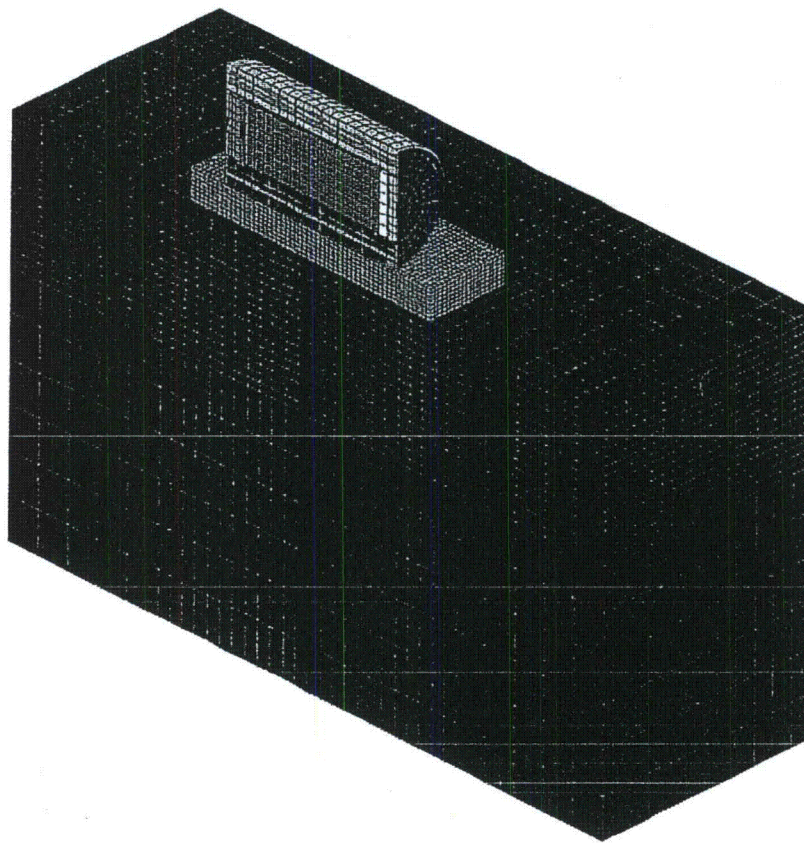


Fig 3.A.1 Tipover Finite-Element Model (3-D View)

HI-2002444  
HI-STORM FSAR

HI-STORM 100 FSAR, NON-PROPRIETARY  
REVISION 12  
MARCH 12, 2014

REV. 0

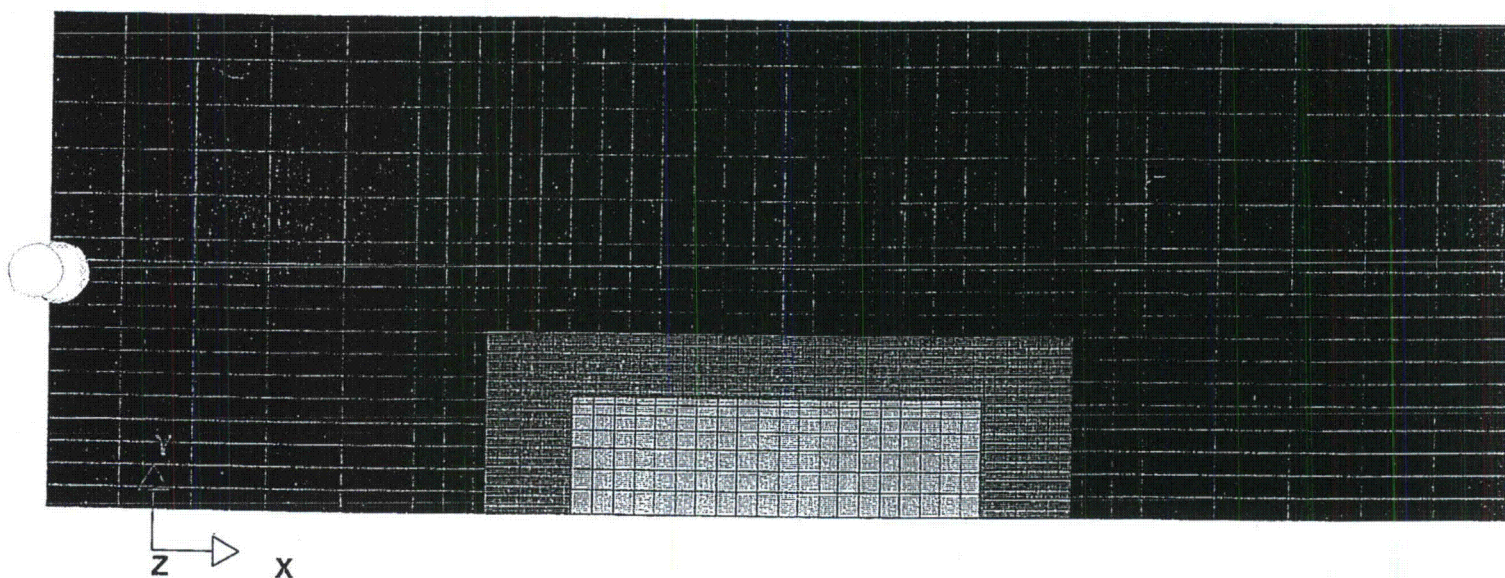


Fig 3.A.2 Tipover Finite-Element Model (Plan)

HI-STORM FSAR

HI-2002444

HI-STORM 100 FSAR, NON-PROPRIETARY  
REVISION 12  
MARCH 12, 2014

REV. 0



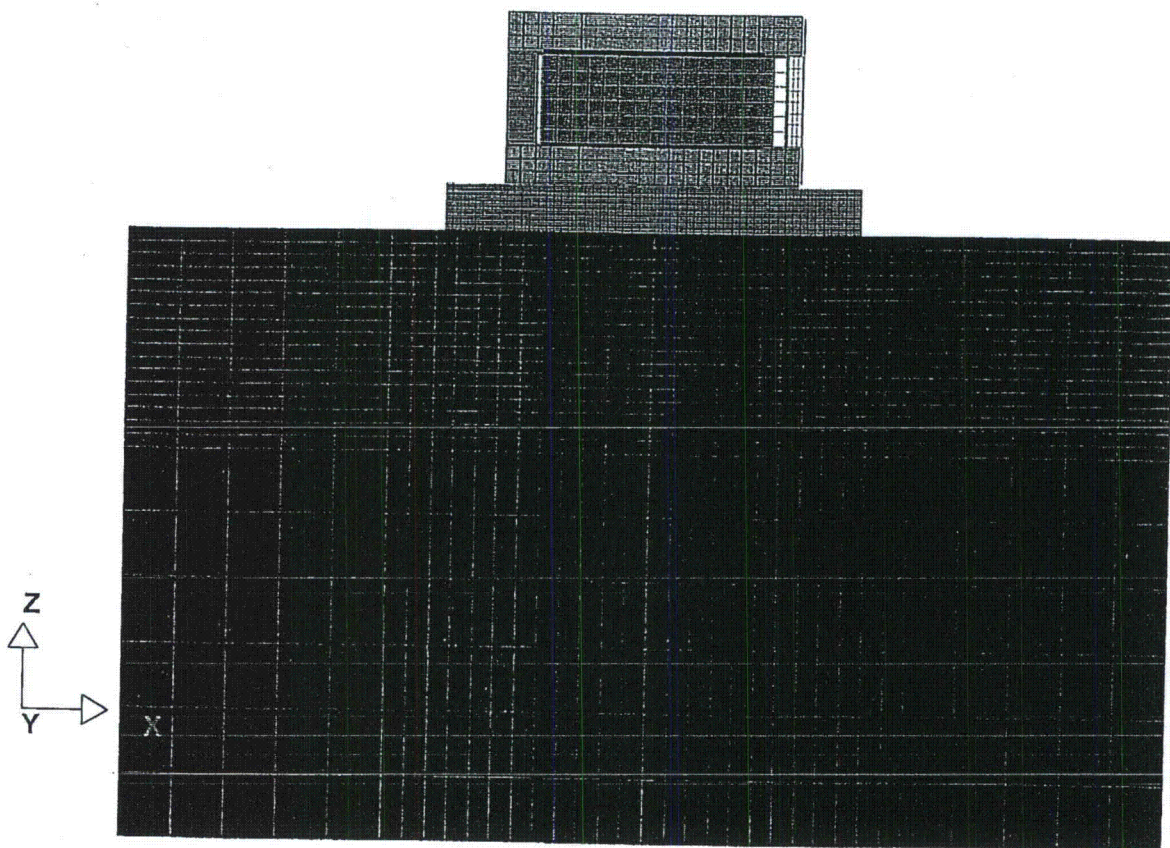


Fig 3.A.3 Tipover Finite-Element Model (XZView)

HI-STORM FSAR  
HI-2002444

HI-STORM 100 FSAR, NON-PROPRIETARY  
REVISION 12  
MARCH 12, 2014

REV. 0

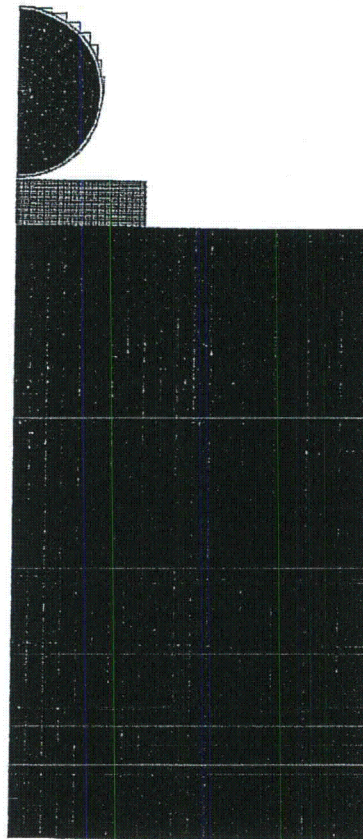
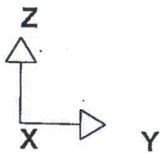


Fig 3.A.4 Tipover Finite-Element Model (YZ View)

HI-STORM FSAR

HI-2002444 HI-STORM 100 FSAR, NON-PROPRIETARY

REVISION 12

MARCH 12, 2014

REV. 0

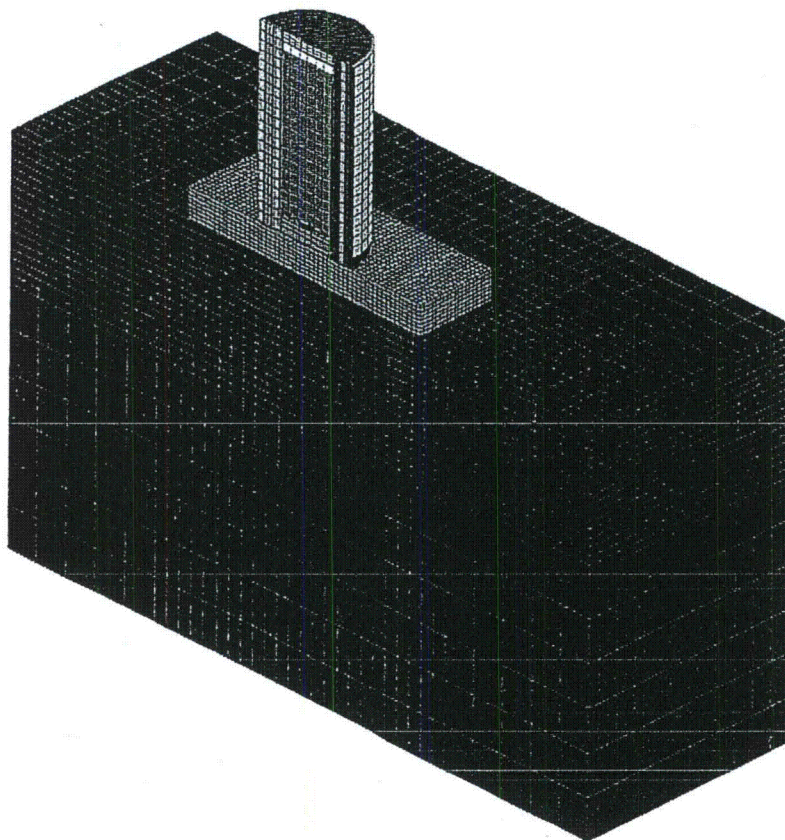


Fig 3.A.5 End-Drop Finite-Element Model (3-D View)

HI-STORM FSAR  
HI-2002444

HI-STORM 100 FSAR, NON-PROPRIETARY  
REVISION 12  
MARCH 12, 2014

REV. 0



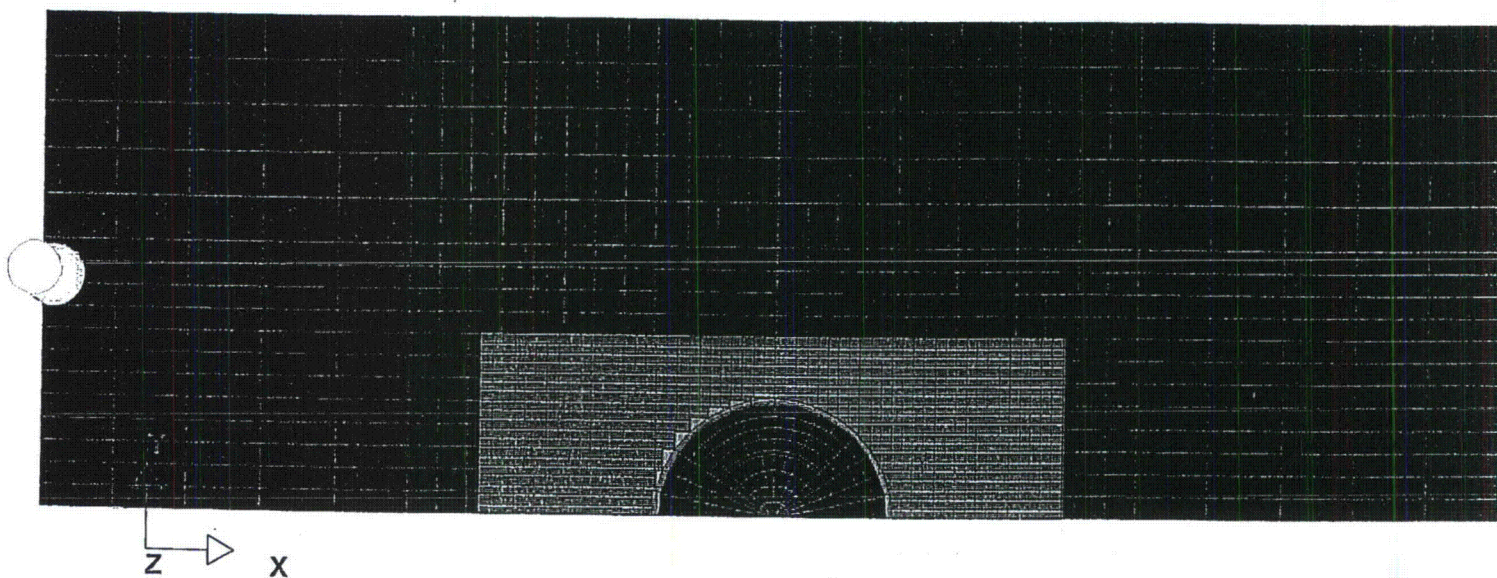


Fig 3.A.6 End-Drop Finite-Element Model (Plan)

**HI-STORM FSAR**

**HI-2002444**

HI-STORM 100 FSAR, NON-PROPRIETARY

REVISION 12

MARCH 12, 2014

REV. 0

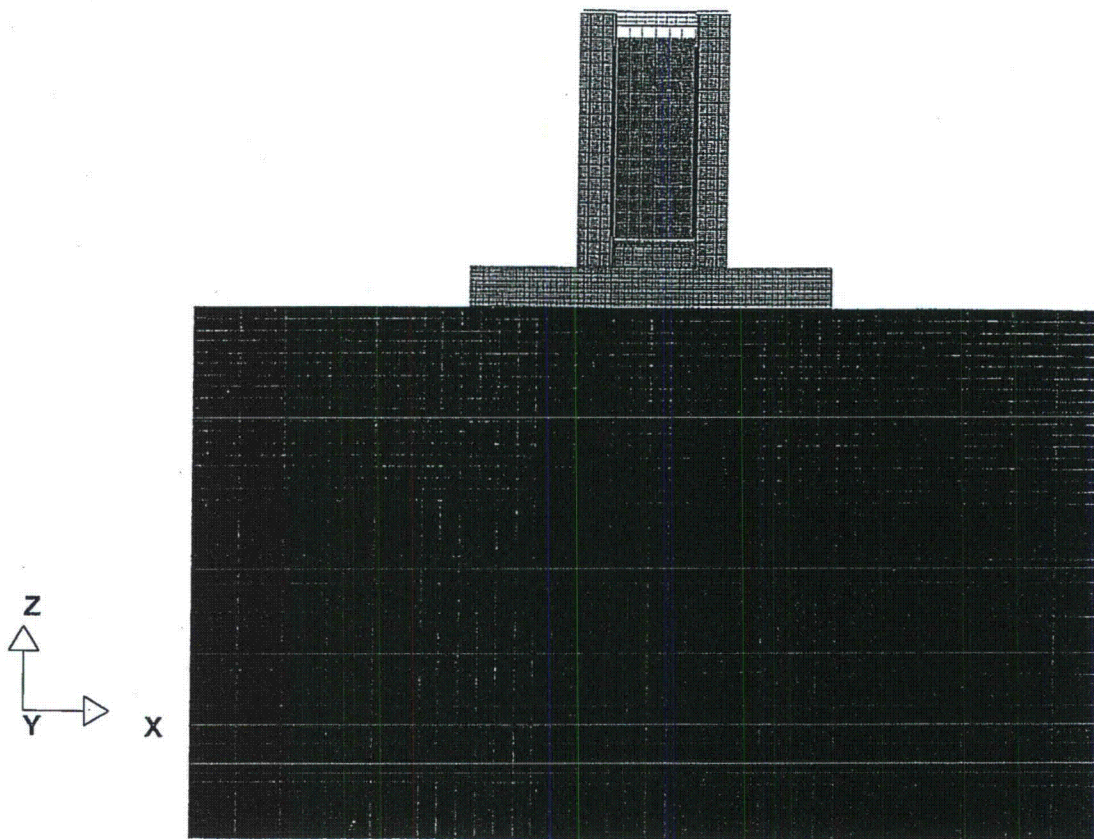
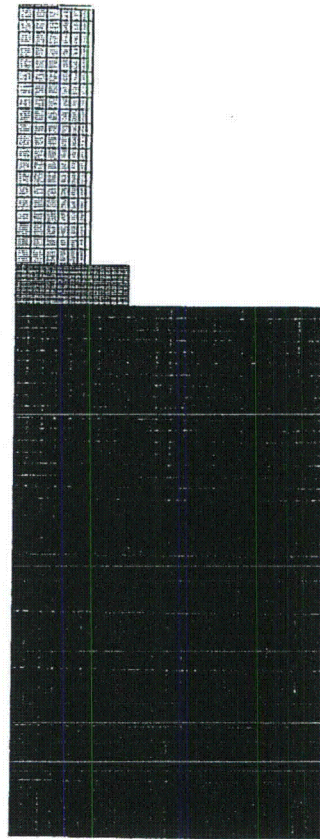
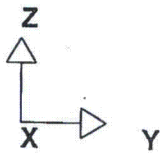


Fig 3.A.7 End-Drop Finite-Element Model (XZView)



HI-STORM FSAR

HI-2002444 HI-STORM 100 FSAR, NON-PROPRIETARY

REVISION 12

MARCH 12, 2014

Fig 3.A.8 End-Drop Finite-Element Model (YZ View)

REV. 0



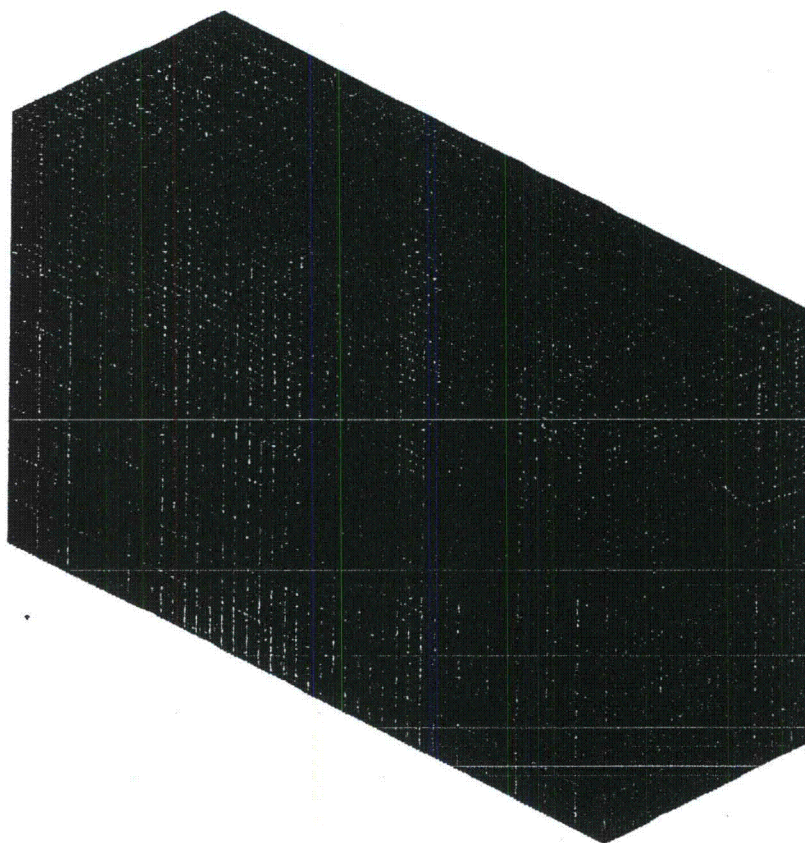
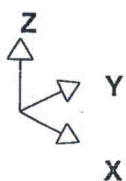
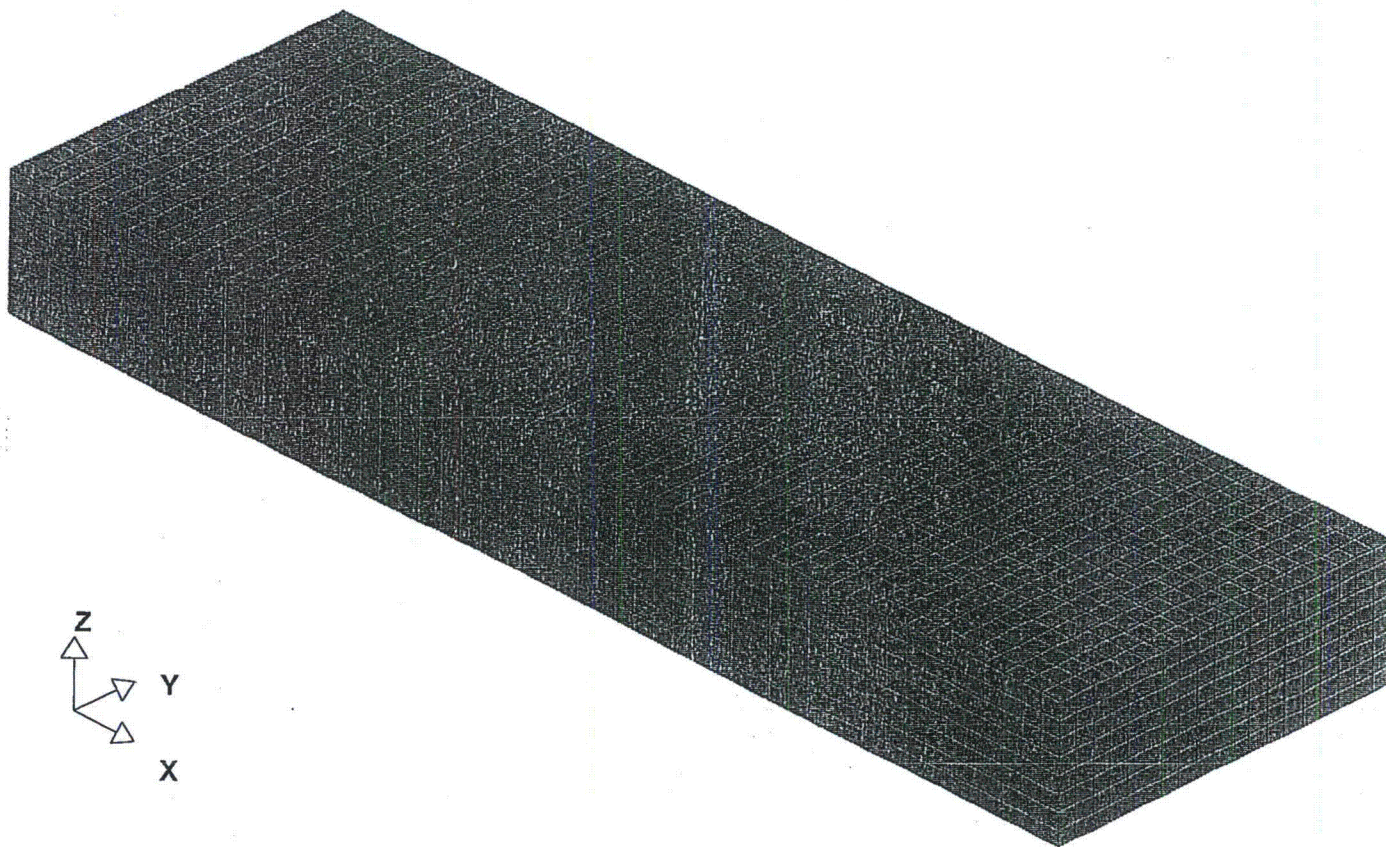


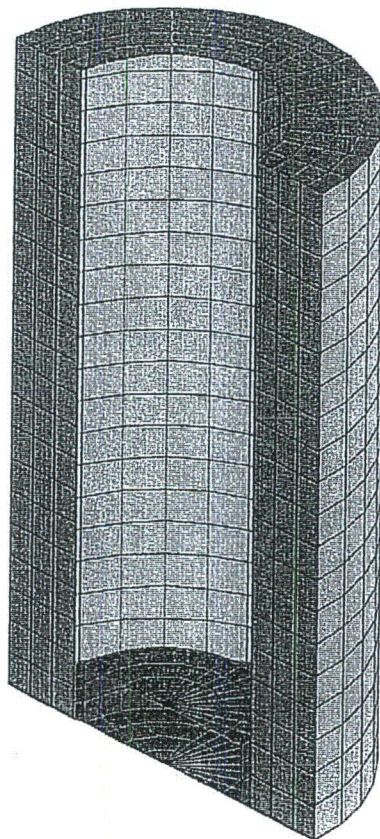
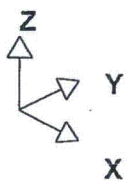
Fig 3.A.9 Soil Finite-Element Model (3-D View)

**HI-STORM FSAR**  
**HI-2002444**

HI-STORM 100 FSAR, NON-PROPRIETARY  
REVISION 12  
MARCH 12, 2014

REV. 0







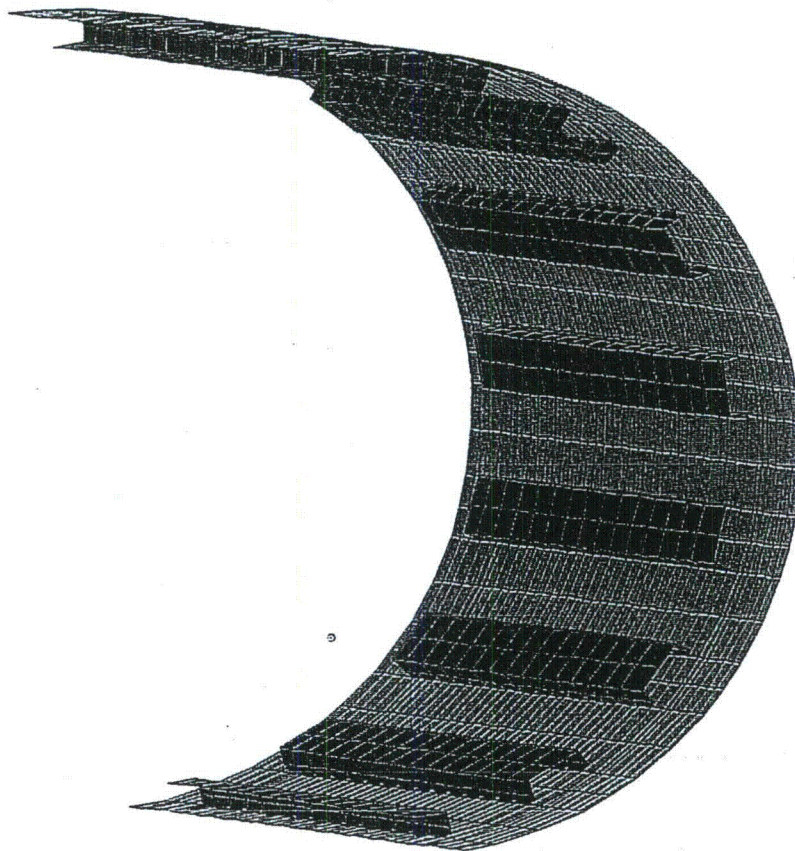
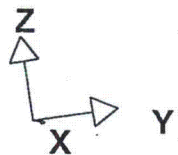


Fig. 3.A.12 Inner Shell and Channels Finite-Element Model (3-D View)

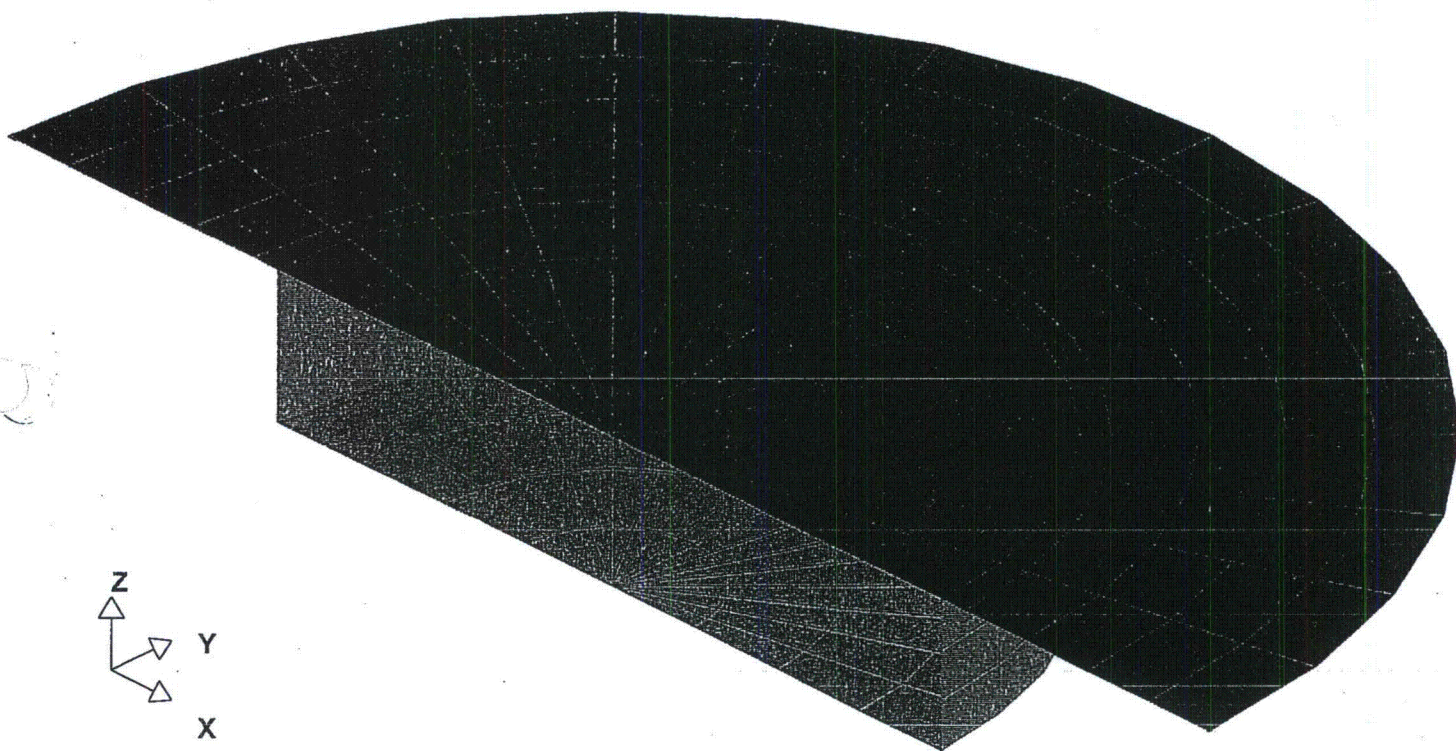


Fig. 3 A-13 Lid Steel Finite-Element Model (3-D View)



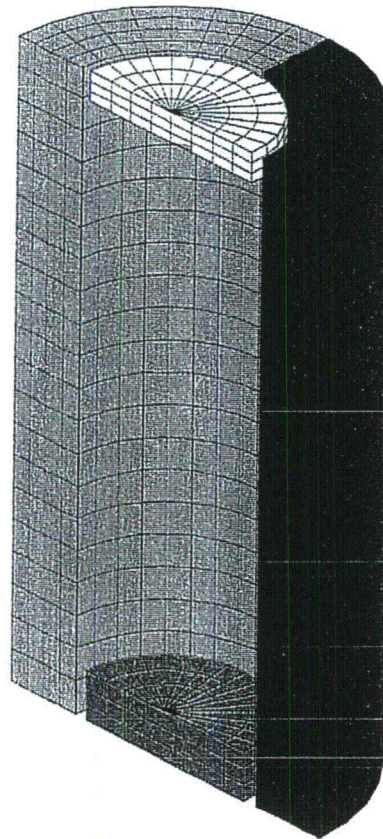
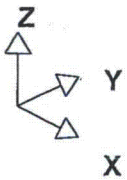


Fig 3.A.14 Overpack Concrete Components Finite-Element Model (3-D View)

HI-2002444

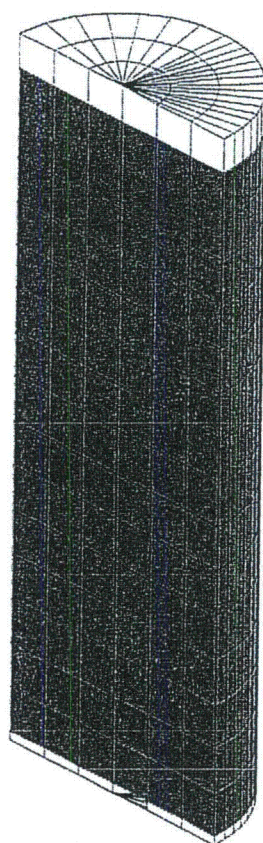
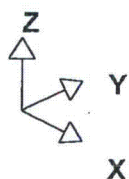
HI-STORM FSAR

HI-STORM 100 FSAR, NON-PROPRIETARY

REVISION 12

MARCH 12, 2014

Rev. 0



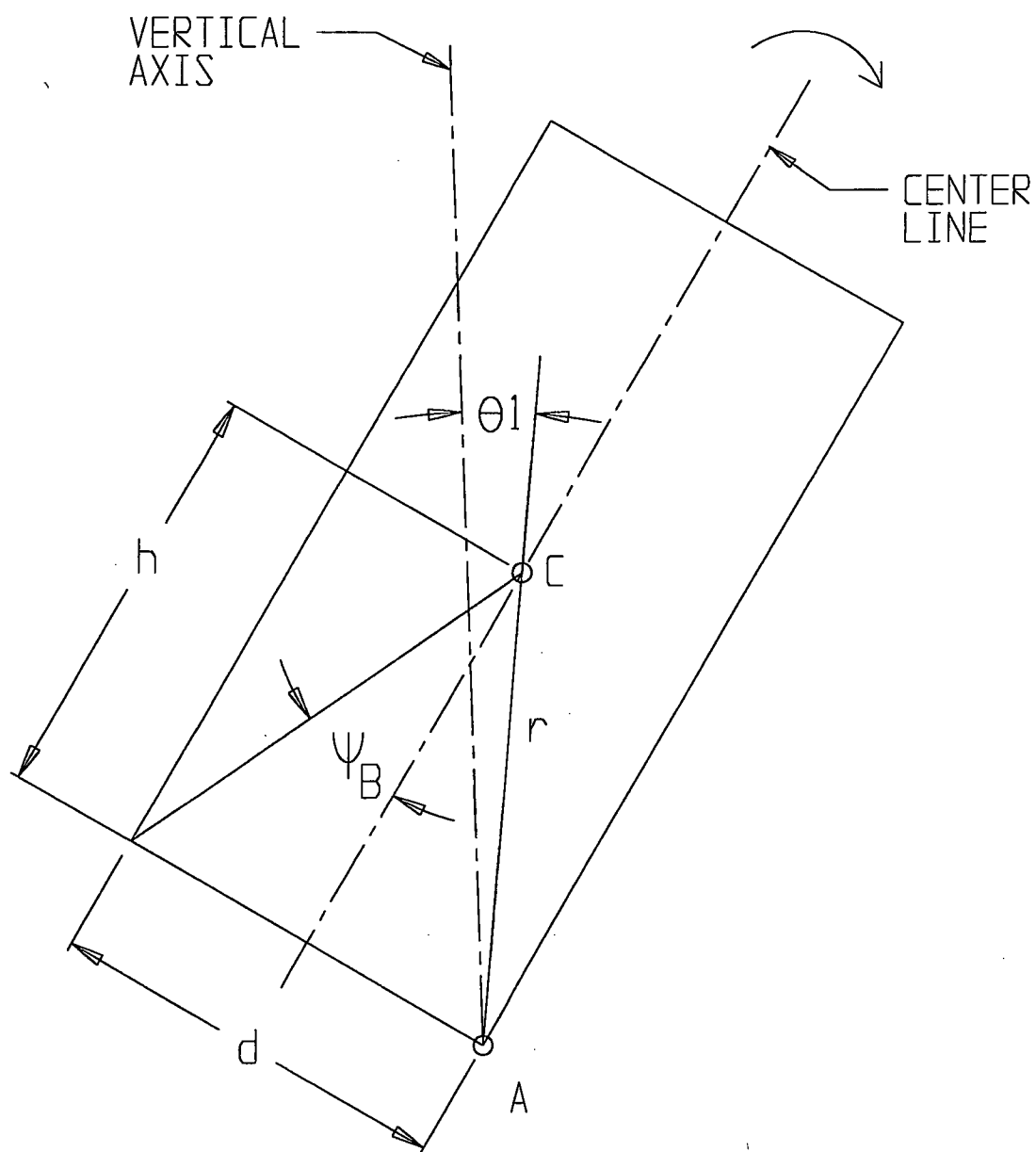


FIGURE 3.A.16; PIVOT POINT DURING TIP-OVER CONDITION

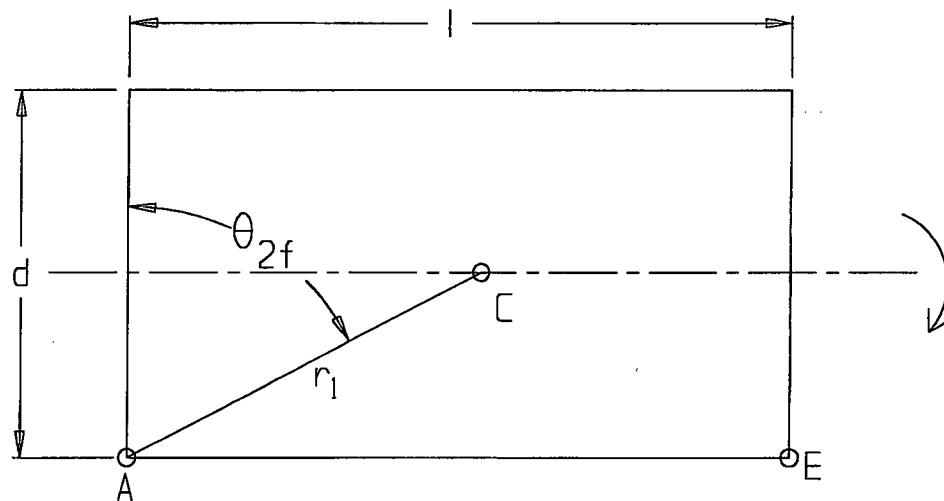


FIGURE 3.A.17; TIP-OVER EVENT OVERPACK SLAMS AGAINST THE FOUNDATION  
DEVELOPING A RESISTIVE FORCE

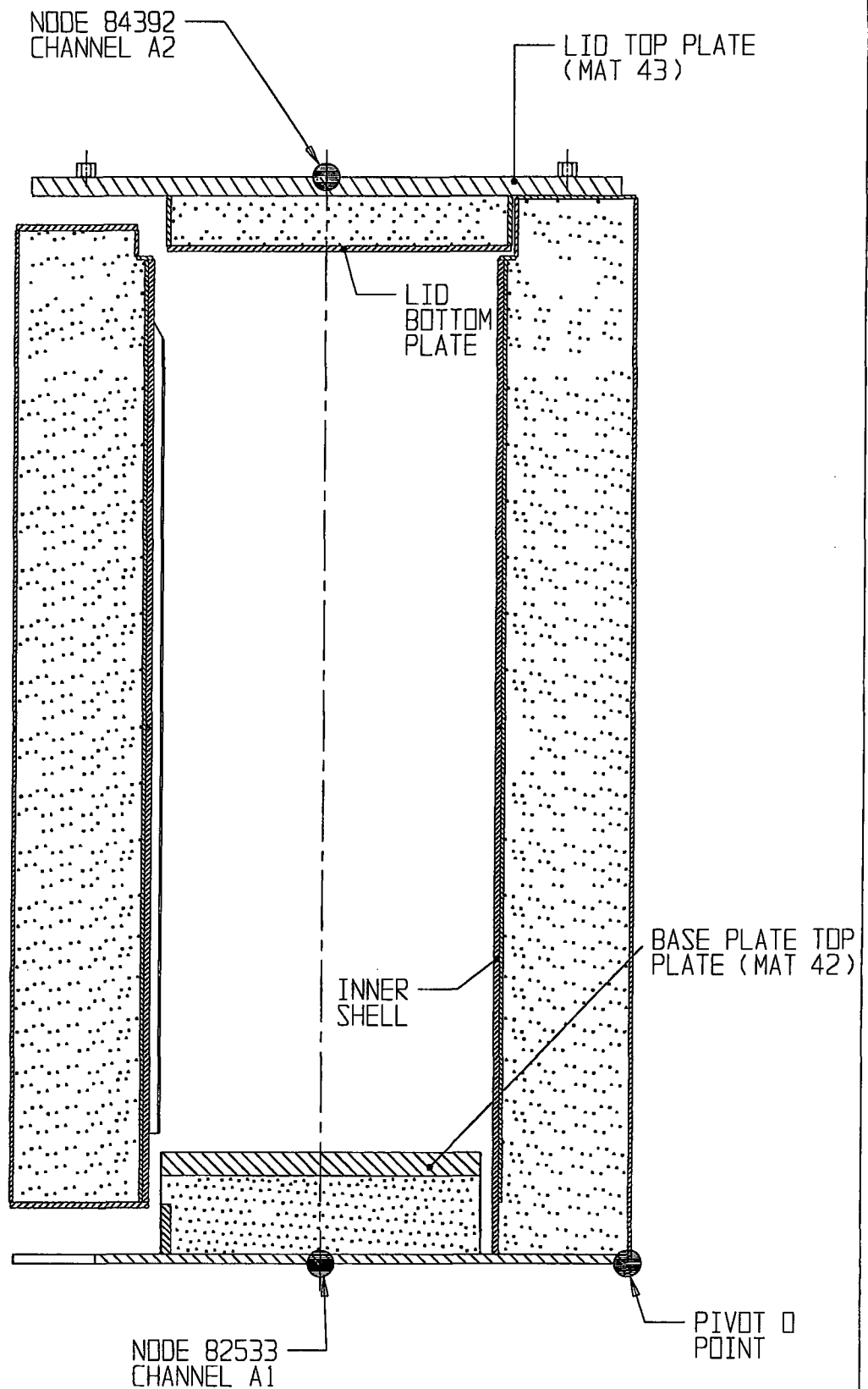


FIGURE 3.A.18; MEASUREMENT POINTS AND CORRESPONDING  
FINITE-ELEMENT MODEL NODES

HI-STORM FSAR

REPORT HI-2002444

HI-STORM 100 FSAR, NON-PROPRIETARY  
REVISION 12  
MARCH 12, 2014

REVISION 0

\\5014\\HI2002444\\CH\_3\\3\_A\_18R0

FIGURES 3.A.19 THROUGH 3.A.30

INTENTIONALLY DELETED